The New Haringvliet Barrier

Conceptual design for the storm surge barrier of the Delta21 project

P. R. I. Onwuachu

TU Delft

Delta 21

Witteveen+Bos

The New Haringvliet Barrier

Conceptual design for the storm surge barrier of the Delta21 project

by

P. R. I. Onwuachu

to obtain the degree of Master of Science

at the Delft University of Technology,

Student number:	4252675	
Thesis committee:	Dr. ir. J. D. Bricker,	TU Delft
	Ir. W. F. Molenaar,	TU Delft
	Dr. ir. R. J. Labeur,	TU Delft
	Ir. G. R. Spaargaren,	Witteveen + Bos
	Ir. L. H. de Vilder,	Witteveen + Bos

Preface

With this thesis, I conclude my Master's degree in Hydraulic Engineering at the TU Delft. This thesis is part of the Delta21 project, an initiative by Huub Lavooij and Leen Berke to find a new solution for the future flood safety challenges the Netherlands faces. I hope this thesis can be a valuable resource in the future research of other students and colleagues.

I would like to express my gratitude to my graduation committee - Dr.ir. Jeremy Bricker, Ir. Wilfred Molenaar, and Dr.ir. Robert Jan Labeur for their guidance and feedback during the course of this project. To my supervisors at Witteveen + Bos, Gerben Spaargaren and Lucas de Vilder, thank you for providing me with constant feedback, encouragement, and many supportive phone calls during the lockdown. I would like to thank the rest of the colleagues and interns at Witteveen + Bos, for their support, and for providing me with a welcoming work environment during my internship.

Lastly I would like to thank my friends, family, and girlfriend for always supporting me.

Peter Robbert Ikenna Onwuachu
Delft, March 2021

Summary

The combination of continuous sea level rise, and more frequent extreme river discharges will become a rapidly developing problem for the Rhine-Meuse delta over the course of the next century. The current Dutch delta management policy mostly revolves around the consistent improvement of the existing dikes to account for the increasing water levels in the region. An alternative solution to this problem is the Delta21 project. The Delta21 project proposes the construction of a large scale storage lake, and a high capacity pumping station at the Dutch coast. The project is meant to allow for the simultaneous closure of the storm-surge barriers on the Dutch coast, while actively discharging river water that would normally be pilling up behind the closed barriers (fig. 1). The Delta21 project foresees it will be able to save up to 5billion euros by the end of the century in dike reinforcement costs.

In order to enable the flood safety operation of the Delta21 project, the project also requires the construction of a new storm-surge barrier in the Haringvliet ebb-tidal delta, roughly 10km away from the current Haringvlietsluices. The objective of this thesis is the conceptual design of the new Delta21 storm surge barrier, the New Haringvliet barrier. The aim of this design process is to identify critical design components, and requirements that could potentially be hurdles in the development of the New Haringvliet barrier, as well as the overall Delta21 project.

For the hydrodynamic design of the barrier, a schematized 1D hydrodynamic model was used to get a first insight into the impact the new barrier will have on the on the tidal range in the tidal delta. As well as how much it could potentially impact the reintroduction of the tide to the Haringvliet. The reopening of the Haringvliet would be a part of Delta21's effort to restore some of the local ecological value to the region as a compensation measure for the project. Additionally, the model was also used to determine the effects of the construction of the barrier on the capability for the system to handle high river discharge rates. The findings of the assessment show that the selection of a small tidal opening in the New Haringvliet barrier will significantly negatively impact the capability for the system to discharge high river water, as well as limit the amount of tidal range that will be available in the system. It was determined that constructing the barrier with a tidal opening with an effective cross-section of 10000m^2 will provide the best balance between hydrodynamic performance of the system, and barrier construction costs.

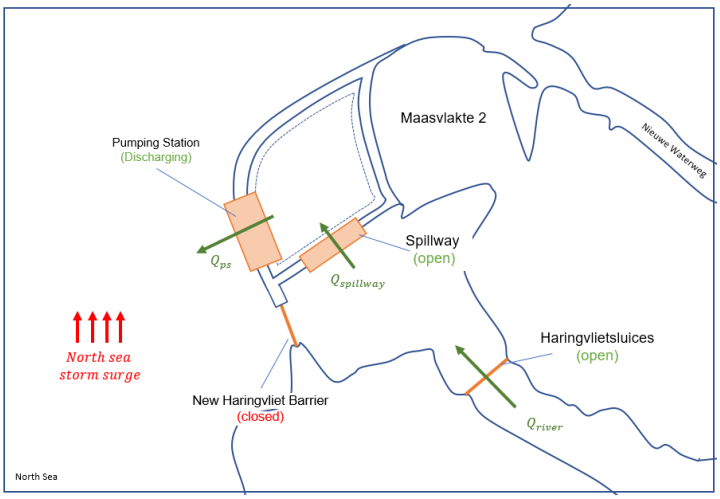

Figure 1: Operation of the Delta21 infrastructure during the combined occurrence of a storm surge on the North sea and a high river Rhine discharge. The New Haringvliet barrier will be closed to stop the storm surge, while the Haringvliet sluices and spillway are opened to allow for river water to flow into the Valmeer. The pumping station is used to simultaneously pump water out of the Valmeer.

An analysis of the possible Delta21 construction sequences was used to determine the preferred construction method for the barrier. In this analysis, an economic construction sequence alternative, and an environmental construction sequence alternative were developed, and consecutively evaluated using a multi-criteria analysis. This MCA revealed that the construction of the New Haringvliet barrier using prefab construction elements and techniques was the desired construction method for the project.

The results of hydrodynamic and construction sequence assessment, were used as the basis for the barrier's spatial design. An overview of this design is shown in fig. 3. The structure was designed with a total of 20 vertical lift gates, each spanning 80m. This would bring the total tidal opening to 10400m^2. Vertical lift gates were chosen for the design due to their great reliability and overall cost effectiveness, which are both important considerations for a barrier of this magnitude. On the southern side of the barrier a shipping lock will be the barrier's primary navigational opening.

The final phase of the conceptual design focuses on the design of the gated barrier section, and includes the validation of the transport stability of the caisson, the design of the vertical lift gates, and the design of the scour protection and it's filter layers. The resulting layouts for the gated barrier section is presented in fig. 2.

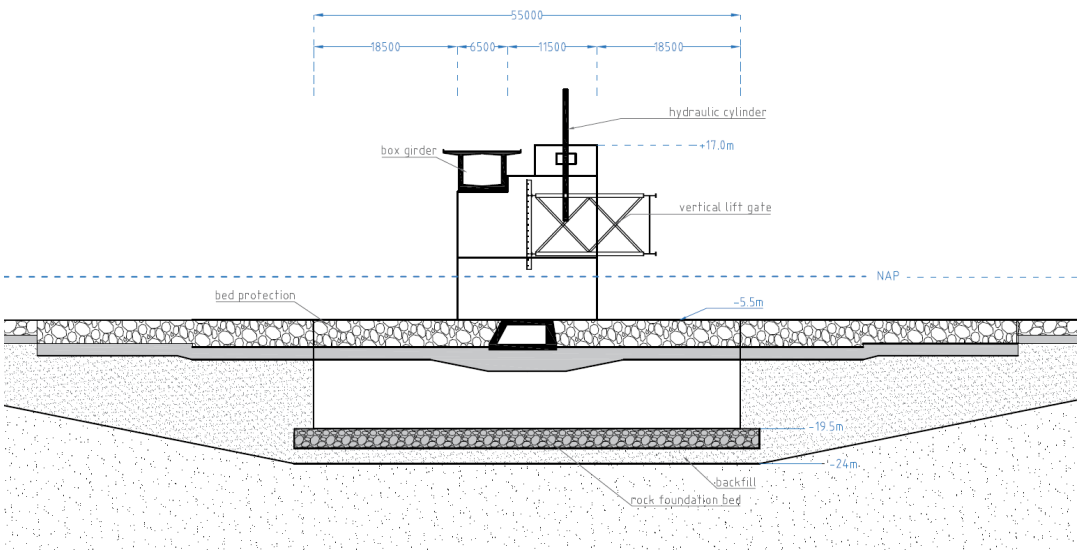

Figure 2: Layout conceptual New Haringvliet barrier design

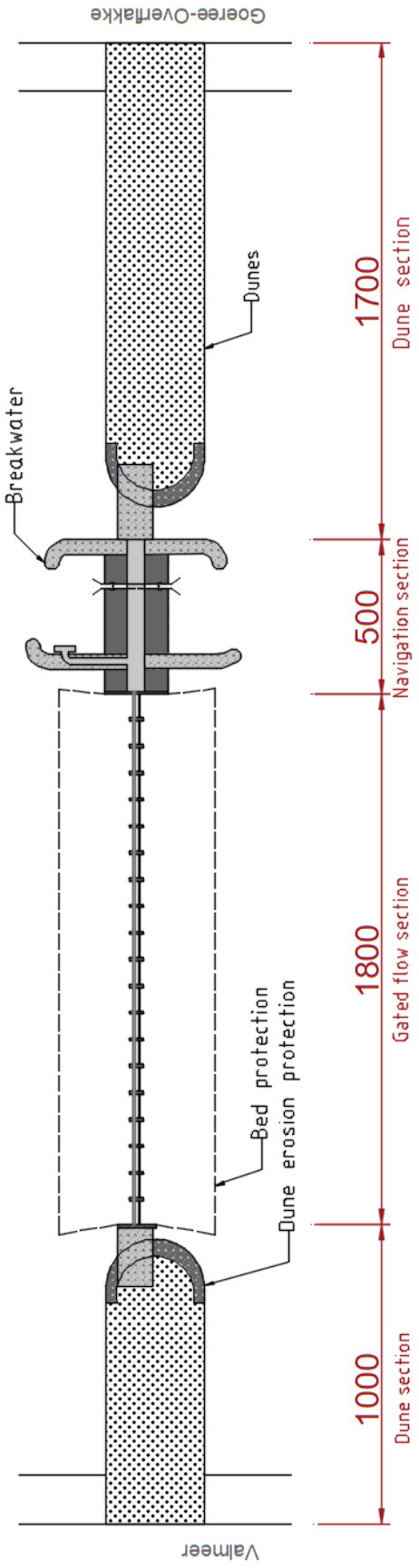

Figure 3: Conceptual spatial design for the New Haringvliet barrier. The dune sections are connected to the structural barrier elements by short breakwater sections. The navigation section is a shipping lock sheltered by breakwaters.

Contents

1

Introduction

After the North Sea flood of 1953, the Directorate-General for Public Works and Water Management (Dutch: Rijkswaterstaat) ordered and started the construction of the Dutch Delta-works, an extensive series of construction projects meant to protect the Rhine-Meuse Delta (RMD) from flooding due to storms on the North Sea. The project effectively shortened the coastline by closing of all major tidal basins in the delta, with the use structures such as dams, storm-surge barriers and locks. Since it's completion, the project has been successfull in ensuring a high level of flood safety for the Rhine- Meuse Delta, and has been globally renowned for it's revolutionary impact on the design of flood defenses, specifically the design and construction of storm-surge barriers.

However, in recent years, concerns about sea level rise (SLR) and increased winter rainfall intensity, once again have brought the future flood safety of the RMD into question. Recent insights have brought to light that the melting of Arctic ice could accelerate the rate of global SLR significantly (Haasnoot et al., 2018). As a result, the current flood defence infrastructure will eventually lose part of it's functionality, and could eventually even fail to provide a sufficient level of safety for regions such as the RMD.

One of the proposed solutions to address the problems related to future flood safety in the RMD is the Delta21 project. The Delta21 project aims to address the future flood safety concerns of the RMD, while also introducing large scale energy storage capabilities, and restorative ecological measures to the region. Figure 1.1 gives an overview of the proposed location of the Delta21 project.The primary attribute of the project is a pumped-storage hydropower-lake ('Valmeer') with a pumping station that is capable of pumping up to 10000 m^3/s of water out of the Haringvliet basin during periods of high river discharge and simultaneous storm surge on the North Sea. During non-critical weather circumstances, the turbines installed at the lake will pump water out during off-peak energy demand periods, and generate energy by filling the lake during peak energy demand periods, basically operating as a massive battery.

To maintain the tidal flow between the Haringvliet Tidal Delta and the North Sea during regular weather conditions, and to ensure the effective flood-safety operation of the pumping station and Valmeer, a storm surge barrier between the Valmeer and the coast of Goeree-Overflakke is proposed as part of the project.

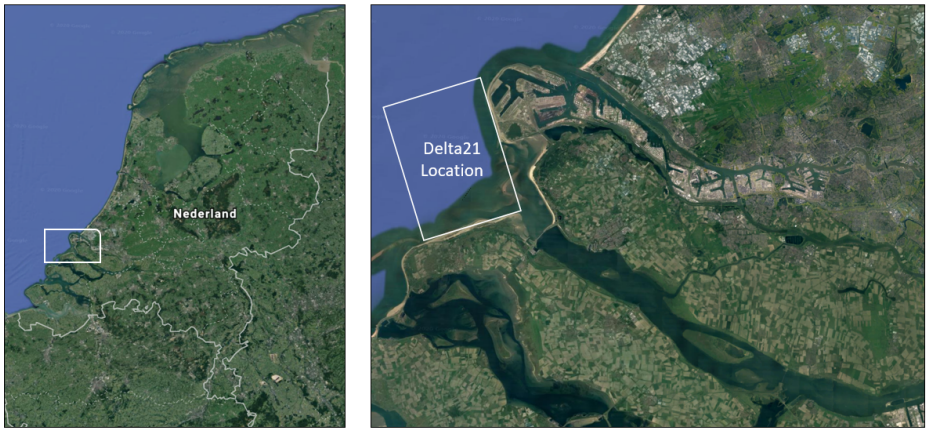

Figure 1.1: Proposed Delta21 project location (source: Google Earth)

1.1. Delta21 and the Rhine Meuse Delta

The current adaptation policy for the Rhine-Meuse Delta mainly revolves around gradually increasing the height of the dikes, in order to maintain a sufficient level of flood safety for the region. The Delta21 project was designed with the aim to provide a robust solution for the Rhine-Meuse Delta by designing water-safety infrastructure that also provides energy storage and nature restoration capabilities. Delta21's main element is a pumped-storage hydroelectricity lake ('Valmeer') (fig. 1.3). The objective of the Valmeer from a water-safety point of view is to install a large pump capacity that can aid in discharging large volumes of water out of the Haringvliet basin ($10.000 m^3/s$). During a potential flooding event the spillway between the Haringvliet and the Valmeer will open and the pumping station on the other side will discharge water from the lake into the North sea, during this time, the New Haringvliet Barrier will also be closed (fig. 1.4). The aim of this measure is to prevent flooding in the scenario that a long lasting storm surge event occurs simultaneously with high Rhine and Muese discharge rates. An overview of the primary components of the Delta21 project can be seen in fig. 1.3.

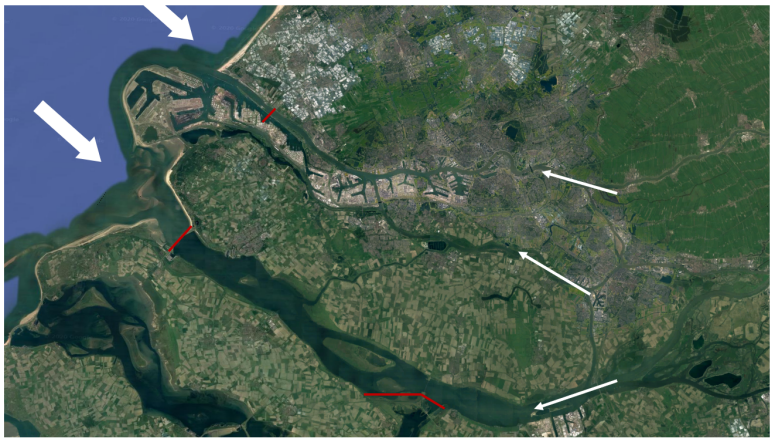

Figure 1.2: An overview for a possible critical flooding scenario for the RMD, during a long duration storm surge on the North sea, combined with a high fluvial discharge from the Rhine and the Meuse. In this situation, the barriers in the region (indicated in yellow) will be closed providing limited storage capacity in the Haringvliet estuary (source: Google Earth)

During non-critical flood scenarios, the pumping station will be used to generate energy by turbining water into the Valmeer during high- energy demand periods, and by pumping water out of the Valmeer during off-peak hours. Therefore Delta21 will provide an important energy storage function for the region, by a multi-functional operational use of the pumping station. As a measure to restore the ecological nature of the region,

during regular conditions, both the New Haringvliet Barrier and the Haringvlietsluices will be reopened to restore the tide in the Haringvliet and the Hollandsche Diep as much as possible. All in all allowing for a integrated flood safety solution allowing for large scale energy storage and the restoration of ecological value in the Haringvliet and the Rhine.

As mentioned previously, the aim for the project is currently to install up to $10000 m^3/s$ of pump capacity in the pumping stations. The preliminary plan for the Valmeer is for it to have up to a total of $500 * 10^6 m^3$ of storage capacity, The exact dimensions of the spillway are yet to be determined, but the aim is to allow a discharge of at least $10000 m^3/s$, as to not limit the pumping station discharge capacity.

1.1.1. Previous Research

The Delta21 project is currently in it's conceptual state and various feasibility studies are still required in order to judge the hydraulic effectiveness of the proposed measures, the economic feasibility of the project, and it's environmental impact on the region. The valmeer's pumping station is expected to be the largest structure within the project. It's feasibility and conceptual design has been addressed in twofold by Ruiz (2020) and Paasman (2020). Other than that, the only currently completed research includes a preliminary design of the dunes surrounding the Valmeer (van Dam, 2020), and an assessment of the primary stakeholders involved in the Delta21 project (Brühl et al., 2020).

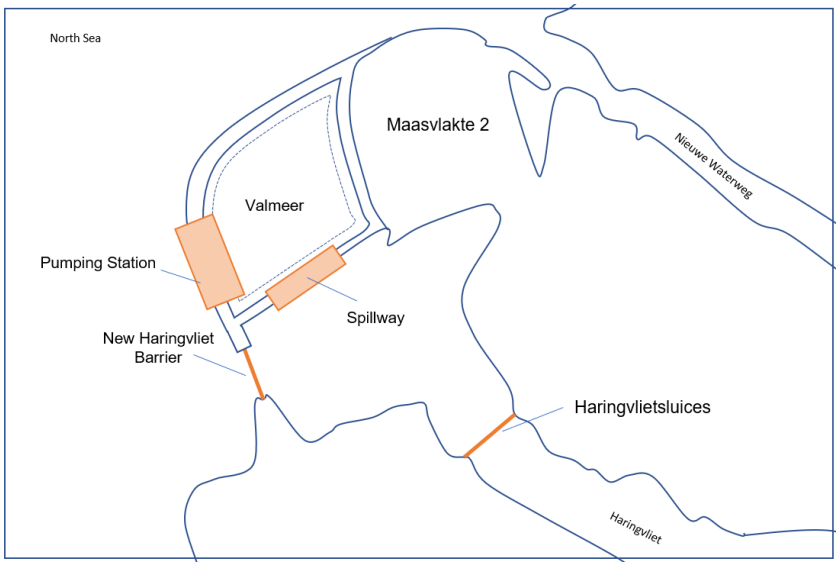

Figure 1.3: Overview of the proposed Delta21 infrastructure

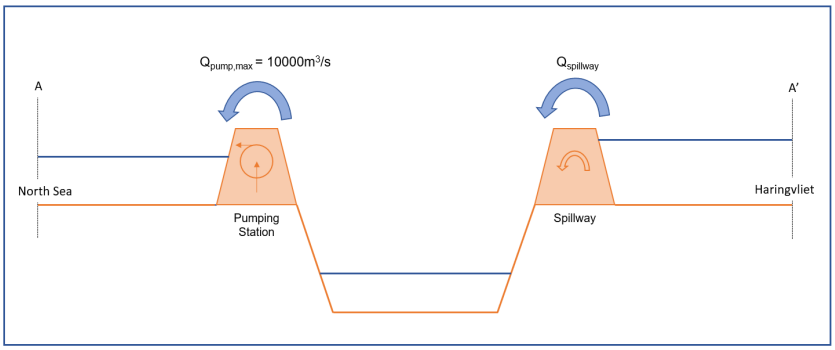

Figure 1.4: Cross-section of the proposed Delta21 infrastructure and discharge scheme during a critical flood scenario (fig. 1.3))

1.2. Problem statement

One key element that has not yet been addressed by the existing research, is the the new storm-surge barrier that is proposed as part of the Delta21 project, the New Haringvliet barrier. Storm-surge barriers are constructed with the goal to prevent flooding of the areas surrounding the inner basin or estuary they are constructed in (Mooyaart et al., 2014). The barrier is opened during regular conditions to allow for functions such as navigation, fish migration and tidal exchange. During storm conditions the barrier closes, effectively shortening the coastline, and therefore limiting the amount of hydraulic load that the flood protections of the inland estuary or basin are subjected to (Figure 1.5). Due to the their scale, often complex construction methods, and strict operational demands, storm-surge barriers tend to be expensive structures. The New Haringvliet barrier is expected to be the second largest structure within the Delta21 project, and it's design could have a large impact on the design, and even the overall economic feasibility of the Delta21 project. Which leads us to the main problem statement of this research:

There is currently no design for the New Haringvliet barrier, that fits the requirements and boundary conditions of the both the Delta21 project and the Rhine Meuse Delta

1.3. Objective

The goal for the storm surge barrier is to design a structure that enables the operation of Delta21's new flood safety infrastructure, allowing for the discharge of river water during a storm surge on the North Sea. At the same time, it is important that the design of the structure has limited negative consequences for the regions ecological value, and is an overall improvement from a flood safety point of view. Taking all these factors into consideration, the main objective of this thesis is formulated as follows:

To create a conceptual design for the New Haringvliet Barrier, that would fit the requirements and boundary conditions of the Delta21 project and the Haringvliet tidal delta.

By making a first conceptual design for the barrier, it will be possible to identify the critical barrier components and design considerations for the New Haringvliet barrier, as well as for and any future barrier that will be constructed in a similar flood safety project as the Delta21 project. The design process will also provide more insight into potential hurdles the Delta21 project faces as a whole with regards to its overall feasibility.

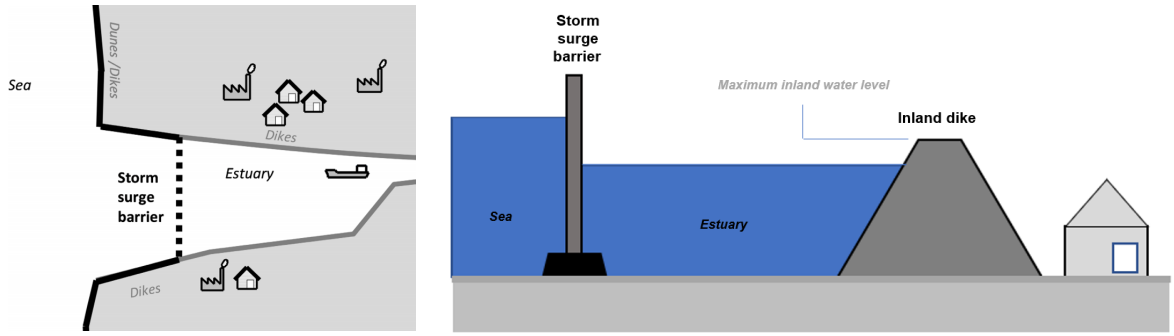

Figure 1.5: Schematic plan of an estuary with a storm surge barrier as a coastal protection strategy (source left image: Mooyaart et al. (2014))

1.4. Approach

This section of the report will elaborate on the approach used in this project. Generally throughout the project, a strongly iterative design approach will be used, where the goal is to work from a general, to a more detailed design over multiple design iterations. A flowchart for the approach and the corresponding relevant chapters is shown in fig. 1.7.

1.4.1. Overview of the relevant system, subsystem and components

The Delta21 project as a whole is currently still in it's initial design stages. Therefor throughout this project, an important consideration will be the function and performance of the barrier within the larger system. For an overview of the relation between the system, sub-system and components relevant to this thesis an overview is provided in fig. 1.6.

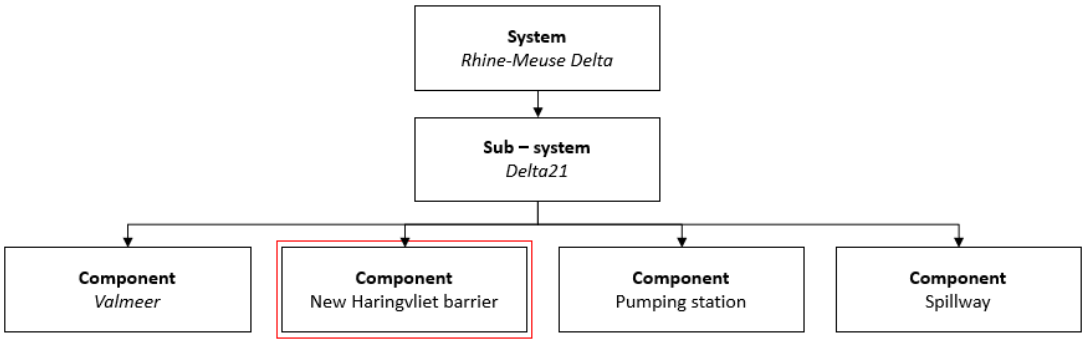

Figure 1.6: Overview of the relevant systems, sub-system and components for the project, and the position of the New Haringvliet barrier within this hierarchical structure.

1.4.2. Overview of the approach

The approach is schematized in three general phases:

1. Project analysis phase
2. System and subsystem level design phase
3. Component level design phase

A short description with the contents of every phase is given below:

Project analysis phase

- **Location and flood safety analysis**
  The first phase of this project will be the analysis phase. The analysis is divided in two different sections: an analysis of the project location, and a flood safety analysis. The purpose of the location analysis is to provide an comprehensive understanding of locations, structures and functions of importance at a system level. Additionally, the potential effect of the construction and operation of the Delta21 project and it's barrier on the region will be assessed. The flood safety analysis' main objective is to review the relevant flood safety regulations and requirements in the region. After identifying the regional requirements, the Delta21 project will be assessed in order to deduce the flood safety requirements and safety levels for the overall Delta21 project, and lastly, for the New Haringvliet barrier itself.

- **Requirements and boundary conditions**
  The findings of the analysis phase, are summarized and concluded, and a programme of requirements is formulated. Additionally, the main hydraulic, meteorological and geo-technical boundary conditions of the project will be defined. This section will function as the basis for the design stages of this project.

System and subsystem level design phase

- **Barrier tidal opening design**
  In the first phase of the design stage, the New Haringvliet barrier and it's hydrodynamic impact on the region will be evaluated. In order to do this an 1D hydrodynamic model is constructed that should give an early idea on the relation between the effective tidal opening in the New Haringvliet barrier and the amount of tide in the Haringvliet and Haringvliet Ebb-Tidal delta. Additionally, the impact of the construction of the New Haringvliet barrier on the discharge capacity of the Haringvliet during high river discharges will be assessed. The final output of this phase is a recommendation for the effective tidal opening in the New Haringvliet barrier and will be used in the preliminary barrier design of this project.

- **Delta21 construction sequence assessment**
  Currently, there has not yet been a systematic review of the Delta21 construction process. The Delta21 project features a total of three different large scale hydraulic structures in close proximity, which makes it necessary to evaluate the construction of a project as a whole, rather than evaluating the construction process of the individual components. Therefor in this project, a preliminary evaluation of the construction sequence for the entire Delta21 construction method is included. This will be a first iteration in the design of the Delta21 construction method as well as the New Haringvliet barrier, as the output of this section of the report will be twofold:

  1. Preliminary evaluation of the Delta21 construction method (sub-system level)
  2. Recommended construction method and foundation type for the New Haringvliet barrier (component level)

Component level design phase

- **Development of spatial design**
  The last phase of the project is based around the design of the New Haringvliet barrier on a component level. The first step in this design process is the barrier's spatial design. In this section of the report, the primary dimensions, and layout of the barriers gated section, navigation opening and dammed sections are all discussed and designed.

- **Gated barrier design**
  The final design step of the project focuses more on the gated section of the barrier, and focuses on the design of the gated sections primary components such as the hydraulic gates, the bed protection and the design of the piers. This step concludes the conceptual barrier design of the New Haringvliet barrier.

Discussion of design choices and considerations

The final step will be the discussion and evaluation of the project, which will give more context on the various problems, uncertainties and premises that were made and used in this study. This section of the report is meant to give more context and reflection to the design and design process, and for potential future studies relating to this topic.

1.5. Report Outline

The approach and it's corresponding chapters are summarized in a final project outline that demonstrates the different phases of the project, including the various iteration points, and chapter outputs throughout the project (fig. 1.7).

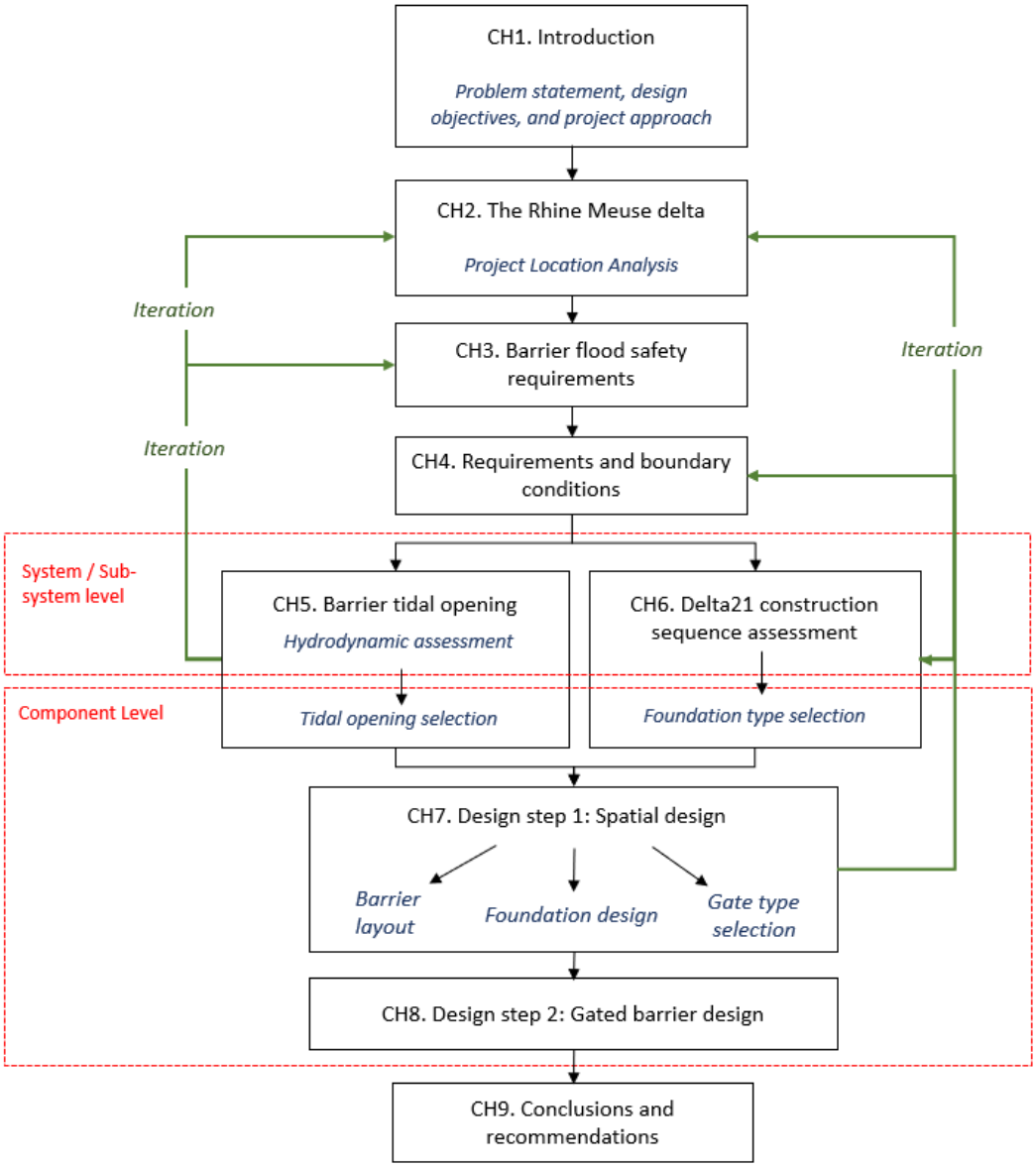

Figure 1.7: Project approach flowchart

2

The Rhine-Meuse Delta

The design and construction of the Haringvliet sluices, was one of the most difficult tasks of the Dutch Delta Works. Not only was the construction process rather complex due to the size of the sluices, the structure also has to satisfy a large number of interests from various stakeholders. This chapter evaluates the historical changes throughout the Rhine Meuse Delta with the aim to understand the current state of the system, and what conditions need to be considered during the design of the Delta21 project, and more specifically the New Haringvliet barrier. Section 2.1 outlines some of the general changes that have occurred over the past century in the RMD, including a technical and operational overview of the Haringvlietsluices and the Maeslantkering. Section 2.2 gives a brief description of the Haringvliet Ebb-Tidal delta, the construction location for the Delta21 project (fig. 2.1). Lastly, in section 2.3, a more detailed description of the Delta21 project is given in addition to an preliminary assessment of it's potential impact on the Haringvliet ebb-tidal delta.

Figure 2.1: The respective locations of the Haringvliet ebb-tidal delta (yellow), and the Haringvliet estuary (orange) withing the Rhine-Meuse Delta. The two areas are separated by the Haringvlietsluices.

2.1. Human interventions in the Rhine Meuse delta

The Rhine-Meuse delta (RMD) as we know it today is a product of centuries of human interventions (Vellinga et al., 2014). Since 1850, three notable interventions were completed in the RMD: the construction of the Nieuwe Waterweg (1872), the relocation of the lower Meuse to avoid confluence with the Rhine Branch Merwede (1904) and the closure of the Haringvliet estuary (1970) (Vellinga et al., 2014). The construction of the Haringvlietsluices, and the consequent closure of the Haringvliet basin, was an important part of the Delta-

works, as the project had some additional objectives besides the improvement of the flood-safety standards in the region:

- To maintain sufficient navigation depth in the Nieuwe Waterweg by minimizing siltation.
- To maintain sufficient navigation depth in the upstream river reaches by maintaining a sufficient waterlevel.
- The creation of a fresh water basin by avoiding salt intrusion into the Haringvliet basin
- To reduce the salt intrusion range in the Nieuwe Waterweg to allow for additional fresh water intake points

Thus effectively, by restricting and regulating the amount of discharge that can pass through the Haringvlietsluices, the Rhine and Meuse river discharges can be redistributed to Northern channels which limits siltation and salt intrusion in the Northern channels of the RMD. The sudden shift in the discharge rates of the Haringvliet compared to the Nieuwe waterweg is shown in fig. 2.2. However, the construction and operation of the Haringvlietsluices has also had profound ecological, hydrodynamic, and morphological impact on the Haringvliet and the Haringvliet tidal delta. Ever since the Haringvlietsluices were constructed, they have almost completely nullified any tide in the Haringvliet and the Hollandsche diep, and have greatly obstructed fish migration across the sluices. Because of this, the Haringvlietsluices currently operate under a new policy, the so called 'kierbesluit'. The kierbesluit went into effect as of 2018, and mandates that the sluices will be partially opened to allow for fish migration into the estuary. The degree the sluices are opened depends on the amount of river discharge at that time, as there should be sufficient discharge to prevent salt water from penetrating the basin. An overview of the changes in the tide related to the closure of the Haringvliet can be found in appendix A.2, while an overview of the effects on the Haringvliet Ebb-Tidal Delta can be found in section 2.2.

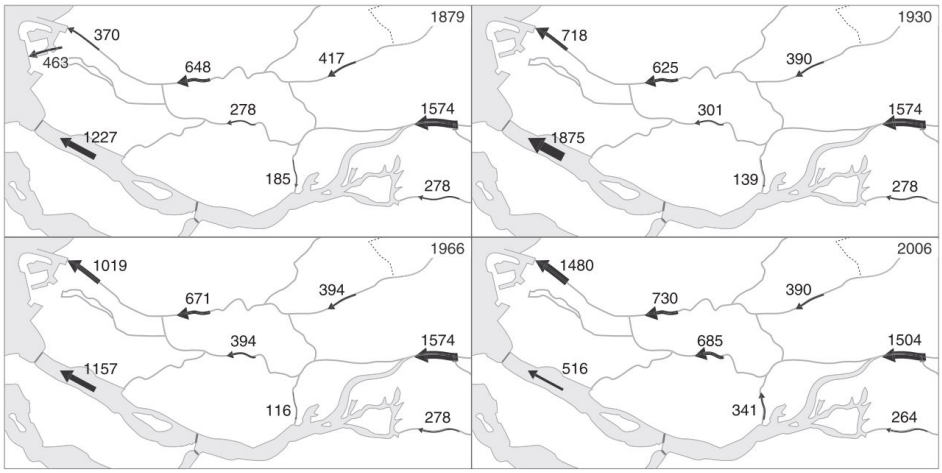

Figure 2.2: Discharge distribution in the channel network from 1879 to 2006. In 1970, a sudden northward redistribution of discharge takes place, as a consequence of closing off the Haringvliet estuary in the south. (Vellinga et al., 2014)

In 1997, 26 years after the completion of the Haringvlietsluices, the Maeslantbarrier was completed as well. The Maeslantbarrier was the final construction to be completed as part of the Delta Works, and is located in the Nieuwe Waterweg (fig. 2.3). In conjunction with the Haringvlietsluices and the Hartelbarrier, the Maeslantkering is capable of closing off the entire RMD from the North Sea in case of an impending storm surge. Together, the structures provide continuous access for navigation to the Port of Rotterdam, while maintaining flood safety standards and a fresh water supply in the RMD. section 2.1.1 and section 2.1.2, will give a brief overview of some of the technical details of the Haringvlietsluices and the Maeslantkering respectively.

Figure 2.3: Locations of the Maeslantkering (top right) and the Haringvlietsluices (bottom right) within the RMD

2.1.1. The Haringvlietsluices (Construction: 1956-1970)

The Haringvlietsluices separate the Haringvliet estuary from the North-Sea. As mentioned previously, the sluices are used to regulate the waterlevel in the Haringvliet estuary and can be used to discharge excess river-runoff to the North Sea when necessary. The structure consists of a total of 17 sluices that are each 56.5m wide, and spans from Voorne-Putten to Goeree-Overflakkee.

The entire sluice complex has a length of approximately one kilometer and when completely opened a total effective cross-section of 6000m^2. Previous to the closure, the wet cross-section of the Haringvliet at this location was about 17000m^2. The foundation of the sluices consists of roughly 22000 concrete foundation piles that are bundled together in groups to improve their total bearing capacity (Ferguson, 1971). The foundation piles hold up the large concrete floor (top of the floor at a depth of -5.5m NAP) of the structure, upon which the 18 piers of the sluices were constructed. The piers hold up, what is considered the core of the entire structure, the NABLA beam (black triangular beam in fig. 2.4). The NABLA beam is the elements to which the hydraulic gates of the structure are attached. The gate on the sea sea side of the structure, when closed, has a retaining height of +3.0m NAP, whereas on the river-side the top of the gate is at +5m NAP. It was determined that, constructing higher gates at the sea-side of the structure would leave the structure vulnerable to large dynamic loads due to wave-loading under extreme storm conditions (Ferguson, 1971). And thus instead the sea-side gate is meant to work as somewhat of a breakwater, while the gate on the river-side of the structure would be normative with regards to potential overflow discharges into the Haringvliet (Ferguson, 1971).

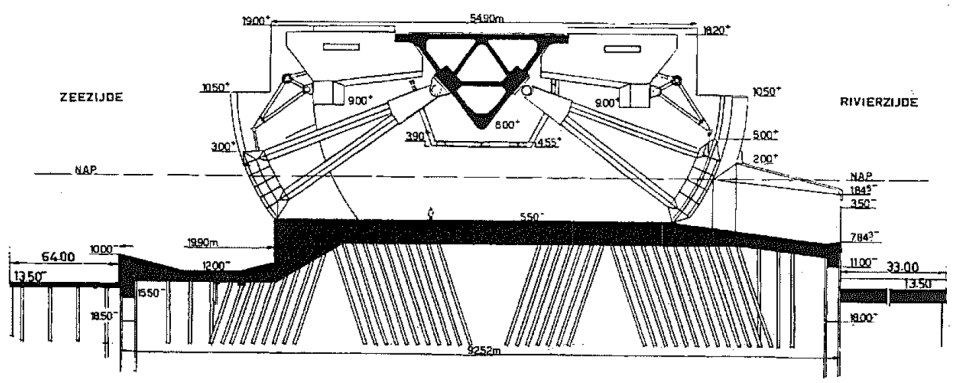

Figure 2.4: Cross-section diagram of the Haringvliet sluices (source: Ferguson (1971))

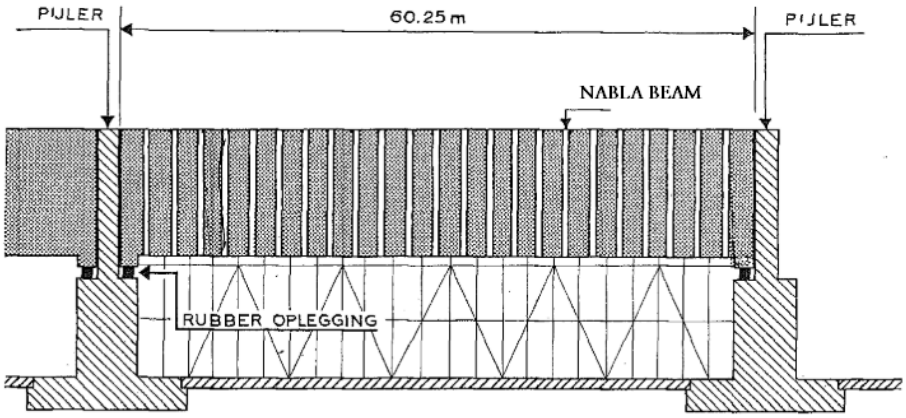

Figure 2.5: Front-view sketch of one Haringvliet sluice without the gates in place (source: Ferguson (1971))

2.1.2. Maeslant Barrier (Construction: 1991-1997)

The Maeslant barrier was the last structure to be completed as part of the Delta Works. The barrier allows for continuous shipping through the Nieuwe Waterweg, while minimizing the need for the reinforcement of the dikes around Rotterdam and other regions around the canal. The barrier consists of two massive gates attached to a ball-hinge which allows for 3-DOF movement of the barrier. When the barrier has to be closed, the gates float up, get moved inwards and then are finally sunk down again to close the Nieuwe Waterweg off. This whole process takes approximately 2.5 hours.

The Maeslantkering is closed when either a waterlevel of +2.9m NAP in Dordrecht, or a waterlevel of +3.0m NAP in Rotterdam is reached. On average it is expected that such a closure will happen once or twice every ten years. From a reliability perspective, the Dutch Water Act (= 'WaterWet'), mandates that the the maximum allowable failure rate of the closure of the Maeslantbarrier is once every 100 closures. The failure of the Maeslantbarrier during a significant storm event, would stipulate a significant hydraulic load on the inland waterways, as there is little to no redundancy for the barrier. The barrier consists of a total of two gates that span a channel that is 360m wide and 15m deep. If one, or both of the gates were to fail, a significantly large wet surface of the channel would be unprotected and the large volumes of water could stream inland.

2.1.3. Functions of the Haringvliet Estuary and Ebb- Tidal Delta

The combination of it's natural functions and the many historic interventions, have made the RMD a unique region that facilitates the interests of many different stakeholders. This subsection will provide a short overview of the primary functions the Haringvliet region fulfills (sluices, estuary, and ebb-tidal delta). By specifically focusing on the Haringvliet area, there will be more clarity on the impact of any potential changes to the area. Conclusively, the main functions of the Haringvliet region were found to be the following:

1. Fresh water storage
2. Flood safety
3. Navigation
4. Nature & Ecology
5. Tourism & Recreation

From the above mentioned functions, the fresh water storage, flood safety, and navigation functions of the Haringvliet were intended results from the construction of the Haringvlietsluices. The current ecological state

of the Haringvliet area on the other hand was a byproduct of the construction of the Haringvlietsluices. Due to the construction of the Haringvlietsluices the ecological diversity in the Haringvliet estuary decreased as the basin changed from a brackish intertidal area to a freshwater basin. Currently, the main area of importance from a nature point of view is the Haringvliet ebb-tidal delta. This area, has become an important ecological area, and is currently also a Natura2000 protected area. More details about the, state of the current Haringvliet ebb-tidal delta is provided in section 2.2. The last function is of the Haringvliet area is recreation and tourism. This function includes things such as recreational fishing, sailing, beach tourism and nature tourism.

2.2. Haringvliet Ebb-Tidal Delta

One of the primary locations of concern for the Delta21 project is the Haringvliet Ebb-Tidal Delta (fig. 2.6). This will be the construction location for the project, and therefor play an important role in the overall design process. This part of the report will primarily outline some general information about the Haringvliet ebb-tidal delta and some of its historical interventions. A complete overview of the significant interventions in the Haringvliet tidal delta since 1950 is shown in Figure 2.7.

The Haringvliet ebb-tidal delta is part of the Dutch Voordelta on South-West coast of the Netherlands, and was originally connected to the Brielse Maas and the Haringvliet estuaries. As many of the estuaries in the Voordelta, the Haringvliet saw most of it's significant changes occur as a result of the Delta Works, specifically the construction of the Haringvliet sluices (Colina Alonso, 2018).

As a result of the closure of the Haringvliet estuary in 1970, the morphodynamics of the Haringvliet tidal delta drastically changed, the limited cross-shore tidal flow made it so that the wave-dominated sediment transport became more important, and as a result, the sea-ward side of the tidal delta eroded and the shore-parallel Hinderplaat grew rapidly in length and height (Elias et al., 2017). The average depth of the tidal delta was reduced, especially towards the landward edge of the delta significant sedimentation occurred, as the wave action pushed the outward edge of the delta land inward (Elias et al., 2017).

The extension of the Maasvlakte by construction of the Maasvlakte2, has further sheltered the tidal delta from NW waves. Additionally, the formation of the Hinderplaat has formed a sheltered area in the delta, causing additional accretion behind it. At this point in time the Hinderplaat has become more of tidal flat-area, rather than a distinct bar (Elias et al., 2017).

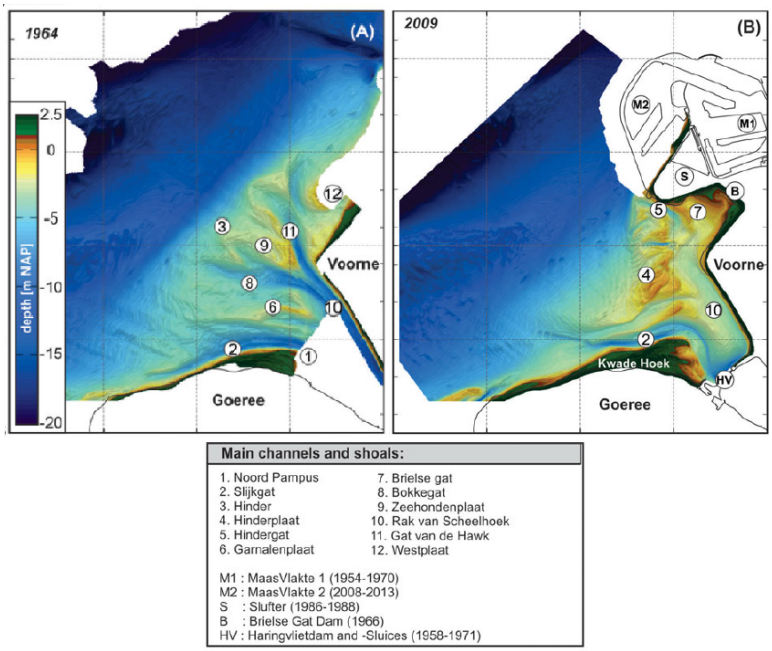

Figure 2.6: Bathymetry of the Haringvliet ebb-tidal delta for 1965 (left) and 2009 (right) (source: (Elias et al., 2017)).

Closure works	
1950	Damming Brielse Maas, creating the Brielse Lake
1957-1970	Construction of the Haringvlietdam
1966	Second closure of the Brielse Gat, creating the Oostvoorne Lake
1971	Closure by the Brouwersdam
Extension Port of Rotterdam	
1964-1966	Construction of Europoort
1967-1976	Construction of Maasvlakte 1
1986-1987	Dredging operations Hindergat and construction of the Slufter(dam)
2008-2013	Construction of Maasvlakte 2
Maintenance dredging operations & nourishments	
1969-1985	Sand nourishments to strengthen the coast of Goerree
1973-1993	Sand nourishments to strengthen the coastline and dunes of Voorne
1983-now	Maintenance dredging Slijkgat channel
1991-2005	Slufterdam sand nourishments
1991	Dynamic Maintenance policy Voorne and Goerree
Haringvliet sluices policy	
1970-2018	Enabling river discharge regulation. Sluice capacity: 25.000 m^3/s
2018	Kierbesluit: partly open sluices, creating a brackish water zone in the Haringvliet

Figure 2.7: Overview main interventions around the Haringvliet (source: (Colina Alonso, 2018))

2.3. The Delta21 project and the RMD

The Delta21 project once again proposes significant changes to the delta region. This section of the report provides an overview of these proposed changes to get a grasp on the scope of the project and it's potential impact. The information in this section will be limited to the core components and operation of the project. For further information regarding the Delta21 project and it's details, please refer to the project's official website (https://www.delta21.nl/).

2.3.1. Delta21 project objectives

The main goal of the Delta21 project is to provide one integrated solution that addresses the future flood safety concerns of the Rhine-Meuse Delta, while also providing the region with a large scale energy-storage resource to aid in the green energy transition. The aim of the project is to achieve both these goals while limiting the environmental and ecological impact of the proposed measures. To achieve the listed main objectives, the Delta21 project proposal consists of the construction of four main elements:

1. **Valmeer**
   The Valmeer is a large scale water storage lake that will be constructed on the west-side of the Maasvlakte 2. The current design of the Valmeer has the following specifications:
   - Total storage capacity: $500 * 10^6 m3$
   - Valmeer bed level: $-27 mNAP$
   - Total surface area: $20 km^2$
2. **Pumping station**
   The pumping station will be located on the west side of the Valmeer. The station will have a maximum discharge capacity of 10000m3/s. The structure can also be used to generate energy by turbining water into the Valmeer during periods of high energy demand.
3. **Spillway**
   The spillway is located in the tidal lake on the south side of the Valmeer and will have a maximum discharge capacity of at least 10000m3/s. This structure can be used to let excess river water from the Haringvliet into the Valmeer.

4. **Storm-surge barrier ('New Haringvliet barrier')**
   The New Haringvliet barrier will be located between the coast of Goerree-Overflakkee and the Valmeer. This structure will protect the RMD against storm-surges while maintaining the ability for the Valmeer to be used as an additional buffer for river water.

The proposed layout of the elements is shown in fig. 2.8.

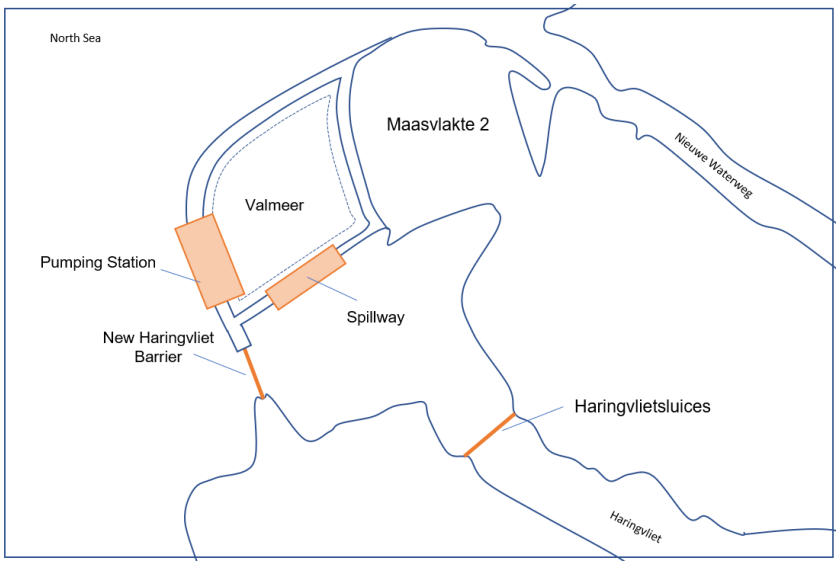

Figure 2.8: Overview of the proposed Delta21 infrastructure

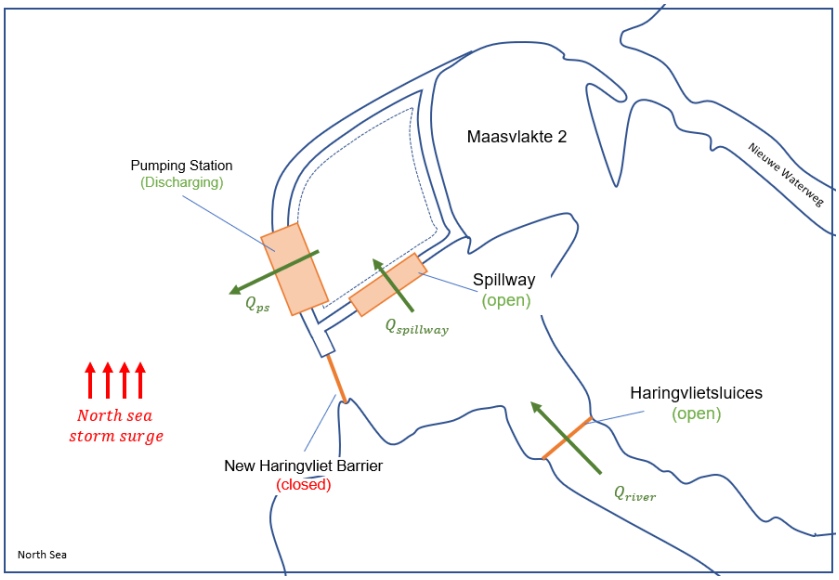

Figure 2.9: Operation of the Delta21 infrastructure during the combined occurrence of a storm surge on the North sea and a high river Rhine discharge. The New Haringvliet barrier will be closed to stop the storm surge, while the Haringvliet sluices and spillway are opened to allow for river water to flow into the Valmeer. The pumping station is used to simultaneously pump water out of the Valmeer.

Flood safety

The primary objective for the Delta21 project is to offer a solution for future flood safety in the RMD. The main flood safety scenario that Delta21 addresses is a situation where there is a simultaneous occurrence of a high river discharge ($Q_{rhine} > 5000 m^3/s$), and a storm-surge on the North Sea. During such a situation, the storm surge barriers along the Dutch coast will be closed to avoid flooding due to the ongoing surge. At the same time, the inland waterlevels will rapidly rise behind the closed barriers, which could cause river flooding in the RMD. Such a scenario occurring is expected to be increasingly likely, as sea levels, and extreme river discharge rates are expected to continue to increase in the future.

Delta21 addresses this scenario by the introduction of additional buffer capacity in the form of the Valmeer, as well as the ability to pump additional river water out of the RMD by use of the pumping station. fig. 2.9 gives an overview of the Delta21 infrastructure during the described flooding scenario. The project will allow for a reduction of necessary dike reinforcements that are currently being planned to account for this scenario. Delta21 claims that this will result in a net saving on the cost of flood safety measures in the region.

During regular conditions, the New Haringvliet barrier will continue to allow for the discharge of river water into the North sea through the Haringvliet, as well as a regular tidal exchange into the tidal lake. It will become the primary storm-surge barrier in the region.

Energy storage

The second objective of the Delta21 project will be to address some of the energy storage demands of the green energy transition. The transition from fossil fuels to more sustainable energy sources, such as solar and wind energy, is causing a large demand for energy storage resources that address the surges in energy supply and demand caused by the weather dependent nature of these energy sources.

The operation of the Delta21 infrastructure from a flood safety perspective is only expected to be required once every 2 to 5 years. During regular weather conditions the Valmeer and pumping station will thus be operated as a pumped hydroelectric storage lake (PHSL). During periods of high energy demand, the pumping station will be used to turbine water from the North sea into the Valmeer, generating energy. During periods of low demand the pumping station will use the excess energy to pump water out of the Valmeer into the North Sea.

Operation Haringvlietsluices

One still unanswered question in the Delta21 plan is the desired operational policy of the Haringvlietsluices once the project is completed. After the completion of the New Haringvliet barrier, the flood saftey function of the Haringvlietsluices will largely become redundant. The structure could still however be critical, in it's operation in regulating river run-off and maintaining a fresh water supply in the Haringvliet. An alternative option that is currently being strongly considered as part of the compensation measures of the Delta21 project, is the permanent reopening of the Haringvlietsluices. This measure would reintroduce a saline environment and tidal dynamics into the Haringvliet, restoring some of the lost estuarine ecosystems of old.

2.3.2. Preliminary impact assessment

The construction of the Delta21 infrastructure in the ebb-tidal delta will have profound effects on the Haringvliet tidal delta. To give insight into the important processes that are to be considered in the first design iterations of the New Haringvliet barrier, appendix A.1 gives additional information regarding the morphological behaviour of the tidal delta. Additionally, appendix A.1.1 presents a case study of the Eastern Scheldt barrier and it's impact on the Easternscheldt estuary. This will provide an idea of the potential impact of the construction of a new barrier in the Haringvliet delta. Using the information from these respective appendices, this section will give an overview of the various changes that are expected in the region related to the construction of the Delta21 project. The primary changes that will affect the state of the Haringvliet tidal delta are the following:

1. **Reopening of the Haringvlietsluices**
   Due to the closure of the Haringvliet for tidal flow in 1970, the wave driven sediment transport became a relatively more dominant morphological process, causing the net sedimentation of the tidal delta. Reopening the Haringvlietsluices would reintroduce a more significant cross-shore tidal flow, causing erosion of the current delta (fig. 2.10.1). However, due to the fact that the Haringvlietsluices have restricted the cross-section in the Haringvliet, it is expected that the delta will not erode to the same extent as it was prior to the construction of the sluices as the tidal exchange will still be less than prior to 1970 due to the restricted cross-section of the Haringvliet sluices compared to the original situation ($6000m^2$ instead of $17000m^2$). The additional restrictions due to the construction of the Valmeer and the New Haringvlietbarrier might further limit the tidal flow.

2. **Construction of the Valmeer**
   The Valmeer and the New Haringvliet barrier would block the majority of the incoming waves, strongly limiting the wave-driven sediment transport into the ebb tidal delta (fig. 2.10.2). At this point the tidal flow and river discharge will once again become important factors with regards to the sediment transport in the tidal delta, which will most likely cause more pronounced tidal channels in the inner delta once again.

3. **Construction of the New Haringvliet barrier**
   The last change that will impact the morphological behaviour of the tidal delta is the construction of the New Haringvliet barrier. The construction of the barrier is likely to affect the average tidal flow into and out of the the inner delta, which also impacts the amount of sediment transport across the barrier. Additionally, depending on the geometry of the barrier relative to the local hydraulic and morphological conditions, there is a possibility for the structure to affect the local sediment transport. In the case study of the Eastern Scheldt, it was found that the barrier became a sediment block, most likely due to the existence of a tidal asymmetry, which caused a residual current away from the tidal inlet. In the case of the New Haringvliet barrier, this is less likely as the barrier is also used as a river discharge outlet. However, it is important to note that the geometry of the barrier could potentially have a profound effect on the state of the inner tidal delta.

The sheltering of the inner delta from waves, the reintroduction of a cross-shore tidal flow, and three-dimensional flow effects related to the New Haringvliet barrier's geometry, will all impact the morphological behaviour of the inner delta. And even though it is qualitatively possible to evaluate each individual change and it's potential effect, it is unclear what the combined effect is of these measures, as well as what the effect is on specific locations such as the Hinderplaat and the Slikken van Voorne without a detailed assesment of the project, and the related conditions. These detailed considerations are out of the scope of this thesis and should be assessed in future research projects. As it pertains to the design of the New Haringvliet barrier, it will be assumed that maximizing the tidal opening of the barrier will provide the

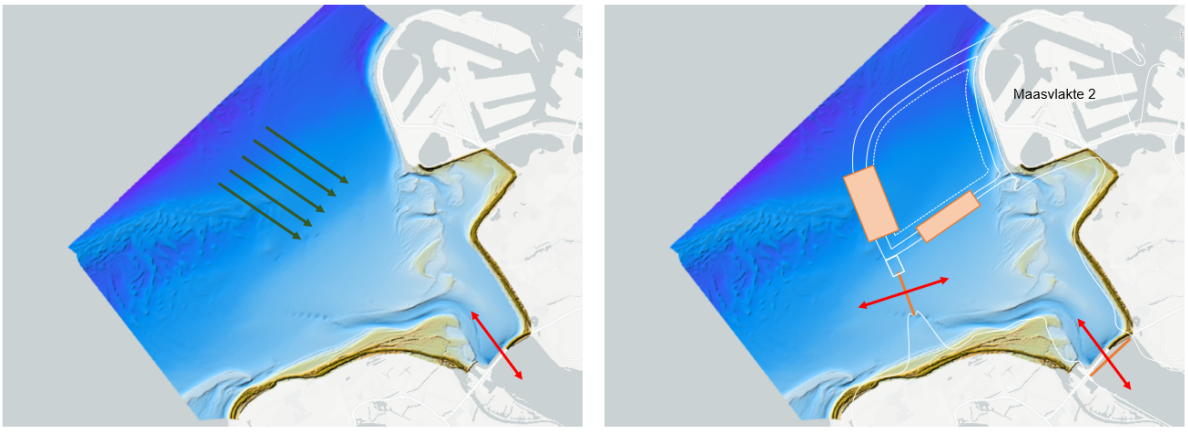

Figure 2.10: Schematic overview of the main hydrodynamic dynamics that are important with regards to sediment transport in the ebb tidal delta when considering the (1) reopening of the Haringvlietsluices and (2) the completion of the Delta21 project

3

Barrier Flood Safety

With flood-safety being the number one function of the Delta21 project and the New Haringvliet barrier, this chapter will evaluate the flood safety requirements for the new barrier. In order to get insight into the flood safety requirements of the barrier, the chapter starts of with a discussion of the Dutch flood management strategies in section 3.1, followed by an assessment of the location of the primary flood defenses in section 3.2. 3.3 offers a discussion of the different failure mechanisms that are considered in the dutch flood management strategy, and 3.4 evaluates how the Delta21 project can be included in the current flood safety approach. This last section leads to the calculation of the preliminary flood safety requirements of the New Haringvliet barrier.

3.1. Flood Risk Management Strategy

In the past, Dutch flood management strategies were based on water level exceedance frequencies. The exceedance frequencies were used to prescribe each dike-ring with a certain safety standard depending on the size of the area encompassed in the dike ring, the economic value of the region and the type of flooding that might occur (sea, river, lake). The current protection standard for all Dutch flood protection infrastructure has been in effect as of 1 January 2017, and is defined in the *'Wettelijk Beoordelings Instrumentatrium 2017'* (WBI2017). The current method includes a minimum safety level for each individual in the country in such a way that fatalities due to flooding in the Netherlands have a chance of occurring of 10^{-5} per individual per year. In order to achieve this, the WBI2017 specifies a **flooding probability** for each section of the primary coastal defence system of the Netherlands. Figure 3.2 shows an overview of the various sections of the primary coastal defense system in the RMD, and their corresponding maximum allowable flooding probability. The flooding probability in the WaterWet is defined as follows:

> *The probability for a flood defence element, to lose it's water retaining functionality, leading to flooding significant enough to cause fatalities (one or more) or significant economic damage.*

Structures, such as storm-surge barrier, that do not directly protect an area of land, but rather close of an estuary or another body of water, are considered as secondary barriers ('b-keringen') in the WBI2017. These barriers, rather than having a corresponding flooding probability, have a level of safety described in the form of a **failure probability**. Failure of these barriers does not directly lead to flooding of the hinterlands, but rather causes steep increases of the hydraulic loads on the coastal defences behind them. Therefor, barriers with a maximum of two gates, have a corresponding 'failure to close' probability, where other barriers with more gates such as the Eastern-Scheldt Barrier, and since more recently the Haringvlietsluices (this structure was reclassified as a storm surge barrier in 2018), have an corresponding failure probability derived from the consequences of various partial failure mechanisms.

In addition to the definition of the failure and flooding probabilities, it is important to note that the maximum

allowable flooding probability of a section as described in the WaterWet, or shown in fig. 3.2, is not dependant on the reliability of an individual flood defence element, but rather depends on the reliability of the whole section (Rijkswaterstaat, 2018). In some cases, mostly with the larger storm surge barriers, the section consists only of on individual structure. The flooding probability of a section is dependant on the probability that one of the elements in the section fails, therefor sections can also be described as a series system (Rijkswaterstaat, 2018). Rijkswaterstaat (2018) , and Deltares (2016) provide descriptions of the failure mechanisms that are to be considered during the design and validation of dikes and hydraulic structures as part of the WBI2017.

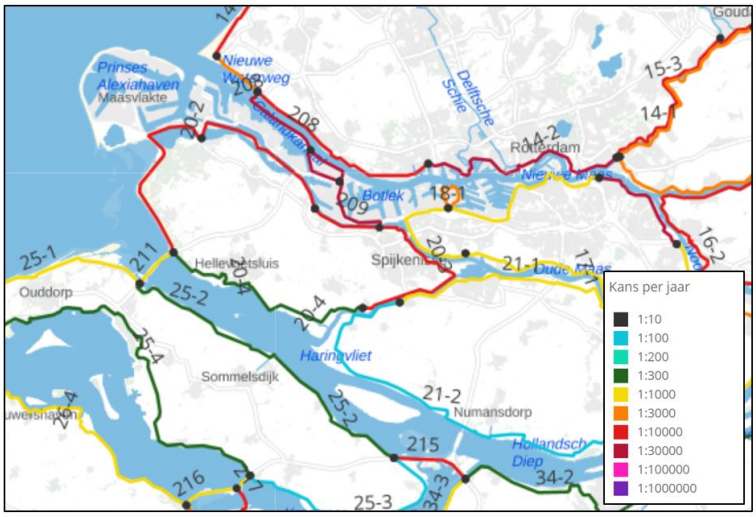

Figure 3.1: The maximum flooding probability of each section of primary coastal defence in the RMD (source: https://waterveiligheidsportaal.nl//home).

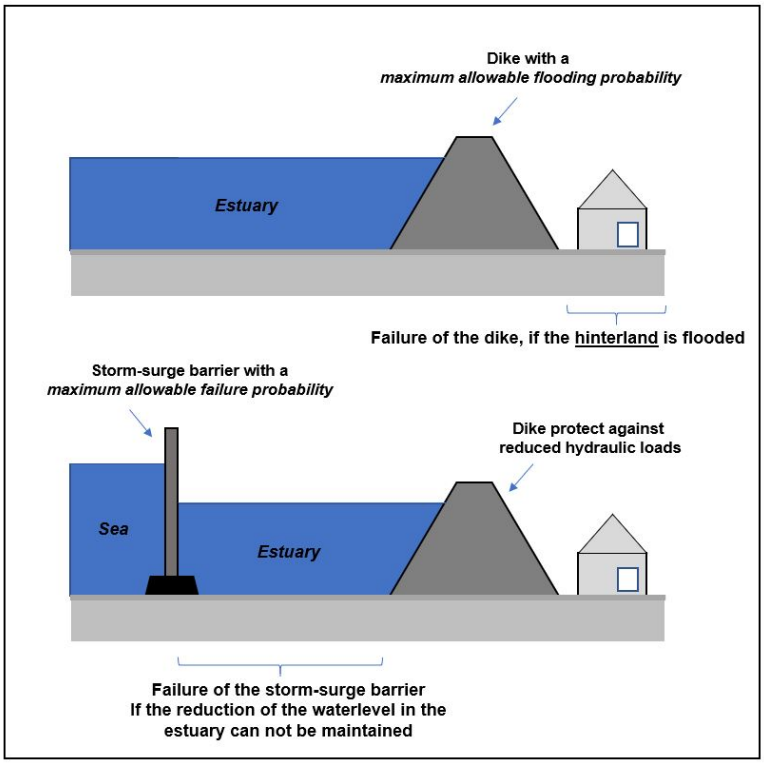

Figure 3.2: The maximum flooding probability of each section of primary coastal defence in the RMD (source: https://waterveiligheidsportaal.nl//home).

3.2. Location Primary Flood Defenses Delta21

The construction location of the Delta21 project, would warrant it to be classified as a part of the network of primary flood defenses along the Dutch coast. The Delta21 project gives two alternatives for the location of the primary flood defense line within the project (fig. 3.3). To give a clear overview of the configuration of the flood defences, the project can be divided into the following sections:

1. Pumping station and accompanying dune section (section 1)
2. New Haringvliet barrier and accompanying dune section (section 2)
3. Spillway and accompanying dune section (section 3)

Figure 3.3 gives an overview of the potential location of the primary flood defence line within the project. In the case of fig. 6.7a, where the primary flood defence layout contains sections #1 and #2, section #3 will have a secondary role with regards to water retaining capabilities of the system. The opposite is valid for the situation in fig. 6.7b, where the primary flood defence consists of sections #2 and #3.

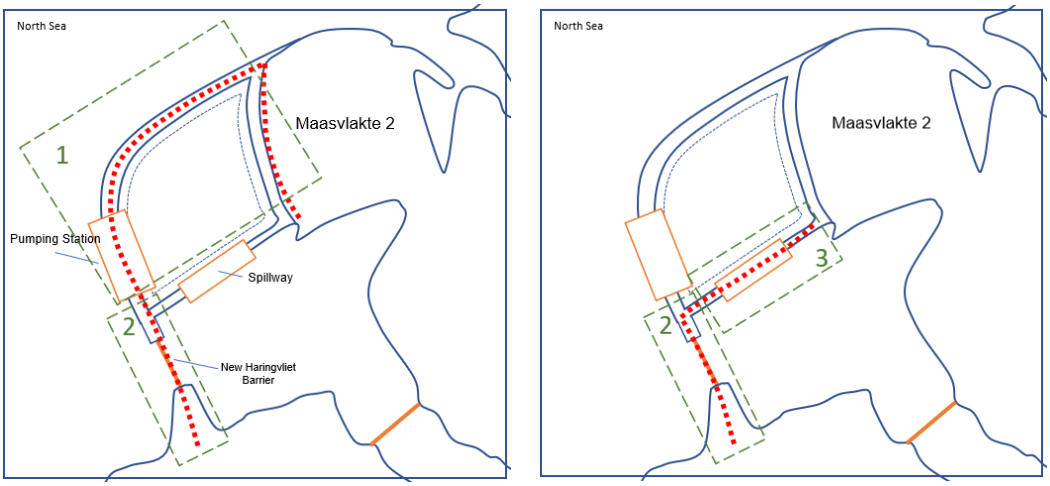

(a) Primary flood defence system option 1

(b) Primary flood defence system option 2

Figure 3.3: Potential configurations for the extension of the Dutch primary flood defense in the Delta21 project (red-dashed line).

The option to place the location of the primary flood defense line as seen in fig. 6.7b, would be quite similar to the current situation, where the Haringvlietbarrier acts as a water retaining structure. In this situation, the effectiveness of the pumping station, and the buffer capacity of the Valmeer during extreme storm surges can not be guaranteed and at most be considered a bonus. However, given the large economic interest in the Valmeer, frequent failure of the dune ring around the lake will be undesirable and a critical design consideration for the plan. There will already be a need for significant flood safety requirements for the Valmeer, in order to guarantee the energy storage operation of the Delta21 project. Therefor the option presented in fig. 6.7a seems like the better option, as it will make the entire Delta21 infrastructure more resilient to extreme storm scenarios, while most likely only being a small increase of the already significant safety requirements for the dunes. The in this case, the inclusion of a significantly high flood safety standard for section #3 would provide the system with a lot of redundancy that will bye required to compensate for the significant increase in length for the section compared to the current entrance of the Haringvliet estuary, the Haringvlietsluices.

3.3. Failure Mechanisms

The failure mechanisms for storm surge barriers can be divided into two categories: failure mechanism related to the structural (gated) sections, and the failure mechanisms related to the dike section. This section will outline the failure mechanism for both respectively, followed by a discussion for the allotted failure probability to each failure mechanism for an entire section in section 3.3.3. The failure mechanisms described in this section are in accordance with the WBI2017 as presented in the documents:

- *Werkwijzer Ontwerpen Waterkerende Kunstwerken – Ontwerpverificaties voor de hoogwatersituatie* (Rijkswaterstaat, 2018)
- *Fenomenologische beschrijving Faalmechanismen WTI* (Deltares, 2016).

3.3.1. Structural failure

For the safety assessment of water retaining structures the following four failure mechanisms have to be considered:

- Overflow and/or Over-topping
- Piping
- Structural failure
- Failure to close

These failure mechanism can cause system failure in a variety of ways. In the case of storm-surge barriers, failure is defined as the failure of the barrier to retain water to the point that a certain critical water level is reached in the hinterlands. This allows for the distinction between two different failure modes for flood defenses. Firstly, structural failure, in the case that an excessive hydraulic load leads to a breach in the flood defence. or secondly, a functional failure, where the water retaining capabilities of a structure are simply exceeded (e.g excessive overtopping without structural failure).

Figure 3.4: Failure mechanisms of water retaining systems from left to right: overtopping/overflow, failure to close, piping, structural failure.

3.3.2. Dike failure

Dikes have different failure mechanisms than structures, the main failure mechanisms to consider in this aspect are the following:

- Overflow and/or overtopping
- Bursting and piping
- Macro- instability (either on the inward or outward slope)
- Erosion of the revetment

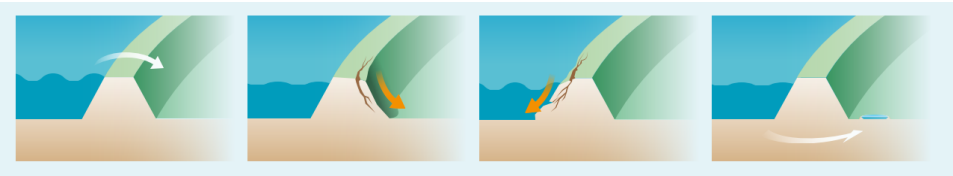

Figure 3.5: Failure mechanisms of dike from left to right: overtopping/overflow, failure of the inner slope, failure of the outer slope, piping.

3.3.3. Determining the reliability of flood defense structures

The failure and flooding probabilities as stated in the WBI2017 are valid for sections of the Dutch primary flood defense system, rather than individual elements or structures (Rijkswaterstaat, 2018). Such a section can be considered as a series- system, meaning that if a part if the section fails, the whole system fails (Jonkman et al., 2016). In order to determine the reliability of individual flood defence elements or structures along a given flood defense section, it is usefull to determine evaluate the fault tree for the given section. The framework of a fault tree, that would be used in a flood safety assessment conform to WBI2017 standards, is shown in fig. 3.6.

From a mathematical point of view, the failure probabilities of various elements of a flood protection standard is formulated in eq. (3.1) (Rijkswaterstaat, 2018). The length factor in the equation accounts for the fact that that it is more likely that a structure fails at one specific location, rather than as a whole. And thus adding the length factor allows for the safety assessment of various components of the overall flood defense section.

$$P_{req,element} = \frac{P_{req}}{N} = \frac{P_{max} * \omega}{N} \tag{3.1}$$

where:

$P_{req,element}$	= failure probability requirement for a specific failure mechanism for an individual flood protection structures per year	[−]
P_{req}	= failure probability of the considered failure mechanism for a flood protection section per year	[−]
P_{max}	= maximum allowable flooding/failure probability of a flood protection section per year	[−]
ω	= failure probability factor (table 3.1)	[−]
N	= length factor	[−]

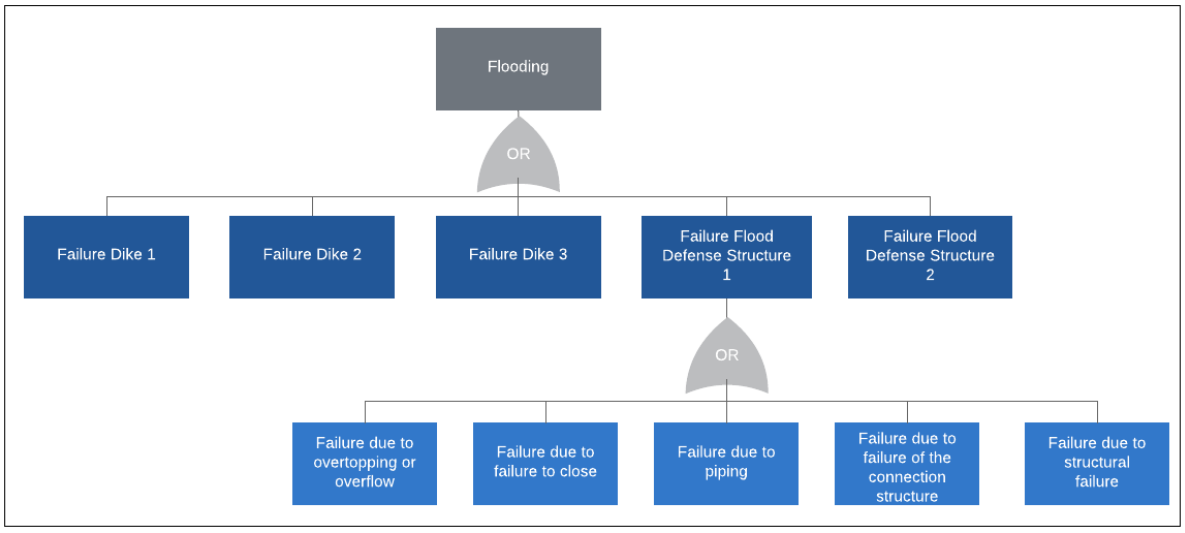

Figure 3.6: Example of a Fault Tree for a series section as defined in the WaterWet (Adapted from:(Rijkswaterstaat, 2018))

Failure Budget Distribution

For a complete flood defence section the WBI2017 prescribes a default failure probability distribution, which is a recommendation for the distribution of the failure probability over the various failure mechanisms for all the flood defense elements in the section (see table 3.1). The default failure probabilities are only a recommendation, and thus changes to the distribution are allowed.

Type of flood defense	Failure mechanism	Sandy coast	Other (dikes)
Dike or structure	Overflow or overtopping	0%	24%
Dike	Bursting and piping	0%	24%
	Macroinstability	0%	4%
	Revetment damage and erosion	0%	10%
Structure	Failure to close	0%	4%
	Piping	0%	2%
	Structural failure	0%	2%
Dune	Dune erosion	70%	0% (10%)
Other		30%	30% (20%)
Total		**100%**	**100%**

Table 3.1: Default failure budget from the WBI2017 (Adapted from Rijkswaterstaat (2018))

3.4. Delta21 Flood Safety

The standard failure mechanisms that the primary flood defenses are designed to withstand, all have to do with maintaining the water retaining capabilities of a structure, or a section. The Delta21 project consists of a total of four civil elements that play a role in the overall flood-safety function the project: the storm-surge barrier, the spillway, the pumping station, and the dunes/Valmeer. As a whole, the project offers a total of three different flood safety functions:

- Storage capacity: Valmeer
- Water retaining capabilities: dunes, pumping stations, spillway, and the storm-surge barrier
- Discharge capacity: pumping station, and spillway

The design of these various elements are not necessarily separate tasks, as the design of each element influences the required reliability for the next element of the overall system. This report, mainly focuses the design of the storm-surge barrier, but in order to do so, the function and reliability of the other elements in the system are also important factors. Given the background information on the WBI2017 and the design of flood defenses in the previous section allows for the assessment of the Delta21 project in more detail. This part of the report will schematize and evaluate the various flood safety elements of the project.

For the schematization of the Delta21 project, the distinction within this report will be made between:

- Water retaining infrastructure
- Water discharging infrastructure

The water retaining infrastructure, and it's impact on flood defenses, can be described by the current WBI2017 and includes: the outer dike sections, the storm-surge barrier and the water retaining function of the pumping-station. An overview of the situation can be seen in fig. 3.7 indicated by the red line. The water discharging infrastructure, consists of the pumping-station and the spillway. These are indicated in green in fig. 3.7. The additional storage capacity of the Valmeer, is not included in this evaluation at first.

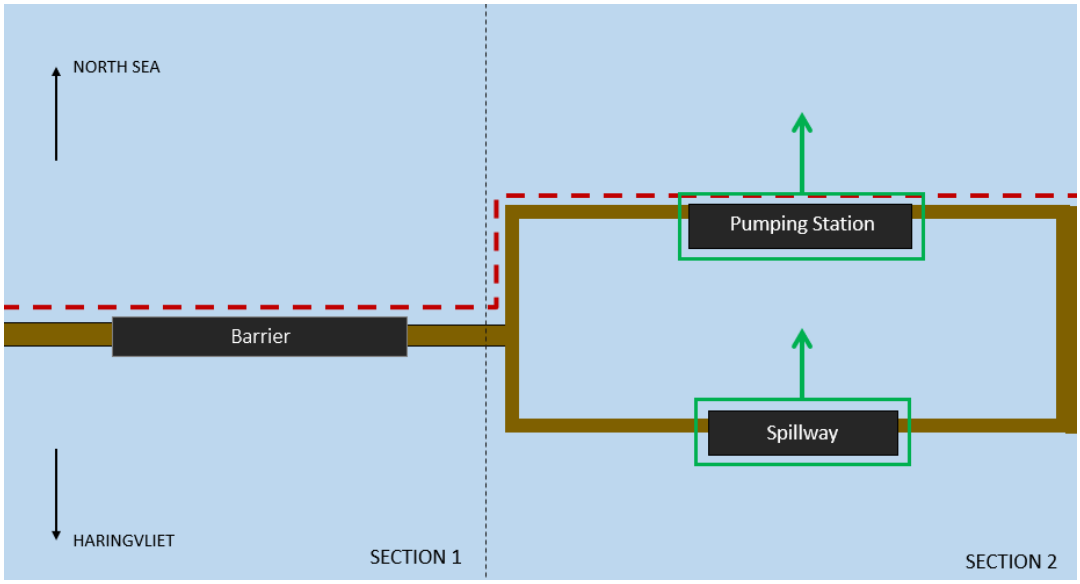

Figure 3.7: Delta21 Flood safety infrastructure overview. With the water retaining infrastructure indicated along the red line, and the water discharge infrastructure indicated in green

At first, in this system, we can evaluate the required safety of the water retaining infrastructure according to the standard set by the WBI2017. This leads to the fault tree as seen in fig. 3.8. It is important to note that flooding due to the potential exceedance of the basin storage capacity behind the barriers during a storm-surge event is not included in the flood safety assessment as, currently, the chance of it happening is very small relative to the maximum allowable flooding probability of a section.

In the future however, it is expected that this scenario will reach a significant probability of occurrence, and in that case, the water discharging infrastructure will become of greater overall importance to the flood safety assessment in the region. For the Delta21 project, or the safety evaluation could be assessed using a fault tree as seen in fig. 3.9. From the fault tree in fig. 3.9, certain observations can be made. Firstly, if there is no high river discharge, in this case from the Rhine and Meuse, the pumping function of the Delta21 project is not needed, and the probability of failure of the system, through failure of the water discharge infrastructure is equal to zero.

Secondly, in the scenario of a high river discharge, the functioning of the discharge infrastructure is conditional on the successful functioning of the retaining infrastructure. If the water retaining infrastructure was to fail, generally speaking in this safety assessment it is assumed that the discharge infrastructure will also be ineffective in preventing a flood.

Lastly, the probability that high river discharges occur during a storm surge, is an actual probability, rather than a failure mechanism that has to be designed for, but it is dependant on the available basin storage capacity for the project region. In this case, the basin capacity would include the Haringvliet, Hollandsche Diep and the Valmeer. Currently, within the Delta21 project, a high river discharge is considered any river Rhine discharge larger than $5000 m^3/s$. The weight of the safety budget allotted to ensuring the successful operation of the water discharge infrastructure, will depend on the probability of the 'high river discharge' scenario occurring. From a qualitative point of view, the failure probability for discharge infrastructure can be compared to the 'failure to close' failure mechanism of a storm-surge barrier, from the perspective that, the reliability is more related to the frequency of occurrence of this scenario the magnitude of a storm with a certain return period. This is also the reason why, the discharge infrastructure might be able to provide some redundancy to the failure to close mechanism.

3.5. New Haringvliet barrier flood-safety requirements

Conclusively, it is important to consider the design failure probability for the New Haringvliet barrier. From the analysis of the Delta21 flood safety operation given in section 3.4, it is concluded that the water discharging infrastructure does not affect the water retaining flood safety requirements for the New Haringvliet barrier. The use of the additional Delta21 elements, should be considered as a contingency plan for the barrier, rather than a replacement for its the water retaining capabilities. For example, in the case of a failure to close, or excessive overtopping, the Valmeer and the spillway could potentially offer additional buffer capacity for the system. However, at this point of the design it is best to consider this as an back-up considering that the use of the Valmeer comes at a cost as well.

Therefor, to determine the design flood safety requirements for the barrier, the entire section from the coast of Goerree-Overflakke was assigned the same flood safety requirement as is currently allotted to section 211 (the Haringvlietsluices). An application of the standard failure budget as shown in section 3.3.3 yields **an overall maximum allowable failure probability for the New Haringvliet barrier of 1.6e-4 per year** (see fig. 3.8).

Due to the uncertainty regarding the future operation of the Haringvlietsluices, these will also not be included in the consideration of the flood safety requirements of this system. This, will most likely lead to a conservative estimate for the flood safety requirements of the barrier at this point. In future studies, the cost benefit of more optimized barrier designs should be considered.

3.6. Conclusions

In this chapter the design flood safety requirements for the New Haringvliet barrier are determined. In addition, the flood safety aspects of the Delta21 project and how they relate to the dutch flood safety management were evaluated. The first main takeaway from this chapter is the location of the primary flood defenses. The primary flood defense 'line' so to speak is most likely preferably along the outside edge of the Valmeer and it's components. If the Valmeer was to become a core component of the Dutch flood defense system, it's integrity should also be guaranteed during extreme storm events.

The second takeaway is the incorporation of the Delta21 project into the current WBI fault tree's. Currently, all the failure mechanisms in the fault tree describe the failure of water retaining infrastructure. In the case that the occurrence of high river discharge In conjunction with a large North sea storm become more frequent, the fault trees will also have to incorporate the potential failure of the water discharging infrastructure. It is recommended that a future study assess the different failure mechanisms related to the failure of the Valmeer, the spillway, and the pumping station to get a clear overview of all the important flood safety design considerations for the Delta21 project.

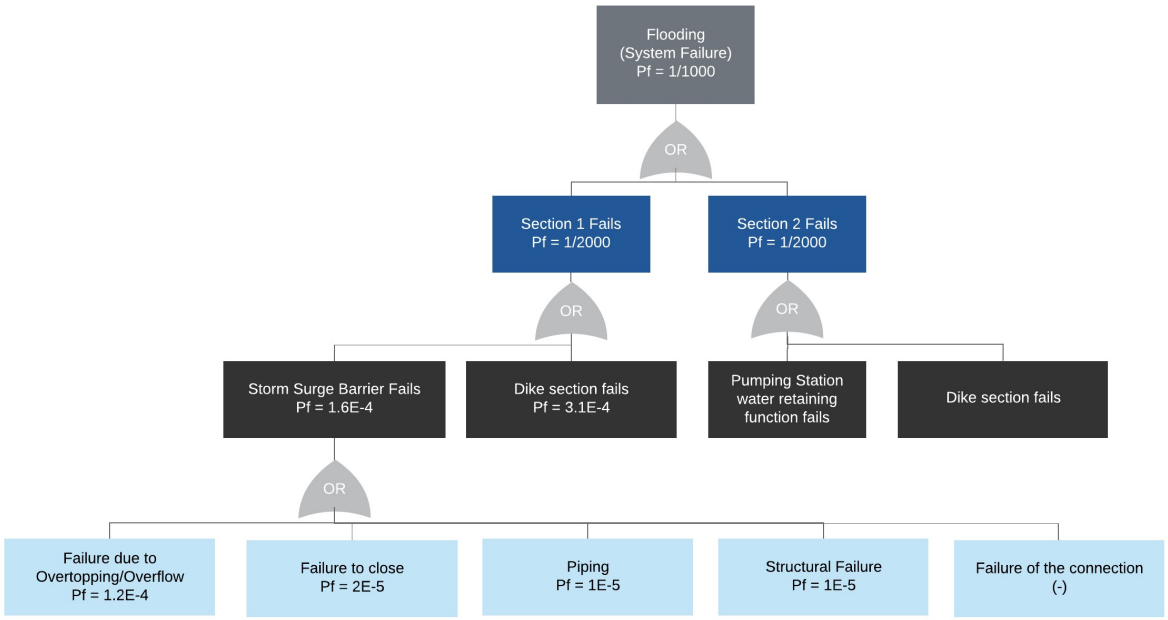

Figure 3.8: Fault tree for the water retaining infrastructure of the Delta21 project according to the WBI2017

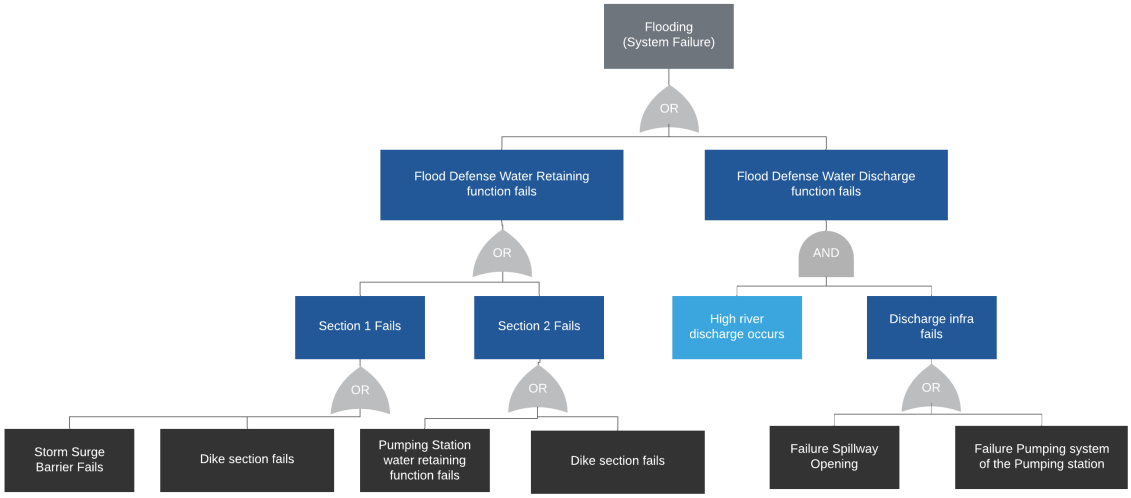

Figure 3.9: Proposed fault tree for the full Delta21 project

4

Functional requirements and boundary conditions

In this chapter the functional requirements and the boundary conditions of the New Haringvliet project are defined. This chapter will form the basis for the design phases of the project.

4.1. Programme of functional requirements

The programme of functional requirements will be described in two different categories, the functional requirements and the aspect requirements. The functional requirements of the project will describes the desired behaviour and performance of the system, while the aspect requirements will provide an overview of the specific characteristics of the system that supports the primary functioning of the system (Molenaar & Voorendt, 2019). It should be noted that some of the functional requirements are limited in detail, as one of the primary aspects of this project is to explore the possible alternatives and solutions for the tidal opening. Having very strict requirements at this state of the project, would limit the possible solutions that could be evaluated by stakeholders.

4.1.1. Functional Requirements

The functional requirements of the project are defined as follows:

- The structure should protect the hinterland from flooding due to storm events on the North Sea.
  - The maximum required failure probability for the storm-surge barrier is set to be $1.6 * 10^{-4}$ (determined in section 3.5)
- There should be sufficient tidal exchange between the North sea and the Haringvliet ETD and the Haringvliet.
  - The tidal opening in the New Haringvliet barrier should be large enough to maintain a tidal range similar to what currently exists in the Haringlvliet ETD.
  - Assuming the permanent reopening of the Haringvlietsluices, the tidal opening in the New Haringvliet barrier should be large enough to reintroduce a significant tidal range to the Haringvliet.
- Discharge river water up to discharge rates of $25.000 m^3/s$. This is the same requirement that is currently used for the Haringvlietsluices.
- Provide a navigational option to allow for sailing access between the North Sea and the Haringvliet.

4.1.2. Aspect Requirements

For the aspect requirements, a total of four different categories were identified that are currently relevant with regards to the project. These are sustainability, construction, maintenance and durability. Under these categories the following requirements were defined:

- Sustainability
  - Emmissions should be kept to a minimum during construction and operation of the structure.
  - No soil pollution is allowed during the construction and operation of the structure.
  - The construction process should have minimal direct impact on important Natura2000 areas (Hinderplaat, Garnalenplaat, Slikken van Voorne).
- Construction
  - Sufficient river run-off should be maintained during the construction of the barrier.
  - There should be limited impact on the tidal exchange between the Haringvliet tidal delta and the North Sea during the construction of the structure.
- Maintenance
  - Maintenance of the structure should have minimal impact on the structure's functional. requirements.
- Durability
  - The barrier should be able to suffice up to a SLR of 1m. (see section 4.2.4)

4.2. Boundary Conditions

This section of the report outlines the various boundary conditions that are applicable to the design of the new Haringvliet barrier, and further analysis in this project.

4.2.1. Bathymetry

The bathymetry of the Haringvliet tidal delta is characterised by a series of long-shore tidal flats, such as the Hinderplaat and the Garnalenplaat, that were partly a result of the construction of the Haringvlietsluices. The construction of the sluices strongly limited the amount of cross-shore tidal exchange that was possible in the region. The tidal delta is not yet in a morphological equilibrium (Colina Alonso, 2018), and thus in the design of the new barrier, various morphological dynamics for the region should be considered carefully. A more in-depth analysis of the bathymetry, and its expected morphodynamic behaviour, with regards to the design of the new barrier can be found in appendix A.1.

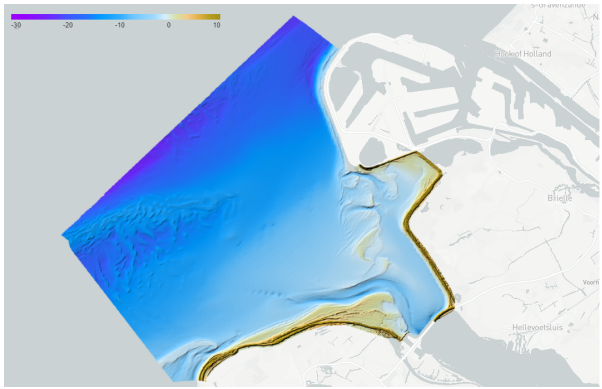

Figure 4.1: The bathymetry from the Haringvliet tidal delta (2015) based on the Vaklodingen dataset (Source: https://www.openearth.nl/coastviewer-static//)

4.2.2. Hydraulic conditions

For the hydraulic boundary conditions HydraNL was used. HydraNL is a probabilistic model that calculates the statistics related to the hydraulic loads on primary flood defences in the Netherlands, and is also part of the WBI2017.

Water level
The expected water levels and their return periods can be found in table 4.1. These values also include 1.0m of SLR, the choice for this amount of SLR is further detailed in section 4.2.4. The water levels represent the respective peak values of the various possible storm events. To determine the actual time dependent behaviour of such a storm, the vertical tide at the location, and the time-dependent behaviour of the storm have to be summed as shown in fig. 4.2.

Return period [years]	100	300	1000	3000	10000	100000
Waterlevel [m +NAP]	4.99	5.31	5.68	6.03	6.43	7.22

Table 4.1: The return period of the normatively expected water levels at the project location, includes the expected 1m of SLR

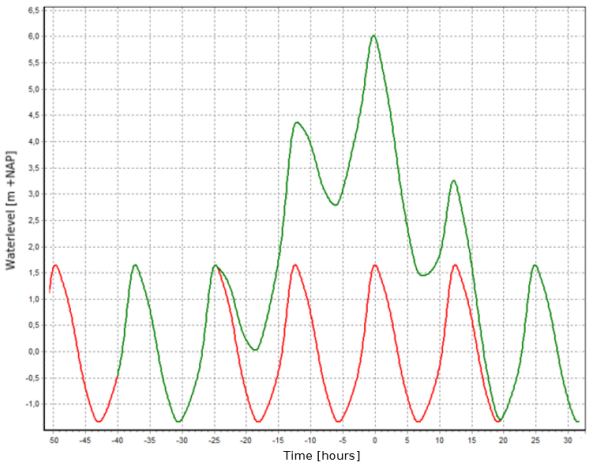

Figure 4.2: The progression of a storm with an expected return period of 3000 years

Waves
The local bathymetry of the delta region plays a large role in several near-shore wave characteristics, such as depth-induced breaking and potential wave-setup. Approximating the wave height using HydraNL could therefor seem to be inaccurate. The waterdepth of the current location is expected to increase as a result of the changes proposed in the Delta21 plan. As a result, due to the depth-limited wave behaviour at the location, the maximum possible wave height is expected to increase. Additionally, the Valmeer will effectively shelter the barrier from waves from a North and North-Western directions further altering the expected wave conditions in the region. Therefore, an extreme value analysis for the waves in the region was done, and SwanOne was used for the near-shore transformation towards the proposed barrier location. The full evaluation of the extreme wave statistics used in this project can be found in appendix B. The final design wave conditions are presented in table 4.2.

Return period [years]	100	300	1000	3000	10000	100000
H_s	2.9	3.06	3.26	3.44	3.62	3.96
T_{m0}	5.35	5.42	5.55	5.58	5.66	5.78

Table 4.2: The return period of the normatively wave conditions at the project location

4.2.3. Geotechnical conditions

The soil profile in the Haringvliet tidal delta mainly consists of sand throughout the depth of 70m NAP (fig. 4.3). Further analysis of CPT measurements in the region indicates that at a depth of around 20m, there is a clay layer of roughly 3m thick. Below a depth of -25m the cone resistance of the CPT's that were considered showed significantly more cone resistance than the more upper sand layers.

The borehole information provided does not include any indication of the depth relative to the waterlevel, and thus the soil model shown in fig. 4.3 is mainly based of of the CPT data for the location.

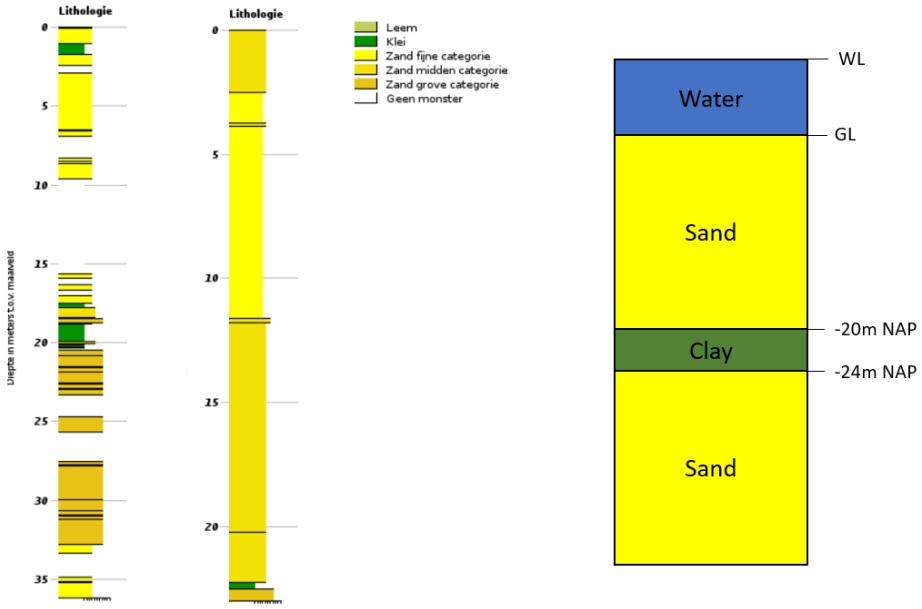

Figure 4.3: Borehole model for the construction location (source: https://www.dinoloket.nl/ondergrondgegevens) and a model for the subsoil to be used in the design of the structure

4.2.4. Sea level rise

Sea level rise (SLR) is an important consideration when designing a storm surge barrier. The functionality of storm surge barriers mainly comes down to their ability to close, their overall strength and stability, and their water retaining capabilities (Haasnoot et al., 2018). SLR has a direct impact on all three of these factors, and can often determine the lifespan of a barrier. Currently there is no general consensus on the degree of sea level rise we can expect in the future. Figure 4.4 presents an overview of all currently considered SLR scenarios, including the Deltascenario's, as well as the newer scenario's that consider a potential acceleration of SLR.

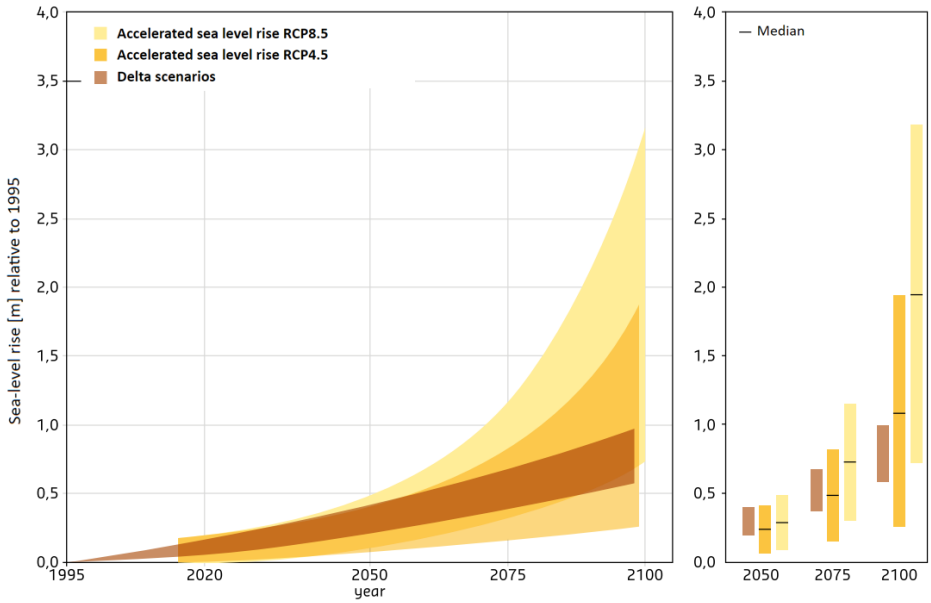

Figure 4.4: Range of SLR scenarios (Haasnoot et al. (2018))

For the design of the New Haringvliet barrier in this project, a sea-level rise of +1.0m will be considered. The reason for this decisions is twofold:

- Currently, according to the Deltascenario's, which are still the most commonly used design guideline, it is not expected that the SLR will exceed +1m before 2100.
- Secondly, designing a barrier for very large levels of SLR (> 1.5m) in a vacuum will not result in an effective barrier. Haasnoot et al. (2018) shows that for a SLR of +1.1m, the Eastern Scheldt barrier would be required to close roughly 100 times per year. If the amount of SLR increases even further (> 1.3m), the barrier would have to be closed year-round. This scenario can only be improved given that the inland dikes will be raised accordingly. Given that doing so is in direct contradiction with the main objective of the Delta21 project, and it is currently unclear what the objective for the inland dikes is, the design SLR value in this thesis is limited to +1m NAP.

4.2.5. Natura2000

One major consideration for the Delta21 project is the fact that the Haringvliet tidal delta, the proposed location for the plan, is a designated Natura2000 habitat. Natura2000 is a network of European designated nature reserve areas that aim to protect core areas for species and habitat types that are deemed of importance to Europe. New activities, especially those on the scale of a construction project such as the Delta21 project, are therefore scrutinized to ensure that their ecological impact is in- line with the goals of the Natura2000 area.

Therefore projects that are thought to have a considerable impact on a Natura2000 site undergo an assessment into their impact on the conservation objectives of the respective Natura2000 area. If a project is found to negatively affect the Natura2000 area, it will be necessary to present a contingency plan, including either detailed mitigation or compensation efforts of the project that are related to specifically the Natura2000 region in question.

A detailed analysis of the ecological impact of the Delta21 project is out of the scope of this project, however due to the importance of this boundary condition for the project, the sustainability, and potential impact of the various alternatives for the project should be strongly considered at all stages of the design process.

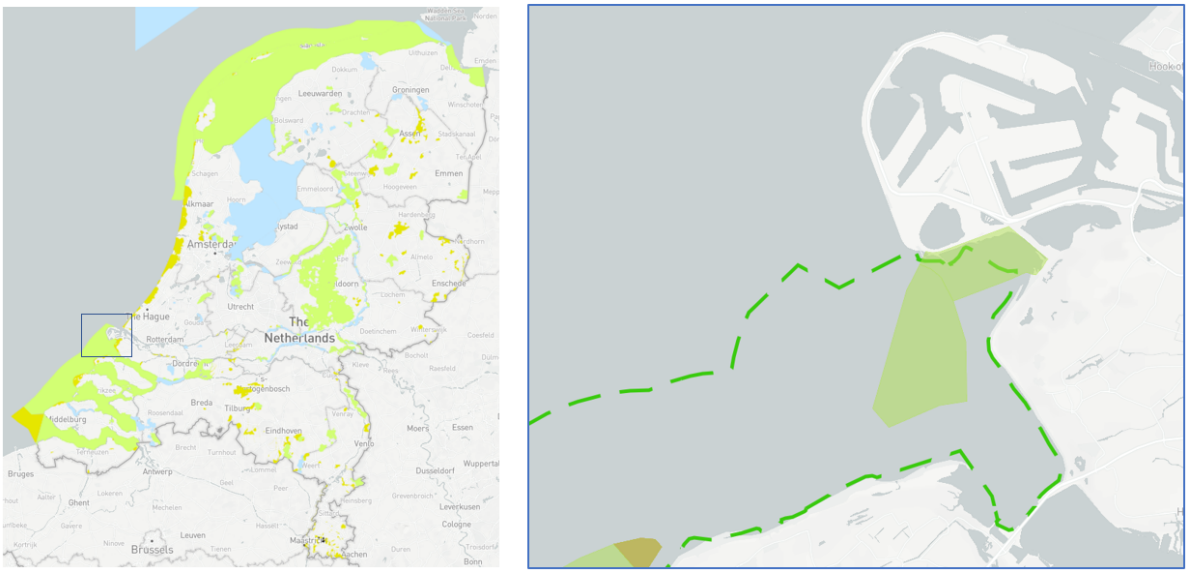

Figure 4.5: Overview of the Natura2000 areas of the Dutch coast (a), and designated rest areas for birds and seals (indicated in green marked areas) and bottom protected areas (surrounded by green dashed line) in the Haringvliet tidal delta (b). (Source: https://www.openearth.nl/coastviewer-static//)

5

Barrier Tidal Opening

In this chapter the effective cross-section of the tidal opening in the New Haringvliet barrier will be evaluated. The size of the barrier's tidal opening is an important design factor as it's choice has a large impact on a multitude of hydrological and morphological processes in the overall region. In order to make a design decision for the barrier's tidal opening, firstly a hydrodynamic assessment of the situation will be given in section 5.1. The aim of this assessment is to gain a first insight into the impact, the size of the tidal opening has on the hydrodynamics in the Haringvliet and Hollandsche Diep (HV/HD), and in the tidal lake (currently the Haringvliet Ebb-Tidal Delta). Following the hydrodynamic assessment of the barrier, several different design alternatives will be formulated in section 5.2. Lastly, a choice is made between the design alternatives for the design tidal opening of the New Haringvliet barrier (section 5.2.4), followed by a discussion of the findings of this chapter and recommendations for further research related to this topic (section 5.3).

5.1. Hydrodynamic assessment

The model used for the hydrodynamic assessment consists of the coupling of an storage basin model, and a 1D channel model. The considered domain is shown in fig. 5.1. The model is used to emulate the behaviour of a system such as the Haringvliet in order to be able to quickly evaluate the impact of various design considerations that are part of the Delta21 project. The main design parameters that will be considered are:

- The tidal opening in the New Haringvliet barrier
- The degree of reopening of the Haringvlietsluices ('kierbesluit' versus complete reopening)

These design parameters will then be evaluated by determining their respective impact on the expected tidal range in the tidal lake, the expected tidal range in the HV/HD, and the performance of the system during high river flood waves. For this purpose a total of four different scenarios were formulated that will be assessed throughout this chapter, an overview of the scenarios is given in table 5.1. The base scenario, will be used as a basis of comparison to evaluate the other scenarios.

5.1.1. Model Setup

For the hydrodynamic assessment of the New Haringvliet barrier, a model was constructed by coupling a storage basin model and an one-dimensional channel model. In this model, the storage basin model was used to emulate the behaviour of the tidal lake, whereas the one-dimensional channel model was constructed to act as the HV/HD section of the model. A short description of the characteristics of the models is given below, a more in depth explanation of the construction of the model is given in appendix C.2.

Figure 5.1: Domain for the hydrodynamic assessment of the barrier. With the tidal lake, located between the New Haringvliet barrier (NHVB) and the Haringvlietsluices (HVS). And the HV/HD channel that reaches from the HVS to the Dortsche Kill.

Scenario	NHVB construction	HVS operational policy	River discharge	Report section
Base	No	Storm surge barrier	Normal	Appendix C.2.4
Scenario 1	Yes	Kierbesluit	Normal	Section 5.1.4
Scenario 2	Yes	Storm surge barrier	Normal	Section 5.1.5
Scenario 3	Yes	-	High	Section 5.1.6

Table 5.1: Scenarios for hydrodynamic assessment

Tidal lake (storage-basin model)

The storage-basin model works using a short-basin approximation. In the case that the length dimension (l) of a basin is small relative to the wavelength of the present tidal wave, phase differences in the basin can be neglected. Indicating a constant surface level elevation across the basin. This means that the tidal lake effectively only has a storage function and it's waterlevel is directly dependent on the incoming and outgoing discharges through the respective barriers (see eq. (5.1)).

$$\frac{d\zeta_2}{dt} A_{b2} = Q_1 - Q_2 \tag{5.1}$$

where:

$\frac{d\zeta_2}{dt}$ = rate of water level elevation change in the tidal lake $[m/s]$
A_{b2} = surface area of the tidal lake $[m^2]$
Q_1 = discharge rate through the New Haringvliet barrier $[m^3/s]$
Q_2 = discharge rate through the Haringvlietsluices $[m^3/s]$

Haringvliet - Hollandsche Diep (1D channel model)

The short basin approximation is not valid for the Haringvliet-Hollandsche Diep. Therefor, this section of the system is modelled as a channel with an exponentially decreasing cross-section and a length of 43km. The model will function by the repeated execution of the shallow water wave equations: the continuity equation (eq. (5.2)), and the momentum equation (eq. (5.3)). As it is a simplified model,the effect of the Spui is not explicitly considered in the model. The Dortsche Kill was left outside of the domain of the model, therefor it

allows for the indirect inclusion of it's impact, as the upstream discharge for the barrier can simply be changed to account for difference discharge distributions between the Dortsche kill and the HV/HD.

$$B\frac{\partial h}{\partial t}+\frac{\partial Q}{\partial s}=0 \tag{5.2}$$

$$\frac{\partial Q}{\partial t}+\frac{\partial}{\partial s}(\frac{Q^2}{A_c})+gA_c\frac{\partial h}{\partial s}+c_f\frac{|Q|Q}{A_cR}=0 \tag{5.3}$$

5.1.2. Boundary conditions

The flow through both barrier's is considered to be quasi-steady, meaning that a waterlevel difference across the barrier will cause an immediate response of the discharge at the structure. The amount of discharge through each barrier is calculated by the discharge relation (eq. (5.4)). The discharge was determined to be negative in cases that the upstream waterlevel was higher than the downstream waterlevel. The subscript 1 and 2 in the equation indicate the NHVB and the HVS respectively.

$$Q_{1,2}=\pm C_d A_{c1,2}\sqrt{2g\Delta h_{1,2}} \tag{5.4}$$

where:

Q	= discharge rate through a barrier	$[m^3/s]$
C_d	= discharge coefficient (assumed 0.7)	$[-]$
A_c	= barrier effective wet cross-section	$[m^2]$
Δh	= head difference over the barrier	$[m]$

Downstream boundary

The average tide on the North Sea was used as the downstream boundary condition. The tide was schematized using a skewed sine function with a tidal range of 2.35m and period of $T = 44700s$ (fig. 5.2). This signal was determined based on an analysis of the local tidal characteristics including the MHW (+1.36m NAP), MLW (-0.98m NAP), and the average tidal water level in the Haringvliet ebb-tidal delta.

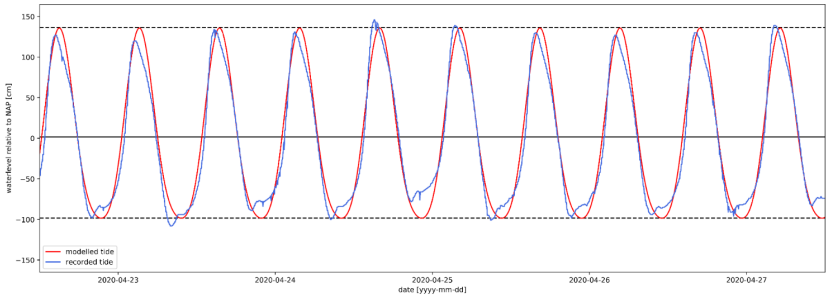

Figure 5.2: Modelled water level on the North Sea, compared to the recorded tide between 22/04/2020 and 27/04/2020

Upstream boundary

For the upstream boundary condition a Riemann boundary is imposed. This boundary is meant to allow waves from within the domain to pass through the boundary undisturbed.

$$Q_3=Q_{3,0}+(Bc)_3\,(h_3-h_{3,0}) \tag{5.5}$$

where:

Q_3	= discharge rate at the upstream boundary	$[m^3/s]$
h_3	= waterlevel at the upstream boundary	$[m]$
B	= channel width at upstream boundary	$[m]$
c	= wave velocity at upstream boundary	$[m/s]$
$Q_{3,0}$	= undisturbed discharge rate at the upstream boundary	$[m^3/s]$
$h_{3,0}$	= undisturbed waterlevel at the upstream boundary	$[m]$

The exact values of the undisturbed situations differ depending on the scenario that was used in the computation of the project, see appendix C.2 for more information regarding the upstream boundary condition values.

5.1.3. Base scenario

The response of the one dimensional channel model was evaluated independently (base scenario) and discussed in detail in appendix C.2.4. The base scenrario evaluates the tidal response in the channel in the case that the Haringvlietsluices would be completely reopened. Figure 5.3 and fig. 5.4 show the resulting maximum and minimum waterlevels, and discharges through the channel respectively. Near the Haringvlietsluices, the tidal range is largest, with increasing dampening along the length of the channel.

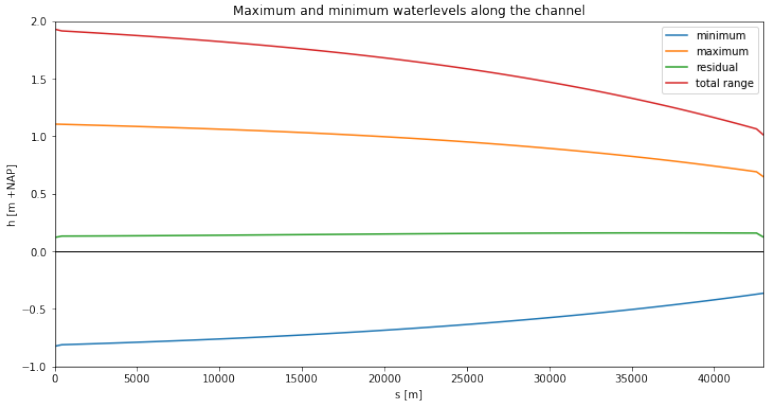

Figure 5.3: Maximum and minimum tidal waterlevel along the length of the channel model for the base scenario, $Q_3 = -800 m^3/s$.

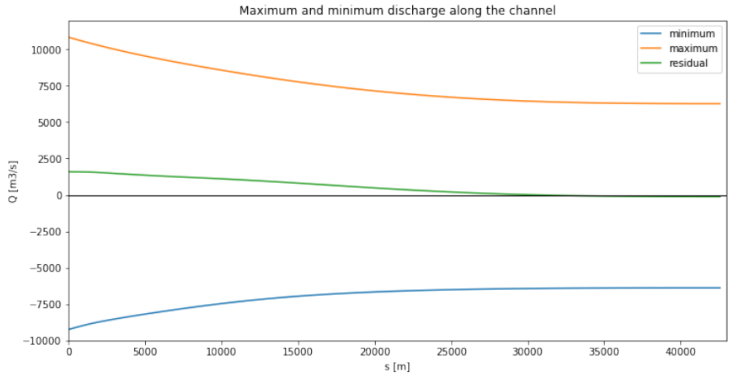

Figure 5.4: Maximum flood and ebb discharges along the length of the channel model for the base scenario, $Q_3 = -800 m^3/s$.

5.1.4. Scenario 1: Kierbesluit

The first scenario that will be evaluated consists of the construction of the Delta21 project, while the current operational policy of the Haringvlietsluices, the 'kierbesluit', is maintained. Under the kierbesluit operational policy the Haringvlietsluices, the Haringvliet sluices are used to discharge river water during times of low tide. During flood tide, there is a small opening in the Haringvlietsluices to allow for migratory fish to travel upstream. This opening is limited in an effort to limit the amount of salt intrusion into the Haringvliet, where large scale fresh water intakes are located. There are no exact measurements available for the amount of discharge that is let through the Haringvlietsluices, but on average it seems that the net difference between ebb and flood flow is roughly $680 m^3/s$. To account for this difference, it is assumed that the flood flow into the Haringvlietsluices is near zero. the schematized version of the Haringvliet discharge is shown in fig. 5.5b.

For this scenario we will be assessing the effects of the tidal opening in the New Haringvliet barrier on the tide in the tidal lake. The maximum tidal range, and tidal flow through the barrier were calculated and are presented in fig. 5.5. From the results we find that for a tidal lake with a surface area of $45 km^2$ a tidal opening that is larger than $3000 m^2$ there is no real significant difference between the tidal range in the basin and that on the North Sea. In this scenario, the surface area of the tidal lake directly affects the tidal response of the lake. A larger lake will also require a larger tidal opening to reach similar tidal ranges in the system.

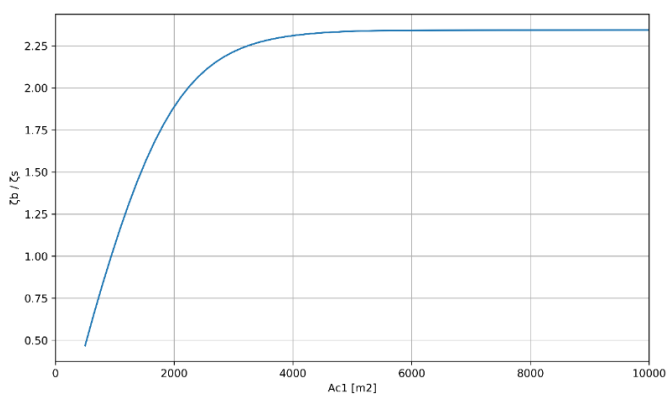

(a) Tidal range in the tidal lake for scenario 1, and a tidal lake area of $45 km^2$

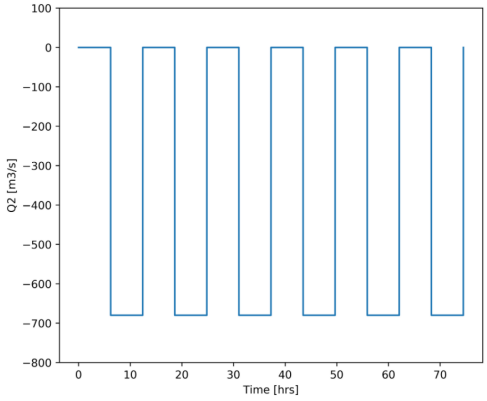

(b) Assumed Haringvlietbarrier discharge for scenario 1, $Q2 = -680 m3/s$ during low tide in on the North Sea

Figure 5.5

5.1.5. Scenario 2: Open Haringvliet

Scenario 2 evaluates the impact of the New Haringvliet barrier's tidal opening on the tidal response in both the tidal lake and the HV/HD channel, in a scenario where the Haringvlietsluices are completely reopened. This is also the primary operational policy proposed as part of the Delta21 project. An overview of the situation is given in fig. 5.6, and the design parameters in table 5.2.

To evaluate this scenario, the hydrodynamic model was ran for varying cross-sections for the New Haringvliet barrier, ranging from $2000 m^2$ to $14000 m^2$, in increments of $500 m^2$. For each cross-section the tidal range induced by the M2 tide on the North Sea were compared. The comparison was done at a total of four locations: in the tidal lake, at the start of the channel , right behind the Haringvliet sluices (s=0), at the halfway length of the channel domain (s = 1/2L), and at the end of the domain (s = L). The resulting maximum tidal ranges at these locations were computed and plotted in fig. 5.8. The respective tidal ranges for the base scenario were also plotted to give a clear overview of the impact of the New Haringvliet barrier in the schematized model.

For smaller cross-sections, the expected tidal range rapidly increases as the size of the opening increases. After the tidal opening become larger than roughly $6000 m^2$, further increasing the tidal opening of the barrier becomes less effective in increasing the tidal range in the system. For cross-sections larger than $10000 m^2$ the reduction in tidal range relative to the base scenario has become less than 20cm at all locations. From this point on the benefits of further increasing the opening size of the New Haringvliet barrier in order to increase the tidal range in the system has very limited efficiency.

A short assessment into the sensitivity of the tidal lake size into the model was also done. This was done by reducing the surface area of the tidal lake from $45m^2$ to $25m^2$, this change had almost no influence on the maximum tidal range in the model. The only significant difference was found in the maximum discharges through the New Haringvliet barrier, as there is less discharge required through the barrier to illicit a water level response in the tidal lake as it is modelled as a storage basin model.

Parameter	Description	Value	Unit
A_{c1}	Opening New Haringvliet barrier	variable	m^2
A_{c2}	Opening Haringvlietsluices	6000	m^2
A_b	Surface area tidal lake	45	km^2
Q_3	Discharge in the upstream channel boundary	-800	m^3/s

Table 5.2: Model Parameters scenario 1

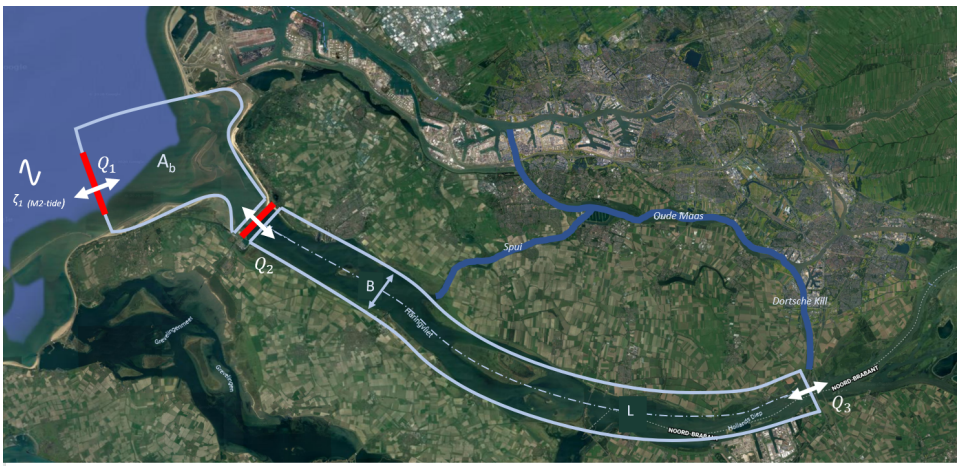

Figure 5.6: Scenario 2: New Haringvliet barrier, while fully reopening the Haringvlietsluices

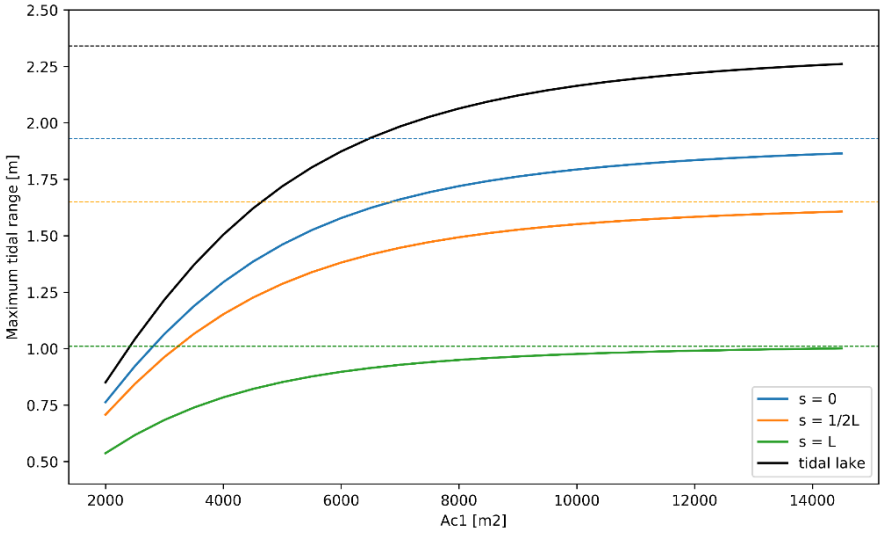

Figure 5.7: Tidal range of the Schematized model depending on the effective cross-section of the tidal opening of the New Haringvliet barrier. Dashed lines indicate the tidal range for the base scenario.

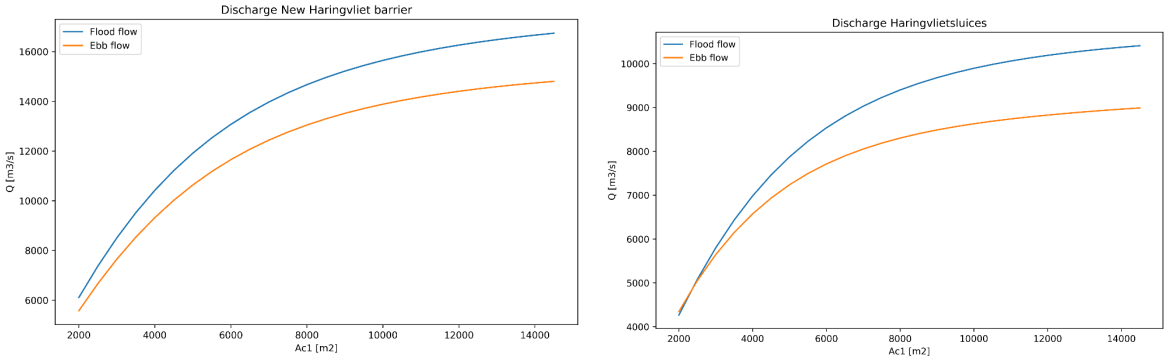

(a) (b)

Figure 5.8: Model results for the maximum ebb and flood discharge rates through the New Haringvliet barrier (a) and the Haringvlietsluices (b), depending on the effective cross-section of the tidal opening of the New Haringvliet barrier.

5.1.6. Scenario 3: High river discharge

The final assessment that was done, was an evaluation of the impact the construction of a second barrier has on the discharge capabilities of the Haringvliet in the case of a high river discharge. Currently, the Haringvlietsluices are only completely opened to discharge water in the case of a river flood wave. The construction of a second barrier right behind the Haringvlietsluices would increase the amount of resistance between the Haringvliet and the North-sea and will inevitably increase the inland waterlevels compared to the current situation. Using the schematized model, the upstream discharge was increased to a very large rate that is expected during a high river discharge ($Q3 = -8000 m^3/s$ / $Q_rhine = 12000 m3/s$). From this point on the base scenario (no New Haringvliet barrier) was be compared with the situation that includes a second barrier. This was be done for a NHVB cross-sections of $6000 m^2$ and $10000 m^2$ respectively. The resulting waterlevels and discharge rates are provided in fig. 5.9 and fig. 5.10 respectively.

As expected, a larger barrier will generally provide a better capability to discharge high river flood waves. During high tide, the model does not show any large differences in waterlevel between the current and the proposed situations. During low tide situations however, having the a barrier with a similar opening size as the Haringvlietsluices, will significantly increase the total head required between the Haringvliet and the North Sea to discharge water at a similar rate as it is currently. Even though the results of this scenario do not indicate any direct increase in the maximum waterlevel in the system, it is unclear how the decrease in water discharge capacity during low tide will affect waterlevels in the rest of the RMD. Limiting the discharge of river water through the Haringvliet, might redirect water to different locations in the RMD. To further review the situation, a review was done of the mean discharges at the upstream boundary of the system. The result of this analysis is summarized in table 5.3. The results show that smaller barrier openings cause a smaller amount of net average inflow into the domain, indicating that this water would typically be redirected to different sections of the RMD. As mentioned previously, to assess this situation in more detail, future studies should be executed using calibrated models for the entire RMD.

Effective barrier cross-section [m2]	6000	10000	14000
Average discharge upstream boundary (Q3) [m3/s]	6960	7342	7474

Table 5.3: Tidal cycle averaged discharge at the upstream boundary

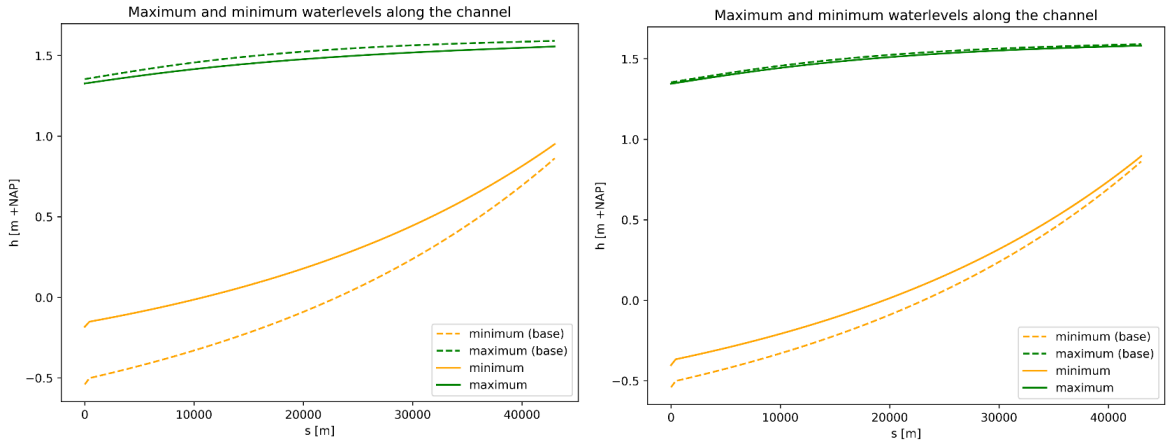

Figure 5.9: Model results for the minimum and maximum waterlevels along the channel for a river discharge of 8000m3/s, in the case of a New Haringvliet barrier openings of $A_c = 6000m^2$ (a) and $A_c = 10000m^2$ (b). Both scenarios were compared with the base scenario.

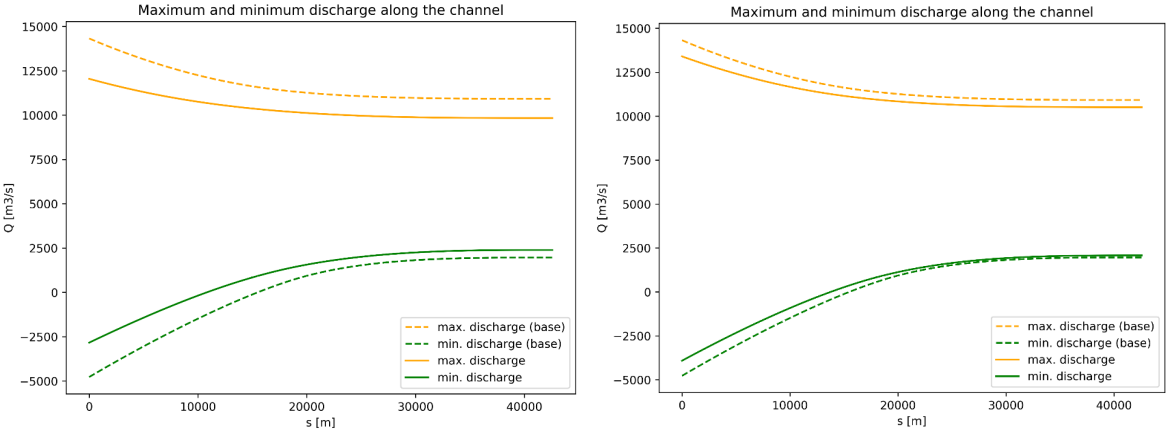

Figure 5.10: Model results for the minimum and maximum discharges along the channel for a river discharge of 8000m3/s, for a New Haringvliet barrier opening of $A_c = 6000m^2$ (a) and $A_c = 10000m^2$ (b). Both scenarios were compared with the base scenario. This plot shows positive discharges for downstream river discharges.

Effectiveness of Valmeer's compensation operation during high river flood

The final scenario that was considered, is the effect of utilizing the spillway and the Valmeer as additional storage during high river discharges for a New Haringvliet barrier of $6000m^2$. This would lower the waterlevel in the tidal lake, while also increasing the head over the Haringvlietslucies. To account for this process in the model the condition was set for an additional $10000m3/s$ to be discharged from the tidal lake during ebb-tide on the North Sea. The results of the calculation are shown in fig. 5.11. As can be seen, the maximum waterlevel in the HV/HD channel for this scenario becomes very similar to the base scenario. This indicates that using the spillway and the Valmeer of the Delta21 project in this manner can indeed present a viable option for improving the discharge of the system in the case of high river discharges, even with the increased resistance of a second barrier. It should be noted that this specific situation needs a far more in-depth analysis before becoming an actual viable option, as operating the Valmeer in this way could potentially cause additional water from the North Sea to flow into the tidal lake, and then into the Valmeer. But this assessment can be seen as an early indication into the effectiveness of the use of the Valmeer in river flood scenarios.

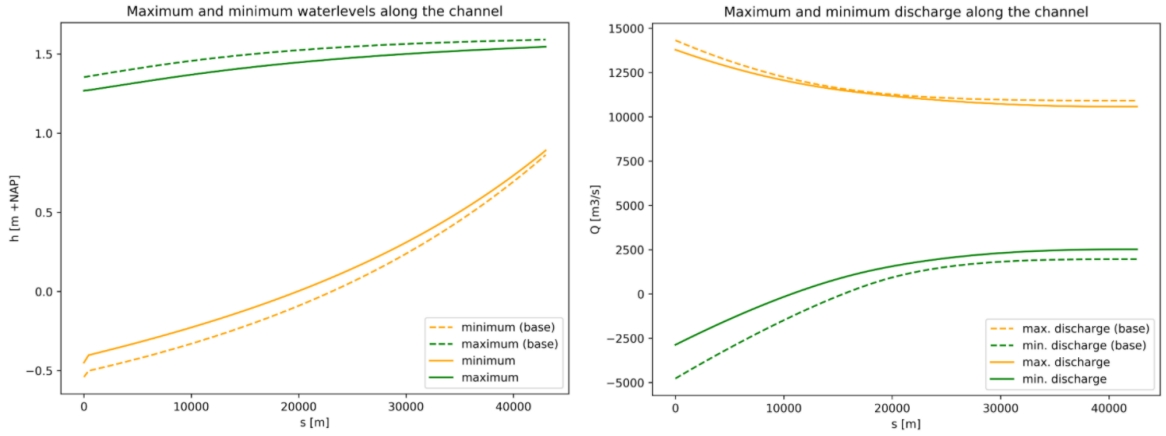

(a) (b)

Figure 5.11: Model results for the minimum and maximum waterlevel (a) and discharges (b) along the channel for a river discharge of 8000m3/s, including an additional $10000 m^3/s$ of discharge across the spillway into the Valmeer during ebb-tide (New Haringvliet barrier opening of $A_c = 6000 m^2$)

.

5.2. Design alternatives

Following the results from section 5.1, a total of three different design alternatives will be formulated. These will be evaluated based on their performance in the hydrodynamic model assessment and based on their expected overall cost. For the alternatives three different discrete cross-sectional areas were considered, $6000m^2$, $10000m^2$, and $14000m^2$. A cross-section of $6000m^2$ was deemed to be the minimal required cross-section for the barrier. If the new Haringvliet barrier was to be smaller than that, the systems ability to discharge river water during river flood events becomes extremely limited.

5.2.1. Effect on the tide

An overview of the hydrodynamic performance of the three alternatives in the schematized model are given in table 5.4. From the perspective of the amount of tidal range it is clear that larger barriers allow for a larger tidal range at all locations. In the case that the Haringvlietsluices will be operated under the kierbesluit, all these alternatives show the same tidal range in the tidal lake in the model assessments.

Effective barrier cross Section [m2]	6000	10000	14000
Average tidal range inside Haringvlietsluices [m]	1.57	1.79	1.86
Average tidal range in the tidal lake [m]	1.87	2.17	2.25
Average peak tidal discharge through NHVB [m3/s]	13073	15646	16663
Maximum flow velocity for an average tide (NHVB) [m/s]	2.18	1.56	1.19

Table 5.4: Results of the Schematised model for the three effective cross-sections of the new barrier, and their corresponding tidal characteristics.

5.2.2. Flood safety

From a flood safety perspective, it was also established that generally larger cross-sections for the New Haringvliet barrier result in a better discharge of river water during river flood events. Table 5.5 shows the tide-averaged waterlevels in the HV/HD based on the schematized model for all alternatives.

Once again it is unclear what the net-impact is on the flood safety in the entire RMD, thus these values should only be used as a first indication on the general choice of tidal opening on the flood safety in the RMD. It was also established that it might be possible to use the spillway and the Valmeer in order to aid in the case of a high river discharge. However this scenario also requires further validation from an hydrodynamic perspective, as well as from an economic perspective.

Effective barrier cross Section [m2]	6000	10000	14000
Avg. waterlevel inside of Haringvlietslucies [$m+NAP$]	0.50	0.37	0.32
Avg waterlevel at the upstream boundary [$m+NAP$]	1.18	1.15	1.14

Table 5.5: Results of the Schematised model for three effective cross-sections of the new barrier during high river discharge scenarios.

5.2.3. Cost evaluation

To evaluate the relative cost of the barrier alternatives at this point in time, an estimation was made based on the expected length of the dynamic barrier components of the respective alternative. Mooyaart and Jonkman (2017), identified a dependence of the cost of storm surge barriers and the length of the gated section of the barriers. The correlation that was found was that a barriers is expected to cost 2.2 million EURO/m of gated section (at a 2013 price level). Kluijver et al. (2017) added additional barriers to the analysis and update the price levels to 2019 euros and found a value of 2.45 million EURO/m. This value will be used to evaluate the relative cost of the different alternatives.

To estimate the length of each alternatives, the wet cross-section of each alternative was divided by the sill depth (-5.5m NAP) to estimate the effective width required for each alternative. From here on each effective

opening width was multiplied by a factor 1.25 to account for piers and supporting structures along the width of the barrier. The results for this assessments and the final estimated cost are given in table 5.6. The result are subject to high variability but as a relative measure of cost this assessment shows a significant impact of the barrier costs to the selected wet cross-section of the barrier.

Effective barrier cross Section [m^2]	6000	10000	14000
Effective opening width [m]	1090	1820	2545
Total barrier span [m]	1363	2275	3180
Expected cost [billion 2019 EUR]	3.3	5.7	7.8

Table 5.6: Expected costs for the three barrier alternatives using a unit cost of 2.45million EURO per meter of gated barrier section

Eastern-Scheldt barrier case study

A second evaluation was done using the cost information of only the Eastern-Scheldt barrier. Due to the close proximity of the barrier's and the fact that both barriers will likely be larger barriers with multiple gates, this was deemed a good reference project for the New Haringvliet barrier. The research data from Kluijver et al. (2017) indicated that the Eastern-Scheldt barrier cost 1.8 million EURO per meter of gated section. The resulting costs are shown in table 5.7

Effective barrier cross Section [m^2]	6000	10000	14000
Expected cost [billion 2019 EUR]	2.5	4.1	5.7

Table 5.7: Expected costs for the three barrier alternatives using a unit cost of 1.80million EURO per meter of gated barrier section (Eastern-Scheldt case-study)

5.2.4. Selection of alternative

The hydrodynamic assessment has shown that larger barriers perform overall better from a flood safety and a tidal perspective, as larger tidal ranges were deemed more preferable in this assessment. However, after a certain point there will be a strongly diminishing return in the effectiveness of the wet cross-section in the hydraulic performance of the system. Whereas, according to the used cost model, the cost of the barrier increases linearly with the wet-cross-section of the barrier. For the Delta21 project, cost is an important parameter, as the projects financial feasibility is dependent on the amount of money that can be saved on dike strengthening projects. A very large barrier (wet cross-section = 14000m^2) will inherently be a very expensive investment and will thus effectively limit the potential for the Delta21 project overall. A barrier with a wet-cross section of 6000m^2 on the other hand could potentially significantly limit the amount of tide that is able to be restored in the Haringvliet estuary. the smaller barrier would also have notable adverse effects on the discharge of high river flood waves through the RMD. Using the spillway and the Valmeer as an additional measure during river floods was shown to have the potential to reduce the waterlevels in the HV/HD channel, even for smaller opening sizes of the New Haringvliet barrier. However, this might not be an acceptable solution, as the frequent use of the Valmeer for flood safety purposes is generally not desirable from a financial perspective. Therefor, a tidal opening wet cross-section of 10000m^2 was selected as the best option. This will be the used in the remainder of the conceptual barrier design.

5.3. Discussion of results and further recommendations

In this section of the report a schematized model was used to gain a first insight into the potential impact of the New Haringvliet barrier on the Haringvliet and Hollandsche Diep, and the Delta21 tidal lake. From the results of the assessment, preliminary design alternatives were formulated, and a wet-cross section of $10000m^2$ was chosen as the design alternative for the remainder of this study.

The hydrodynamic assessment in this chapter was done by utilizing a schematised version of the actual scenario in the Haringvliet. The resulting recommendation for the wet-cross section is thus only meant to be a first indication into the size of the opening in the New Haringvliet barrier. Relative to the opening size of the Haringvlietsluices ($6000m^2$) and considering the fact that the desired hydrodynamic effect, a wet-cross section of $10000m^2$ does seem like a realistic recommendation for the New Haringvliet barrier overall.

5.3.1. Recommendations

This section will describe the recommendations with regards to the future studies related to this topic.

Tidal range

For the study of the tidal range, it is recommended to determine the impact of the Delta21 project on a model that has been calibrated for the RMD. Additionally, it should be determined what the desired tidal range is at different locations along the Haringvliet and the Hollandsche Diep. This will help in further determining and verifying the final wet cross-section of the New Haringvliet barrier.

River flood safety

The most crucial conclusion for Delta21 and the New Haringvliet barrier project that can be taken away from this assessment is the potential impact of a second barrier on the waterlevels in the RMD during high river discharges. The model tests showed a significantly noticable impact of the opening size of a second barrier on the waterlevels, and discharge rates through the channel. The flood safety of the RMD during a river flood wave is likely to be the normative factor in determining the minimum cross-section of the New Haringvliet barrier. More frequent river flooding, or the requirement for additional dike strengthening due to the Delta21 project is not a desirable outcome for the overall feasibility within the Delta21 project. Because of this it is recommended that the opening size of the barrier will be re-evaluated for their impact on waterlevels in the RMD during a river flood wave travelling down the river Rhine using a calibrated hydrodynamic model. Such a study would give a better insight in the actual changes in the RMD, and would give a higher confidence in the selected barrier cross-section.

Potential Measures

In addition to simply evaluating the impact of the barrier opening, varying measures can be taken in order to potentially lower the resistance of the overall system during high river discharge.

The first intervention that can be considered is the (partial) removal of the gates of the Haringvlietsluices. Currently, when fully opened, the gates are opened to a level of +0.5m NAP. Limiting the maximum effective opening area of the sluices to $6000m^2$. Removing or raising the gates, could improve the discharge of the sluices during high waterlevels on the Haringvliet and the Hollandsche Diep.

The second intervention that could be considered is the operation of the spillway and the Valmeer to discharge river water during high river discharges. As mentioned previously, the financial feasibility of such a measure should be investigated, as the Valmeer will serve as a very large resource in the European energy market. For this it is recommended that Delta21 determines something like a maximum usage frequency for the flood safety use of the Valmeer. This would allow for a better design integration for the use of the Valmeer, with the design of other Dutch flood safety infrastructure.

6

Delta21 Construction Sequence

One of the primary design choices with regards to the construction of the New Haringvliet barrier is the type of foundation and bed protection that will be used in its construction. However, this choice is often dictated by the chosen construction method of a barrier. The two traditional options for this are:

- Piled foundation in the case of in-situ construction
- Shallow (caisson) foundation in the case of prefab construction

In order to establish the preferred construction method for the New Haringvliet barrier, it is important to evaluate the various possible construction sequences for the Delta21 project as a whole. Due to the scale of all the different structures in the Delta21 project, assessing the construction sequence of just the barrier in a vacuum will not give a complete perspective with regards to the most desired choice of the construction method for the structure.

This chapter of the report will discuss the various elements of the Delta21 project (section 6.1), as well as describe two potential different alternatives for the construction sequences that could be utilized in the construction of the Delta21 project:

- Alternative 1: Economic (section 6.2)
- Alternative 2: Environmental (section 6.3)

Following the description of the alternatives, in section 6.4, a multi-criteria analysis (MCA) will be used to determine the preferred construction sequence. Based on the results of the MCA, a preferred construction method for the New Haringvliet barrier is determined. This preferred construction sequence will then be the basis for the design of the barrier in the final design stages of this project.

6.1. Delta21 Elements

The elements proposed in the Delta21 project are all the in early stages of their design process. This section of the report will summarize the currently available technical details of the project, and where necessary will provide an estimate for the primary dimensions of the Valmeer, the pumping station, and the spillway.

6.1.1. Valmeer

The Valmeer will be constructed by dredging the interior region of the lake, while using the dredged material to construct dunes that will separate the Valmeer from the North-sea. The design of the dune protection of

the Valmeer is detailed in van Dam (2020), and the various dike sections that will be used to describe the project in this report can be seen in fig. 6.1. Figure 6.4 shows a cross-section of the final designed dunes that will be surrounding the Northern and Western edges of the Valmeer.

The dune section location North of the Pumping station, Dune section North, currently has an average waterdepth of roughly -15m NAP. For dune section west of the station this is -7m NAP. Using these waterdepths, the dune designed per van Dam (2020) and the preliminary design sketches of Valmeer are used to make an estimate of the Valmeer dimensions and total required sand volumes. Doing this will be useful in gauging viable construction methods for the spillway, New Haringvliet Barrier and the pumping station in relation to the overall Delta21 project. For dune section south, we assume smaller sand dunes, as in this section of the Valmeer the dune does not have to protect against large storm-surges or wave attack. On both sides of the dune a slope of 1:12.5 is assumed and the maximum height of the section will be roughly 4.5m as well (fig. 6.5). On transition East, we assume a similar slope from a height of +4.5m NAP to the bottom of the Valmeer at -25m NAP.

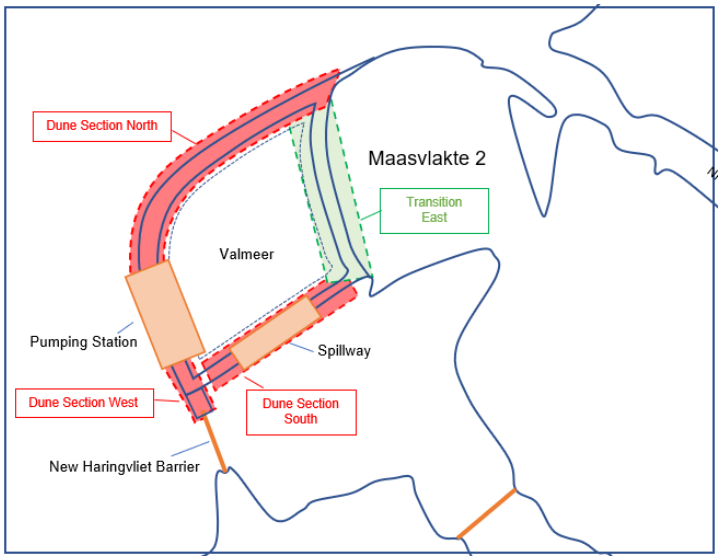

Figure 6.1: Overview image of the Delta21 elements, including an overview of the location of Dune Section North. A cross-section of this dune section can be found in fig. 6.4

Section	**Avg. required sand volume** $[m^2/m]$	**Section length** $[m]$	**Total sand volume** $[m^3]$
North	11668	6194	72271592
West	5937	500	2968500
South	1835	4000	7340000
Transition East	1702	4500	7659000
		Total:	$90 * 10^6$

Table 6.1: Required sand volumes for the construction of the Valmeer dike (these figures do not include maintenance of the dunes due to erosion

From the geometry of the sand dunes it was determined that the total sand volume required to construct the sand dunes in Dune section North is $11668 m^2/m$, whereas in Dune section West this value is $5937 m^2/m$. Dune section south has relatively low sand requirements relative to the Northern and Western sections, here the required sand volumes are roughly $1835 m^2/m$ given the geometry of the sand dunes presented in fig. 6.5. As a final step in order to estimate the project's required sand volumes for the constructions of the Valmeer, the length of both the pumping station and the spillway are required. The pumping station is currently expected to be a section of 2200m long (Ruiz, 2020). For the spillway no initial dimensions are known as no preliminary design was made yet, however as an assumption, this section is assumed to be 1500m long. The resulting computations of the required sand volumes for the Valmeer's dunes shown in table 6.1.

In order to construct the dunes around the Valmeer the material extracted from the interior of the Valmeer

can be used. The Valmeer with the dimensions given in fig. 6.2 has a surface area of $17.5 * 10^6 m2$ at a depth of -25m NAP, up to a surface area of $23.3 * 10^6 m^2$ at a waterlevel of +4.5m NAP. The average ground-level at the site of the Valmeer is at -12m NAP, and thus excavation to a depth of -25m would mean that in total $240 * 10^6 m^3$ of sand would have to be excavated to form the interior of the Valmeer. This means that after the construction of the Valmeer's dunes there will still be an excess of sand that will have to be accounted for within the project.

Options such as a more conservative dune design, or reallocation the excess sand from the project to other projects or locations are all viable options that can be considered. Further elaboration of the possible options for the excess sand are however out of the scope of this project.

The Valmeer will have an operational range for energy storage purposes by pumping and turbining water between the range of -22.5m NAP and -5m NAP. This coincides with storage volumes of $44 * 10^6 m^3$ and $387 * 10^6 m^3$ respectively, fig. 6.3 gives an overview of the storage capacity of the Valmeer for any given waterlevel in the Valmeer. At a waterlevel of +0m NAP the Valmeer would contain up to $500 * 10^6 m^3$. of water.

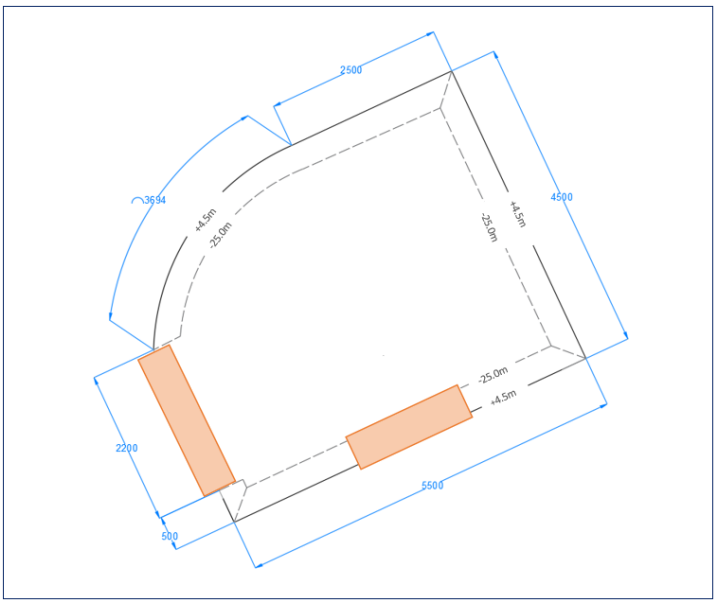

Figure 6.2: Preliminary interior Valmeer dimensions and bathymetry

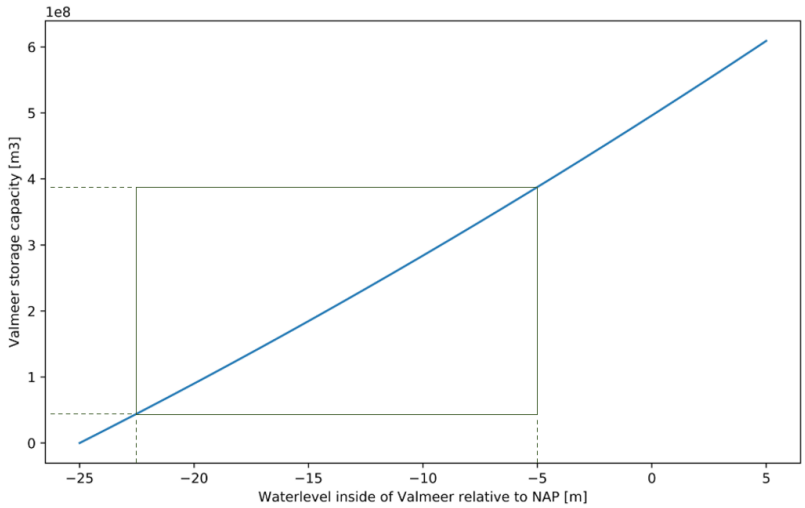

Figure 6.3: Storage capacity for the proposed Valmeer dimensions depending on the waterlevel inside the Valmeer relative to NAP

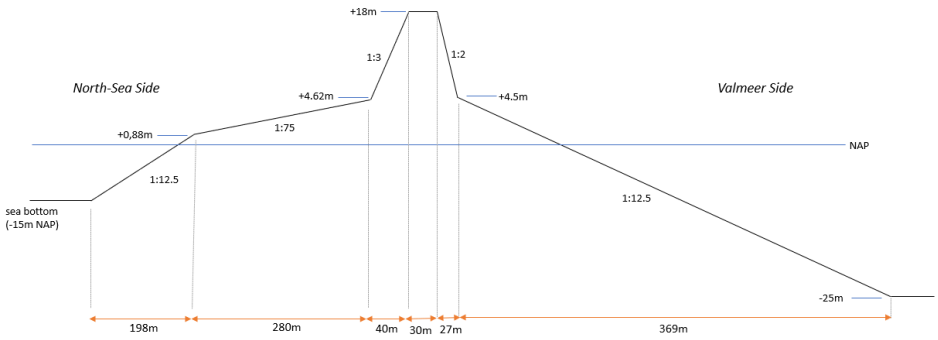

Figure 6.4: Overview of the proposed sand barrier dimensions around the Valmeer assuming a seaside bottom depth of -15m NAP [Image NTS] (Adapted from van Dam (2020))

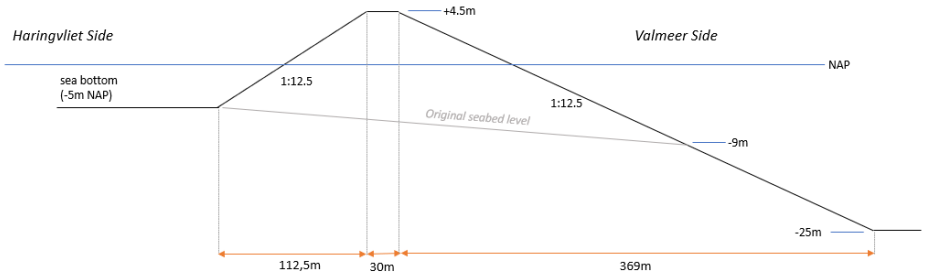

Figure 6.5: Preliminary design estimate for the sand protections in dune section south [Image NTS]

6.1.2. Pumping Station

The pumping station is generally expected to be the largest structural element of the Delta21 project. Currently, the only existing design for the station is detailed in Ruiz (2020), this report is referred to for any additional details pertaining to the pumping station that will not be addressed in this section of the report.

The pumping station is designed to house a total of 167 pump-turbines capable of discharging $60 m^3/s$ each and are rated at 11.1MW per pump. The total structure would span a total of 2228m with the bottom of the structure being at a depth of -32m NAP. Both in-situ, as well as prefab construction methods, were considered as a construction method for the pumping station. Eventually the options of an in-situ construction method was recommended as the main construction method because, even though the in-situ construction pit would be significantly larger than the prefab construction pits, the ease of construction and minimization of specialty equipment requirements were estimated to outweigh the additional cost related to the size of the in-situ building pit.

For the in-situ construction pit, a pit with interior dimensions of 125m x 2800m ($350000 m^2$) at a depth of -34.5m was recommended. The construction pit dimensions were selected in such a way to limit the costs of the building pit, due to the large depth and length of the building pit, any additional width added to the construction site would pose significant increases in the costs related to the pit. For the pre-fab construction alternative Ruiz, 2020 recommends that the structure would be built using bottom and top caissons layered on top of each other as this would strongly limit the overall size of the to be constructed caissons and their eventual draught.

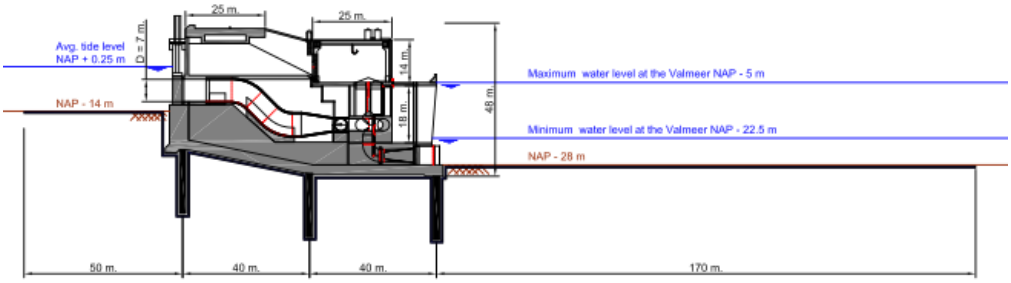

Figure 6.6: Cross-section of the pumping station design (Ruiz, 2020)

6.1.3. Spillway

Currently there are no details regarding the design of the Spillway between the Valmeer and the Haringvliet Delta. From a functional point of view, it is known that during the most critical flood safety operation, the pumping station will be able to discharge a maximum $10000 m^3/s$ of water from the Valmeer into the North - Sea. This means that for the spillway, the maximum capacity should at least match that discharge capacity. But there could be an added benefit to having a spillway with an higher maximum capacity than $10000 m^3/s$ to effectively use the large storage area the Valmeer provides as an additional buffer to the discharge capacity of the pumping station. The type of spillway is also still an unknown, some of the more applicable types of spillways for these project are overflow of siphon spillway (fig. 6.7).

Given all these factors it is important to note that the spillway will most likely be another large structure, in the order of 1-2km long, and could also require a large bed protection to protect against potential erosion. However, given the fact that these factors are indeed unknown, the evaluation of the construction sequence of the Delta21 plan in the upcoming sections will not explicitly take into account the construction of the spillway. Instead the spillway will be considered as another large infrastructural project that could also be constructed using either in-situ or prefab construction methods.

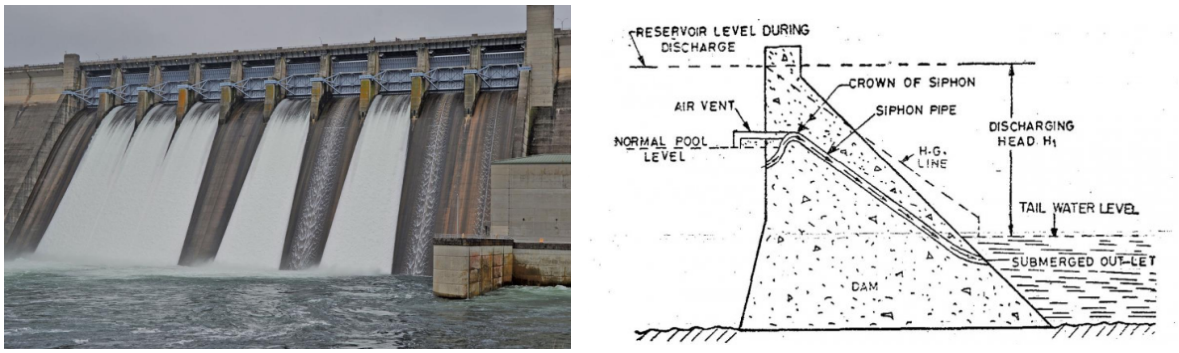

(a) (b)

Figure 6.7: Overflow spillway located at Table Rock Dam, USA (a), and a schematic overview of a siphon spillway (b)

6.2. Construction sequence alternative 1: Economic

The first alternative for the Delta21 construction sequence that will be presented in this assessment is focused on the economic succes of the project. This alternative is centered around optimizing the financial return of the project by planning the construction sequence in a way that allows for economical return as fast as possible. The Delta21 project has two main ways of generating a net profit as a project:

1. Generating revenue by the operation of the Valmeer as a pumped hydro-electric storage lake
The operation of the pumping station and the Valmeer during normal conditions is expected to roughly generate a revenue of 280 million EUR/year. Early estimates for the Valmeer are that it will have a capacity of roughly 1.8MW and the round-trip efficiency of roughly 72%. (source: https://www.delta21.nl/het-grote-geld-van-delta21/).

2. By saving money on potential future dike reinforcement projects
From a flood-safety perspective, Delta21 has the aim to strongly reduce the amount of required dike reinforcements in upstream river reaches by providing a solution for a scenario where both high river discharge and a storm-surge occur, a scenario that is currently accounted for by simply increasing the height of the dikes to satisfy this criteria. Early estimates from Delta21 indicate that the project, could save as much as 5 billion EUR on dike reinforcements by the end of the century. However, this estimate is currently still highly volatile as the amount of potential savings on dike reinforcements is strongly related to the amount of sea-level rise that will occur, and the effects of the Delta21 project on the inland waterlevel during a storm.

It is also important to note that during the consideration of this alternative, there will still be limiting factors due to the environmental boundary conditions of the project. The project is being planned in a Natura2000 area and therefor it is of high importance that all the different alternatives suffice from an environmental point of view as well.

If we consider both financial incentives of the Delta21 project, the operation of the Valmeer as a PSHL can happen independent from the other Delta21 infrastructure (the New Haringvliet barrier and the spillway). However, in order to unlock the full flood safety capabilities of the project and thus to be capable of saving costs on future dike reinforcements, all elements of the Delta21 project are required. Therefor, prioritizing the construction of the Valmeer and the pumping station would allow for the fastest return of investment of the project. This alternative follows this concept, and mandates that the pumping station and Valmeer would be the first elements to be constructed. An overview of the overall phases of this construction alternative can be seen in section 6.2.

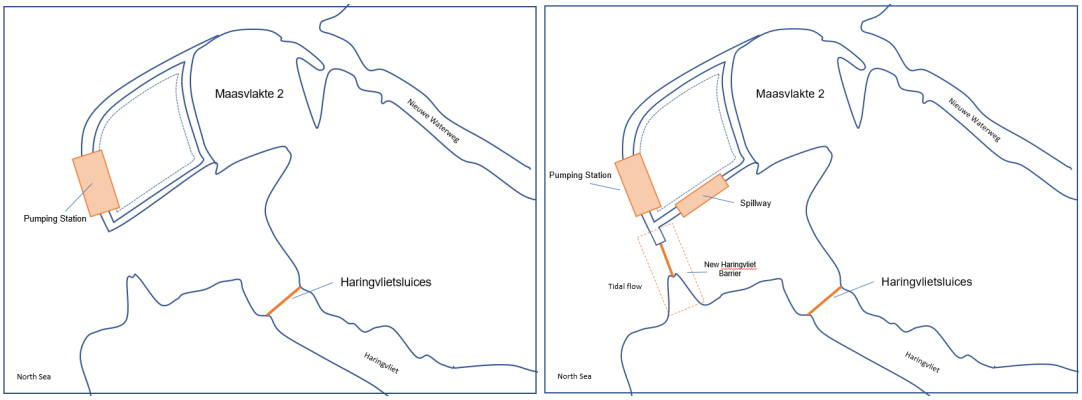

(a) Construction phase 1 of Alternative 1, construction of the Valmeer and the pumping station

(b) Construction phase 2 of Alternative 1, construction of the New Haringvliet Barrier and the spillway

Figure 6.8: The two main construction phases of Alternative 1

6.2.1. Construction alternative 1: Phase 1

Ruiz (2020) recommends an in-situ construction process for the construction of the pumping station. The main benefit for an in-situ building pit was found to be the fact that a prefab construction method would require special vessels for the positioning of the finished elements and the construction of the foundation and bottom protection. The main downside with the in-situ construction of the pumping station would be that the costs of the construction, maintenance, and operation of the pumping installation of the large building pit would be rather expensive.

For this alternative, the choice is made to focus on the in-situ construction of the pumping station, as the primary concern related to the pumping station is to construct the station as fast as possible. In doing so, the in-situ construction method is most likely to provide the largest degree of control over the project at this stage. Additionally the construction of the Valmeer will require large volumes of sand to be dredged, which means that the construction infrastructure require to construct the pumping station building pit will already be required at the location.

The dimensions used for the building pit are derived from the preliminary calculations done in (Ruiz, 2020). As mentioned previously in this report a in-situ building building dock with a work area of 2800m x 125m ($350000 m^2$) was recommended. The final structure proposed by Ruiz (2020) is a total of roughly 2200m long and 80m wide, with the bottom foundation at a level of -32m NAP. This thesis will continue to use the dimensions of a more conservative building dock of 2400m x 250m ($600000 m^2$) which yields more general construction area within the dock (fig. 6.9). This is only a primary design assumption and is subject to change as more detailed iterations of the design process are done in the future. A dock of this size at the location shown in fig. 6.8, where the average groundlevel is at a depth of -10m NAP, would required the following volumes of sands to be dredged or deposited:

- Building pit dikes: $14.6 * 10^6 m^3$
- Interior building pit dredge volume: $24.2 * 10^6 m^3$

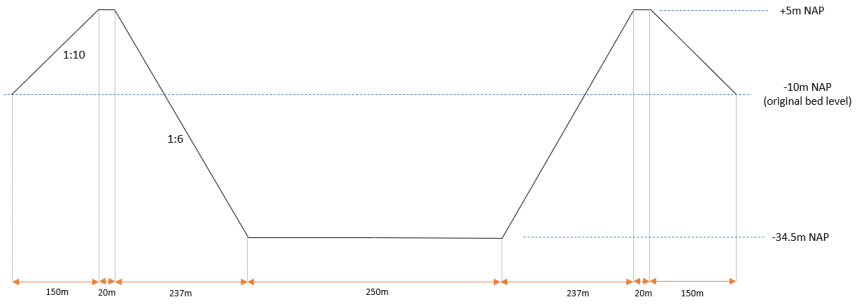

Figure 6.9: Initial design of the cross-section of the building pit and it's dimensions [Image NTS]

6.2.2. Construction alternative 1: Phase 2

For the completion of phase 2, the construction of the New Haringvliet Barrier and the spillway this thesis will consider two general options that will be evaluated:

- Option 1

  In-situ construction of the New Haringvliet Barrier

  In-situ construction of the spillway

- Option 2

  Prefab construction of the New Haringvliet Barrier

  In-situ construction of the spillway

The above mentioned options do not include the possibility of the prefab construction of the spillway. This is mainly due to the combination of two factors: the limited knowledge related to the final spillway structure and dimensions, and the need for a prefab construction dock. The current location of the spillway is in a sheltered location, where the construction of a building dock will not cause any additional disturbance to the tidal flow, river discharge and navigation in the region. Therefor applying a potentially more difficult prefab construction process here is most likely not optimal and therefor is not considered in this report. As the design of the spillway becomes more detailed, this might still change. One of the additional possibilities for example might occur if it is found that the spillway requires a limited amount of prefab elements, to the point where the use of the Barendrecht building dock (fig. 6.10) becomes a viable project option. However, given the scale of the other elements of the Delta21 project, this does not seem like a likely scenario.

Short Note on Bouwdock Barendrecht
The Barendrecht building dock has been frequently used to construct tunnel elements for various projects throughout the Netherlands. The dock has a size of 200m x 400m (10ha), with the bottom at -10m NAP, and transport of the elements to the Delta21 project location would roughly take 25 hours. The dock is a potentially viable resource for the Delta21 project, however given the scale of the dock in relation to the project, it will not be considered as a primary resource.

Figure 6.10: Bouwdock Barendrecht during the constrcution of the tunnel elements of the Tweede Coentunnel

Option 1: In-situ construction of the spillway and barrier

The first option is to construct both the spillway and the barrier in-situ. A rough schematic overview of this option is given in fig. 6.11. This construction sequence is the most straightforward of all the construction options as it requires the in-situ construction of all Delta21 elements. The benefits and downsides of this construction method are listed below:

Benefits:

- Good control of the construction of the bed protection and structures foundation
- Enables the use of piled foundations for the spillway and the barrier
- Minimizes the need for specialty vessels used for transport of the caissons, soil improvement, and construction of the bed protection.

Disadvantages:

- Requires the construction of two large scale building docks
- New Haringvliet Barrier building dock would take up a large section of the remaining opening between the Haringvliet and the North Sea.

Given the length of the barrier, a building dock would obstruct roughly 2500m - 3000m of the remaining 5000m long section between the coast of Goeree and the Valmeer. It is unlikely that this obstruction would be large enough to limit the discharge potential of the Rhine river water, causing potential flood safety concerns. Additionally, the obstruction would further affect the tidal flow patterns in the Haringvliet Delta, how this impacts the morphology of the tidal flats such as the Hinderplaat is unknown. The detailed assessment of these factors is out of the scope of the project However, during the assessment of the various alternatives, estimates of the effects of the chosen measures will be considered.

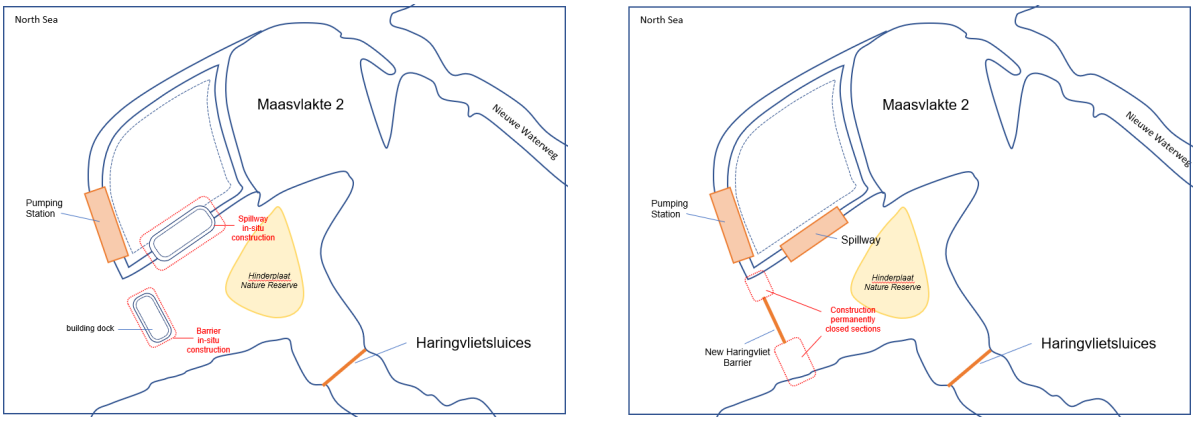

(a) In-situ construction of both the barrier and the spillway in their respective building docks

(b) Construction of the permanently closed dammed sections of the barrier

Figure 6.11: Phase #2 Option #1 project outline

Option 2: Prefab construction of the barrier and In-situ construction of the spillway

The second option for phase 2 is to construct the spillway in-situ while the barrier is constructed using pre-fabricated elements. This option plays into the fact that the final spillway location is in close proximity from the New Haringvliet barrier and generally has a good location for the construction of a building dock.

The construction sequence for this option is laid out in fig. 6.12. The construction sequence would start with the construction of a building dock at the location of the spillway (this would most likely coincide with construction of the Valmeer). This dock would then firstly be used to construct the prefab elements for the New Haringvliet barrier. Once these elements are completed, the building dock can be opened up and the elements can be transported to the barrier assembly location . In order to do so an access channel and construction trench at the assembly location would have to be dredged (fig. 6.12b). After the construction of prefab elements is done, the building dock can be closed up again and re-purposed as an in-situ construction dock for the Valmeer spillway. Lastly the whole section of the New Haringvliet barrier can be closed of to complete the construction of the Delta21 project. The benefits and downsides of this construction method are listed below:

Benefits:

- Economic and efficient use of one building dock
- Limited obstruction to the remaining waterway during construction of the New Haringvliet barrier

Disadvantages:

- Increased complexity for the construction of the New Haringvliet barrier
- Limited possibility for the simultaneous construction of the New Haringvliet barrier and the spillway

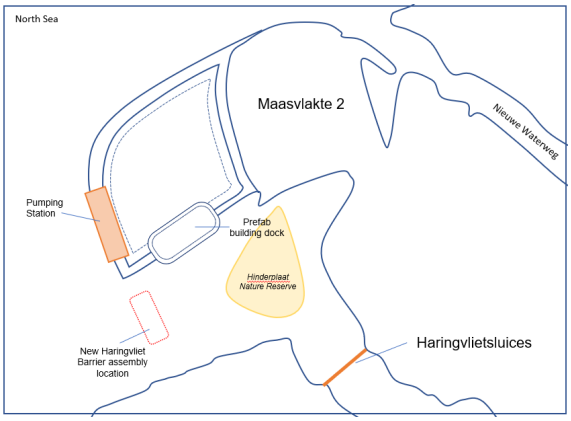

(a) Construction of building dock for the construction of the caisson elements of the New Haringvliet Barrier / Preparation of the final barrier assembly location

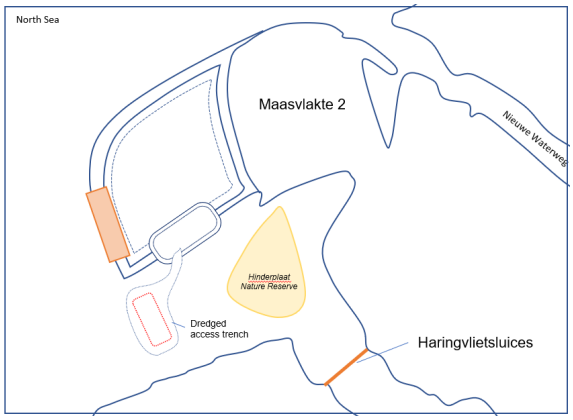

(b) Transport of the foundation elements to the final assembly location, this will require that a access channel and trench at the final construction location

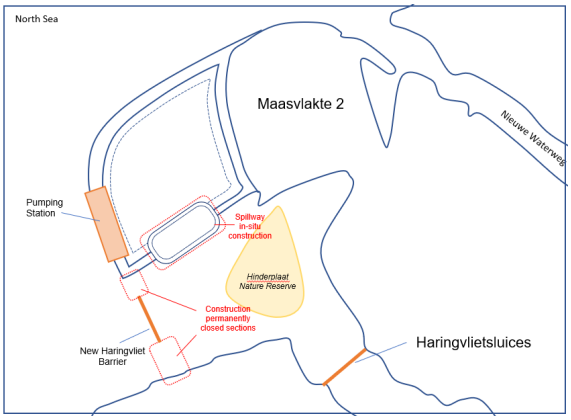

(c) Construction of the permanently closed dammed sections of the barrier and the start of construction of the spillway in the building dock

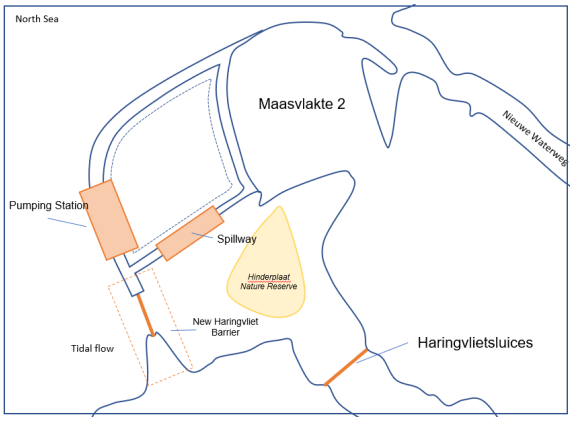

(d) Project completion after disassembly of the building pit of the spillway

Figure 6.12: Phase #2 Option #2 project outline

6.3. Alternative 2: Environmental

The second alternative for the construction method of the Delta21 project is centered around minimizing the adverse environmental effects of the construction process as much as possible. Delta21 as a project is proposed to be constructed in a Natura2000 area, making the environmental impact of the project a critical variable in the design process of the project. The environmental alternative is designed with the following aims:

1. Limiting actions with a potential negative environmental impact

This criteria is focused on limiting any construction processes that might negatively affect the Haringvliet tidal delta's natural value. This includes limiting actions that affect regions such as the Hinderplaat, the Slikken van Voorne and the wider Haringvliet Delta beyond what is strictly necessary to construct the Delta21 infrastructure.

2. Minimizing emissions during the construction process

An important consideration when choosing the construction method of the New Haringvliet Barrier is the emissions that come with the project. As per 2019, in the Netherlands, an estimated 18000 building and infrastructure projects were put on hold due an excess of nitrogen that is present in nature across the country. The excessive amount of nitrogen are harmful to the biodiversity in nature, as it harmful to flora that normally flourish in areas with a lack of nitrogen. In the construction industry the main source of nitrogen is due to the emission of construction machinery in the form of nitrogen oxides (NOx). In the Delta21 plan limiting the amount of nitrogen oxide emitted is a crucial factor, as the plan is located in the middle of a Natura2000 area, of which 118 of a total of 160 already are experiencing an excess of nitrogen.

In order to address the emission concerns related to the construction of the Delta21 project, the main focus in this section of the report will be on evaluating the potential use of electrically powered construction equipment during the construction process. Other technologies, such as nitrogen oxide filters, might also aid in the reduction of emissions during the construction process, however those will not be included in this primary assessment of the construction sequences. In section 6.3.1 the current state of electrical construction equipment is outlined and discussed. The recommendations and findings of this section were used to determine an alternative that facilitates the use of electrically powered construction equipment, this alternative is presented in section 6.3.2.

6.3.1. Electrical Construction Infrastructure

Currently, the most common fuel source for high powered construction machines is diesel. The use of diesel powered machines currently offers great reliability and robustness to a project. In order to limit the emissions during the construction of the Delta21 project, the operational limitations of electrically powered machines need to be considered during all stages of the design and construction process. The aim should be to design a construction infrastructure that facilitates the use of electric construction machinery. Only then will the use of electric construction equipment potentially become technically and economically viable for the project.

At this stage of the design process we consider the general limitations of the use of electric machinery in the construction process in order to make recommendations for the overall construction sequence. The main limitations are listed below.

- The applicability of batteries in high powered construction equipment is currently limited by the high cost and weight of the batteries that come as a result of the high power-storage requirements for the machines
- Charging times for battery powered machines cause operational downtime which is not seen in diesel powered machines
- The use of a net connection through a power cable strongly limits the mobility of the respective ma-

chines

- The current developing state of high powered electrical construction equipment means that they are currently very expensive to purchase.

From the above-mentioned limitations it is clear that the use of batteries is currently only applicable in relatively small machines that require mobility. Larger machines such as dredgers, larger cranes, excavators, and wheel loaders are currently only able to be powered through a direct net connection when looking at electric alternatives. Due to the current state of battery technology in large-scale construction equipment, it is unlikely that they will provide a reliable and financially feasible alternative for traditional diesel powered machines, depending on the technology's rate of development. fig. 6.14 gives an overview of some examples of machines that are currently being produced or developed to operate fully electrically in order to give an idea of the current capabilities with regards to heavy construction equipment for the use in the construction of hydraulic structures.

For this reason, when considering the construction of the Delta21 project using electrical construction equipment the main focus at this point in time should be on constructing a carefully designed infrastructure consisting of cranes and machines with relatively long spans that can be powered electrically. Constructing a larger scale machine, that could potentially replace a multitude of smaller diesel powered machines is currently the most applicable way to reduce emissions in the construction process. A good example for a piece of construction equipment would be the Nestum bridge-crane used during the construction of the Haringvlietsluices (fig. 6.13). This crane was a mobile crane on tracks that moved along the construction site while providing the required materials to their respective locations. Developing and using a similar crane powered by, for example, overhead power lines, could be an effective measure in order to reduce emissions during the construction process of the Delta project. Optimizing the workflow of the construction site, and careful planning of the transport of material across the building site could greatly minimize emissions during the construction process by facilitating the use of high powered zero-emissions construction equipment.

Whether the large-scale implementation of electrically powered construction equipment is applicable to the construction of the Delta21 project is currently difficult to asses, given the uncertainty related to the state of electric construction technology and the state of the project. In order to get a better overview of the respective necessities during the construction process, table 6.2 provides an overview of the respective construction steps within the Delta21 project, and whether or not the it is deemed likely or unlikely whether the large-scale implementation of the electrically powered construction equipment could be used during the construction step. The assessment is mainly based on the electrically powered construction equipment that is currently available or in development.

Figure 6.13: Nestum bridge-crane during the construction of the Haringvlietsluices

Model	Type	Power source	Technical Specifictions
DAMEN RSD-E Tug 2513	Tug Boat	2800kWh battery pack	70 tonne bollard pull 3-4 hours of continuous operation 2 hour fast charge using 1.5MW charger
DAMEN ECSD 650	Cutter Suction Dredger	Onshore powerline	3035kW total installed power 18m dredgin depth 7000 m3/h production rate
Cat 323F double Z-line	26 ton excavator	300kWh battery pack (3.4t)	122kW electric mototr 5-7 hours of operation 12 hour charging time on 63A/400V connection 1-2 hour charging time on 150-350kW chargers

Figure 6.14: Brief overview of recently developed modern electric heavy construction equipment that could be used in the construction of hydraulic structures

6.3.2. Construction Sequence Alternative 2

This alternative for the construction sequence of the Delta21 project, is centered around the construction of a single reusable building dock. This dock will be located at the final Delta21 pumping station location (fig. 6.15a), and will initially be used to construct prefab elements for the spillway and New Haringvliet barrier. After all the elements of the respective structures are completed and transported out of the dock, the dock can be re-purposed for the in-situ construction of the Delta21 pumping station. An overview of the general construction steps is given in fig. 6.15.

This construction sequence was recommended based on a few principle considerations related to the environmental impact of the construction process:

- The use of a single building dock is beneficial as it minimizes the potential changes in tidal flow patterns and wave dynamics in the Haringvliet tidal delta during the early stages of the construction process.
- This alternative prioritizes the construction of the New Haringvliet barrier, which would ensure sufficient tidal in-and-outflow and river discharge capacity during the later stages of the construction process when the Valmeer is being constructed.
- The most labour intensive structure, the pumping station, will be built in-situ, which would most likely increase the construction efficiency of this structure.

As it pertains to the assessment of the use of electrically powered construction machinery presented in section 6.3.1, the choice was made to center the construction process around one primary building dock. Doing so will allow for the space within the project to establish a controlled construction environment within the primary dock. This gives the most potential to establish a primarily electric construction environment as the use of multiple building docks would mean that at each location a separate electric infrastructure would have to be assembled, and eventually disassembled. Both of these processes are currently unlikely to be able to occur electrically (table 6.2).

One of the main downsides of this construction method is the location of the building dock. The dock is roughly 5km away from the nearest coastline, which means that access to the dock will only be available by ship. This includes transport of materials and personnel. For this reason the the final location of the New Haringvliet Barrier was also briefly considered as the primary building dock location as it would allow for a connection to land. However, this would mean that a large part of the above mentioned benefits would no longer apply. Additionally, the pumping station location also has a larger draught, making the transport of construction materials by boat to the building dock more difficult, as it would require intensive dredging.

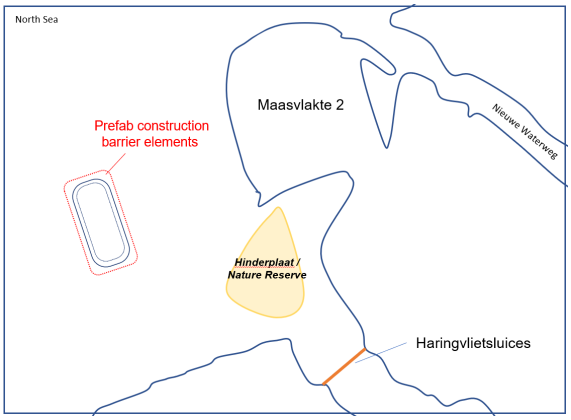

(a) Construction of the primary building dock at the pumping station location. Start of construction barrier prefab elements.

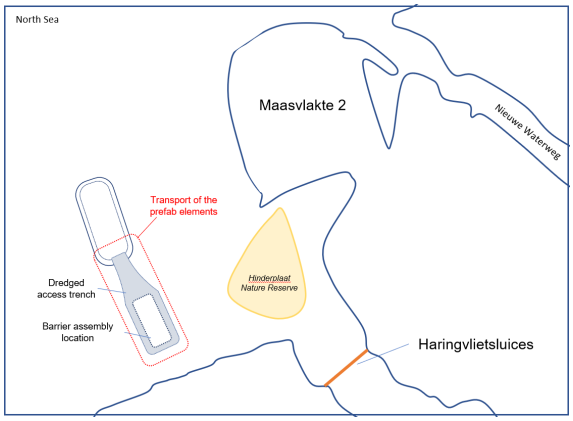

(b) Dredge access trench. Transport of prefab elements to barrier assembly location

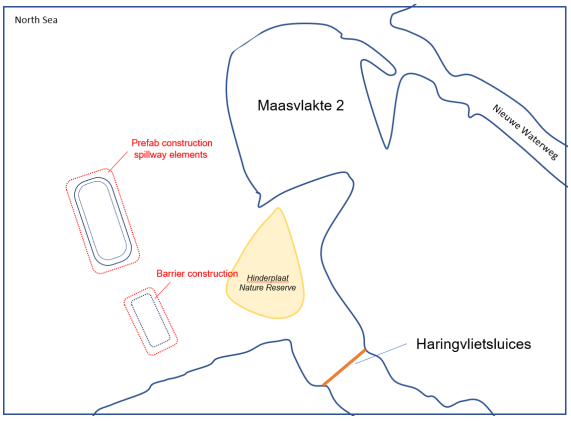

(c) Start construction of prefab spillway elements. Completion of barrier construction

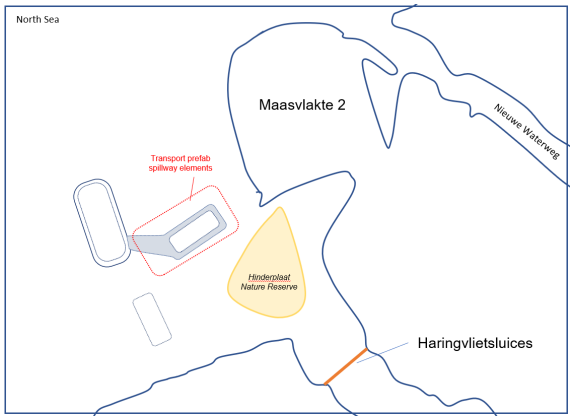

(d) Transport Spillway elements

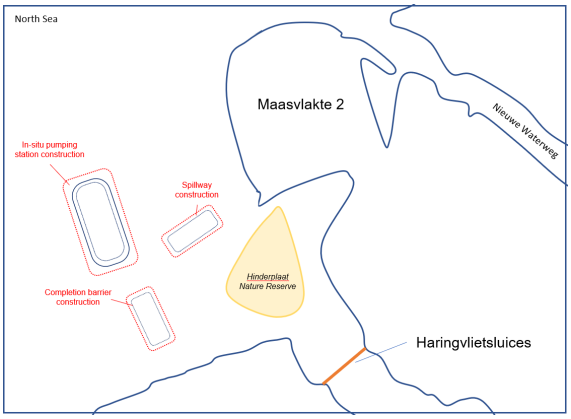

(e) Complete spillway construction, start in-situ construction of the pumping station. Start construction of sand dunes

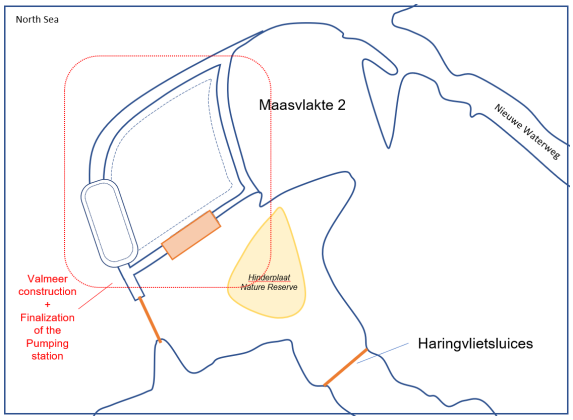

(f) Complete Valmeer construction. Complete pumping station construction

Figure 6.15: Phase #2 Option #2 project outline

	Construction step	Technical feasibility use of electric construction equipment	Description
1	Construction building dock (dredging)	Likely	Currently fully electrical dredgers are availible and have been used in construction projects, these dredgers get supplied with electricity through a power cable that is fed through the dredging line.The main problem arises with the fact that currently, these dredgers have a limited production rate relative to the total dredging volume required in the Delta21 project. But regarding the construction of the building pits the use of these electric dredgers is considered feasible.
2	Preparation of building dock workspace	Unlikely	This construction step includes the transport of materials and construction equipment to the building pit and the preparation of the building pit for construction purposes. This includes the construction of access roads, setup of the local electrical infrastructure, leveling of work areas, and the setup of the overall construction infrastructure. This construction step is highly dependant on standardized transport and construction equipment. Thus at this point in time, the use of electrical machinery for this step is deemed unlikely.
3	Construction of the structure or prefab elements	Likely	The actual production of a structure or its prefab elements could very well occur using, if not exclusively, with mainly zero-emission construction machinery. When setting up a construction infrastructure, this step is the primary step that will be accounted for, therefor this is deemed feasible
4	Transport of the elements to the final construction site (prefab only)	Neutral	Depending on the required vessels required to move the prefab elements to the construction site, this step might be deemed feasible or not. There are currently plans to develop fully-electric tugboats for the Port of Auckland that are to be delivered in 2021. If such vessels are more widely available and technically capable of transporting the caisson elements for the various structures the transport of these elements might be possible.
5	Assembly at the final construction site (prefab only)	Unlikely	The assembly at the final construction location is very unlikely at this point in time to be able to occur electrically. The construction of the Eastern-Scheldt barrier required several specialty vessels for the placement of the bed protection, soil improvements, and placement of the piers. Coordinating and powering these large vessels electrically is considered unlikely at this point.
6	Deconstruction building dock	Unlikely	The deconstruction of the building-dock has a similar transport element as construction step #2. Therefore this construction step is also deemed unlikely.

Table 6.2: Assessment of the technical feasibility of the various possible construction steps of the Delta21 project, and whether they are deemed unlikely or feasible to be executed using primarily electrically powered construction equipment

6.4. Assessment Construction Alternatives

In order to determine the preferred construction method for the New Haringvliet barrier, the Delta21 construction sequence alternatives will be evaluated using a Multi-criteria analysis (MCA). The following criteria were used in the MCA:

1. Environmental Impact
Under this criteria, the various construction sequence alternatives are judged based on their respective potential to incorporate electric construction techniques and machinery, and the overall expected impact of the construction process to the inner tidal delta. Due to the sensitive nature of the Natura2000 areas, it is expected that in the future a large part of the environmental considerations of the project will most likely become project requirements. Therefor, at this stage of the design process, this criteria will be the highest weighted criteria in this MCA (fig. 6.16).

2. Economic Potential
The economic potential of the various alternatives will be primarily assessed based on the time it will take within an alternative to complete the Valmeer and the pumping station. The the overall expected efficiency of the construction process is also considered at this stage of the project. Completion of the Valmeer and the pumping station will allow for the most reliable, and quickest return on investment for the project, making it an important factor for the project's overall financial feasibility.

3. Constructability
The constructability of the project is important as it indirectly indicates the potential project cost. The criteria includes factors such as access to the construction site, difficulty of the applied construction techniques, and the efficiency of the overall construction process.

4. Public Disturbance
The final criteria judges the alternatives based on the amount of disturbance the construction process causes. This includes factors such as obstruction or pollution of the view, noise and smell pollution, and disruption of navigational channels in the area.

In order to determine the weighted factor of the various MCA criteria, they were ranked based on relative importance within the project. Based on this relative importance a final score was assigned to every criteria and the weight factor was calculated. An overview of the priority matrix used for this assessment is shown in fig. 6.16. The MCA for the construction alternatives in presented in fig. 6.17.

		a	b	c	d	total	final scores	weight factor
Environmental impact	a		1	1	1	3	6	0.46
Economic potential	b	0		1	1	2	4	0.31
Constructability	c	0	0		1	1	2	0.15
Public disturbance	d	0	0	0		0	1	0.08
							13	1

Figure 6.16: Priority matrix for the assessment criteria in order to determine the weighted criteria factors used in the MCA

		Alternative 1: Option 1		*Alternative 1: Option 2*		*Alternative 2*	
Criteria	Weight factor	Score	Weighted score	Score	Weighted score	Score	Weighted score
Environmental impact	0.46	3	1.38	5	2.31	8	3.69
Economic potential	0.31	8	2.46	8	2.46	4	1.23
Constructability	0.15	8	1.23	6	0.92	6	0.92
Public disturbance	0.08	4	0.31	6	0.46	8	0.62
Total:	1.00	23	5.38	25	6.15	26	6.46

Figure 6.17: Multi criteria analyis of the construction sequence alternatives

From the MCA it is found that Alternative 2 is best overall construction sequence. The relatively low negative environmental impact of this alternative, and the relatively low public disturbance are the main positive attributes of this construction method. The primary downsides of this alternative are the location of the building pit, which might make it difficult to access, and the relatively late completion of the Valmeer and the pumping station. The top two scenarios of the MCA, both utilize a prefab construction method for the New Haringvliet Barrier. During the process of evaluating the construction of the entire Delta21 project, there was no clear upside for the overall project found for the in-situ construction of the New Haringvliet barrier. Therefor this iteration of the design will be focused on the use of a prefab construction process for the New Haringvliet Barrier.

6.5. Discussion Location Pumping Station

In the development of the construction sequence alternatives, no alternate layouts of the Delta21 project were considered. However there were some general findings in relation to the location of the pumping station that should be considered in future iterations of the project.

Environmental considerations

The current location of the pumping station was mainly decided on based on the beneficial wave attack related to the more sheltered location compared to a more northern location (Ruiz, 2020). However, the entire Delta21 infrastructure is proposed to be constructed in the Dutch Voordelta, which is a Natura2000 area. The Haringvliet tidal delta is a critical area of the Voordelta as there are additional specified areas of environmental importance. These areas are the bottom protected area, and the designated bird and seal rest areas. fig. 6.18a shows the location of these area in relation to the proposed Delta21 infrastructure. All the major structures within the project are currently either located in, or in close proximity of these important areas. A more northern location for the pumping station (fig. 6.18b) would put some distance between the pumping station and these important environmental areas. The pumping station is not only the largest piece of infrastructure within the project, it will also the most frequently used. Thus additional distance might not just be beneficial to the environmental aspects of this project, it might even be a requirement given the noise, vibrations, and additional currents that are expected to occur related to the operation of the pumping station.

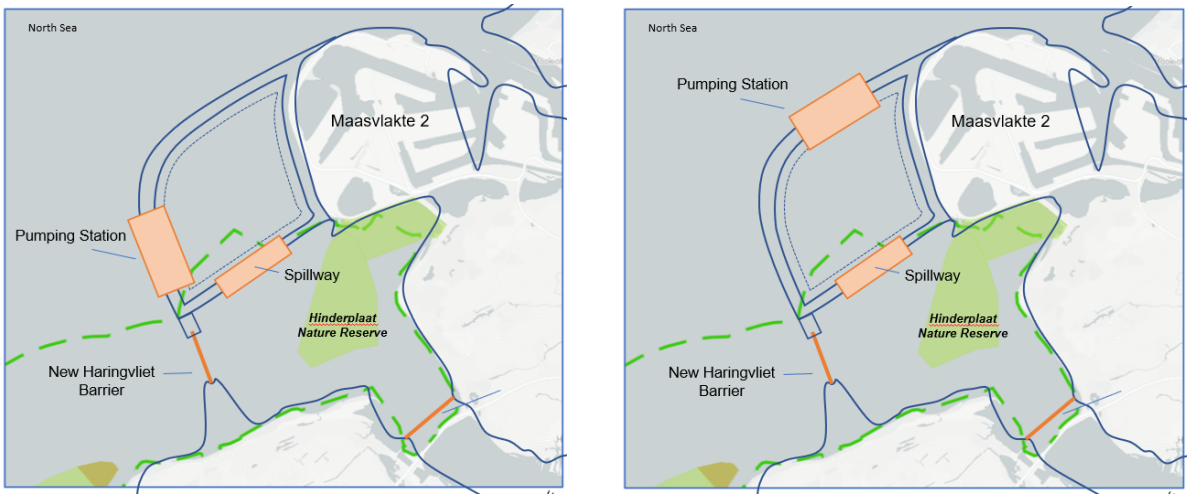

(a) Delta21layout

(b) Alternate layout with Northern location for the pumping station

Figure 6.18: An overview of Delta21 infrastructure in relation to the bottom protected area (green dashed line), and the designated bird and seal rest area (green area) of the Haringvliet tidal delta

Construction considerations

A more northern location of the pumping station also has additional benefits from a constructability perspective. This location for the pumping station's building dock, puts it in close proximity to the Maasvlakte 2.

Making it far easier to access, than at the original location fig. 6.18a. Over the course of the entire construction process, the reduction in distance to the building pit, can have large impacts on the total amount of transport of materials that is required and reduce the total amount of navigation that has to occur in the tidal delta.

Additionally, similar to the environmental concerns related to the pumping station's operation, having the construction process further removed from the inner tidal delta would be an added benefit, when considering the noise, vibrations, and visual disturbances for the local community. This benefit only increases if this pumping station is also used as a prefab construction dock for the other structures of Delta21. As this means that construction in the inner delta is limited to the assembly of the spillway and New Haringvliet barrier, and the dredging operations for the Valmeer.

7

Design step 1: Spatial design

In this chapter the spatial design of the New Haringvliet barrier is presented. The aim is to determine the primary dimensions of the barrier and it's components. This will be done for the the three main barrier components: the gated section section 7.1, the dune section section 7.2, and the navigational section of the barrier section 7.3. The barrier location consists of the span between the Valmeer and the coast of Goeree-Overflakkee, and has a total length of 5km (fig. 7.1). This location gives ample space for the construction of the spillway between the tidal lake and the Valmeer, and is the shortest overall span between the Valmeer and the coast of Goeree, and was therefor chosen as the preferred construction location for the barrier.

Figure 7.1: Proposed barrier location (indicated in red) relative to the Delta21 Valmeer and the Haringvliet Ebb-Tidal delta

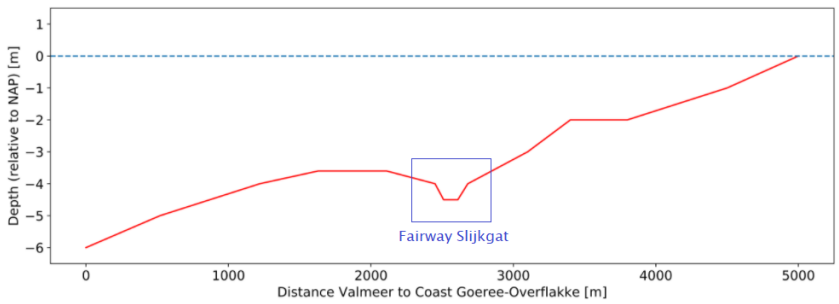

Figure 7.2: Bathymetry at barrier location from the Valmeer (left) to the coast of Goeree-Overflakke (right)

7.1. Gated barrier section

This section will outline the primary barrier dimensions and how they were determined. This includes the barrier retaining height, sill level, gate span, and a general overview of the barrier layout. Based on the results of chapter 6, the design of the gated barrier section is based on the premise that its construction will be done primarily with the use of prefabricated elements. This means that the basis of the design will be the use of caisson elements for the barrier's foundation.

7.1.1. Barrier Type

The barrier type selection for the New Haringvliet barrier was chosen based on a multi-criteria assessment of a total of six design criteria. The design criteria for the assessment were ranked and weighted using a priority matrix and each alternative was ranked on a scale of 1 to 5. In the case of the New Haringvliet barrier, there is no need for a navigational opening with a large span as the navigation in the region is limited to relatively small vessels. For more details on the navigational demands for the barrier more information is given in section 7.3. Therefor the gate type options in this assessment are limited to gates that excel in flow openings: vertical lift gates, flap gates, vertically rotating segment gates, radial gates, and inflatable gates (fig. 7.3). The full MCA, including the description of the specific criteria and the priority matrix is given in appendix E.

Results MCA

From the MCA (fig. 7.4), it can be found that the best suited barrier gate type for the New Haringvliet barrier is the vertical lift gate, followed closely by the radial gate. These gate types are some of the most used hydraulic gate types in flood barriers, and are well proven and generally cost effective solutions for barriers for barriers where a limited clearance height is acceptable. Given the length of the gated section (ca. 2000m), and the fact that the barrier will become part of the primary flood defence system of the Netherlands, gate types with large construction costs, or with reduced reliability such as rotating segment gates and inflatable gates become less desirable. The fact that vertical lift gates, are a well proven commodity, well maintainable, relatively low in cost and offer high reliability means that they are the best option for this barrier.

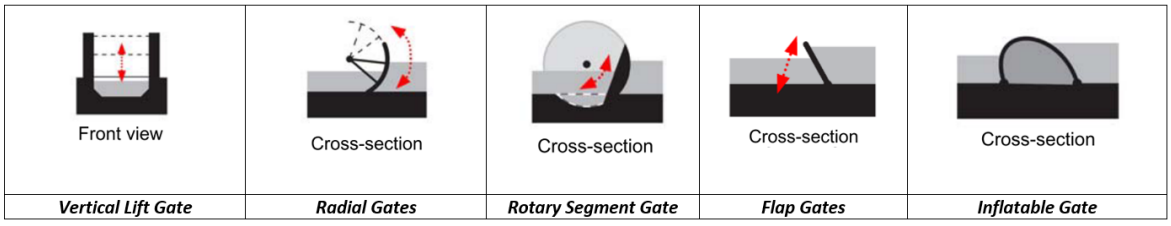

Figure 7.3: Schematic overview of the considered gate types for the New Haringvliet barrier. (images: Dijk and Van der Ziel (2010))

		Flap gates		Radial Gates		*Rotating Sector Gate*		*Inflatable Gate*		Vertical Lift Gate	
Criteria	Weight factor	Score	Weighted score	Score	Weighted score	Score	Weighted score	Score	Weighted score	Score	Weighted score
Maintenance	0.19	1	0.19	5	0.97	5	0.97	5	0.97	5	0.97
Construction Cost	0.32	3	0.97	4	1.29	2	0.65	4	1.29	4	1.29
Reliability	0.26	4	1.03	5	1.29	4	1.03	3	0.77	5	1.29
Ship collision	0.06	5	0.32	5	0.32	5	0.32	3	0.19	5	0.32
Operation in current + waves	0.13	3	0.39	4	0.52	4	0.52	3	0.39	5	0.65
Visual Impact	0.03	5	0.16	1	0.03	5	0.16	5	0.16	1	0.03
Total:	1.00	21	3.06	24	4.42	25	3.65	23	3.77	25	4.55

Figure 7.4: Multi-criteria analysis of the selection of the gate types

7.1.2. Construction location

The bathymetry of the construction location would suggest that the barrier would be best suited to be placed as much towards the Valmeer as possible (fig. 7.2), as this is the deepest part of the cross-section. However, due to the proximity of the barrier to the pumping station, it is at this point suggested to move the barrier slightly more south starting it roughly 1000m south from the end of the Valmeer. At this location, the barrier is still in a naturally relatively deep part of the section, while having some distance from the pumping station. The main concern here is that the operation of the Pumping Station during a storm event would locally increase the waterlevel. This could thus also effect the hydraulic demands on the New Haringvliet barrier during a storm event. The degree of this impact should be considered in future studies relating to the Delta21 project.

7.1.3. Retaining height

The retaining height of the barrier should be chosen in such a way that the amount of overtopping and overflow over the closed structure stays within reasonable bounds. During, a storm event, overtopping and overflow could pose a danger to the inland basin behind the barrier in two ways (Rijkswaterstaat, 2018):

1. The overtopping and overflow discharges reach a critical rate, at which the storage capacity of the basin behind the barrier is exceeded.

2. The overtopping and overflow discharges cause significant damage to the bottom protection, which leads to the erosion of the bottom around the structure, and eventual instability of the structure.

The area behind the New Haringvliet barrier consists of the tidal lake and the Haringvliet and Hollandsche Diep estuaries (surface area $\approx 200 km^2$). This makes it so that the system can accept large overtopping volumes during storms. The bed protection near the barrier is governed by the situation where a barrier gate fails to close during a normative storm event, thus from this perspective large overtopping discharges are also acceptable.Appendix D features the full overview of design calculations for the barrier's retaining height.

The minimum acceptable failure probability due to overtopping and overflow of the structure is $P_{f_{HT}} = 6.0e-5$. The corresponding design water level is $h_{NS} = 6.5m$, while the design wave-height is $H_{m0} = 3.76m$. After evaluating the impact of the barrier's retaining height on the overtopping and overflow discharge during a normative storm, a retaining height of +6m NAP was selected. Figure D.4 shows the combined overflow and overtopping discharges for a retaining height of +6m NAP. The maximum expected discharge over the storm duration is $q_{ot+of,max} = 3.6 m^3/s/m$, while the mean discharge is equal to $q_{ot+of,max} = 1.2 m^3/s/m$.

The total gated length of the barrier is $1600m$. This means that on average, during a storm, there will be an influx of roughly $1920 m^3/s$ of water into the basins behind the New Haringvliet barrier. Over a period of 25 hours that the barrier is expected to be closed, this yield a net inflow of $173 * 10^6 m^3$ of water into the basin. This amount to roughly a 0.9m increase of the waterlevel in the region behind the barrier (excluding river water inflow). This is generally well acceptable for a normative storm. In the case that the river water inflow is also high, the Valmeer and the spillway can be utilized to lower the waterlevel in the region behind the barrier. One consideration that should be noted is the effect of the overtopping discharge on the design of the hydraulic gates. Large overtopping/overflow rates ($q > 1.0 m^3/s/m$) can induce high dynamic load on the gates (Rijkswaterstaat (2018). The detailed dynamic design of the hydraulic gates is however out of the scope of this research and should be considered in a future study.

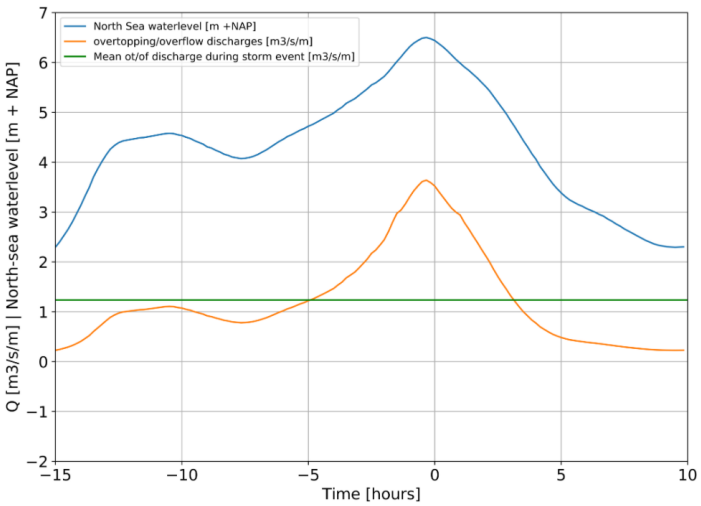

Figure 7.5: Combined overtopping and overflow discharges for a New Haringvliet barrier with a retaining height of +6m NAP for a normative North Sea storm (orange). The Corresponding North Sea waterlevel is also plotted (blue)

7.1.4. Sill level

The sill level for this project is chosen to be -5.5m NAP. The bathymetry of the construction location shows that the bed level ranges from roughly -3 to -4m NAP at the proposed barrier construction location (fig. 7.2). It is expected that the section will experience erosion due to the construction of the Valmeer restricting the cross-section of the tidal delta, and the final equilibrium bed level will indeed be lower (see appendix A). Due to the uncertainty related to the equilibrium depth, the choice was made to use the Haringvlietsluices as a reference structure for this design step, and to match the sill level of the New Haringvliet barrier to that of the Haringvlietsluices. This leaves a sill-level of -5.5m NAP.

7.1.5. Gate span

The gate span was determined by evaluating the effect the gate span has on the requirements for the foundational caisson elements on the barrier. This assessment was chosen as a primary metric due to the importance of the caisson elements in the overall cost and constructability of an prefab storm-surge barrier such as the New Haringvliet barrier. The full detailed analysis, including the hydraulic boundary conditions, the stability calculations and the caisson dimensions as a result of the assessment are given in appendix F.

In the assessments, gate span sizes of 40m, 60m, 80m, and 100m were compared. A span of 100m is roughly around the largest gate span seen in current barriers with vertical lift gates, so this was chosen as a upper limit for the assessment. The results of the calculation and is shown in table 7.1. Figure 7.6 gives an sketch of the storm surge barrier model that was used for the calculations.

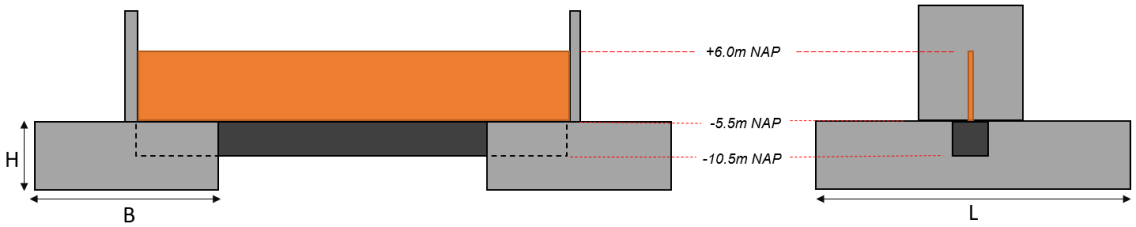

Figure 7.6: The primary dimensions and relative positions of the primary barrier elements [image NTS]

Gate span [m]	40	60	80	100
Caisson width (B) [m]	20	25	30	30
Caisson length (L) [m]	50	50	55	60
Caisson height (H) [m]	12	14	14	16
Total caisson volume [m3]	12000	17500	23100	28800
Relative span increase [-]	1.0	1.5	2.0	2.5
Relative caisson volume increase [-]	1.0	1.46	1.93	2.41
Total number of caissons required [-]	46	32	24	19

Table 7.1: Caisson dimensions for each respective gate span

From the results for the caisson dimensions, it can be seen that the total volume of the caissons increases roughly proportional to the gate span of a section. This means that the choice in gate span will not significantly impact the total amount of material that is required for the construction of the caissons.

From a construction process point of view, a larger span would be greatly beneficial as it strongly reduces the construction of a smaller number of caissons to reach the desired wet-cross section for the barrier. For the construction process this would have the following implications:

- There would be a reduction in the total amount of transport of caissons between the building dock and the final assembly location. Even though the elements might be larger, and thus would require more effort to transport and place accurately. However, even the largest caissons in this case are of a feasibly manageable size.
- A smaller construction dock would be required. In the building dock, the individual caisson elements would have to be separated to allow for transport of materials and construction equipment throughout the building dock. Having fewer total elements to be constructed in the building dock would lead to a net reduction in the amount of space needed for these spaces, and thus also the total amount of space required in the building dock.

Based on the caisson elements and their relation to the gate span, it would be recommended to choose the section of a single gate opening as large ass possible. However, it should be noted that the relation between the number of gate openings and the span of each gate is an inverse relation (see eq. (F.9)). Thus the larger the span becomes, the less effective the impact of increasing the gate span is on the total number of required caisson elements. On the other hand however, the other structural elements, such as the gate, walkway, and sill beam are subject to distributed loads, and are subject to large bending moments, which scale quadratically with the span of the respective elements.

The final choice for the gate span is to select a single gate span of 80m. This was done as increasing the gate span to 100m would have a relatively small impact on the total number of caisson elements that would have to be constructed and transported. While on the other hand there would still be a significant lower normative bending moment (36% reduction for a 80m span relative to 100m spans under a uniform distributed loads on a simple supported beam) that the sill-beam, walkway and gates would be subjected too.

7.1.6. Spatial design gated barrier

With all the design considerations from the previous sections, the spatial design of the gated section is summarized in table 7.2. In the original gate span assessment, the number of caisson elements were decided by dividing the desired effective barrier opening by the sill level. In this iteration of the design it was assumed that the barrier gates will be recessed at a level of +1.0m NAP. Effectively creating an maximum opening height of 6.5m. Thus only 20 gates are required for a maximum opening cross-section of over $10000 m^2$.

	Description	Value	Unit
Gate dimensions	Sill level	-5.5	m NAP
	Retaining height gates	+6.0	m NAP
	Gate span	80	m
	Total gate height	11.5	m
Caisson dimensions	Height	14	m
	Width	30	m
	Length	55	m
	Placement level caissons	-19.5	m NAP
Total barrier overview	Number of gates	20	-
	Effective barrier opening	10400	m^2

Table 7.2: Spatial design gated barrier section

7.2. Permanently Closed Section

Delta21 recommends the construction of a dune-like dam section for the permanently closed sections of the Haringvliet barrier (fig. 7.9). The sand-dam would allow for an extension of the dune and beach area of Goeree, providing a natural and ecologically friendly barrier solution. Additionally, it would provide the option to re-use the large amounts of sand that will be yielded from the construction of the Valmeer.

The use of a dune like structure as a dam to close an estuary, has not been done before in the Netherlands. As a result there is currently no standard for the design of such structures within the WBI2017. Coastal dunes are typically morphologically active parts of the foreshore of a coast. During a storm, when the storm surge reaches the dune face, the dune will rapidly erode and retreat (fig. 7.7). In the case that there is no sediment gradient along the coast, the waves, wind, and the tide will restore the profile of the eroded dune. The timescale for the recovery however, is much larger than that of the initial erosion. In the case that there is a net erosion along the foreshore, there might be structural losses to the dune, which would require maintenance or other interventions to prevent.

To get an first idea of the dimensions of the dune sections of the barrier, the design of the dunes on the western side of the Valmeer were used. The full design of these dunes can be found in van Dam (2020). The dunes were designed for a storm with a water-level of $h_{NS} = 4.0m + NAP$, a wave-height of $H_{m0} = 4.0m$, and a wave period of $T_s = 12.85s$. The design of these dunes will still have to be verified from a flood safety perspective for their use in the storm surge barrier section of the Delta21 project. Figure 7.8 shows a sketch of the dune section and it's primary dimensions. To account for the construction of an access road to the barrier, the design of the original dune was altered slightly, and an extra section with a width of 20m was added to the interior (river) side of the dune. The structural integrity of this road, and it's inclusion in the dune design is not considered in this project, and should be verified at a later stage of the dune design as well.

The dune consists of a base layer that ranges from the sea bed to a level of +1.0m NAP. At the North sea side of the dune there is a foreshore ranging from +1.0m NAP to +4.0m NAP, with a slope of 1:63. The main dune is a steep dune with a slope of 1:3 up to a crest level of +18m NAP. The backside of the dune has a slope of 1:2 on the main dune section, after which the slope reduced to 1:12.5 from a level of +4.5m NAP to the sea bed. In total if we consider the sea bed level to be similar to the sill level of the barrier, this amounts to a base width of 485m. it should however be noted that due to the fact that this dune would be part of the primary flood defense system of the Netherlands, it's dimensions would still have to be verified for all of it's failure mechanisms, which could still have a significant impact on the dune's dimensions.

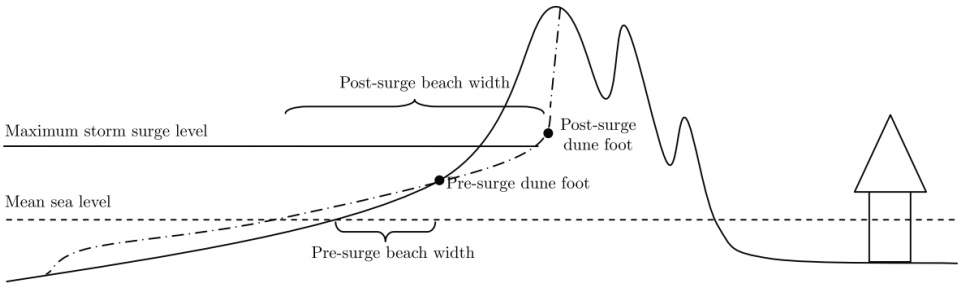

Figure 7.7: Typical dune erosion due to storm surge, when the surge reaches the dune face (source: Van Thiel de Vries (2009))

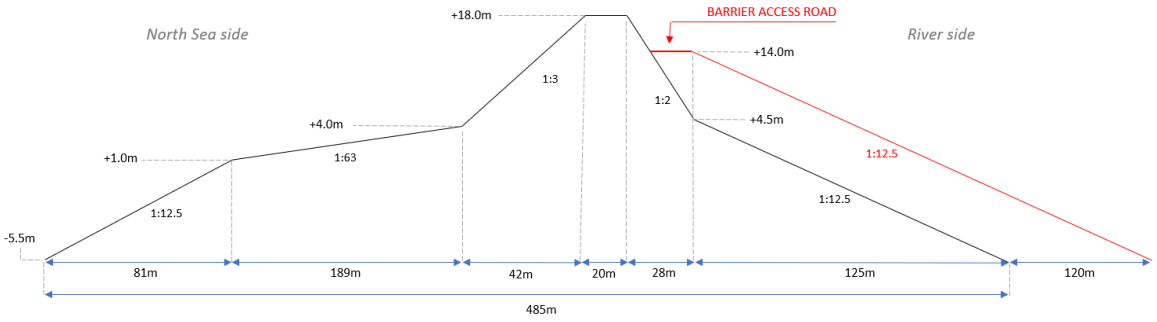

Figure 7.8: Sketch of the dune design as described by van Dam (2020). The sea bed in this image is set to a level of -5.5m NAP. Alterations to the original design, for the inclusion of an access road to the barrier, are shown in red. [image NTS]

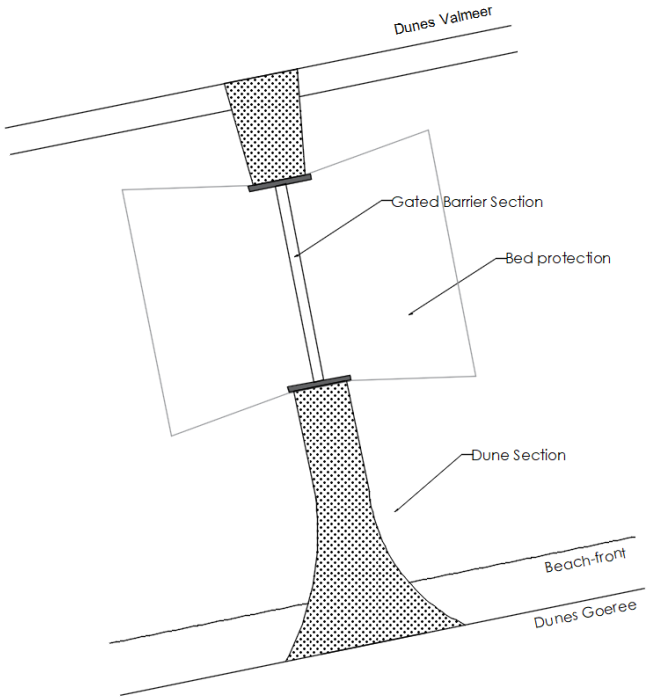

Figure 7.9: Proposed Delta21 sand-dune barrier layout

7.3. Navigation Options

This section will outline the navigation options for the New Haringvliet barrier.

7.3.1. Navigation route Haringvlietsluices

Currently, navigation past the Haringvlietsluices occurs through the Goereese Sluis, a navigation lock located south of the Haringvlietsluices (fig. 7.10). The lock is most commonly used by recreational and fishing vessels, but the lock chamber has a length and width of 144.5m and 16.38m respectively, which allows for vessels such as dredgers, floating cranes and barges to pass as well. The bottom of the chamber is located at a depth of -5m NAP, such that vessels with a draught of 3.5m can pass the lock during low tide. When sailing North through the Haringvliet tidal delta, all sailing passes through the Slijkgat (fig. 7.10a). The Slijkgat is a fairway that is maintained by the Port of Rotterdam to allow sufficient navigation depth (-4.5m NAP) for the design vessels in the location.

(a) (b)

Figure 7.10: Navigation route past the Haringvlietsluices through the Goereese Sluis and the Slijkgat (a), and an overview of the Goereese sluis layout (b)

7.3.2. Possible navigation options

Due to the location of the current navigation routes in the region, the navigation option for the New Haringvliet barrier should also be located at the south side of the barrier. For the navigation options of storm surge barriers the option exists between having a gated navigation opening, or a navigation lock to pass the barrier.

For average tidal flow velocities larger than 1.5m/s, a navigational opening in the storm-surge barrier is not generally feasible (Mooyaart et al., 2014). In the case of the New Haringvliet barrier, where the main traffic consists of smaller vessels, this criteria might even be more stringent. In the case that the tidal currents are too strong for a navigational opening, a shipping lock will be necessary in order to allow shipping into the Haringvliet. This would mean that sailing from the Haringvliet to the North sea would require a ship to pass through two locks. Although inconvenient, there is no large scale commercial shipping happening through the Haringvliet, and therefore, there will not be significant economic downside to the extra lock being installed.

Navigation Opening

The option for having a navigation opening depends on many factors but is mostly limited based on the preceding hydraulic conditions near the barrier. Many barriers, are subject to the high local currents making a navigation opening in the barrier a non-viable option. The individual gate span in this project is chosen

to be relatively large (80m) so the possibility for a navigation opening exists. However, this would require an alternate gate design for this particular opening as currently, the use of vertical lift gates would strongly limit the clearance height of the opening.In order to determine the feasibility for this option however, a more in-depth hydrodynamic assessment is required.

Shipping Lock

A shipping lock would remove all the navigational requirements from the barrier itself. An example overview of a navigation lock for the New Haringvliet barrier is given in fig. 7.11. The main downside of a navigation lock is that there are waiting times depending on the traffic intensity at the location. Constructing a lock to pass the New Haringvliet barrier, would thus mean that vessels planning to ship from the Haringvliet onto the North Sea would have to pass two shipping locks, which is generally undesirable. The navigation lock does have the added benefit that it provides sheltered berthing locations. Such a berth will be highly beneficial in the supply of maintenance materials and equipment to the barrier by water.

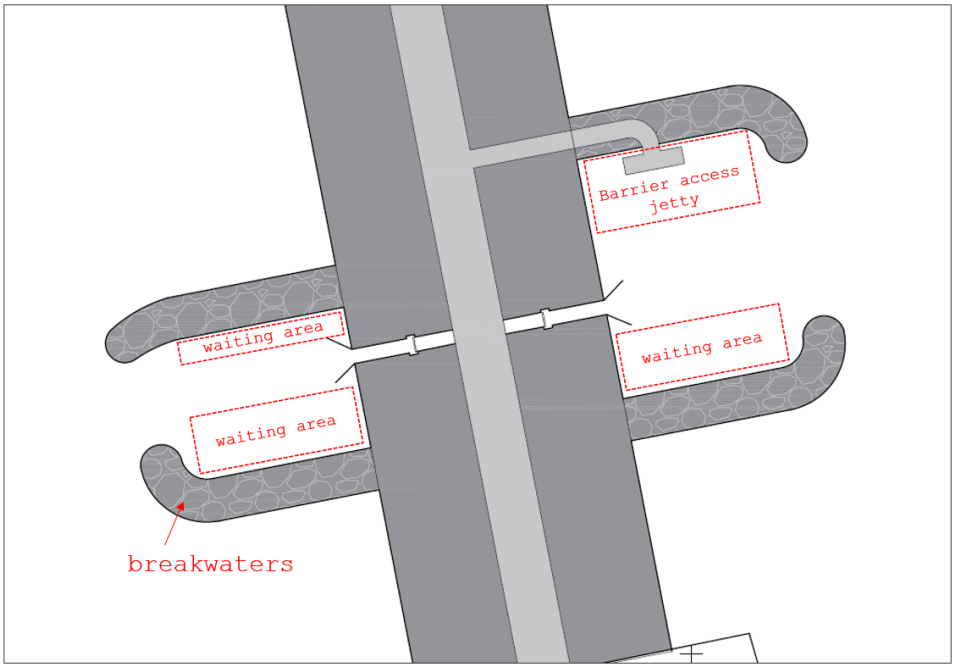

Figure 7.11: Potential navigation lock layout

7.3.3. Conclusion navigation opening

The choice in the type of navigational barrier strongly depends on the final hydraulic boundary conditions near the barrier. Given the fact that the traffic across the barrier in this case mainly consists of smaller recreational and fishing vessels, the choice was made to opt for a lock as the barriers primary navigation opening. The lock can guarantee save sailing conditions for all vessels past the barrier for a wider range of weather conditions. Additionally, the lock area can be feature additional berthing locations that allow access to the barrier over any of the breakwaters.

7.4. Combined spatial design

The full spatial design sketch of the barrier is given in fig. 7.12. Due to the large width of the sand-dunes, a transitional structure between the gated barrier section and the dune sections of the barrier is required. For this connection, it is recommended to apply erosion protection to the edges of the dunes, as well as a transitional structure in the form of a short breakwater.

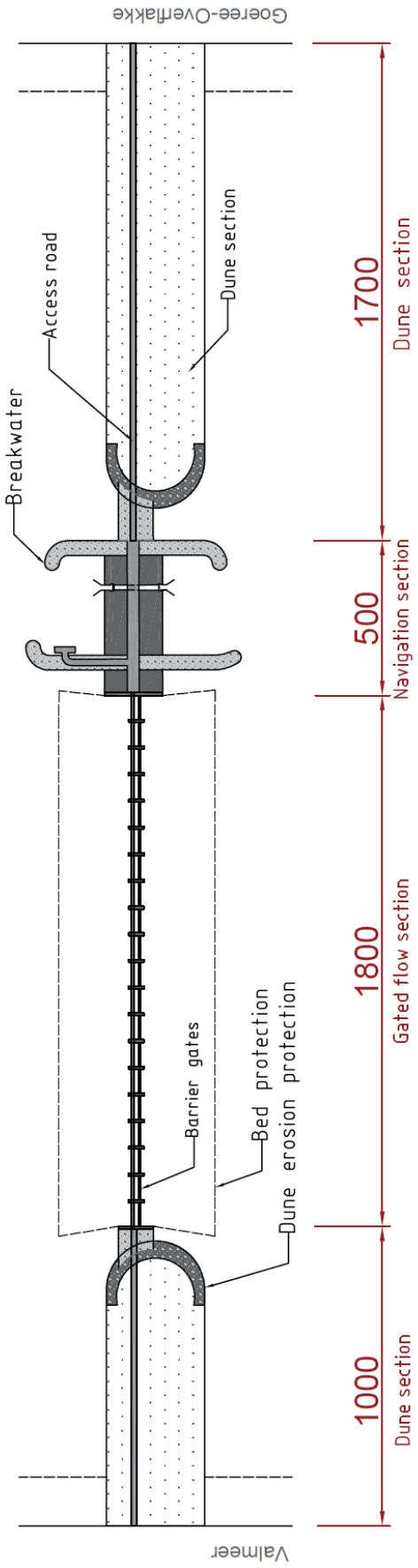

Figure 7.12: Spatial design for the New Haringvliet barrier. The dune sections are connected to the structural barrier elements by short breakwater sections. The navigation section is a shipping lock sheltered by breakwaters.

7.5. Spatial design conclusions and discussion

In this chapter the spatial design of the New Haringvliet barrier was designed. Firstly the gated barrier section of the structure was evaluated. The large barrier span made it so that reliability, cost and inspection and maintenance capabilities were the primary determining factors in the selection of the gate type for the barrier. A multi-criteria analysis showed that the most desirable gate type for these criteria was a vertical lift gate.

The gate span of each individual gate was chosen to be 80m. A gate span assessment was done by evaluating the impact of the gate span on the total number of caisson elements that were required for the construction of the barrier, and their dimensions. This was done based on the assumption that the construction and placement of the caissons will be a driving factor in the costs of the overall project. From this assessment, it was found that there was no real benefit to be found in the total amount of concrete required for the caissons, based on the overall gate span of the structure. And eventually the choice was made to opt for a large single span gate as it would require overall less caisson elements that would have to be transported between the dry dock and the final location, as-well as less space in the dry dock.

A smaller span gate would definitely also be a possibility however. In that case the project would generally experience a higher repetition factor and it would be easier to design and construct the additional barrier elements such as the gates, sill beam and walkway, that now each have to span significant distances. It is recommended that this choice is optimized on in future studies, by evaluating the impact of the single gate span on the cost total cost of all the barrier elements.

For the permanently closed barrier section of the barrier, Delta21 recommends the use of sand dunes. This was also incorporated into the spatial design by using the design of the Valmeer dunes designed by van Dam (2020). The design of the dunes was slightly altered to feature a 20m wide flat section for an access road behind the crest of the dune. Additionally, the choice was made to incorporate a navigation lock with berthing locations that can be used to access the barrier by water. The construction of the access road, and the the overall flood safety of the dunes still needs to be designed in full detail to get a better idea of the final dimensions of the dunes.

8

Design step 2: Gated barrier design

In chapter 7, an overview of the desired layout for the overall Haringvliet barrier and it's components was provided. In this chapter the gated barrier section of the barrier will be designed in more detailed. From the spatial design, and the construction sequence assessments, the following elements were identified as core barrier components:

- **Piers**: the barrier piers consist of a foot (caisson) that functions as the structure's foundation, and a pillar to support the hydraulic gates, walkways and the barrier mechanical infrastructure.
- **Scour protection**: the barrier is in need of a scour protection to prevent erosion of the bed near the barrier. Bed erosion could lead to significant damage or instability of the structure.
- **Hydraulic gates**: the preferred gate type for the structure was determined to be a vertical lift gate.
- **Walkway:** to ensure barrier access for inspection and maintenance purposes a walkway should be added to the barrier.
- **Sill beam:** in the case of a granular bed protection, a sill beam is required to allow for the proper closure of the vertical lift gates

A sketch of the various components is given in fig. 8.1. From these element this chapter will be focused on the design of three primary components: the base of the piers, the hydraulic gates and the scour protection. These three elements were identified as the most normative design components for the barrier's overall feasibility, cost, and construction method.

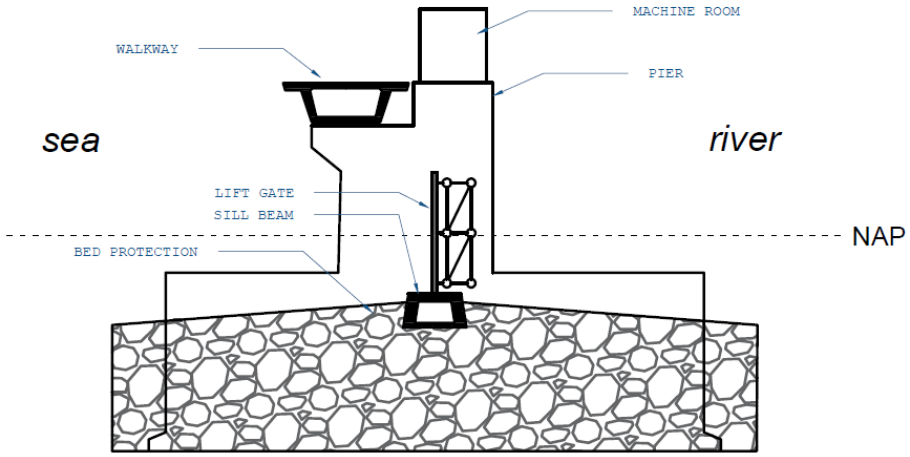

Figure 8.1: Sketch of an example layout for a lift-gate configuration of the gated barrier section

8.1. General construction sequence

To get a clear overview of the requirements for the design of the gated barrier section the construction sequence of the barrier is given below.

1. Construction of a prefab dry dock for the construction of the barrier elements
2. Start construction of the prefab caisson elements
3. Dredging of a trench for the transport and placement of the caisson elements
4. Soil improvement and preparation at the barrier construction location
   (a) Replacement of unsuitable subsoil (removal of the subsoil down to a level of roughly -24m NAP to remove any clay layers)
   (b) Soil compaction of the remainder of the subsoil to improve the bearing capacity of the subsoil
   (c) Bed leveling and placement of a rock foundation bed for the caissons
5. Transport and placement of the caissons at the final location
6. Completion of the piers at the final location using prefab elements
7. Back-filling of trench, placement of the sill, and construction of bed protection
8. Placement of the hydraulic gates and road girder elements

8.2. Caisson transport stability

The initial dimensions for the foundation caisson were determined in the gate span assessment (see appendix F). These caisson were designed based on their stability during a normative storm event. However, the stability of the caissons during transport has not yet been verified.

From the construction sequence, and the caisson dimensions it can be concluded that the caisson elements will have to be placed at a level of -19.5m NAP. This puts the top of the caisson at the sill level of -5.5m NAP. From a constructability point of view, it is necessary for the base of the pier to be transported as part of the caisson. This base should extend above the local water-level to allow for the pier to be finished at the final barrier location using prefab construction elements. As a first estimate a it is deemed acceptable for the pier base to be placed to reach a level of +3.0m NAP.

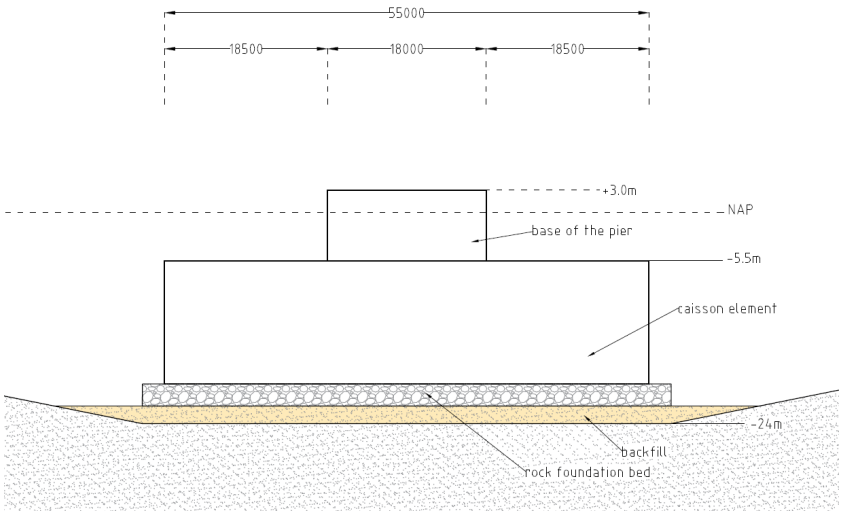

Figure 8.2: Caisson element placed on the rock bed foundation after soil improvements

The addition of the base of the pier, can make the caisson element less stable for transport as it raises the center of gravity of the structure. It is preferable for the element to be independently stable during transport as it would eliminate the need for the construction of special hoisting vessels (e.g. the Ostrea, a large custom hoisting vessel that was used in the construction of the Eastern Scheldt barrier).

8.2.1. Static stability

To avoid instability during transport of the elements, the metacentric height of should be larger than 0.5m (Molenaar & Voorendt, 2019). If this is the case, any rotation of the element will be counteracted by a correcting moment. For the weight of the caisson, 30% of the volume of the caisson was assumed to be concrete, with the remainder being available for ballasting material. For the pier, a slightly higher concrete volume percentage of 40% was used. The weight of the respective elements is calculated and shown below.

$$F_{w,caisson} = 55 * 14 * 30 * 0.3 * 25 = 173250 kN/m^3 \tag{8.1}$$

$$F_{w,pier} = 18 * 6 * 8.5 * 0.4 * 25 = 9180 kN/m^3 \tag{8.2}$$

The next step was to determine the center of gravity of the structure. As the detailed structural design of the caissons is out of the scope of this research, the following caisson dimensions were estimated for the caisson stability calculations:

- thickness top slab: $t_t = 1.0m$
- thickness bottom slab: $t_b = 1.0m$
- thickness outer walls: $t_{w,o} = 0.7m$
- thickness inner walls: $t_{w,i} = 0.5m$
- number of length-wise oriented inner walls: n = 3
- number of width wise oriented inner walls: n = 8

The distribution of the inner walls was chosen to be as uniform as possible, while the total amount of concrete used come down to 30.4% of the total caisson volume. Equation (8.3) shows the equation used to determine the center of gravity of the caisson element.

$$\overline{KG} = \frac{\sum F_{w,i}\, e_i}{\sum F_{w,i}} \frac{173250 * 7 + 9180 * 18.25}{173250 + 9180} = 7.57m \tag{8.3}$$

where:

$F_{w,i}$	= weight of an element i	$[kN]$
e_i	= distance from the bottom edge of the caisson to the center of an element i	$[m]$

The center of buoyancy of the element is halfway between the bottom of the structure and the waterlevel while the element is floating. The draught is calculated by using Archimedis' law.

$$d = \frac{F_w}{b\, l\, \gamma_w} = \frac{182430}{55\ m * 30\ m * 10.25\ kN/m3} = 10.8\ m \tag{8.4}$$

$$\overline{KB} = 0.5d = 5.4\ m \tag{8.5}$$

Lastly, the distance between the meta-centre and the centre of buoyancy is determined using eq. (8.6)

$$\overline{BM} = \frac{I}{V} = \frac{\frac{1}{12} * 55 * 30^3}{55 * 30 * 10.8} = 6.94m \tag{8.6}$$

I	= mass moment of inertia of the area that intersects the water surface	$[m^4]$
V	= volume of displaced water	$[m^3]$

Lastly the metacentric height is calculated and is found to be equal to $h_m = 4.8m$. Thus there is no problem with the static stability of the caisson and pier combination during transport.

$$h_M = \overline{GM} = \overline{KB} + \overline{BM} - \overline{KG} = 5.40 + 6.94 - 7.57 = 4.8m. \tag{8.7}$$

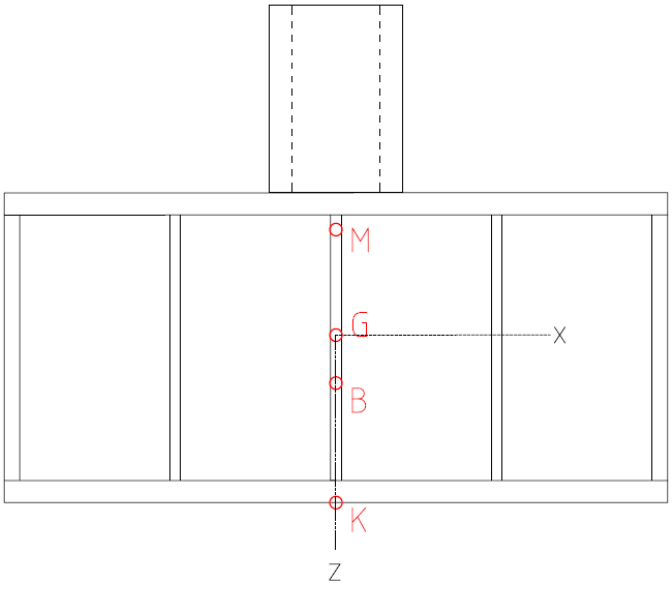

Figure 8.3: Locations of the meta-centre (M), center of buoyancy (B), centre of gravity (G) and the base point (K)

8.2.2. Dynamic stability

For the dynamic stability during transport two general evaluations are done. The first evaluation criteria is that, the caisson dimensions (width and length) should be large compared to the local wavelength to avoid the caisson rolling or pitching with the incoming waves. The common rule of thumb is that the wavelength should be smaller than 0.7 times the width or length of the transported caisson:

$$L_w < 0.7\,L = 0.7 * 55 = 38.5m \tag{8.8}$$

$$L_w < 0.7\,B = 0.7 * 30 = 21.0m \tag{8.9}$$

This criteria is easily satisfied for the expected wave conditions.

The second criteria is that the period of wave movements should not come close to the natural oscillation period of the transported caisson. The natural oscillation period of the structure is given by:

$$T_o = \frac{2\,\pi\,j}{\sqrt{h_m\,g}} \tag{8.10}$$

T_o	= natural oscillation period		$[s]$
I_p	= polar mass moment of inertia	$(= I_{zz} + I_{xx})$	$[m^4]$
h_m	= metacentric height		$[m]$
j	= polar inertia radius	$(= \sqrt{\frac{I_p}{A_c}})$	$[m]$

As a first estimate, only the caisson dimensions are considered in this dynamic stability assessment (see fig. 8.3 for the caisson geometry that was considered in the calculations). The final mass moment of inertia for the respective axes was determined to be the following:

$$I_{zz} = 1688 m^4 \tag{8.11}$$

$$I_{xx} = 7181 m^4 \tag{8.12}$$

$$I_p = I_{zz} + I_{xx} = 8867 m^4 \tag{8.13}$$

This yields a polar inertia radius of:

$$j = \frac{I_p}{A_c} = \frac{8867\ m^4}{154.8\ m^2} = 57.3 m \tag{8.14}$$

Lastly the natural oscillation period is determined. The natural oscillation period of the caisson far exceed the wave periods that can be expected during the transport of the caisson, and therefor the dynamic stability of the element is found not to be a problem.

$$T_o = \frac{2\,\pi\,57.3}{\sqrt{4.77\,9.81}} = 52.7 s \tag{8.15}$$

8.3. Gate Design

This section of the report will outline the design of the vertical lift gates in the New Haringvliet barrier. The aim of this section is to get a first overview of the gates dimensions and weight.

8.3.1. Gate system design

For the design of the vertical lift gates, the Hartelkering and the Hollandsche Ijsellkering were used as reference projects. Both barriers are among the largest single span vertical lift gates in the world, with the Northern gate of the Hartelkering spanning 100m, and both gates of the Hollandsche IJsselkering having a span of 80m. Both barriers have a rather similar design, both consists of a skin plate , backed by a load bearing frame in the form of a tied-arch. The main difference between the structures is the fact that the skin plate in the case of the Hartelkering is curved, this allows for a more preferable center of mass for the structure. Both the arched beams, and the beams between the back arch and the skin plate are vertically cross-braced for more stability and structural rigidity in both gates.

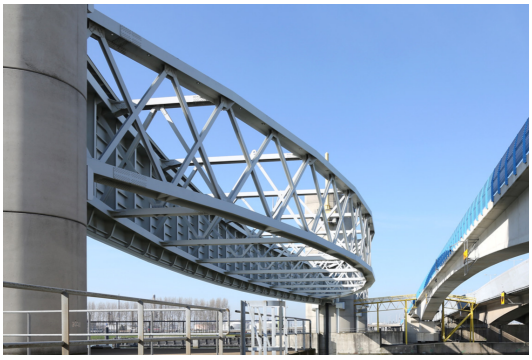

(a) Hartelkering

(b) Hollandsche IJselkering

Figure 8.4

New Haringvliet vertical lift gate system
A schematization for the gate system design of the New Haringvliet barrier is given in fig. 8.5. As mentioned, the barrier is designed to consist of a stiffened skin plate, backed by the an arched load bearing frame. To determine the size and the and spacing of the structure, the barrier will be schematized as a simply supported

beam, where the skin plate, and the arch carry the bending, and the supporting beams transfer the shear forces.

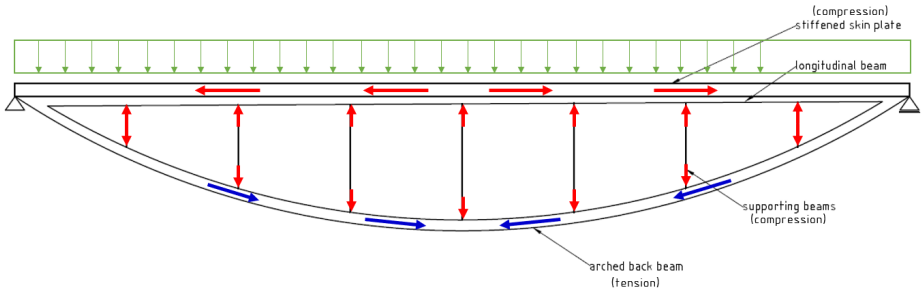

Figure 8.5: Schematized top view for the New Haringvliet barrier, including the force distribution throughout the system for a distributed load

8.3.2. Design load

For the design of the gates, the same design loads will be used as those for the design of the hydraulic caissons. An overview of the design conditions is given in fig. 8.6. The hydrostatic pressures are determined using the hydrostatic pressure equation (eq. (8.16)), and the normative wave load is calculated using the Sainflou method (see appendix F.2 for a complete overview of the Sainflou method). With these design conditions and the given equations, the hydrostatic pressures along the gate length were determined (fig. 8.7). Integration of the net hydrostatic pressure diagram yields that the design load on the gates is, $q = 798kN/m$. It should be noted that this design does not take into account the dynamic interaction between fluid and structure. This will have to be addressed in future research.

$$p = \rho_w g h \tag{8.16}$$

where:

p	= water pressure	$[Pa]$
ρ_w	= density of water$(= 1025kg/m^3)$	$[kg/m^3]$
h	= pressure head	$[m]$

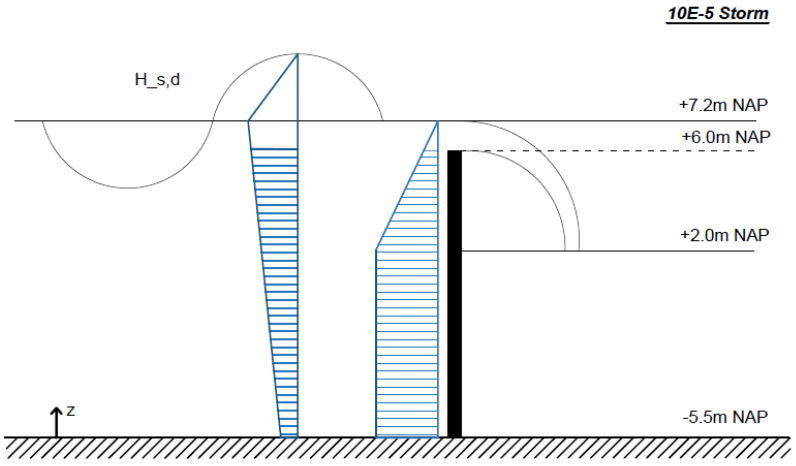

Figure 8.6: Quasi-steady diagrams for wave and hydrostatic loads on the gate ($H_{s,d} = 3.96m$)

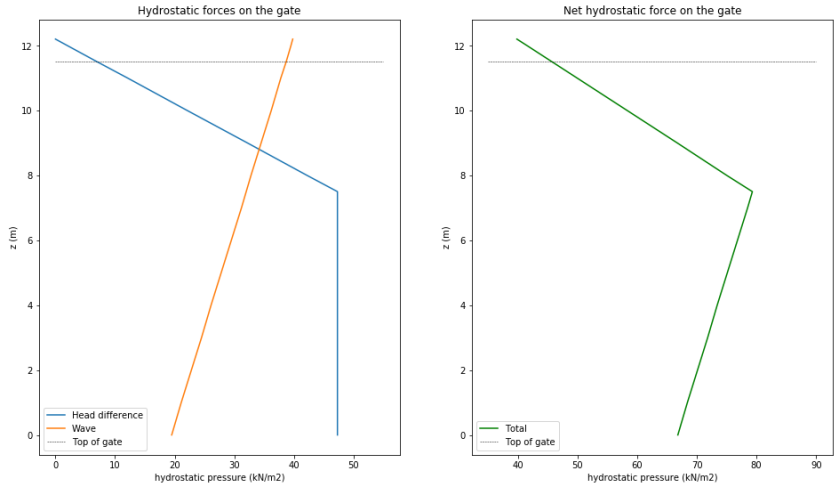

Figure 8.7: Design hydrostatic and wave pressure distributions (net positive forces indicate a loads on the North Sea side of the gate)

8.3.3. Skin plate design

The first step in the design process, is the design of the skin plate and it's stiffeners. The skin plate thickness of the gates was chosen to be $t_{skin} = 20mm$. The skin plate will be supported by both longitudinal stiffeners and transverse girders that will transfer the forces to the main supporting structure of the gate. The stiffeners are oriented horizontally along the structure, spaced 750mm apart from each other. The girders on the other hand span along the vertical axis of the gates and are separated by 2500mm. The design process of these stiffeners is given in appendix H. The profiles for the longitudinal stiffeners and the transverse girders are given in fig. 8.11, and fig. 8.10 respectively.

8.3.4. Load bearing frame design

For the design of the load bearing frame, the system was evaluated as a simply supported beam loaded by a uniformly distributed load. The mid-section of the gate was used to determine the design of the arched beam and the longitudinal beam. For the longitudinal beams, a HE500A profile was chosen. For the arched beam a custom profile was designed, see fig. 8.8.

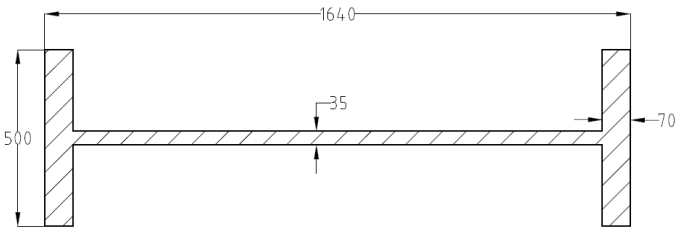

Figure 8.8: Custom cross-section for the arched beam (dimensions given in mm)

Global bending evaluation

The maximum bending moment for the gate occurs at the middle of the span and is equal to $M = 640000 kNm$ (eq. (8.17)) After application of a design safety factor of $\gamma_s = 1.2$, the design bending moment is equal to $M_{ed} = 768000\, kNm$.

$$M = 0.125 * q * L^2 = 0.125 * 800\, kN/m * (80\, m)^2 = 640000\, kNm \tag{8.17}$$

To evaluate the bending moment resistance of the gates all longitudinally oriented elements are considered. This includes the skin plate (including longitudinal stiffeners), the arched beam, and the longitudinal support beams. A sketch of the middle cross-section and it's relevant elements is given in fig. 8.9. Firstly the centroid of the cross-section is determined using eq. (8.18). The distance between the arched beam and the longitudinal beams in this case is 14000mm. After calculation of the centroid location, the mass moment of inertia is determined around the z-axis of the centroid. The results of the computation is given in table 8.2.

$$y_{n,centroid} = \frac{\sum y_{n,i}\, A_{total,i}}{\sum A_{total,i}} = 9627\ mm \tag{8.18}$$

Once again the maximum bending stresses in the outer most fibres of the cross-section is evaluated, and it is determined that a steel type of S355 suffices for the designed cross-section.

$$\sigma_{b,skin} = \frac{M_y\, y_{skin}}{I_{yy}} = \frac{7.68 * 10^{11}\, Nmm * -7143\, mm}{2.40 * 10^{13}\, mm^4} = -288.8\, N/mm^2 \tag{8.19}$$

$$\sigma_{b,arch} = \frac{M_y\, y_{arch}}{I_{yy}} = \frac{7.68 * 10^{11}\, Nmm * 9627\, mm}{2.40 * 10^{13}\, mm^4} = 308.3\, N/mm^2 \tag{8.20}$$

where:

σ_b	= bending stresses	$[N/mm^2]$
y_{arch}	= distance from the centroid to the outer edge fibres of the arched beam	$[mm]$
y_{skin}	= distance from the centroid to the outer edge fibres of the skin plate	$[mm]$
M_z	= design bending moment	$[Nmm]$
I_{zz}	= mass moment of inertia in the z- plane	$[mm^4]$

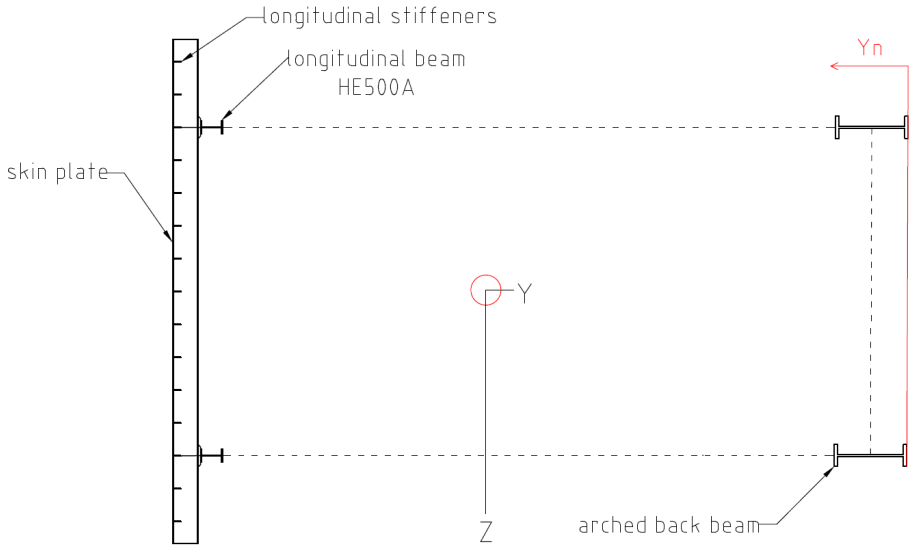

Figure 8.9: Cross-section for the bending moment assessment

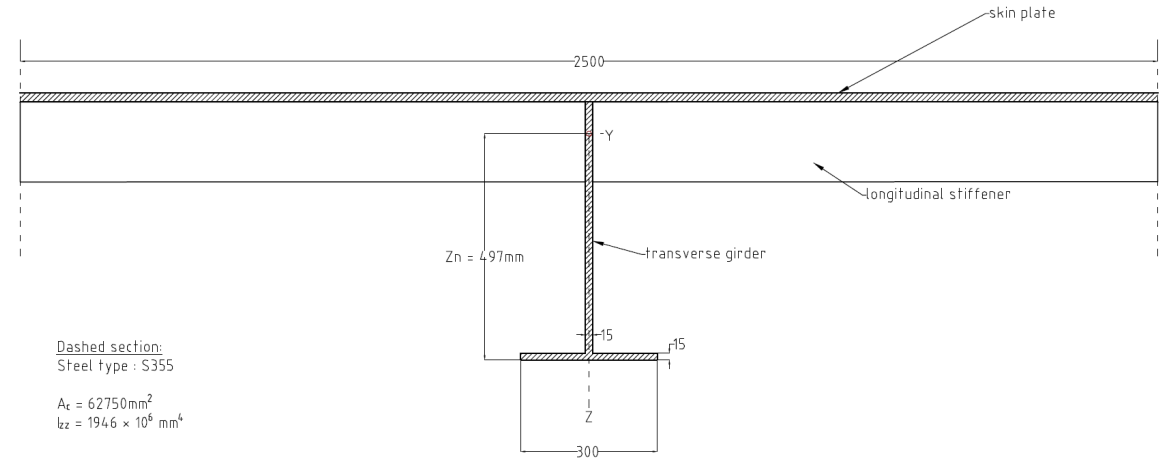

Figure 8.10: Design dimensions of the transverse girders (skin plate and transverse girder)

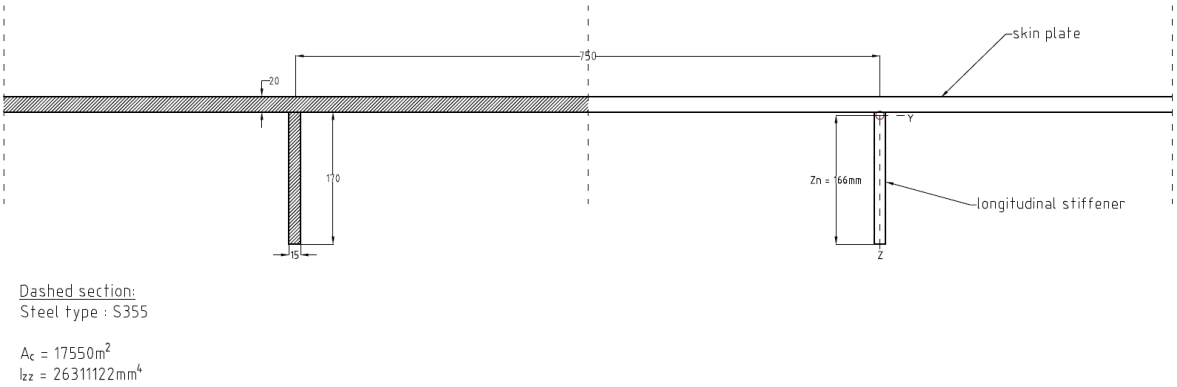

Figure 8.11: Design dimensions of the longitudinal stiffeners, the right side indicates the location of the centre of mass of each section (skin plate and stiffener)

Element	*number of elements [-]*	$b\,[mm]$	$h\,[mm]$	$t_w\,[mm]$	$t_f\,[mm]$	$A\,[mm^2]$	$A_{total}\,[mm^2]$	$y_n\,[mm]$
Skin plate	1	11500	20	-	-	230000	230000	16760
Longitudinal stiffeners	15	15	170	-	-	2550	38250	16665
Longitudinal beam	2	300	490	12	23	19800	39600	15885
Arched beam	2	500	1640	35	70	122500	245000	820

Table 8.1: Dimensions of the elements that contribute to the bending assessment, see eq. (8.18) for a visual overview of the cross-section

Element	I_{yy} x 10^6 $mm4$	*y- distance to centroid* $[mm]$	$I_{yy,steiner}\,[mm]$	$I_{yy,total}\,[mm]$
Skin plate	7.67	-7131	1.17E+13	1.17E+13
Longitudinal stiffeners	92.12	-7038	1.89E+12	1.89E+12
Longitudinal beam	1739.4	-6258	7.75E+11	7.77E+11
Arched beam	106016	8807	9.50E+12	9.61E+12
Total				2.40E+13

Table 8.2: Mass moment of inertia contribution of the various elements that contribute to the bending assessment, see eq. (8.18) for a visual overview of the cross-section

8.3.5. Overview of gate design

Following the primary design assessments of the vertical lift gate, the design geometry was imported into Matrix-Frame for the final structural validations (see appendix H). The supporting beams were modelled with hinged connections, so that the only transfer axial loads. To reduce the deformations of the structure, additional diagonal supported beams were added to the edges of the barrier.The final displacement diagram of the structure is given in fig. 8.12. For a complete overview of the gate design, see fig. 8.13.

The supporting beams are taken to be a HE500A profile, these easily suffice the axial loading and buckling strength criteria. However, to minimize the deformations of the barrier these were selected. For the cross-bracing members, a HE260A profile was chosen, these were also used in the Hartelkering, no additional checks for the requirements of these members was done, as that is out of the scope of this project.

Total barrier weight

A summation of all the steel elements used for the gate design yields a total steel mass of roughly 460ton. This does not include the weight of any detailing, or the additional connecting elements between the barrier and the piers. This could easily increase the mass of the barrier towards the range of 500ton. For reference the weight and spans of the reference gates are listed below.

- Hartelkering - Northern Gate (span: 98m) - 640ton
- Hollandsche IJsell - Northern Gate (span: 81m) - 590ton

The modelled weight of the barrier is very comparable to that of the reference structures. One thing to note however is that these gates are part of barrier that consist out of either a single or double barrier span. The New Haringvliet barrier would require a total of 20 gates to span the entire section. From this perspective is might be beneficial to evaluate the cost of construction in addition to the cost of material, as ease of construction become increasingly valuable in the case that 20 gates are required.

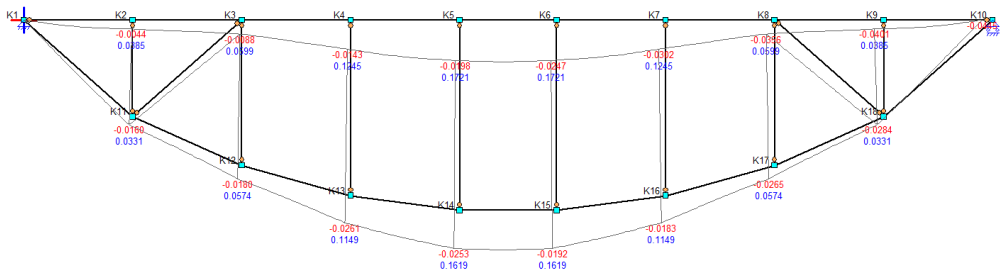

Figure 8.12: Displacement diagram for the vertical lift gates

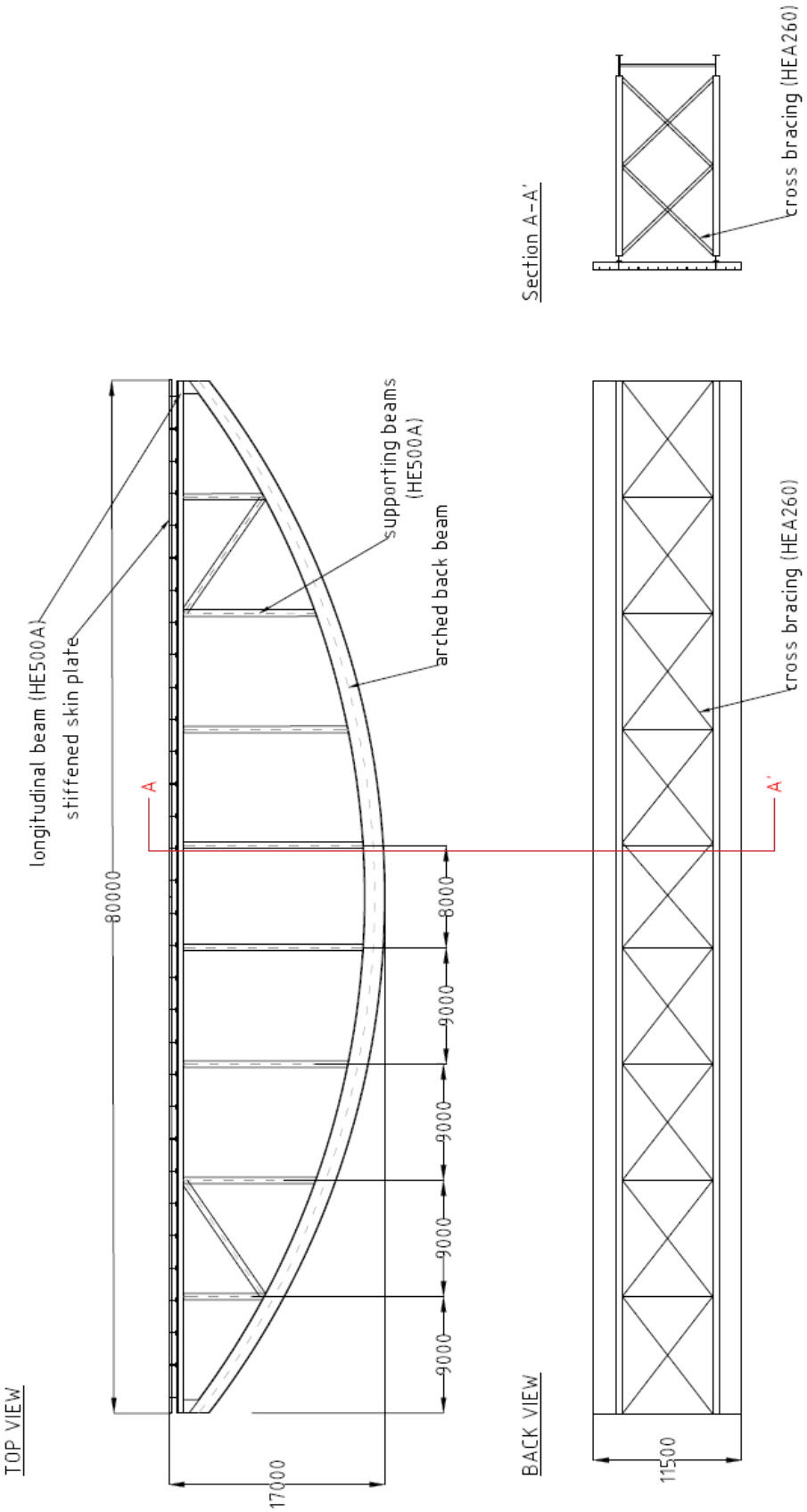

Figure 8.13: Design drawings for the vertical lift gates

8.4. Scour protection

In this section of the report a preliminary design for the bed protection of the New Haringvliet barrier is made and the feasibility of the use of a granular bed protection is evaluated. The scour protection design is part of the failure to close failure machanism, appendix G gives an overview and discussion of the failure to close failure mechanism for the New Haringvliet barrier, as well as a description of possible mitigation strategies.

Because the barrier construction sequence in this project is centered around the use of pre-fab construction methods, the main focus of this section of the report will be to investigate the feasibility of the use of a granular bed protection. Therefor the focus of the design will be to design the armour layer of the bed protection, this will be the most critical element in determining the overall bed protections feasibility.

8.4.1. Scour protection length

For financial reasons, the length of the bottom protection is often limited to the minimum required length to ensure the stability of the structure. The depth of the scour hole at the end of the bottom protection will be normative for this stability, and thus also for the length of the scour protection. Figure 8.14 shows an overview of the scour protection around a hydraulic structure.

The development of the scour hole can be described in four distinct phases: the initial phase, a development phase, a stabilisation phase, and an equilibrium phase (Hoffmans & Verheij, 1997). In order to determine the required length of the bottom protection of the New Haringvliet barrier, the equilibrium depth and slope of the scour holes are most important. Given that the scour holes occur at the end of the bed protection, there should be enough distance between the scour hole and the structure to prevent any soil instability as a result of the scour holes of reaching the structure.

To give an initial estimate for the equilibrium depth of a scour hole, the clear water scour equation is used to estimate at which depth the transport capacity of the flow at the bottom of scour hole is equal to the critical flow velocity of the soil in the scour hole (eq. (8.21)). The equation uses the velocity at the edge of the scour hole which might overestimate the equilibrium scour depth, to account for this this Schiereck (2004) recommends a factor of 0.5 to the equation.

$$\frac{h_{se}}{h} = \frac{0.5\,\alpha\,\bar{u} - \bar{u_c}}{\bar{u_c}} \tag{8.21}$$

where:

h_{se}	= equilibrium scour depth	$[m]$
h	= water depth at the end of the bed protection	$[m/s^2]$
$\bar{u}$	= average flow velocity at the end of the bed protection	$[m/s]$
$\bar{u_c}$	= critical flow velocity of the soil ($= 0.3 m/s$)	$[m/s]$
α	= turbulence factor ($= 1.5 + 5r$ if $\alpha > 1.8$)	$[-]$

The disturbance factor α is a function of the relative turbulence intensity at the location the bed protection ends. The intensity of this turbulence depends on the intensity of the flow conditions, the bed roughness and the length of the protection. The expected mean flow velocity at the location during mean tidal flow is in the order of 1.0m/s assuming a scour protection length in the order of 200m. The water depth at the end of the scour protection is also set to be 5.5m. For structures with a low sill, during hydraulically rough conditions, the relative turbulence intensity is about $r = 0.10$ at the end of the bed protection (Hoffmans & Verheij, 1997). Using that value to compute the equilibrium scour hole depth according to eq. (8.21) yields the following results.

$$h_{se} = \frac{0.5 * 2.0 * 1.0 - 0.3}{0.3}\, h = 12.8m \tag{8.22}$$

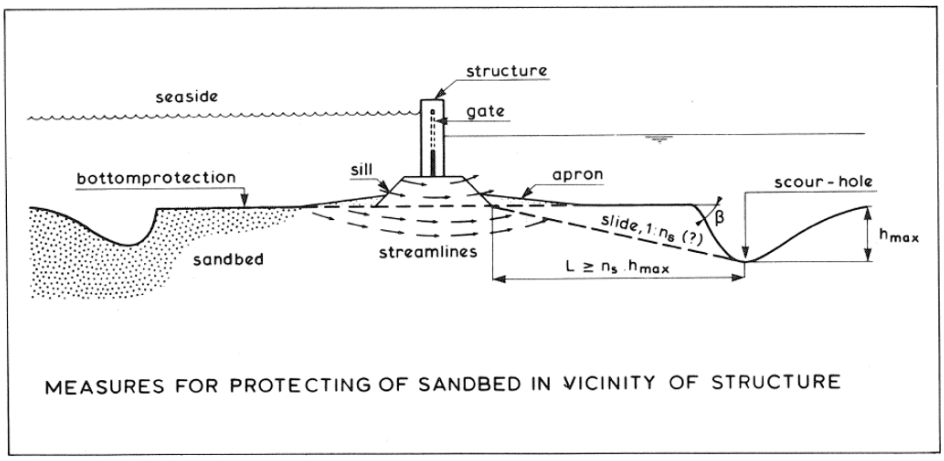

Figure 8.14: Scour overview near a hydraulic structure (Hoffmans & Verheij, 1997)

The equilibrium scour depth according to a first estimate is 12.8m. Depending on the stability of the subsoil near the structure, the required length of the bottom protection need to be a minimum of 6-15 times the maximum equilibrium depth of the scour hole (Hoffmans & Verheij, 1997). A value of 15 can be used in cases that the subsoil is loosely packed and susceptible to effects such as liquefaction, whereas lower values are given to tightly packed or even cohesive sub-soils. For a project of this magnitude, if required, subsoil improvements can be used to ensure better subsoil stability, however such measure for the entire bed protection are also quite expensive.

It should be noted that recent research by Broekema (2020) has shown that eq. (8.22) can underestimate the depth of the scour hole at the end of the bed protection, as it does not take into account any velocity gradients in the horizontal plane. Most notably, Broekema (2020) shows this is the case for the scour holes at the end of the bed protection of the Eastern Scheldt barrier. To account for this, an conservative estimate for the length of the bed protection was chosen (length of 15 times the equilibrium scour depth). Other solutions, such as a sill at the end of the bed protection could also be a viable solution, as that would force vertical flow separation. But for such detailed design, more in-depth research is required.

$$L_s = \gamma_s * n_s * h_{max} = 1.2 * 15 * 12.8 = 230m \tag{8.23}$$

where:

γ_s	= safety factor (1.2)	$[-]$
L_s	= minimum required scour protection length	$[m]$
$1:n_s$	= average slope of the sliding plane	$[-]$

8.4.2. Design conditions of the New Haringvliet barrier

The chosen design water-level coincides with a return period of 3000 years. The normative failure situation would be the a scenario where early barrier closure occurs (during the turning of the tides), and only a single gates fails to close. This coupled with a low river discharge, would lead to the highest possible head difference across the New Haringvliet barrier.

After a potential early closure, the design storm develops further towards it's maximum potential level of +6.07m NAP over a period of 20 hours. Once the peak is reached, it takes an additional 5 hours for the design storm to reach a waterlevel of +3m NAP, after which the barrier can potentially be re-opened. In the 20 hour period between the initial closure and the peak of the storm, the waterlevel behind the New Haringvliet barrier will still slightly rise due to the combined effects of overtopping discharges, through-flow of the single

opened gate, and the river discharge into the Haringvliet over that time period. Therefor it is assumed that during the peak of the storm, the waterlevel behind the barrier has reached a level of roughly +2m NAP. This makes the design head difference over the New Haringvliet barrier's bottom protection, $\Delta h = 4.0m$.

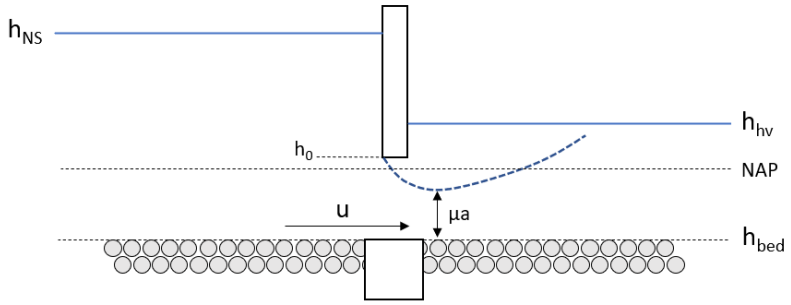

Figure 8.15: Schematic o

Parmater	Value [m +NAP]
h_{ns}	6.07
h_{hv}	2.0
h_0	1.0
h_{bed}	-5.5

Table 8.3: Parameters used in the design of the bed protection

Design flow velocity

In the case of a failed gate closure as described in section 8.4, the water will exit the New Haringvliet barrier in a similar fashion as a wall jet. A wall jet is generally very similar to a submerged hydraulic jump (Schiereck, 1996). In a wall jet one side of the jet is free, while the other is bound by a wall. Within the core region of the jet, which has a length of 6.1 - 6.7 times the initial jet thickness, the flow velocity of the jet is best approximated by the jet's initial velocity (Rajaratnam, 1976). The main distinction between the jet in this case and classical wall jets, is the fact that the jet exiting the New Haringvliet barrier is limited by the relative shallowness of the water in the basin. Due to the relatively shallow water level, there is little room for the flow to spread in the vertical plane, while the bottom friction from the bed plays an important role in the development of the flow field (Broekema, 2020). Modelling this flow, and the exit velocities over the length of this bed protection in detail is out of the scope of this research.

In order to get a rough estimate of the velocities along the bed protection the following approach was used:

- In the flow development region of the jet (the first 35m [$\approx 6.4 * \mu a$] behind the gate) , the design flow velocity of is assumed to be equal to the initial jet velocity.
- After the flow development zone, it is expected that the boundary layer from the bed has reached the mixing layer and that the turbulence has fully penetrated into the core of the jet. At this point the flow from the jet will uniformly penetrate into the stagnant areas surrounding the jet. Typically we seen mixing layers penetrate stagnant areas with a slope of 1:6 (Schiereck, 2004). However, given the fact that the this method is based on a simplified approach that assumes the uniform spreading of the flow, this method will underestimate the center-line flow velocity of the exiting jet (see fig. 8.17 for a more accurate representation for the flow profile). Therefor a more conservative slope of 1:10 was used in the calculations.

Due to the shallow nature of the water in the basin, there will only be a limited spread of the flow in the vertical plane. Additionally, this approach neglects the potential losses due to the bed friction and turbulence at the

bed. But as a first estimate this is found to be acceptable. Figure 8.16 shows an side profile of the schematized outflow through the barrier. Figure 8.17 shows a top-view sketch of typical shallow jet exiting a hydraulic structure.

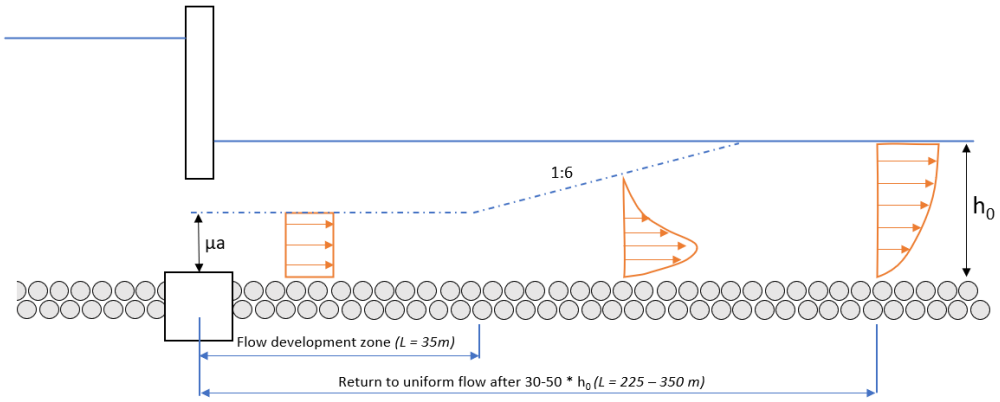

Figure 8.16: Flow pattern of the jet exiting the New Haringvliet barrier

The initial velocity velocity of the water through the barrier in the case one gate fails to close is calculated using the Toricelli equation (eq. (8.24)). For the initial jet thickness the contracted jet thickness is used. In this case a contraction coefficient of 0.8 is assumed. The final design flow velocities along the length of the bed protection are given in fig. 8.18.

$$u = \sqrt{2\,g\,\Delta h} = 8.9 m/s \tag{8.24}$$

where:

u	= flow velocity	$[m/s]$
g	= gravitational acceleration	$[m/s^2]$
Δh	= head difference over the gate	$[m]$

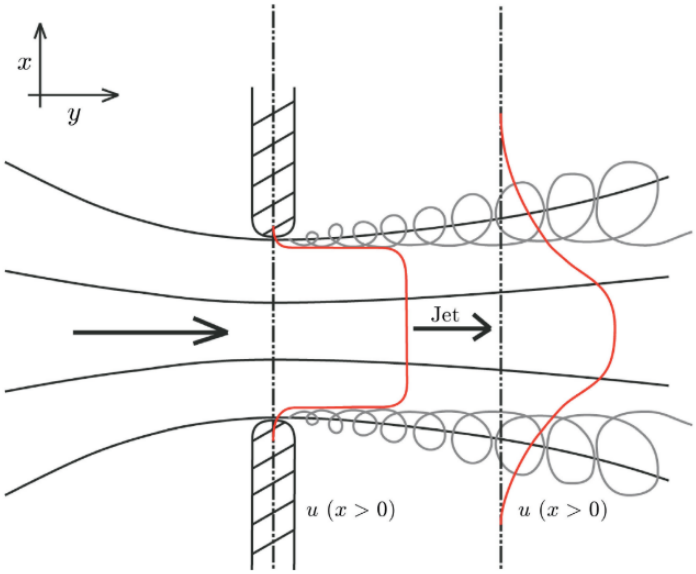

Figure 8.17: Top-view sketch of a shallow jet in the horizontal xy-plane induced by a local cross-section reduction at a hydraulic structure. The hydraulic structure is located at x = 0, and downstream of the structure a free shear layer containing large vortical structures develops on either side of the jet, causing the flow to spread laterally for x > 0. (source: Broekema (2020))

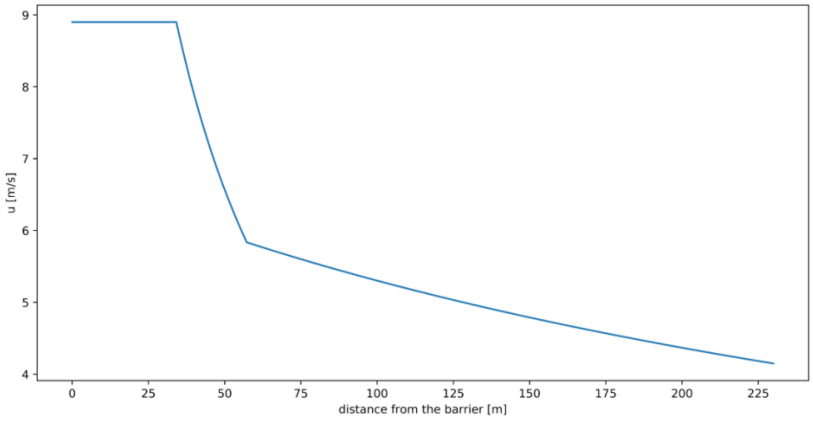

Figure 8.18: Design flow velocities along the length of the bed protection, for the failure to close scenario

8.4.3. Armour layer design

In order to come to evaluate the stability of the top layer of the bed protection the shield equation was used (eq. (8.29)). For flow acceleration due to a vertical (underflow) constriction, the shields stability relation accurately describes the behavior of the system when the contracted jet height is used as the waterdepth in the equation.

For the choice in the shield parameter (ψ_{cr}), Schiereck (2004) states that it's choice remains subjective as long as there has not yet been an quantitative assessment for the costs related to the construction and maintenance of the entire bed protection. A combination of $\psi_{cr} = 0.03$, and $k_r = 2d_{n50}$ are considered as practical choices at preliminary design stages.

$$d_{n50} = \frac{\bar{u}^2}{\Psi \Delta C^2} \tag{8.25}$$

$$C = 18\log\left(\frac{12\,h}{k_r}\right) \tag{8.26}$$

where:

d	= characteristic size of the protection element (= d_{n50} for armourstone)	$[m]$
$\bar{u}$	= depth averaged flow velocity	$[-]$
ψ_{cr}	= critical shields parameter (=0.03)	$[-]$
Δ	= relative buoyant density	$[-]$
k_r	= roughness coefficient	$[-]$
h	= local flow water depth	$[m]$

In the first 50m behind the structure, there are no rock elements available (heaviest rock class considered was $HM_A6000-10000$) that satisfy the shields stability relation. In order to asses the feasibility of using a rock protection near the structure a second evaluation was done using the Izbash equation. The Izbash equation considers the individual forces working on a single grain or element in order to determine it's stability. Similar to the situation at the New Haringvliet barrier, the Izbash equation works best, with large elements in a shallow flow environment, and is especially useful in cases of non-uniform flow or jets (Schiereck, 2004). These criteria are all met in the region closest to the New Haringvliet barrier. The resulting design for the bed protection is given in table 8.4 and fig. 8.19. For the North Sea side of the barrier, it is a less conservative bed protection is required as this section has to be designed for the wave loads near the barrier, or for reverse flow scenario's. Both of these scenario's typically are much smaller hydraulic loads. The design of this section is however out of the scope of this project and should be discussed in future research project.

$$u_c = 1.2\sqrt{2\,\Delta\,g\,d} \tag{8.27}$$

Equation (8.29) yields the following critical flow velocities for rock class $HM_A6000-10000$ and $HM_A10000-15000$ respectively:

$$u_c = 1.2\sqrt{2*1.7*9.81*1.44} = 8.3m/s \tag{8.28}$$

$$u_c = 1.2\sqrt{2*1.7*9.81*1.7} = 9.0m/s \tag{8.29}$$

Distance to the barrier [m]	Class name	Weight range
0 - 40	HMA 10000-15000	10 - 15 ton
40 - 50	HMA 6000 - 10000	6 - 10 ton
50 - 60	HMA 1000-3000	1-3 ton
60 - 115	HMA 300-1000	300 - 1000 kg
115 - 230	LMA 60-300	60 - 300 kg

Table 8.4: Armour layer elements for the Haringvliet side of the New Haringvliet barrier.

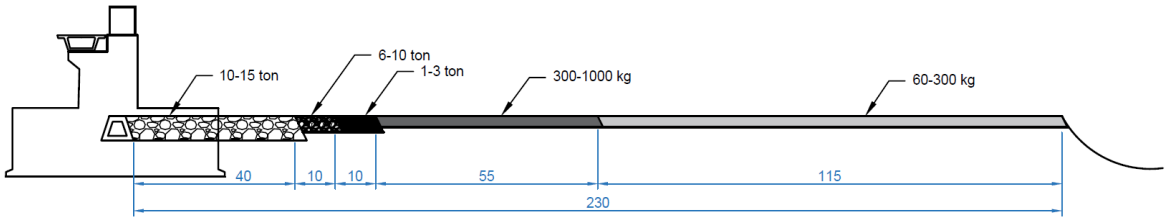

Figure 8.19: Design of the armour layer composition of the scour protection

8.4.4. Filter construction

The primary option with regards to the construction of the filter, is the construction of a geometrically closed filter. This is mainly due to the requirements of the barrier to withstand large hydraulic gradients, and for the barrier to have a long lifespan.

The stability, permeability and internal stability requirements for the design of a geometrically closed barrier are given below. In these equations, the subscript f always describe the top 'filter' layer of any two layers, whilst the b subscript indicates the bottom 'base' layer. Using these relations, the filter design given in table 8.5 was developed. The layer thickness was determined by doubling the d_{n50} of each rock class, with a minimum layer thickness of 300mm for construction purposes. The total thickness of the bed protection layer near the structure is thus roughly 5m.

$$\text{stability:} \quad \frac{D_{f15}}{D_{b85}} < 5 \tag{8.30}$$

$$\text{permeability:} \quad \frac{D_{f15}}{D_{b15}} > 5 \tag{8.31}$$

$$\text{internal stability:} \quad \frac{D_{60}}{D_{10}} < 10 \tag{8.32}$$

Description	**rock class**	$d_{15}\ [mm]$	$d_{85}\ [mm]$	**Layer thickness [mm]**
Armour layer	rock 10-15ton	1600	-	3500
Base layer 1	rock 40-200kg	290	410	1000
Base layer 2	gravel 30-100mm	30	100	300
Base layer 3	gravel 3-10mm	3	10	300
Bottom layer	Sand	-	0.6	-

Table 8.5: Filter layer design for the New Haringvliet barrier under the first armour layer

8.4.5. Discussion bed protection design

In this section of the report, the critical load scenarios for the bed protection were determined. From this the required length of the bed protection was determined, and a design was made for the bed protection's armour layer on the Haringvliet side of the barrier. This side of the barrier is most critical as it is subject to higher design loads than the North sea side of the bed protection.

The most important finding in this assessment is the fact that a granular armour layer is indeed feasible. This is a positive conclusion with regards to the feasibility of the use of prefab construction methods in the barrier construction. Secondly, it was determined that the length of the protection should be 230m on each side of the barrier. Comparing this to the Eastern Scheldt barrier (bed protection length of 600m on each side) that is very short. This is mainly due to the limited depth at the end of the bed protection, which limits the depth of a potential scour hole according to equilibrium scour theory.

In the design of the bed protection's armour layer, the Izbash and Shields equations were used to assess the required granular elements along the bed protection. Both equations evaluate the stability of granular elements, given the respective hydraulic conditions. However, it is important to note that mobility of the bed protection elements does not equate to a failure of the system. Instead, in order to come to a more economically optimized design for the barrier, the elements in the bed protection, should be evaluated for the ultimate limit state (for a schematized overview see fig. 8.20). This means, that during the design storm conditions, which last a couple of hours, significant damage to the bed protection is acceptable, as long as the barrier stability is not directly threatened. For the best evaluation for the optimal bed protection design, it is therefor recommended to do a study using scale models of the barrier, in which armour layer is designed based on the maximum damage expected during storm conditions.

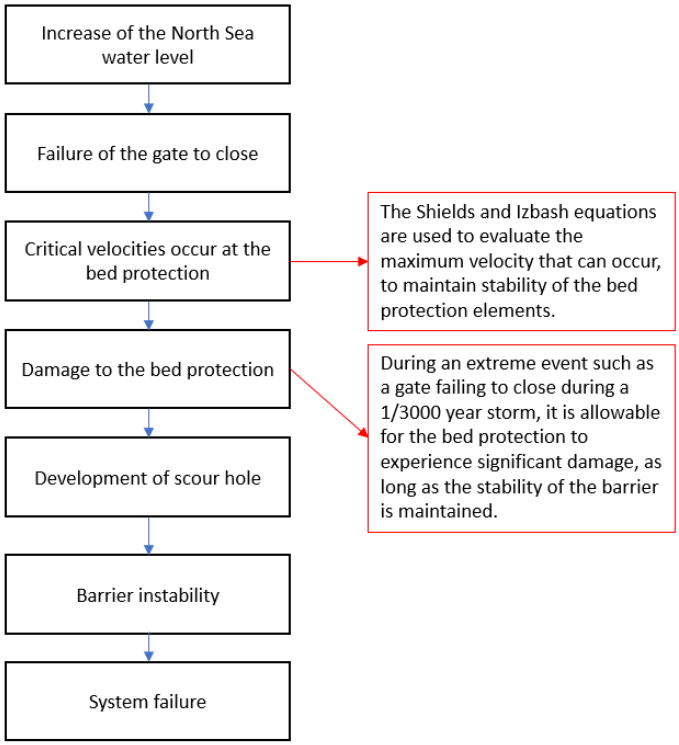

Figure 8.20: Events leading to the failure of the barrier when a gate fails to close, including comments on the application of bed protection design, given the events.

8.5. Final design overview

The final conceptual design for the gated barrier section is shown in fig. 8.21. This chapter looked into the design of the bed protection, the vertical lift gates, and pier base of the structure. The walkway, sill beam and lifting equipment were not designed in detail but were included in the sketch to give a complete overview of the conceptual design. the walkway is located on the sea-side of the structure, so that the skin plate of the vertical lift gate can be located in the middle of the caisson. Due to the elevation of the walkway (bottom at roughly +12m NAP), it is not expected to be subject to any significant impact loading. For in the case that the walkway is deemed vulnerable to wave loading, additional MatrixFrame calculations for the reverse orientation of the gates was done (skin plate facing the river side, see appendix H.3 for MF diagrams). The calculations show that doing so will simply reverse the direction of the forces through the gate, thus the gate would still suffice the general strength calculations done in this design. This would however also have to be verified in a dynamic strength assessment of the gate.

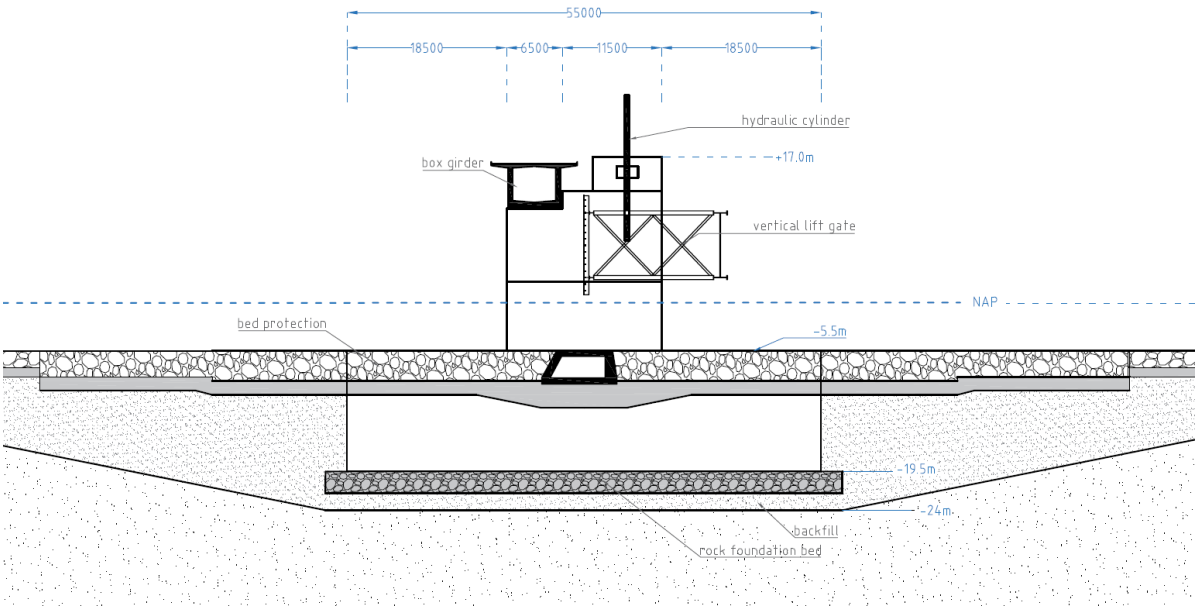

Figure 8.21: Side view of gated barrier design

9

Conclusion and recommendations

This chapter will outline the main conclusions and recommendations formed in this thesis. In addition to the conclusions an additional discussion of the project methodology is given.

9.1. Design Results

The output of this thesis, is a conceptual design for the New Haringvliet barrier that would fits the requirements and boundary conditions of the Delta21 project and the Haringvliet tidal delta. The design sketches for the barrier are given in fig. 9.1 and fig. 9.2. The design consists of a total of 20 vertical lift gates that each span 80m. The effective cross-section of the tidal opening in the barrier is 10400m^2

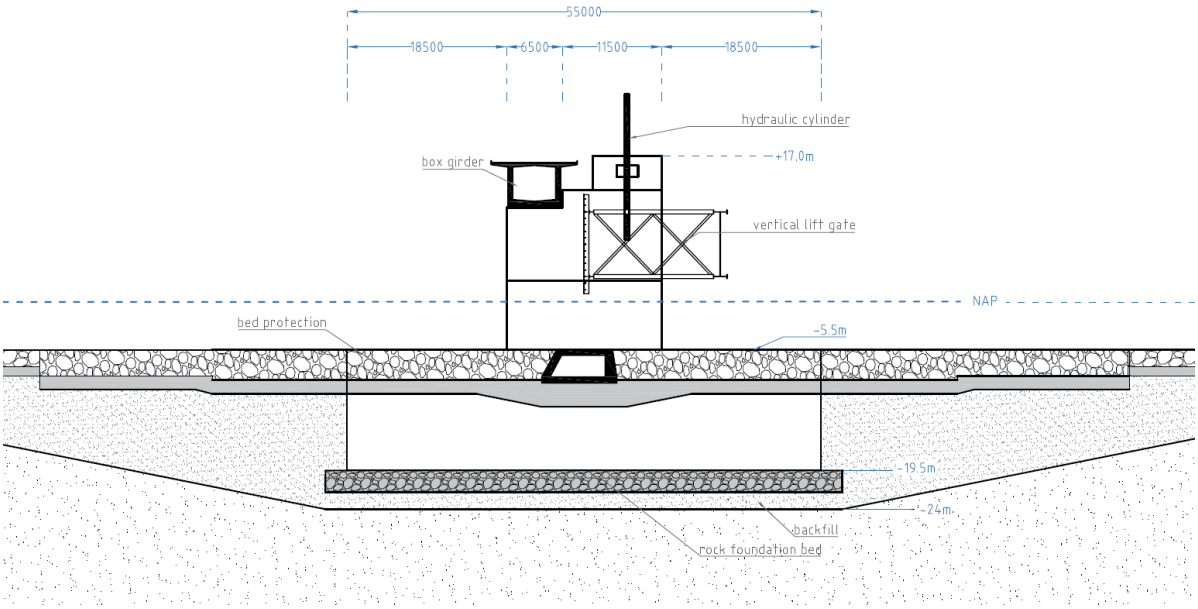

Figure 9.1: Side-view conceptual barrier design

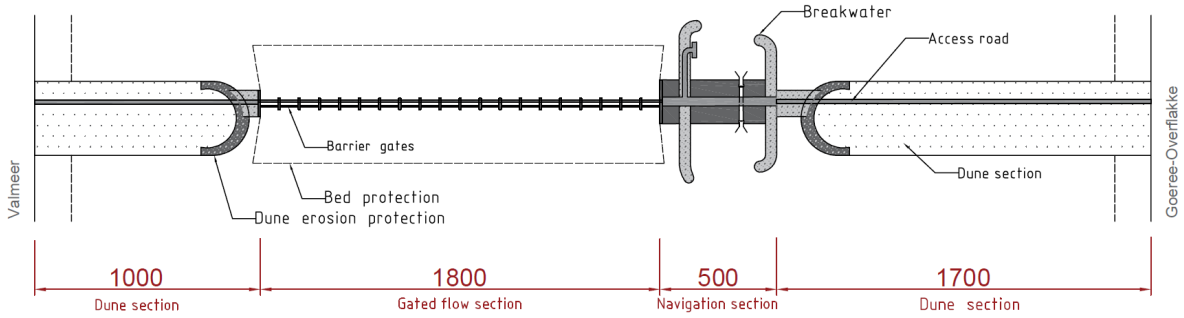

Figure 9.2: Spatial design for the New Haringvliet barrier. The dune sections are connected to the structural barrier elements by short breakwater sections. The navigation section is a shipping lock sheltered by breakwaters.

9.2. Conclusions

In addition to the conceptual design, some notable conclusions were drawn throughout the barrier design process. Both in regards to the construction of the New Haringvliet barrier, as well as the overall Delta21 project. This section presents an overview of the most notable conclusions.

- **Hydrodynamic impact New Haringvliet barrier**
  In this thesis the hydrodynamic impact of the construction of the New Haringvliet barrier was evaluated using a schematized model of the situation. From this model it is clear that the construction of a second barrier definitely will have a noticeable impact on the capability of the system to discharge water into the North Sea during high river discharge rates, as well as on the maximum available tidal range in the region. Given the fact that the goal of the Delta21 project is to save money on future dike strengthening projects, the potential for the New Haringvliet barrier to cause an increase in waterlevels in the case of a river flood, is a critical design consideration. To minimize any negative impact with regards to flood safety, and to maximize the amount of tide possible in the system, a large cross-section for the barrier is required (roughly $10.000 m^2+$). In very extreme cases, the model shows that there is potential for the Valmeer and the spillway to be used to mitigate the majority of the negative impacts of the barrier.

- **Barrier construction costs**
  The expected costs for the barrier were estimated based on the construction costs of the Eastern-Scheldt barrier. The barrier was estimated to cost roughly 4.1 billion Euro's. This is a very significant cost, when considering one of the primary objectives of the Delta21 project is to save on future dike reinforcement project in the delta region.

- **Construction method**
  The prefab construction of the New Haringvliet barrier is the preferred construction method in the context of the overall Delta21 project. The construction sequence for the entire Delta21 project was considered as the primary starting point for determining the construction method of the New Haringvliet barrier. To this effect two different design objectives were formulated, one that prioritized a quick financial return on investment, and one that prioritizes that minimizes the environmental impact of the construction process. When optimizing the construction process from an economic perspective, the construction of the Valmeer and the Pumping station should be prioritized to ensure the fastest return on investment on the project. If this is the case, the in-situ construction of the New Haringvliet barrier would strongly restrict the remaining tidal opening between the Haringvliet and the North Sea. In the environmental alternative, the re-use of a single dry-dock is emphasized. In this case the New Haringvliet barrier will also have to be built using prefab construction elements.

- **Vertical lift gates are the best gate alternative for the New Haringvliet barrier**
  Due to the size of the barrier, vertical lift gates are the preferred gate type. The total number of gates (20) and the total barrier span, require a gate type that is reliable, cost efficient and easy to maintain. For this case, less researched barriers such as the inflatable barrier, or structures with expensive sill structure such as the rotating sector gate are not desirable for the structure. The vertical lift gate on the

other hand, is relatively cheap, easy to maintain and inspect, and the most frequently used of flood gate around the world.

- **The application of a granular bed protection is feasible.**
  Using the stability relations of Izbash and Shields, a granular bed protection was designed for the New Haringvliet barrier. In the case that such a protection was not realistically feasible, it would complicate the prefab construction process of the barrier.

9.3. Discussion

This section will outline the primary discussion points related to the assumptions and design choices that were made throughout the project:

- **Gate span selection**
  The gate span assessment was mainly based on the amount of caisson elements that were required for the construction of the barrier. Given the shallow sea-bed and the large dredging requirements, it was assumed that the construction and transport of the caisson elements would be a important consideration in the overall cost of the project. What was not included in the gate span assessment explicitly, was the impact of the span on the overall cost, size, and construct-ability of elements such as the sill beam, hydraulic gates and the road girder. A detailed cost-benefit analysis of the influence of gate span selection on all barrier components could thus give a different output for the the desired barrier gate span.

- **Construction method**
  The construction method for the new Haringvliet barrier was determined based on an assessment of desired construction sequence of the entire Delta21 project. As mentioned in the conclusion, this assessment yielded that the prefab construction of the New Haringvliet barrier is preferable over an in-situ construction method. However, during the design stages of this project, it was generally found that the prefab construction of the barrier would require the dredging of large trenches due to the shallow sea-bed around the construction location. From this perspective it might actually be more beneficial to construct the New Haringvliet barrier using alternative construction methods.

- **Sea level rise**
  In this project, the barrier is designed to account for +1m of SLR. Given the desired lifetime of the project, this might be on the optimistic sides for SLR estimates. Part of the choice for the barrier's design SLR, is the consideration that Delta21 wants to limit the future reinforcement of dikes as much as possible. However, if the dikes are not raised, the closure frequency of the barrier will rapidly increase to the point where designing a barrier that is structurally able to withstand significant SLR is not optimal. As the structure will still lose the majority of it's functionality. Considering future changes to the Delta21 policy or SLR predictions, a more conservative estimate might be more beneficial.

9.4. Recommendations

For future research it is recommended to investigate the effect's of the construction of the New Haringvliet barrier on the waterlevels throughout the RMD during a high river flood wave using a calibrated model. As mentioned previously, the results in this project indicate an overall negative impact of the construction of the New Haringvliet barrier on the discharge capacity of the system. Given the importance of this flood safety parameter, it requires a detailed evaluation, as it will most likely be the normative criteria in determining the final size of the New Haringvliet barrier. A good addition to this research would be to include the effects of using the Valmeer during these river discharges, and evaluating the effectiveness of that measure as well.

Similar to the previous recommendation, it is also recommended that the impact of the effective opening in the New Haringvliet on the tidal flow through the barrier is studied using a calibrated model. Additionally it should be evaluated what the ecological impact is of a reduction in the tide in the tidal lake. This will allow for a more accurately estimate for the amount of reduction in tide that is deemed acceptable.

To get a more optimized barrier design in future iterations, an detailed cost assessment study is recommended. Quantifying the costs of the various elements will allow for more quantitative optimization choices and design decision for the barrier. This applies to both the construction methods used for the barrier, as well as the costs of the final barrier elements.

Lastly, it is recommended to develop a detailed construction framework for the entire Delta21 project. The construction sequence assessment in this project was a first glance at the construction process of the entire Delta21 project. For a project of this magnitude, getting a better understanding of the constructive demands of the project will give more options for design optimization of the individual elements. Additionally it will provide clarity towards the potential environmental impact the construction process will have on the Haringvliet ebb-tidal delta

Bibliography

Battjes, J., & Labeur, R. J. (2017). *Unsteady flow in open channels*. Cambridge University Press.

Broekema, Y. (2020). *Horizontal shear flows over a streamwise varying bathymetry* (Doctoral dissertation). https://doi.org/10.4233/uuid

Brühl, C., Helsen, G., Kempen, G. V., Kivits, D., & Toorn, M. V. (2020). *Connecting Delta21 to its stakeholders : The Haringvliet case* (tech. rep.). Wageningen University.

Colina Alonso, A. (2018). Morphodynamics of the Haringvliet ebb-tidal delta.

Daniel, R., & Paulus, T. (2019). *Lock Gates and Other Closures in Hydraulic Projects* (Vol. 53). https://doi.org/10.1016/b978-0-12-809264-4.00017-3

Deltares. (2016). Fenomenologische beschrijving.

de Vriend, H. J., Dronkers, J., Stive, M. J. F., & Wang, J. H. (2002). Coastal inlets and Tidal basins. *Delft University of Technology*, *1*, 1–84.

Dijk, A., & Van der Ziel, F. (2010). Multifunctionele beweegbare waterkeringen. www.royalhaskoning.com

Eelkema, M. (2013). *Eastern Scheldt inlet morphodynamics*.

Elias, E. P., Van Der Spek, A. J., & Lazar, M. (2017). The 'Voordelta', the contiguous ebb-tidal deltas in the SW Netherlands: Large-scale morphological changes and sediment budget 1965-2013; Impacts of large-scale engineering. *Geologie en Mijnbouw/Netherlands Journal of Geosciences*, *96*(3), 233–259. https://doi.org/10.1017/njg.2016.37

Ferguson, H. A. (1971). De afsluiting van de Haringvliet. *Weg en Waterbouw*. https://doi.org/10.1017/CBO9781107415324.004

Groen, M., & Walburg, L. (2002). Haringvlietmonding : reconstructie van een afsluiting Beschrijving , verklaring en modelaanpak van de effecten. (november).

Haasnoot, M., Mosselman, E., Sloff, K., Huismans, Y., Mens, M., Ter Maat, K., Weiler, O., Bouwer, L., Diermanse, F., Kwadijk, J., Van der Spek, A., Oude Essink, G., & Delsman, J. (2018). *Mogelijke gevolgen van versnelde zeespiegelstijging voor het Deltaprogramma*. https://www.deltares.nl/app/uploads/2018/08/Deltares%7B%5C_%7DMogelijke-gevolgen-van-versnelde-zeespiegelstijging-voor-het-Deltaprogramma.pdf

Hoffmans, G., & Verheij, H. (1997). *Scour Manual*. AA Baalkema.

Hoogduin, L. (2009). *Sediment transport through the Eastern Scheldt storm surge barrier* (Doctoral dissertation). Delft University of Technology Faculty of Civil Engineering and Geosciences.

Huis in 't Veld, J., Stuip, J., Walther, A., & van Westen, J. (1982). The closure of tidal basins. https://doi.org/10.1016/0378-3839(82)90006-0

Jonkman, S. N., Vrouwenvelder, A. C. W. M., Steenbergen, R. D. J. M., Morales-nápoles, O., & Vrijling, J. K. (2016). Probabilistic Design: Risk and Reliability Analysis in Civil Engineering, 271.

Kluijver, M., Dols, C., Jonkman, S. N., & Mooyaart, L. F. (2017). Advances in the Planning and Conceptual Design of Storm Surge Barriers – Application to the New York Metropolitan Area.

Molenaar, W., & Voorendt, M. (2019). Manual Hydraulic Structures - TU Delft. (February).

Mooyaart, L. F., & Jonkman, S. N. (2017). Overview and design considerations of storm surge barriers. *Journal of Waterway, Port, Coastal and Ocean Engineering*, *143*(4). https://doi.org/10.1061/(ASCE)WW.1943-5460.0000383

Mooyaart, L. F., Jonkman, S. N., De Vries, P. A., Van Der Toorn, A., & Van Ledden, M. (2014). Storm surge barrier: Overview and design considerations. *Proceedings of the Coastal Engineering Conference*, *2014-Janua*(October 2016). https://doi.org/10.9753/icce.v34.structures.45

Paasman, Y. (2020). *Design for the in- and outlet structure of the Energy Storage Lake within the Delta21 plan* (Doctoral dissertation).

Rajaratnam, N. (1976). *Turbulent Jets*. Elsevier Science; Technology.

Rijkswaterstaat. (1985). Tienjarig Overzicht der waterhoogten, afvoeren en watertemperaturen 1961-1970. *1*(1), 207. https://doi.org/10.1002/ajim.20908

Rijkswaterstaat. (1998). MER Beheer Haringvlietsluizen: Deelrapport 1 Water-en Zoutbeweging.

Rijkswaterstaat. (2011). Beschrijving huidige situatie Haringvliet. Achtergrondrapportage voor onderzoek naar alternatief voor het Kierbesluit., 19.

Rijkswaterstaat. (2018). Werkwijzer Ontwerpen Waterkerende Kunstwerken – Ontwerpverificaties voor de hoogwatersituatie. (november).

Ruiz, R. A. (2020). *Conceptual Design of the Valmeer ' S Pump Storage Station of the Delta21 Plan* (Doctoral dissertation January). https://repository.tudelft.nl/

Schiereck, G. J. (1996). *Introduction to bed, bank and shore protection.*

Schiereck, G. J. (2004). *Introduction to Bed, Bank and Shore Protection.* https://doi.org/10.4324/9780203397879

Van Thiel de Vries, J. S. M. (2009). *Dune erosion during storm surge conditions.*

Van Vessem, P. (1998). Morfologie monding Haringvliet, verandering van een dynamisch onderwaterlandschap.

van Dam, J. (2020). *Ontwerp Duinenrij Energie-Opslagmeer* (tech. rep.).

Vellinga, N. E., Hoitink, A. J. F., Vegt, M. V. D., Zhang, W., & Hoekstra, P. (2014). Human impacts on tides overwhelm the effect of sea level rise on extreme water levels in the Rhine – Meuse delta. *Coastal Engineering, 90*, 40–50. https://doi.org/10.1016/j.coastaleng.2014.04.005

Vissers, M., de Swart, E., & Baretta-Bekker, J. (2013). Stroomgebiedsafstemming Rijn-.

Wijsman, J., Escaravage, V., Huismans, Y., Nolte, A., van der Wijk, R., Wang, Z. B., & Tom Ysebaert, T. (2018). *Potenties voor herstel getijdenatuur in het Haringvliet, Hollands Diep en de Biesbosch.* https://doi.org/10.18174/440424

A

Haringvliet Impact Assessment

In chapter 2, an overview of the human interventions in the RMD is given. This appendix is meant as a supplement to this chapter and will further evaluate the impact of the human interventions on the Haringvliet ebb-tidal delta and the Haringvliet respectively. At this point in the Delta21 project it is unknown what the impact of the Delta21 project will be on the local hydrodynamics, morphology and ecologically, therefor this appendix will also do a rough assessment of the potential effects of the construction of the Delta21 infrastructure in the Haringvliet ebb-tidal delta. This will be done using the information gathered from the previous results of human interventions on the Haringvliet tidal delta, aswell as a case study of the Eastern Scheldt barrier in appendix A.1.1. This assessment is meant to give a preliminary idea of the potential effects of various design choices within this project.

A.1. Haringvliet Tidal Delta Morphology

After completion of the Haringvliet barrier in 1970, the dynamic equilibrium in the Haringvliet tidal delta was disrupted, as there was no longer an exchange of water and sediment between the Haringvliet estuary and the tidal delta, and a large reduction in the tidal volumes entering the tidal delta. Since the construction of the sluices, sediment transport from the haringvliet estuary into the tidal delta is only possible through suspended sediment loads as the high sill structure of the sluices limits bed load transport (Van Vessem, 1998). As a result of the disruption of the dynamic equilibrium related to the closure of the estuary, the Haringvliet tidal delta experienced net sedimentation in addition to causing a long-shore reorientation of the channels and flats that were originally in cross-shore direction, causing the creation of shoals such as the Hinderplaat (fig. A.1) (Colina Alonso, 2018; Van Vessem, 1998). Since the creation of the Hinderplaat, the flat has become a important factor for the local ecology, as it functions as a resting place for different animals such as birds and seals, and is nowadays considered an important part of the Natura2000 area.

As of 2018 Colina Alonso (2018) argued that the tidal delta was close to an new equilibrium state, however, application of the Kierbesluit policy is likely to disturb the new equilibrium. With regards to potential morphological adaptations to a potential operation of the Haringvlietsluices as a storm-surge barrier Van Vessem (1998) had some of the following conclusions:

- A change from the current sedimentation trend to an erosion trend in, especially the southern part of the Haringvliet tidal delta
- Net sediment transport in sea-ward direction
- Reduction in the size of the Hinderplaat, the Kwade hoek and an increase in the size of the Slijkgat and the Rak van Scheelhoek (tidal channels) fig. A.2.
- An increase in morhodynamics. The new morphological activity will likely not be larger than prior to 1970

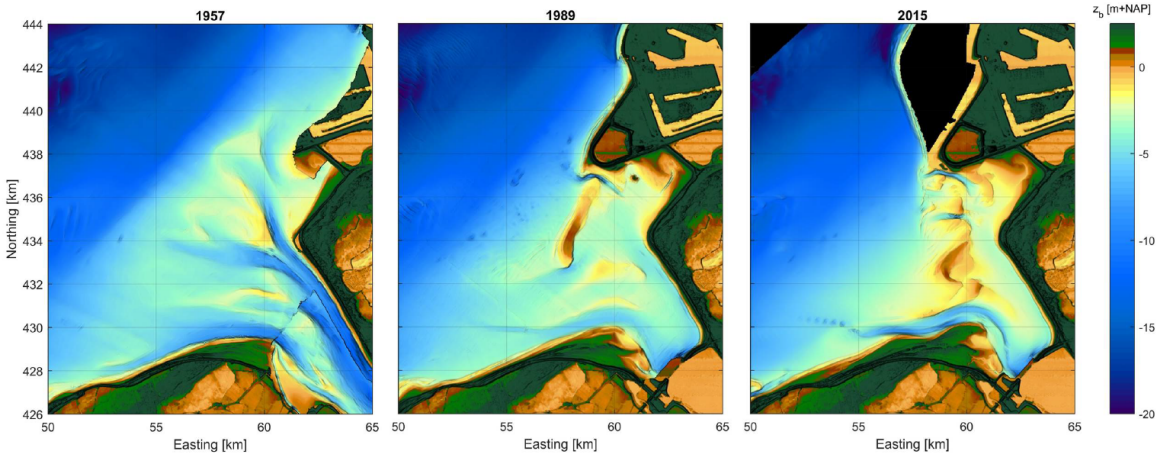

Figure A.1: Different stages of the evolution of the Haringvliet outer delta, based on the Vaklodingen data (source: Google Earth)

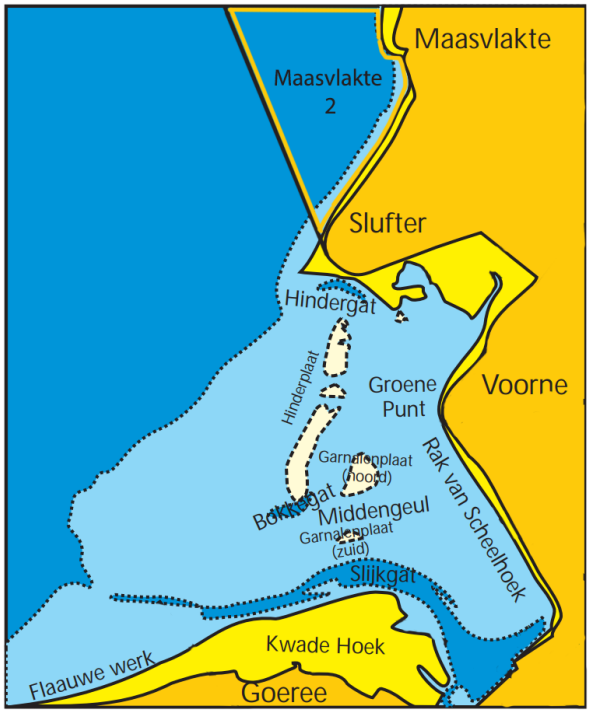

Figure A.2: Haringvliet tidal delta, with indications of the flats and channels (Adapted from: Groen and Walburg (2002))

A.1.1. Case-Study Eastern-Scheldt Barrier

Tidal inlet morphology is a function of the complex interactions between waves, currents and sediment, that all interact on varying temporal and spatial scales (Eelkema, 2013). Human interventions such as damming, and land reclamations in or near a tidal basin can significantly affect the inlet morphodynamics, and therefor, knowledge on the effects off such interventions is important for the coastal zone managment (Eelkema, 2013). Given the proximity of the Eastern Scheldt to the Delta21 project location, as part of this project, an analysis from the Hydrodynamic and Morphological effects of the construction of the Eastern Scheldt Barrier will be applied to gain better insight into important design considerations for the New Haringvliet Barrier.

The Eastern Scheldt is the former mouth of the Scheldt river. Just like the Grevelingen Dam and the Haringvlietsluices, the closure of the Basin was part of the Deltaplan, as a response to the storm surge of 1953. The construction of the back barrier dams as part of the Deltaplan cut of all river influence, turning the Eastern scheldt from an estuary into a basin (Eelkema, 2013). The construction of the Eastern Scheldt Barrier was completed in 1986, the barrier was designed as an open-barrier but yet yielded great effects on the ebb-tidal deltas morphology and hydrodynamics. Eelkema (2013) describes the effects of the construction of the Eastern Scheldt barrier in detail, a summary of his findings are presented here:

- Due to the construction on the barrier, the average tidal flows inside and outside of the basin have decreased.
- The decrease in tidal flows has led to a decrease in sediment transport towards the tidal flats
- The flats in the Eastern Scheldt experience net erosion due to the the fact that the main erosive mechanism for the tidal flat in the estuary, the wind waves, are not limited due to construction of the barrier.
- Ever since the completion of the barrier, there has been virtually no exchange of sediment between the basin and the tidal delta. Indicating that the barrier has been a blockage for sediment transport.

With regards to the sediment blocking behaviour for the barrier, it has been hypothesised that the scour holes at each side of the barrier play a significant role in the sediment blockage of the barrier. However results from research done by Hoogduin (2009), and Eelkema (2013) show that the blocking behaviour near the barrier is most likely not due any complicated three-dimensional flow effects around the barrier and the scour holes. The results from Hoogduin (2009), does indicate that the tidal jets play an important role in the amount of net sediment transport around the barrier.Tidal jets are the phenomena where in a tidal inlet, the tidal flow enough momentum to the degree that the out-flowing flow, forms a jet of the length scale of hundreds of times the water depth de Vriend et al. (2002). This causes a residual current pattern away from the tidal inlet, both for ebb and flood conditions (fig. A.3).

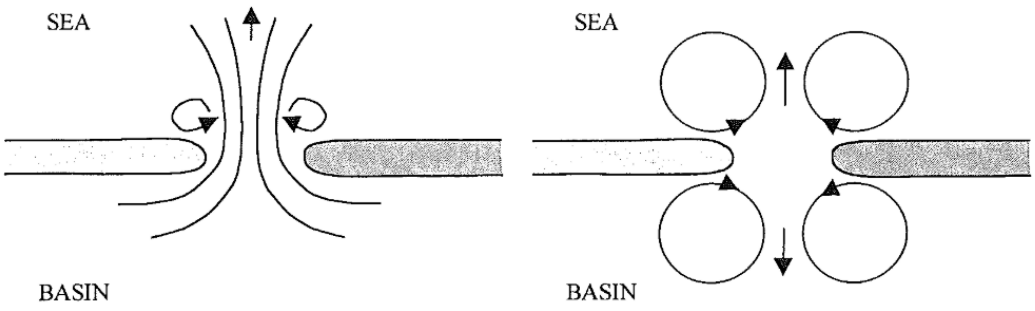

Figure A.3: Ebb- tidal jets (left) and the tidal residual currents around the inlet (right) (de Vriend et al., 2002)

Figure A.4: Overview of the Eastern-Scheldt Barrier and estuary relative to the Delta21 project location (source: Google Earth)

A.1.2. Bathymetry Construction Location

The proposed location for the New Haringvliet barrier has experienced relatively little changes in bathymetry due to the various interventions in the delta fig. A.1. At the location of the gated section of the barrier, the seabed is roughly at a depth of -4m NAP fig. A.5. The construction of the Delta21 project would restrict a large part of the ebb-tidal delta, making it so that tidal channels will for near the barrier and that the sea-bed will locally erode due to the tidal flows, and river discharges. What the correct equilibrium depth for this barrier is hard to say without an in-depth morphological analysis of the final location.

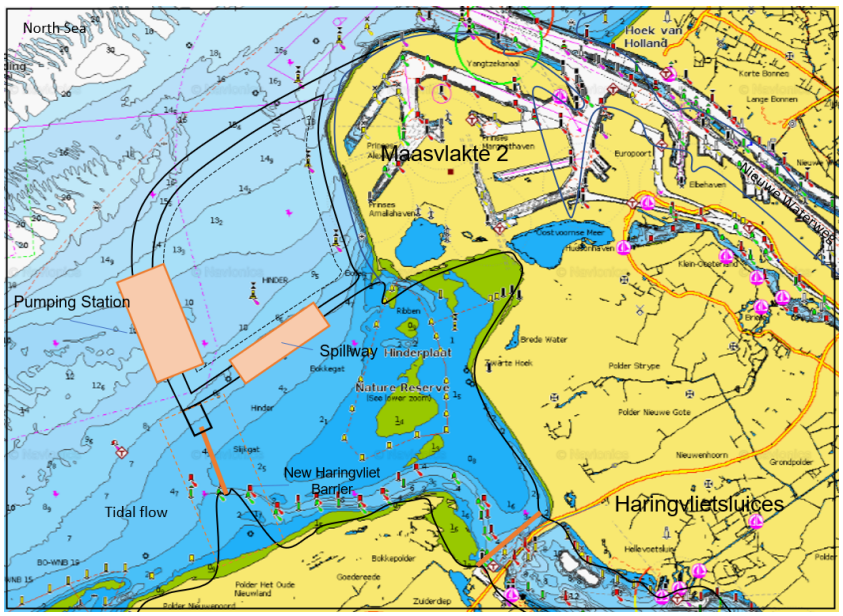

Figure A.5: Caption

A.2. Haringvliet, the Hollandsche Diep, and the Biesbosch

Another important area to pay attention to with regards to the construction, and operational ionterventions related to the Delta21 project, is the Haringvliet estuary, and the more inland Hollandsche Diep and the Biesbosch (fig. A.6). Similar to the Voordelta, these more inland waterways have also been highly affected by the various closure projects of the Delta works.

The largest changes that affected the overall area were the construction of the Volkerrakdam (completed in April 1969) and the completion and closure of the Haringvlietsluices (operational per 2 November 1970). The construction of these structures cause some of the following changes in the region:

1. A strong reduction in the tide. Some limited vertical tide still remains due to the connection of the Haringvliet to the Nieuwe Waterweg through the Spui and the Dordtsche Kill.

2. The original dynamic salt-brackish-fresh water intertidal nature of the Haringvliet, Hollandsche Diep and Biesbosch has been turned into a near stagnant fresh water environment.

3. As a result of the limited intertidal interaction, the ecological nature of the region has completely changed.

4. The Haringvlietsluices, have formed an obstruction for migratory fish from the North-Sea to the Rhine. The current Kierbesluit operation of the sluices, aims to alleviate this problem. However the longterm effects of this measure are not yet clear.

A.2.1. Effects of interventions on the tide

Prior to the construction of the Volkerrakdam and the Haringvlietsluices, the time average tidal range on the Haringvliet, Hollandsche Diep and the Biesbosch were 1.85m (Hellevoetsluis), 2.30m (Moerdijk), and 2.30m (Deeneplaat) respectively (Rijkswaterstaat, 1985). The Volkerrakdam disconnected the Eastern-scheldt estuary from from the Hollandsche Diep, and the Haringvliet, allowing for the creation of a fresh water environment behind the Haringvlietsluices. The tidal range reduced as the Volkerrakdam was closed of with 0.55m (1.75cm tidal range) on the Hollandsch Diep, and 0.2m (1.65m tidal range) on the Haringvliet. From February 1970 untill November 1970 the dammed section of the Haringvlietdam had been completed and, the tide was able to flow in and out of the estuary through the opened barrier. In this period (April 1970 - November 1970) the tidal range at Hellevoetsluis and Moerdijk was 1.20m and 1.60m respectively (Rijkswaterstaat, 1998). After the Haringvlietsluices became fully operational, the tidal range in the overall region reduced to 0.2m - 0.3m. In the Haringvliet tidal delta, in the period Februari - November 1970 the average tidal range was between 170 and 190cm. After the sluices became operational the tidal range in the Delta increased to averages of 220cm in 1971 and up to 235cm in 1991.

In an previous evaluation of the potential effects of different operational regimes for the Haraingvlietsluices, anlyses were done to evaluate the effects of operating the sluices as a storm-surge barrier. Meaning, that unless a significant storm occurs, the sluices would be completely opened. The first research done was Rijkswaterstaat (1998), and included a full analysis of the morphological, ecological, hydraulic effects of these measures. Wijsman et al. (2018) evaluated the effects of alternative operation of the sluices, and how much of an increase in the amount of tide, and therefor the amount of increases of the areal inter-tidal was possible. table A.1 shows an overview of the amount of tidal range, was calculated to occur due to the permanent reopening of the Haringvlietsluices, as was found in Rijkswaterstaat (1998). Wijsman et al. (2018) found average tidal ranges, of 1.30m, 1.34m, and 1.35m for the operation of the sluices as a storm surge barrieri in the Haringvliet, Hollandsche Diep, and Bieschbosch respectively.

An important factor to note is the fact that Rijkswaterstaat (1998) states, that the bathymetry of the tidal delta played a big role in the expected tide in the Haringvliet. In the calculations, the bathymetry from 1990 was used, but when doing the same calculations while using the tidal deltas 1970 bathymetry instead, it showed that the tide in the inland areas would on average increase approximatly 30-40cm compared to the findings presented in table A.1. Therefor, the findings of Wijsman et al. (2018), should be more of an indication of the

Figure A.6: An overview of the southern section of the RMD. From left to right: The Haringvliet Tidal Delta, the Haringvliet, the Hollandsch Diep and the Biesbosch. (source: Google Earth)

what the current tidal situation would be when reopening the Haringvlietsluices. However, the findings are not applicable when considering the potential long term effects of such a measure.

Location	**Mean tidal range**	**Mean slack water level**	**Mean low tide**	**Mean high tide**
Haringvliet 10	2.05*	0.0	-0.85	1.25
Haringvlietsluices (outside)	1.4	0.30	-	-
Haringvlietsluices (inside)	0.9	0.30	-	-
Middelharniss (Haringvliet)	0.9	0.35	-0.15	0.75
Moerdijk (Hollands Diep)	1.25*	0.40	-0.20	1.00
Gat van Kampen (Biesbosch)	1.30	0.40	-0.25	1.05

Table A.1: Tide characteristics in case the Haringvlietsluices would completely be opened (source: Rijkswaterstaat (1998)).
*values might be inconsistent with high-, and low tide levels due to rounding

B

Wave Heights - Extreme Value Analysis

This appendix will elaborate the Extreme Value Analysis computed for the Haringvliet Tidal Delta. The underlying dataset was downloaded through the website of Rijkswaterstaat Waterinfo (https://waterinfo.rws.nl/), and entails 29 years of wave data in terms of, the significant wave height (H_s), the mean wave direction, and the mean absolute wave period (T_{m02}). The location of the measurements the data was taken from was the Europlatform fig. B.1, and includes data from 1990-2018.

Figure B.1: Location Europlatform

B.1. Evaluating the Dataset

After filtering and aligning the various datasets, the first evaluation was done towards the overall wave characteristics at the Europlatform. The proposed location of the New Haringvliet barrier will be subject to waves from directions of 240 - 330 Deg. North. This is also in the general direction of the wave dominant conditions in the overall wave spectrum.

The wave period and the wave height was also plotted, it should be noted that in plot such as fig. B.2, the swell waves are often seen in the bottom right of a H,T- plot (relative low wave height, with long periods). The plot also includes a relation between the wave height and the period. This relation is in the general form:

$$T_{m02} = \alpha\sqrt{H_s} \tag{B.1}$$

Figure B.2 also shows the plotted lines for this relation for different values of alpha. An value of $\alpha = 3.2$ seems to have a good fit for the wind waves in the spectrum, especially for the more extreme wave conditions.

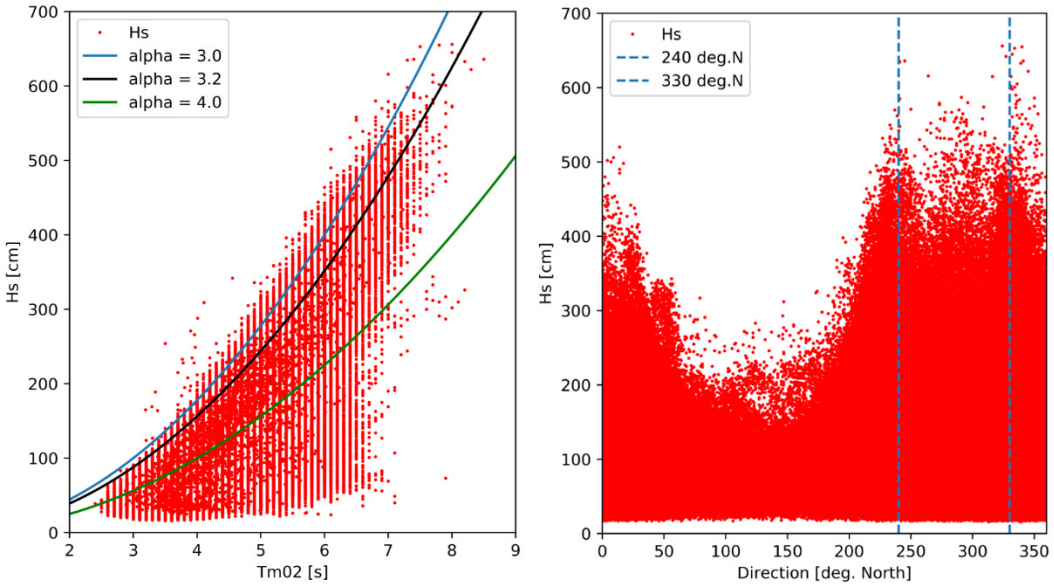

Figure B.2: Check of the assembled dataset

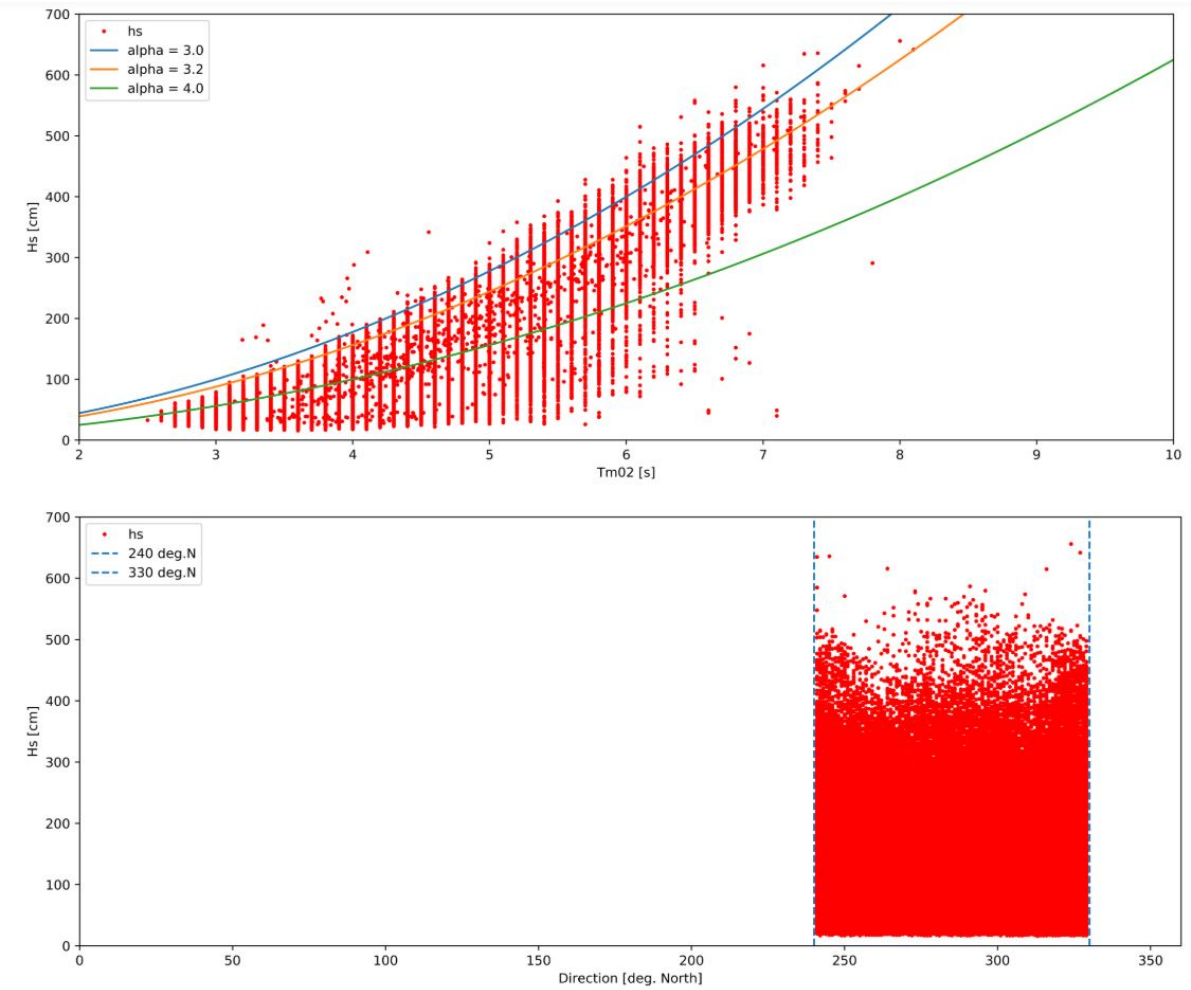

Figure B.3: Wave height versus mean absolute wave period (a), and Wave height versus direction (b) plots (240-330deg. North)

B.2. Extreme Value Distribution Fit

Firstly, the dataset was processed into a series of storms with a maximum occurring wave height. To do this, initially a Peak-over Threshold analysis was done. In such an analysis, a storm is defined as the period of time in which the wave height exceeds a certain threshold. Only the highest point over this period of time is considered for each storm, doing so gives a certain number of storms per year (N_s). However, analyzing the results of this analysis shows a certain problem with storms with a peak around the threshold, as it registers one storm event as a multitude of storms with various peaks, skewing the extreme storm events towards more frequent lower intensity storms. An example of this can be seen in fig. B.5.

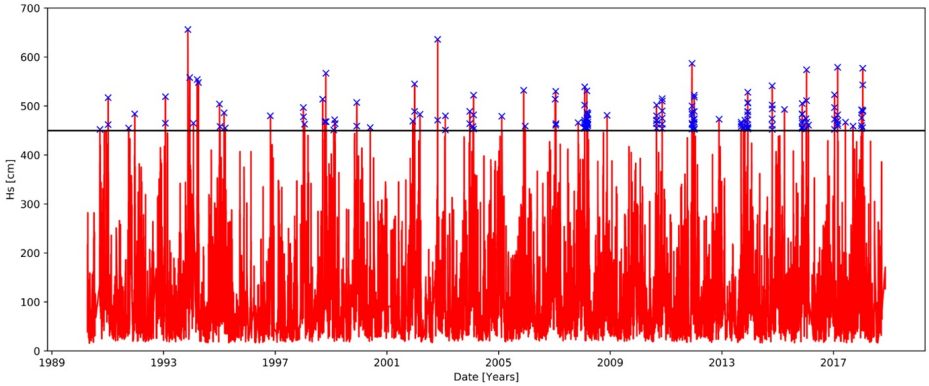

Figure B.4: Results Peak over Threshoild analysis (threshold: $H_s > 450$ cm)

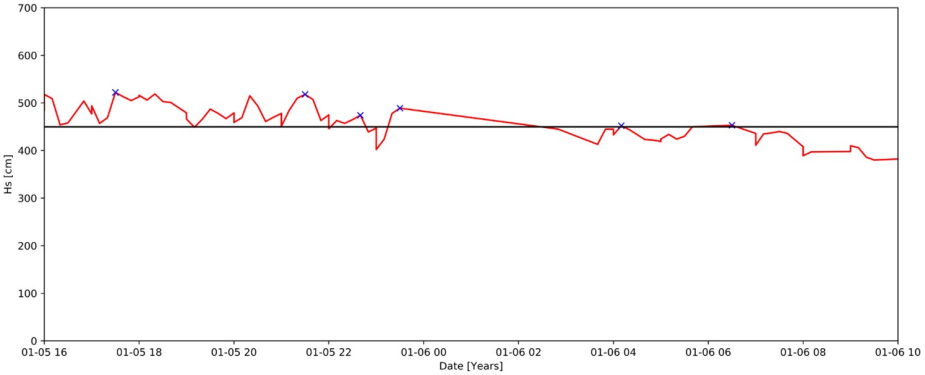

Figure B.5: One storm being counted as multiple storms using the PoT method (threshold: $H_s > 450$ cm)

To solve this problem, the PoT analysis was limited to include a maximum of one storm event per day. Table B.1 shows an overview of the results of the various PoT methods for two thresholds. In the final analysis a threshold of $H_s > 450cm$, using the PoT analysis including a maximum of 1 storm per day was used.

Threshold	PoT points	PoT Datapoints (including daily maxima)	Ns (PoT)	Ns (PoT + Daily Maxima)
Hs >450cm	163	83	5.62	2.86
Hs >400cm	324	169	11.17	5.83

Table B.1: Results from the Peak-over-Threshold

B.2.1. Results

The extreme value analysis was done using the method of moments top estimate the distribution parameters for the Exponential, Gumbel, Weibull and Generalized Pareto distributions, additionally, the Weibull and Generalized Pareto distributions were fitted with an alpha to ensure the smallest RMSE possible. The results of the analysis can be found in fig. B.6, and the RMSE of each method is shown in table B.2. The final results of the analysis is that the Generalized Pareto distribution yields the most accurate results., followed closely in accuracy by the Weibull distribution, which at the the top end of extreme wave scenarios is slightly more conservative than the Generalized Pareto distribution. Finally due to accuracy, the results of the GDP were used in further analysis of the wave height at the project location.

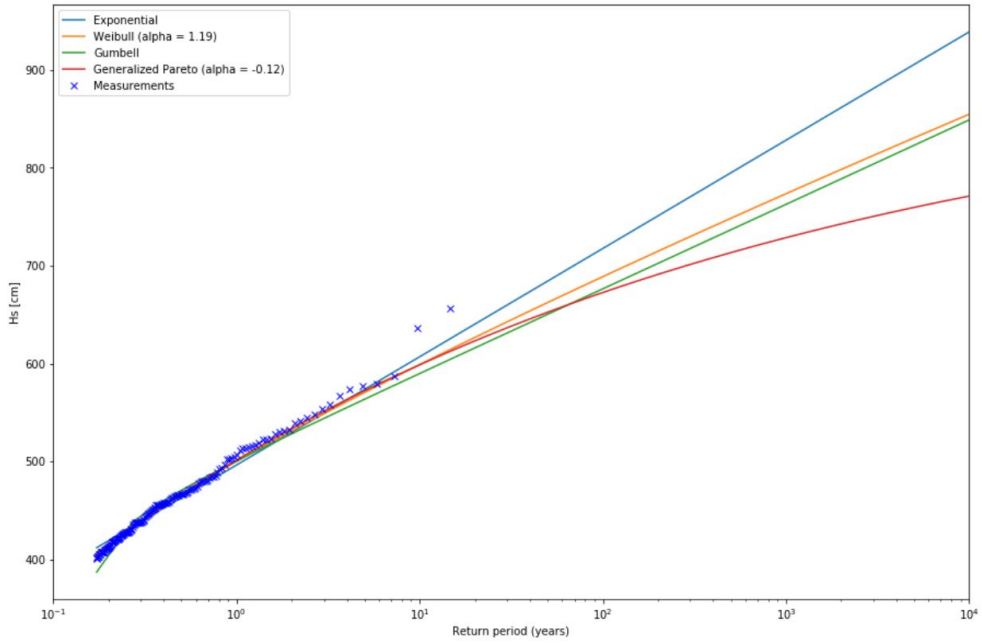

Figure B.6: Fitted Extreme value analysis of the extreme storm wave heights

	Exponential	Gumbel	Weibull (alpha = 1.19)	Generalized Pareto (alpha = -0.12)
RMSE	6.833	8.256	5.709	5.609

Table B.2: RMSE of the fitted Extreme value distributions

B.3. Nearshore Wave Transformations

For the transformation of the Wave characteristics, from the Europlatform towards the Haringvliet Tidal Delta, SwanOne was used.

In order to determine the nearshore wave-conditions using SwanOne, the future bathymetry was roughly estimated. An overview of this bathymetry and the current bathymetry of the location are shown in fig. B.7. Furthermore, the normative conditions such as the wind-speed and set-up that coincide with the return periods of the extreme wave conditions, were extracted from HydraNL. An overview of all parameters and the final results of the SwanOne calculations are shown in fig. B.8.

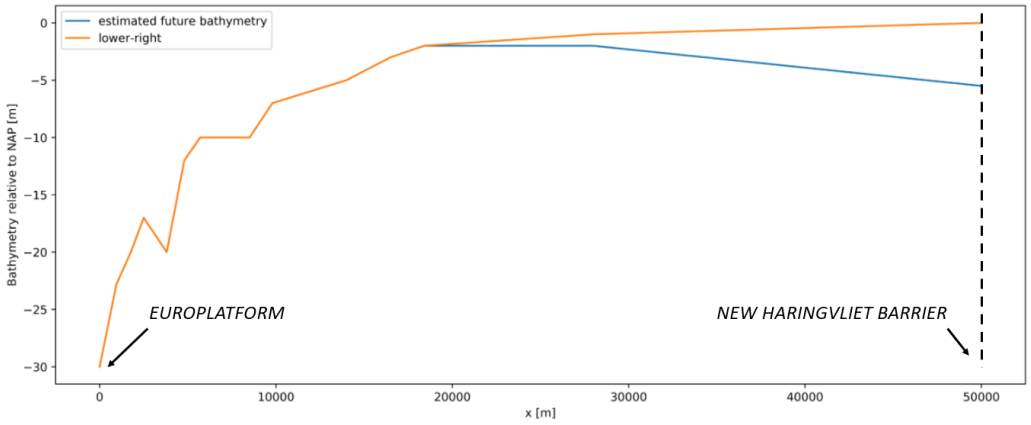

Figure B.7: Current and estimated bathymetry between the Europlatform location and the expected location of the New Haringvliet barrier

	Offshore conditions				Nearshore wave conditions			
Return Period	Hmo [m]	Wind Speed [m/s]	Set-up [m]	Tp [s]	Hmo [m] (HydraNL)	Hmo [m] (Swan)	Tp	Tm0
100	6.72	27.1	4.73	10.37	2.291	2.9	6.45	5.35
300	7	28.9	5.04	10.58	2.508	3.06	6.46	5.42
1000	7.28	30.9	5.43	10.79	2.734	3.26	6.45	5.55
3000	7.49	33.1	5.75	10.95	2.924	3.44	7.2	5.58
10000	7.66	35.2	6.15	11.07	3.131	3.62	7.2	5.66
100000	8	39.4	6.87	11.31	3.508	3.96	6.45	5.78

Figure B.8: Results of the SwanOne calculations

C

Hydrodynamic model setup

This appendix provides additional information concerning the models and methods used in chapter 5.

C.1. System Overview

The model that was used to asses the potential impact of the tidal opening in the New Haringvliet barrier is the function of the coupling of a storage-basin model and a 1D channel model. The storage basin model was used to evaluate the reaction of the tidal lake in the system, whereas the 1D channel model was used to describe the Haringvliet and the Hollandsche Diep. An overview of the system is provided in fig. C.1

Figure C.1: Overview of the considered domain within the hydrodynamic assessment. The tidal lake is being considered as a short basin located in between the New Haringvliet barrier and the Haringvliet sluices, while the Haringvliet/Hollandsch diep is being considered as a canal reaching from the Haringvlietsluices to the Dortsche kill

C.2. Model Setup

This section will describe the setup of the hydrodynamic model that was solved using Python.

C.2.1. Shallow water equations

The basis for the model are the shallow water equations. The propagation of tidal waves into canals and tidal channels can be described using the shallow water equations; the momentum balance and the continuity equation. The complete long-wave equations are at the root of many numerical models and calculations of

unsteady flow in open channels. However, if certain terms are expected to be small for a certain case, the equations can be simplified and solved.

$$B\frac{\partial h}{\partial t}+\frac{\partial Q}{\partial s}=0 \tag{C.1}$$

$$\frac{\partial Q}{\partial t}+\frac{\partial}{\partial s}(\frac{Q^2}{A_c})+gA_c\frac{\partial h}{\partial s}+c_f\frac{|Q|Q}{A_cR}=0 \tag{C.2}$$

In the case of low waves in a prismatic conduit, the advective acceleration is relatively small compared to the local acceleration term and can therefor often be neglected in a first approximation. In the case of flow into tidal entrances or over tidal flats the advective acceleration term starts becoming of a greater importance in describing the behaviour of the tidal wave accurately. In cases such as flow over control structures, the advective acceleration term can often become dominant over the local acceleration term, allowing for the flow to be modelled as quasi-steady; meaning that the flow, instantly adapts to the boundary conditions at the structure.

C.2.2. Basin-storage model

For the basin-storage model, the tidal lake is simplified to where the basin only has a storage function. In order for this simplification to be valid, the length dimension (l) of a basin has to be small relative to the wavelength of the present tidal wave. If this is the case, phase differences in the basin can be neglected, indicating a constant surface level elevation across the basin. This approximation is also known as the 'short basin approximation'. To evaluate the validity of the short basin approximation, firstly the wavelength of the tidal wave is computed (eq. (C.3)). This wavelength is compared to the length of the respective basins. Generally speaking, a basin can be considered short if the basin is 0.05 times the wavelength. Equation (C.5) shows the short-basin approximation is valid for the tidal lake, and can therefor be used.

$$\lambda = T\sqrt{g*d} \tag{C.3}$$

where:

λ	= wavelength	$[m]$
g	= gravitational acceleration	$[m/s^2]$
d	= water depth of the basin (4m)	$[m]$

$$\lambda_1 = 44700\sqrt{9.81*4} = 280km \tag{C.4}$$

$$\frac{l_{b1}}{L_1}=\frac{10}{280}=0.036 \tag{C.5}$$

The final model for the tidal lake is thus described as a basin with only a storage function, and a connection with negligible length and only expansions losses. The schematisation of the model and the set of equations used to solve the numerical scheme for the model are listed below.

$$Q_i = C_d A_c\sqrt{2g|\zeta_i-\zeta_{i+1}|} \tag{C.6}$$

$$\frac{d\zeta_2}{dt}A_{b2}=Q_1-Q_2 \tag{C.7}$$

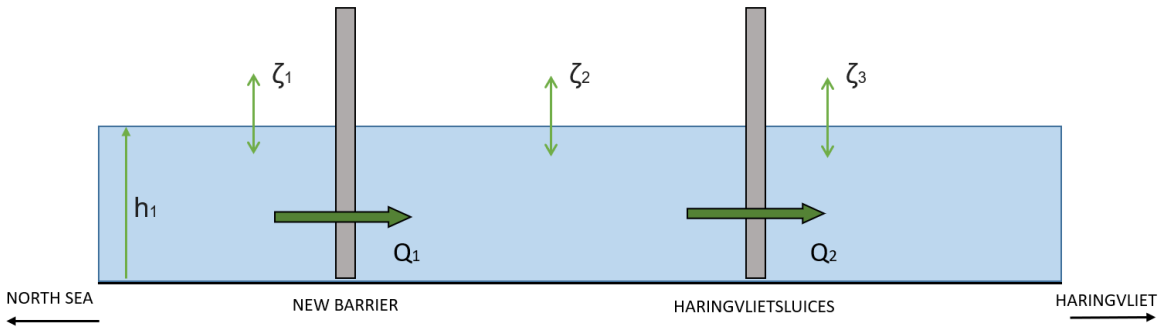

Figure C.2: Basin-storage model

C.2.3. 1D Haringvliet- Hollandsche Diep model

In the hydrodynamic impact assesment of the Delta21 project and the New Haringvliet barrier, the Haringvliet and Hollandsche Diep, will be treated as a 1D channel and will be evaluated using a one-dimensional model for shallow water flows in channels. In reality, the Haringvliet and Hollandsche Diep are part of a much more complex system in the Rhine-Meuse Delta. Thus in order to get a workable model, some simplifications need to be made to the system. Most notably, is the impact of the Spui and the Dortsche Kill need to be considered (see fig. C.1). Both rivers, connect the Haringvliet and Hollandsche Diep with the Oude Maas, which connects to the Niewe Waterweg, the northern sea outlet of the Rhine - Meuse Delta. Therefor depending on the given hydraulic conditions at any time, as well as the operational policy of the Haringvlietsluices, the distribution of discharges and water levels throughout the system can change significantly. However, as the main objective of this model is to gain some insight in the impact of tidal opening of the New Haringvlietbarrier on the tidal range in the tidal lake and the Haringvliet/Hollandsch Diep, the following parameters are set:

- The Spui being the smaller of the two channels is not incorporated in the model. It is a relatively small channel that is close to the North Sea. The Nieuwe Waterweg will experience a similar tidal range near the start of the basin as the Haringvliet, and thus it is expected that during average tides the impact of the discharge through the Spui will have minimal impact on the overall system.

- The Dortsche Kill will also no explicitly be considered in our model. The model domain is chosen such that the Dortche Kill is outside of the domain of the model. The river has a significant impact on the discharge distribution into the Haringvliet/Hollandsche Diep, and the Oude Maas. By keeping the Dortsche Kill outside of the domain of the model, it's impact can be evaluated using a sensitivity analysis of the discharge at the upstream boundary.

Channel dimensions

In order to determine the dimensions of the modeled channel, various cross-sections along the Haringvliet and Hollandsche Diep were assessed fig. C.3. From these locations the cross-sectional areas fig. C.4a and the total section width fig. C.4b, excluding any tidal flats, were measured. As can be seen from the data, we can see a decrease of the cross-sectional area and width as the channel reaches further inland. Generally speaking, alluvial tidal rivers have such a exponentially varying cross-section, where the width and wet surface are of the river increases in seaward direction (Battjes and Labeur (2017)). The convergence of alluvial tidal rivers can be described by the following relations for the conveyance area and width respectively:

$$A_c = A_{c,0}\, exp(-2\lambda s) \tag{C.8}$$

$$B_c = B_{c,0}\, exp(-2\lambda s) \tag{C.9}$$

where:

A_c	= The conveyance area of a cross section	$[m^2]$
B_c	= The storage width of a cross section	$[m]$
$A_{c,0}$	= The conveyance area at the river mouth	$[m^2]$
$B_{c,0}$	= The storage width at the river mouth	$[m^2]$
λ	= The convergence parameter	$[-]$
s	= distance from the cross-section from the mouth	$[m]$

For the model of the Haringvliet/Hollandsche Diep channel, a similar convergence relation was assumed. To fit the model to the bathymetry data taken from the Haringvliet, a convergence parameter of $\lambda = 8e-6$ was used, and initial values of $A_{c,0} = 21000m^2$ and $B_{c,0} = 2900m$ were chosen. The depth over of the tidal river is assumed to be constant at a depth of 7.25m. A sketch of the final model geometry is given in fig. C.5.

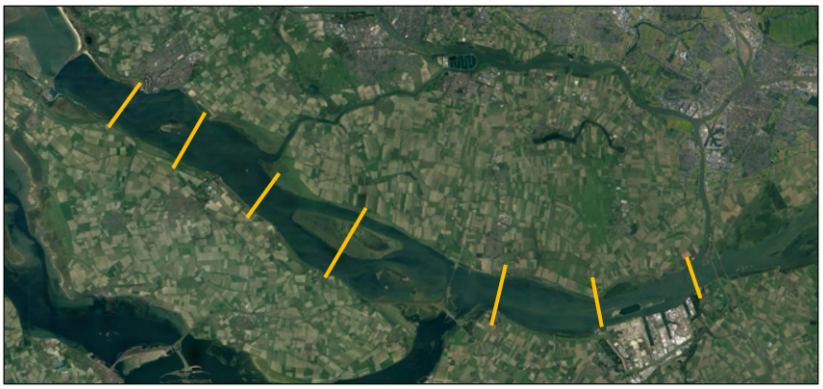

Figure C.3: Map with the locations for the collected bathymetry data of the Haringvliet and the Hollandsch Diep

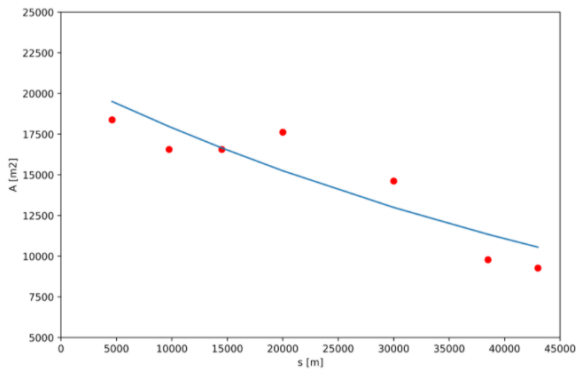

(a) Conveyance area data, and model for $A_{c,0} = 21000m^2$ and $\lambda = 8e-6$

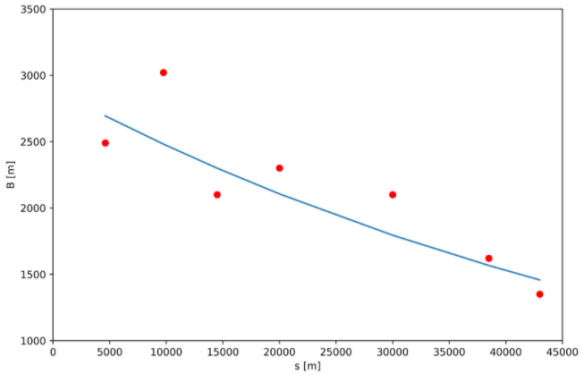

(b) Storage width data, and model for $B_{c,0} = 2900m$ and $\lambda = 8e-6$

Figure C.4: Overview of the collected bathymetry data (red), and the bathymetry used for the hydrodynamic model (blue). (Bathymetry data source: https://www.navionics.com/)

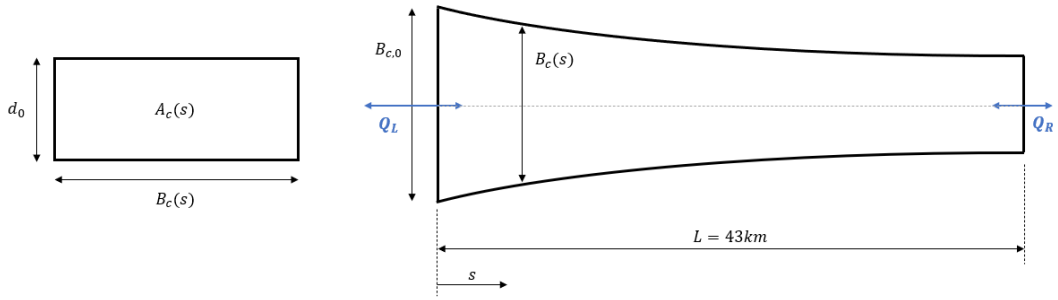

Figure C.5: Sketch of HV/HD model geometry

Numerical computation

This subsection will elaborate on the numerical method that was used to solve the shallow water equations in the HV/HD channel model. In the one-dimensional model, the discharge and water level vary both in time and space. Therefor the time domain was divided in N sections, each of length Δt, while the channel was divided in M sections of length Δs. Each section has a corresponding surface area (A_m), discharge (Q_m), and hydraulic radius (R_m). Between every section additional nodes that hold the water level are defined. These nodes also are specified a local storage width (B_m). From this point the Python script was set up to progress through time from $t = 0$, where the initial conditions are defined, to $t = t_n$, by using a semi-implicit method. Firstly, the continuity equation is used first to compute an updated water level, followed by an update of the discharge by using the momentum equation.

Boundary conditions

Downstream boundary
For the left side (sea side) boundary of the HV/HD model the avergae North-Sea tide is specified as a boundary condition. This is then directly used to calculate the discharge through the Haringvliet sluices. The discharge relation for this is derived from the Bernoulli equation and is as follows

$$Q_L^n = C_d A_c \sqrt{2g\,\Delta h} \tag{C.10}$$

A_c	= The effective opening cross-section of the barrier	$[m^2]$
C_d	= The discharge coefficient (assumed ≈ 0.7)	$[m]$
Δh	= head difference over the barrier	$[m]$

The barrier's discharge coefficient is assumed to be roughly 0.7 and in the case of the New Haringvliet sluices the maximum opening area is $6000 m^2$.

Upstream boundary
For the upstream boundary condition, a Riemann boundary is specified. Specifying a Riemann boundary condition, avoids the occurrence of artificial reflections within the domain by adapting to the local waterlevel at the boundary. The local Riemann invariant is based on the assumed flow state outside of the boundary, and for the upstream boundary is defined as follows

$$R^- = Q - Bch \tag{C.11}$$

For the right boundary this yields:

$$Q_R^n = Q_{R,0} + (Bc)_R^n (h_M^n - h_{R,0}) \tag{C.12}$$

where:

$Q_{R,0}$ = undisturbed discharge rate at the upstream boundary $[m^3/s]$
$h_{R,0}$ = undisturbed waterlevel at the upstream boundary $[m]$

The exact values of the undisturbed situations differ depending on the scenario that was used in the computation of the project.

Normal river discharge
The average annual river discharge for the river Rhine is roughly $Q_{rhine} = 2200m3/s$. On average this leads to a discharge of $800m^3/s$ into the Hollandsche Diep (Vissers et al., 2013). Therefor, for scenarios with regular river discharge rates (scenario's 1, 2 and base), the upstream boundary conditions are set to be:

$$Q_{R,0} = 800m^3/s$$
$$h_{R,0} = 0.1m$$

The undisturbed waterheight is an estimate for the undisturbed waterlevel in this situation relative to the undisturbed waterlevel at the downstream boundary.

High river discharge
In scenario 3, the high river discharge of the system is evaluated. To formulate the boundary conditions for such a scenario, HydraNL was used to find the hydraulic conditions in the system during a high river discharge. The following scenario from HydraNL was eventually used:

$$Q_{Rhine} = 11865m^3/s$$
$$h_{northsea} = 1.36m$$
$$h_{upstream} = 1.6m$$

The waterlevel on the North Sea corresponds with the MHW tide level at the North Sea. For a rhine discharge of $12000m^3/s$, roughly $8000m^3/s$ will be discharged through the Haringvliet (Rijkswaterstaat, 2011). Through iteration in the model it was found that an undisturbed waterlevel $h_{R,0} = 1.1m + NAP$, and a undisturbed discharge of $Q_{R,0} = 8000m^3/s$ yields a waterheight of $h = 1.6m + NAP$ at the upstream boundary during high tide. Conclusively, the following values were used for the upstream boundary conditions for a high river discharge:

$$Q_{R,0} = 8000m^3/s$$
$$h_{R,0} = 1.1m$$

C.2.4. 1D HV/HD model assessment

In order to be able to asses the impact of the Delta21 measures, firstly the channel model was ran independently. This means that at this point no Delta21 measures would be taken into account in the model, and only the impact of reopening the Haringvlietsluices was evaluated (fig. C.6). An overview of the parameters that were used in the computations are presented in table C.1. It should be noted that negative discharge rates indicate downstream flow.

Parameter	Description	Value	Unit
A_{c2}	Opening Haringvlietsluices	6000	m^2
ζ_1	North Sea tidal range	2.0	m
Q_3	Discharge in the upstream channel boundary	-800	m^3/s

Table C.1: Model Parameters scenario 1

Figure C.6: Base scenario: Channel model assessment, No Delta21

Results and discussion

The results from the 1d model assessment are given in fig. C.7.

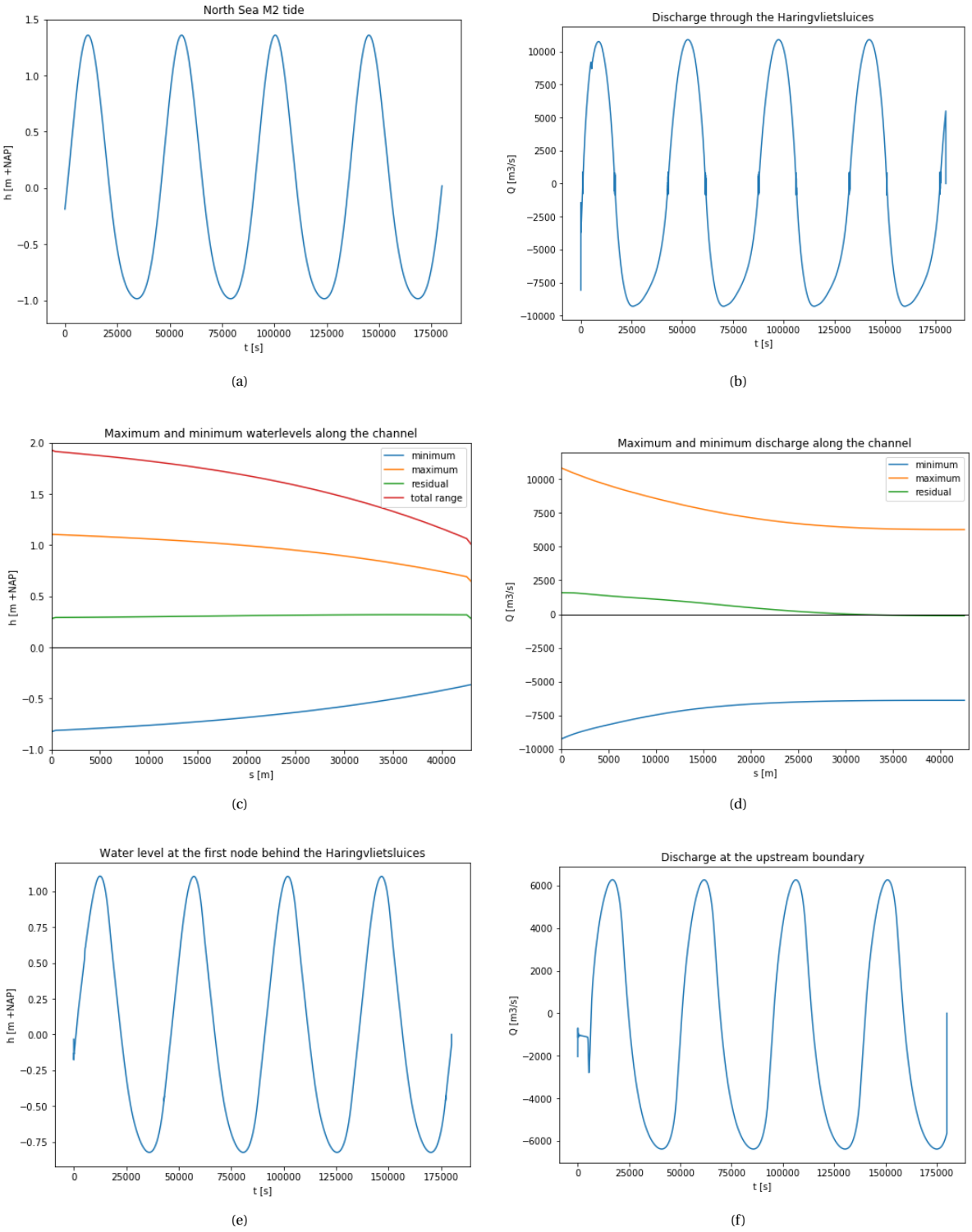

Figure C.7: Output of the 1D channel model for the base scenario, assuming no presence of any Delta21 infrastructure

C.3. Validation hydrodynamic model

In order to evaluate the accuracy of the model used, this section will outline a validation calculation for the model. The validation calculation compares the model, to the real life scenario of at Hellevoetsluis for the period of 05-05-2018 to 17-05-2018, over this period in time the Rhine river was recorder to have a average discharge rate of roughly $Q_{rhine} = 2000m3/s$. For average Rhine discharges of $Q_{rhine} = 2200m3/s$, the Haringvlietsluices will have the following respective opening sizes during the kierbesluit operational policy:

- $A_{flood} = 180m^2$
- $A_{ebb} = 450m^2$

These were the values used in the validation model calculations. The results of the calculations can be found below:

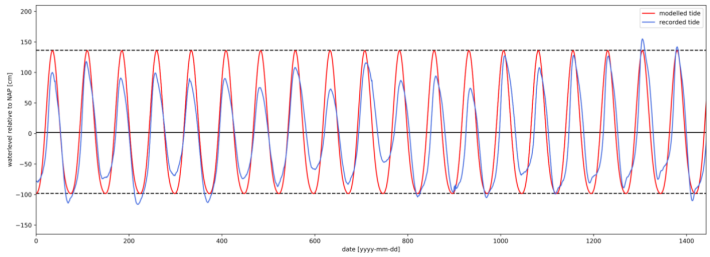

Figure C.8: Modelled and recorded tide for the validation calculation

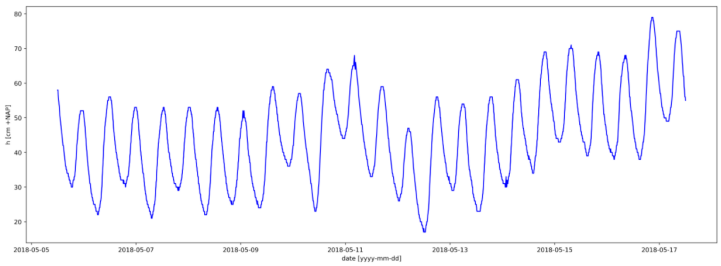

Figure C.9: Recorder waterlevel at Hellevoetsluis

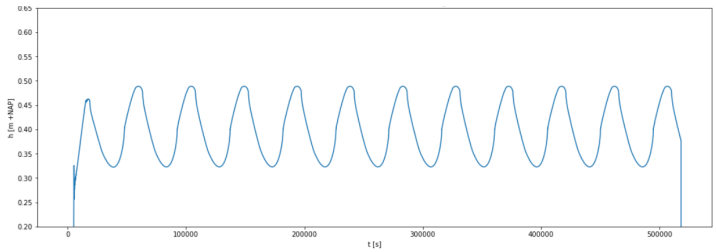

Figure C.10: Modelled waterlevel at Hellevoetsluis (this plot shows a shorter time-span, as the inputs for the model are averaged anyway)

C.3.1. Validity discussion

As can be seen from the model calculations, the model underestimates the amount of tidal range range available for the current situation. This is due to the fact that the Spui is not incorporated into the hydrodynamic

model. Even in situations with extremely low river discharge, the presence of the Spui will still induce a significantly noticeable tidal range into the system. The Spui is expected to have less of an impact, in the case of the full reopening of the Haringvlietsluices.

The second large takeaway for the model is that the model only functions for average situations. The fact that the upstream boundary condition requires an estimate for the undisturbed water height and discharge, makes it so that variation at the downstream boundary that is not average, is not taken into account properly. As such a change would also change the required input for the upstream boundary conditions.

C.4. Python scripts numerical model

In this section of the appendix screenshots are provided of the python script, in which the hydrodynamic model was developed. The presented screenshots are for scenario 2 as described in chapter 5. The other scenario's were simply calculated by changing the boundary conditions of the system.

```
"""
This cell is used to calculate the tidal response of the system for varying cross-sections of the New Haringvliet barrier
"""

# physical constant
g = 9.81                                          # gravitation [m/s2]
T = 44712                                         # M2 tide period [s]

# time stepping
t0, tN = 0, 180000                                # start and end of time domain [s]
N = 70000                                         # number of time steps [-]


# New Haringvliet barrier
mu1 = 0.7                                         # discharge coefficient New Haringvliet barrier [-]
Ac1 = 1500                                      # effective opening New Haringvliet barrier [m2]

#intermediate basin
Ab2 = 45 * 10**6                                  # surface are of tidal lake [m2]

# section data
L = 43000                                         # length of the channel [m]
M = 100                                            # number of sections [-]
s = np.linspace(0,L,M+1)

ds = s[1:M+1] - s[0:M]                            # section length [m]
dS = np.zeros(M+1)                                # section length at nodes [m]
dS[0:M] += ds/2
dS[1:M+1] += ds/2


# channel geometery
def geometry(s,h):
    d = 7.25 + ( h[0:M] + h[1:M+1] ) / 2          # depth in section [m]
    B = 2900 * np.exp(-2 * 0.000008 * s[0:M+1])   # storage width [m]
    A = 21000 * np.exp(-2 * 0.000008 * s[0:M])    # conveyance area [m2]
    R = A / (B[0:M] + 2 * d)                      # hydraulic radius [m]
    return A, B, R, d


# resistance coefficient
cf = .004

# array for results
a = 26

res1 = []                                       # storage array for the water level at the end of a simulation
res2 = []                                       # storage array for the discharge at the end of a simulation

max_Q = []
min_Q = []

max_h = []
min_h = []

z2a = np.zeros(a)
z2b = np.zeros(a)

Qhva = np.zeros(a)
Qhvb = np.zeros(a)

Qla = np.zeros(a)
Qlb = np.zeros(a)



for j in tqdm_notebook(range(a)):
    Ac1 = Ac1 + 500
    print(Ac1)

    t = np.linspace(t0, tN, N+1)                    # time instances
```

Figure C.11: Python script for Scenario 2 (pt. 1/3)

```
# initial conditions
h = np.zeros(M + 1)                          # initial water level channel [m]
Q = np.zeros(M)                              # initial discharge channel [m3/s]
Q2 = 0                                       # initial conditions left boundary of channel
A, B, R, d = geometry(s, h)                  # initial geometry

# intitial conditions tidal lake
Q1 = np.zeros(N+1)                           # initial discharge [m3/s]
zeta2 = np.zeros(N+1)                        # initial waterlevel tidal lake [m]


# storage arrays
Ql_t = np.zeros(N+1)                         # storage array left boundary of channel
Qr_t = np.zeros(N+1)                         # storage array right boundary of channel


#imposed water level boundary (outside of HVSluices)
h1 = 1.17 * np.sin((2*np.pi/T * t)) - 0.19 *  np.sin(2*(2*np.pi/T * t  + T))  # M2 tide at the North Sea


# time loop
for n in tqdm_notebook(range(N)):
    dt = t[ n + 1 ] - t[n]                   # time step

    # discharge relation through the New Haringvliet barrier
    if h1[n] > zeta2[n]:
        Q1[n] = mu1 * Ac1 * np.sqrt(2*g*np.abs(h1[n]-zeta2[n]))
    else:
        Q1[n] = - mu1 * Ac1 * np.sqrt(2*g*np.abs(h1[n]-zeta2[n]))

    # relation through the Haringvlietsluices (left boundary condition channel)
    if zeta2[n] > h[0]:
        Q2 = + 0.7 * 6000 * np.sqrt(2 * g * np.abs(zeta2[n] - h[0]))
    else:
        Q2 = - 0.7 * 6000 * np.sqrt(2 * g * np.abs(zeta2[n] - h[0]))

    # computation of the tidal lake water level
    zeta2[n+1] = zeta2[n] + dt * (Q1[n]-Q2) / Ab2

    #right boundary condition
    Q3 = -800 + B[M-1] * np.sqrt(g * R[M-1]) * (h[M] - 0.1)

    # continuity equation
    dh = np.append(Q, Q3) - np.append(Q2,Q)          # discharge difference
    h  = h - (dt * dh / (B * dS))                    # water level update

    #momentum flux
    F = np.zeros( M + 1 )
    F[0 : M]     += 0.5 * ( Q - np.abs(Q)) * Q/A     # left momentum flux contribution
    F[1 : M + 1] += 0.5 * ( Q + np.abs(Q)) * Q/A     # right momentum flux contribution
    F[0]         += np.max(Q2, 0) * Q2 / A[0]        # inward flux contribution (left boundary)
    F[M]         += np.min(Q3, 0) * Q3 / A[M-1]      # inward flux contribution (right boundary)

    #new geometry update
    A, B, R, d = geometry(s, h)                      # updated geometry (n+1)
    chi = cf * ds / R                                # resistance coefficient of the section
    kappa = chi * np.abs(Q)/A                        # linear resistance factor

    #momentum equation
    dQ = g * A * (h[1:M+1] - h[0:M]) + kappa * Q     # surface slope and resistance of the momentum equation
    dQ += F[1 : M + 1] - F[0:M]                      # momentum flux difference of the momentum equation
    Q  -= dQ / (ds/dt + 2*kappa)                     # discharge update

    Ql_t[n] = Q2                                     # storage of the left boundary value
    Qr_t[n] = Q3                                     # storage of the right boundary value


    if n > 20000:
        res1.append(h)                               # storage of the simulation waterlevels
        res2.append(Q.tolist())                      # storage of the simulation discharge

minima_h = pd.DataFrame(res1).min(axis = 0)
maxima_h = pd.DataFrame(res1).max(axis = 0)

minima_Q = pd.DataFrame(res2).min(axis = 0)
maxima_Q = pd.DataFrame(res2).max(axis = 0)

#computation of the minima and maxima of the channel waterlevel and discharges
min_h.append(minima_h)
max_h.append(maxima_h)
```

Figure C.12: Python script for Scenario 2 (pt. 2/3)

```
min_Q.append(minima_Q)
max_Q.append(maxima_Q)

z2a[j] =  np.max(zeta2[15000:])
z2b[j] =  np.min(zeta2[15000:])
Qhva[j] = np.max(Q1[15000:])
Qhvb[j] = np.min(Q1[15000:])
Qla[j] = np.max(Ql_t[15000:])
Qlb[j] = np.min(Ql_t[15000:])
```

Figure C.13: Python script for Scenario 2 (pt. 3/3)

D

Barrier retaining height

This is an appendix to chapter 7. This appendix provides an overview of the over-topping and overflow calculations used to determine the retaining height of the New Haringvliet barrier.

D.1. Storm development and barrier closure

Figure D.3 shows a storm surge in combination with the average tide at the Hoek van Holland. As a primary design choice, the closure of the New Haringvliet Barrier is set to occur when water levels of higher than +3m NAP are expected. This closure level is in line with the closure demands of the Maeslantkering. When such a storm is expected to occur, there are several closure strategies that are possible to use, depending on the conditions of the storm. These factors include, storm length, storm intensity, and the river discharges behind the barriers. Average river discharge rates for the Rhine and Meuse are $2200 m^3/s$ and $250 m^3/s$ respectively. If these moderate river discharges occur during a storm-surge that is slightly higher than the mandated closure level, the barrier could be closed using a 'late closure'. Closing the structure at a relatively late stage will minimize the head difference across the structure, reducing the risk of structural complications on the barriers. This is a strategy also used during the operation of the Maeslantkering, but can only be used during situations where the storage capacity in the Rhine-Meuse Delta is sufficient to account for the given river discharge during a the time the barriers are closed.

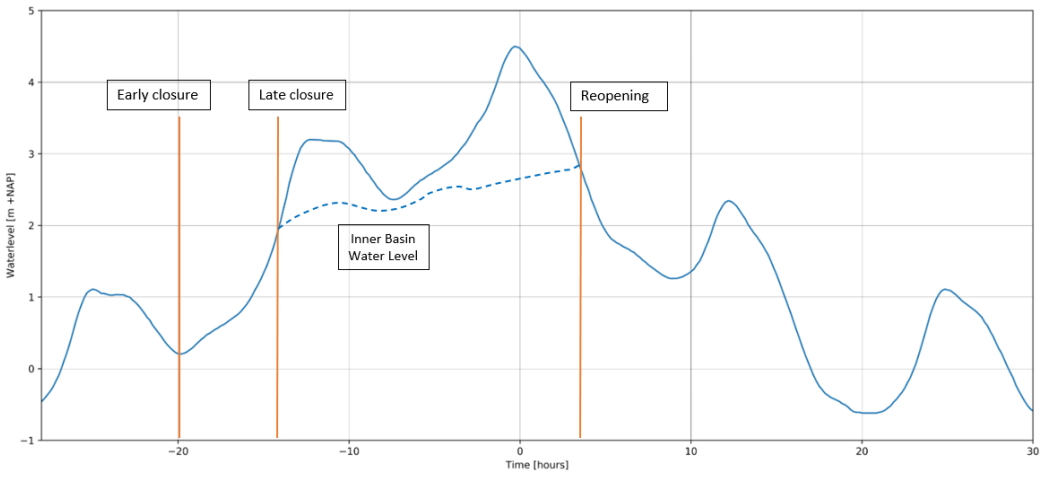

Figure D.1: Waterlevel during a storm with a peak of 4.5m +NAP (Location: Hoek van Holland). The inner basin water-level is a fictional value and only used as an example.

When there is a large amount of river discharge, the barrier can be closed when the tide changes from a ebb to a flood-tide. This allows the areas behind the barriers a larger storage capacity for the in-flowing river discharges. In the case that there is an excessive storm that has multiple peaks over the mandated closure level, if at any time in between those two peaks the water level in the inland basins, exceeds the waterlevel on the North Sea, the barriers can be partially opened to relief some of the water behind the barriers. The operation of the Valmeer and the pumping station in the Delta21 plan will most likely prevent this from being part of the barrier operation during a storm surge. Once the storm subsides and the water-level on the North Sea is lower than that on the inland side of the barrierr, the New Haringvliet barrier can be reopened.

D.2. Failure due to Height

The barriers failure due to a limitation in the a structures height is described by the fault tree shown in fig. D.2. In the WBI2017, it is assumed that when the bottom-protection of a structure is damaged due to erosion, that this will lead to structural failure as-well. Therefor the limit state function can be written in the following manner:

$$P_{f,HT} = P(min[Z_{HT1}; Z_{HT3} < 0]) \tag{D.1}$$

where:

$P_{f,HT}$ = failure probability of the structure due to overtopping/overflow [-]

$P(Z_{HT1} < 0)$ = probability failure of the bottom protection [-]

$P(Z_{HT3} < 0)$ = probability exceedance of the storage capacity behind the barriers [-]

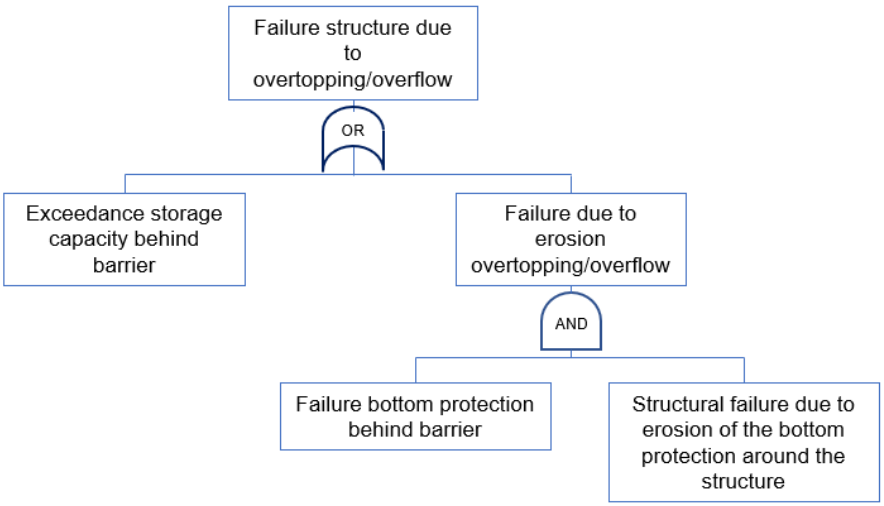

Figure D.2: Fault tree due to overtopping/overflow

D.2.1. Failure probability requirement

The total failure probability allotted to this failure mechanism is $P_{f_HT} = 6.0e-5$. The corresponding desiogn water level is $h_{NS} = 6.5m$, while the design waveheight is $H_{m0} = 3.76m$.

$$P_{f,HT} = \frac{P_{req} * \omega_{HT}}{N_{HT}} = \frac{5e-4 * 0.24}{2} = 6.0e-5 \tag{D.2}$$

where:

$P_{f,HT}$	= failure probability of the structure due to overtopping/overflow	[−]
P_{req}	= required maximum failure probability of the flood defense section	[−]
ω_{HT}	= failure probability factor for overtopping/overflow = 0.2	[−]
N_{HT}	= length factor for the height = 2	[−]

D.2.2. Overtopping and Overflow discharge

The amount of discharge that occurs during a storm event by overtopping and overflow depends on a total of three factors: the structures height, the outside water-level, and the wave-height occurring during the storm. Overtopping only occurs when the water-level outside of the structure exceeds the height of the structure. If this is not the case the only discharge over the structure is caused by overtopping, which is caused by the momentum of the waves crashing against the structure and water spilling over the structure periodically. In the case of the New Haringvliet barrier, the discharge under consideration, only consists of two scenarios, discharge due to overtopping, or discharge due to the combination of overtopping an overflow.

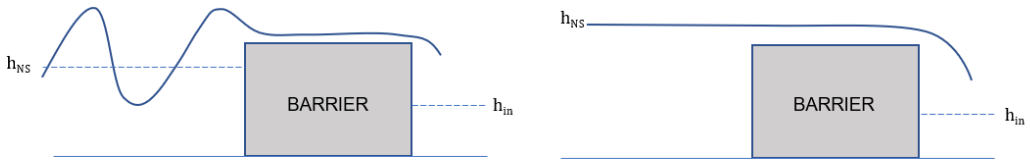

Figure D.3: Schematic examples of overtopping (left) and overflow (right)

Overtopping
The overtopping discharge is given in eq. (D.3), and describes the average discharge over the closed structure.

$$q_{ot} = m_{ot} * \sqrt{g H_{m0}^3} \exp\left(-2.61 \frac{h_b - h_{NS}}{H_{m0}}\right) \tag{D.3}$$

where:

H_{m0}	= significant wave height on the North Sea	[m]
h_b	= retaining height of the barrier	[m]
h_{NS}	= water level on the North Sea	[m]
m_{ot}	= model factor for overtopping = 0.13	[−]

Combination Overtopping and Overflow
The discharge related to the combined effect of overflow and overtopping is given in eq. (D.4).

$$q_{ot+of} = m_{ot} * \sqrt{g H_{m0}^3} \exp(-2.61 \frac{h_b - h_{NS}}{H_{m0}}) + m_{of} * 0.55 \sqrt{g * (h_{NS} - h_b)^3} \quad \text{(D.4)}$$

where:

H_{m0}	= significant wave height on the North Sea	$[m]$
h_b	= retaining height of the barrier	$[m]$
h_{NS}	= water level on the North Sea	$[m]$
m_{ot}	= model factor for overtopping = 0.13	$[-]$
m_{of}	= model factor for overtopping = 1.1	$[-]$

D.2.3. Discharge during normative storm event

With the overtopping/overflow relations provided in appendix D.2.2 were taken and the discharge due to the overtopping and overflow were computed for the normative storm event. In this calculation, the barrier retaining height was set to +6m NAP. The results are shown in fig. D.4. The maximum expected discharge over the storm duration is $q_{ot+of,max} = 3.6 m^3/s/m$, while the mean discharge is equal to $q_{ot+of,max} = 1.2 m^3/s/m$.

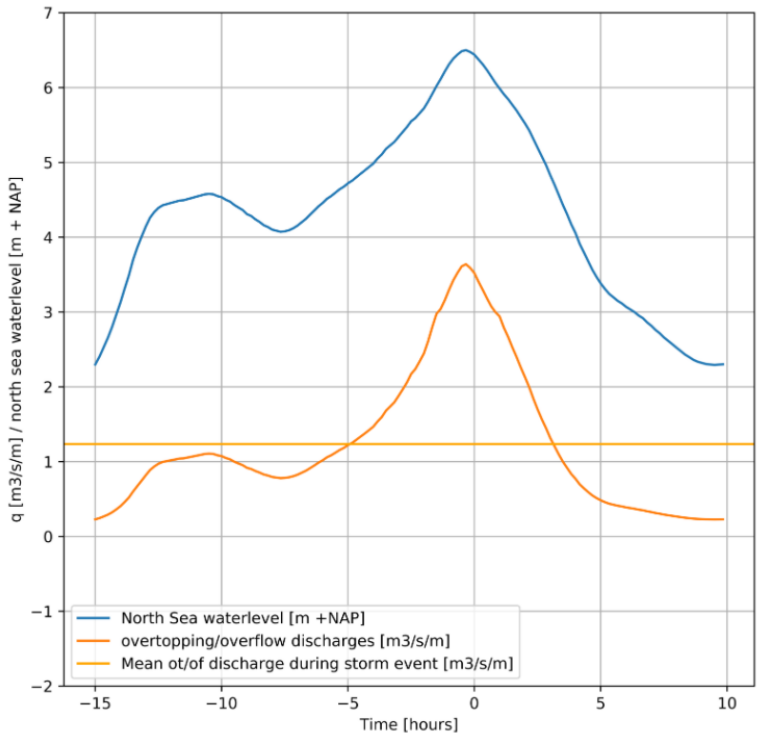

Figure D.4: Combined overtopping and overflow discharges for a New Haringvliet barrier with a retaining height of +6m NAP for a normative North Sea storm (orange). The Corresponding North Sea waterlevel is also plotted (blue)

E

Gate Type

This is an appendix to section 7.1.1. This appendix features the MCA that was done for the gate type selection.

The gate type selection for storm surge barriers is dependent on the local requirements and boundary conditions in relation to the barrier. Flowgates in a storm surge barrier are generally more simplistic and smaller in scale than navigational openings, due to their limited requirements with regards to their clearance height, draught and opening width (Mooyaart et al., 2014). Some common gate types for navigational gates are: floating sector gates, barge gates, and rolling gates. Many of these gates require large amounts of storage space next to the opening for the gates, but excel in closing of a single opening of a long span.

In the case of the New Haringvliet barrier, there is no need for a navigational opening with a large span as the navigation in the region is limited to relatively small vessels. For more details on the navigational demands for the barrier more information is given in section 7.3. Therefor the options with regards to the gates of the New Haringvliet barrier in this assessment are limited to vertical lift gates, flap gates, vertically rotating segment gates, radial gates, and inflatable gates (fig. E.1). Figure E.2 gives an overview of the effectiveness of different barriers to different design criteria and requirements.

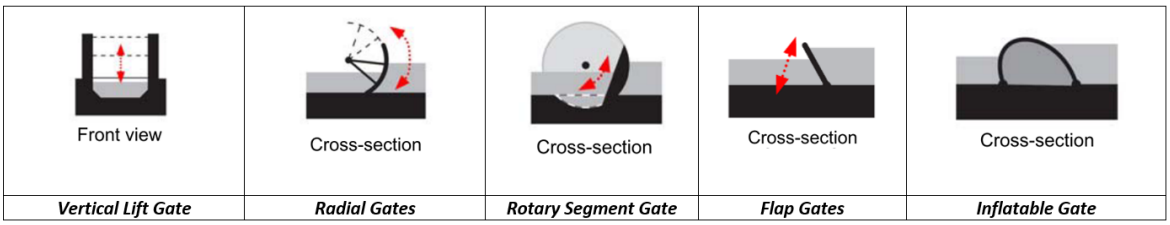

Figure E.1: Schematic overview of the considered gate types for the New Haringvliet barrier. (images: Dijk and Van der Ziel (2010))

	Mitre gate	Vertical lifting	Flap	Horizontal rotating	Vertical rotating	Inflatable
Span > 30m	-	+	+	+	+	+
Span > 100 m	-	-	+	+	-	+
Water depth > 10 m	+	+	+	+	+	+
Impact upon landscape	+	-	+	+	-/+	+
Maintenance	+	+	-	0	+	+
Currents and waves	-	+	0	0/+	0/+	0
Closure time	+	+	+	+	+	+
Space required	+	+	+	-	+	+
Colliding ships	0/-	+	+	0/-	+	0
Reliability	-/+	+	0/+	-/+	+	0
Clearance height	+	-	+	+	-/+	+

Figure E.2: Comparison of the different barrier types: - Not favorable up to not feasible, 0/- Below average/vulnerable, 0 Average/possible, 0/+ Above average, + Favorable/proven technology, -/+ Score depends ondesign choices and conditions (source: based on Dircke et al. (2012))

E.1. Assessment Gate Type New Haringvliet barrier

Based on the comparison of the various gate types presented in fig. E.2, a pre-assessment of the various possible gate types is made. The New Haringvliet barrier is expected to have individual openings with a span of between 50-100m, with the bottom of the opening at a depth of -5.5m NAP. There is no need for an unlimited clearance height in the gated sections as the barrier will have a dedicated navigational opening or shipping lock. Lastly, the barrier will form a part of the primary flood defense system of the Netherlands, therefor the reliability and ease of inspection and maintenance of the structure are primary concerns in the assessment of the gate types for this project.

Based on the description of the general requirements of the New Haringvliet barrier and the characteristics of the different gate types presented in fig. E.2, the criteria for the pre-assessment were selected and are presented below. In the MCA, the final score of the gate types will strongly coincide with the scores received in fig. E.2, however, additional explanation of the chosen criteria is given for additional context and clarity of the assessment procedure.

1. Maintenance
Maintenance scores often come down to the expected cost of maintenance and the reliability of maintenance demands for a specific gate type. However, at this stage of the assessment, this score is mainly estimated based on the ease of maintenance and inspection of the various gate types. Therefor gates that can be inspected above water, and that have the majority of their crucial mechanical components such as hinges and above water, will generally have a better score in this part of the assessment.

2. Reliability
This criteria rates the possible failure modes a specific gate type can have during their respective operation. This includes things such as a gate's possible mechanical failures, vulnerability to obstructions, and structural failures. Generally, more frequently seen gate types will have an advantage in this criteria as well, as there is more expertise and better insight into their operation and possible failure mechanisms.

3. Construction Costs
The expected cost of a structure is not a factor that is included in the assessment criteria presented in fig. E.2. However, in the scope of a large construction project, construction costs are often of the primary determining factors in the project's success. For the use in flood barriers, vertical lift gates, inflatable gates and tainter gates are often considered to have low-moderate construction costs (Daniel & Paulus, 2019). Flap gates are also often relatively affordable, however, larger gates can become more complex and expensive. Lastly, rotating segment gates, are generally more expensive as they are some of the heaviest gates, and require a large, and complex sill structure to operate effectively (Daniel & Paulus, 2019).

4. Ship Collision
The occurrence of a ship collision is often not considered a likely scenario, however, it can have a significant impact on the structural integrity of a structure. Therefor the impact of such a collision on the respective gate types will be considered.

5. Operation in currents and waves
The operation of a storm surge barrier is especially important in the construction of coastal storm-surge barriers, such as the New Haringvliet barrier, which are subject to large wave-loads and currents when they are required to close.

6. Visual Impact
The visual impact of a barrier on the local landscape can be an important parameter for locals and possible tourism industries. In this assessment, the a large visual impact of the gates is considered negative. This will mostly affect radial and vertical lift gates, due to their visual presence above the waterline.

E.2. Multi-Criteria Assessment Gate Types

In order to determine the weighted factor of the various MCA criteria listed above, once again a priority matrix was used (fig. E.3). Based on the priority matrix, the MCA in fig. E.2 was made. As can be seen in the priority matrix, the visual impact of the barriers is the least highly rated criteria in the assessment, as it is the only criteria with no impact on the operational performance or total project costs of the barrier.

		a	b	c	d	e	f	total	final scores	weight factor
Maintenance	a		0	0	1	1	1	3	6	0.19
Reliability	b	1		1	1	1	1	5	10	0.32
Construction Cost	c	1	0		1	1	1	4	8	0.26
Ship collision	d	0	0	0		0	1	1	2	0.06
Operation in current + waves	e	0	0	0	1		1	2	4	0.13
Visual Impact	f	0	0	0	0	0		0	1	0.03
									31	1.00

Figure E.3: Priority matrix for the assessment criteria in order to determine the weighted criteria factors used in the MC

		Flap gates		Radial Gates		*Rotating Sector Gate*		*Inflatable Gate*		Vertical Lift Gate	
Criteria	Weight factor	Score	Weighted score	Score	Weighted score	Score	Weighted score	Score	Weighted score	Score	Weighted score
Maintenance	0.19	1	0.19	5	0.97	5	0.97	5	0.97	5	0.97
Construction Cost	0.32	3	0.97	4	1.29	2	0.65	4	1.29	4	1.29
Reliability	0.26	4	1.03	5	1.29	4	1.03	3	0.77	5	1.29
Ship collision	0.06	5	0.32	5	0.32	5	0.32	3	0.19	5	0.32
Operation in current + waves	0.13	3	0.39	4	0.52	4	0.52	3	0.39	5	0.65
Visual Impact	0.03	5	0.16	1	0.03	5	0.16	5	0.16	1	0.03
Total:	1.00	21	3.06	24	4.42	25	3.65	23	3.77	25	4.55

Figure E.4: Multi-criteria analysis of the selection of the gate types

From the MCA, it can be found that the best suited barrier gates for the New Haringvliet barrier are the vertical lift gates and the radial gates. These gate types are some of the most used hydraulic gate types in flood barriers, and are well proven and generally cost effective solutions for barriers for barriers where a limited clearance height is acceptable. However, given the fact that the New Haringvliet barrier, is proposed in a current Natura2000 area, there might be an increased desire for the use of barriers with a low visibility. Therefor a second assesment was done in the where the importance of the visual impact of the barrier was increased, an overview of this was shown in fig. E.5. In this assessment, only the barrier reliability is ranked as more important than the visual impact of the barrier on the landscape. The assumption here is that the visual impact of the barrier is a priority in the project. Doing so yields the results that the inflatable gate is the most desirable barrier type, followed by a rotating sector gate.

		a	b	c	d	e	f	total	final scores	weight factor
Maintenance	a		0	0	1	1	0	2	4	0.13
Reliability	b	1		1	1	1	1	5	10	0.32
Construction Cost	c	1	0		1	1	0	3	6	0.19
Ship collision	d	0	0	0		0	0	0	1	0.03
Operation in current + waves	e	0	0	0	1		0	1	2	0.06
Visual Impact	f	1	0	1	1	1		4	8	0.26
									31	1.00

Figure E.5: Priority matrix for the assessment criteria in order to determine the weighted criteria factors used in the MC, increased value for the visual impact of the barrier

		Flap gates		*Radial Gates*		Rotating Sector Gate		Inflatable Gate		*Vertical Lift Gate*	
Criteria	Weight factor	Score	Weighted score	*Score*	*Weighted score*	*Score*	*Weighted score*	*Score*	*Weighted score*	*Score*	*Weighted score*
Maintenance	0.13	1	0.13	5	0.65	5	0.65	5	0.65	5	0.65
Construction Cost	0.32	3	0.97	4	1.29	2	0.65	4	1.29	4	1.29
Reliability	0.19	4	0.77	5	0.97	4	0.77	3	0.58	5	0.97
Ship collision	0.03	5	0.16	5	0.16	5	0.16	3	0.10	5	0.16
Operation in current + waves	0.06	3	0.19	4	0.26	4	0.26	3	0.19	5	0.32
Visual Impact	0.26	5	1.29	1	0.26	5	1.29	5	1.29	1	0.26
Total:	1.00	21	3.52	24	3.58	25	3.77	23	4.10	25	3.65

Figure E.6: Multi-criteria analysis of the selection of the gate types, increased value for the visual impact of the barrier

E.2.1. Discussion MCA

From the MCA, the following conclusions can be drawn:

- The vertical lift and radial gates provide the best general solutions from a cost, reliability and maintenance perspective for the New Haringvliet barrier.
- In the case that there is a high demand for a low visual impact the inflatable gate and rotating sector gates gain increases importance.

The MCA mainly uses general criteria from fig. E.2 to asses the effectiveness of various gate types in application of the New Haringvliet barrier. However, when we consider the length of the gated section (ca. 2000m) and the fact that the barrier will become part of the primary flood defence system of the Netherlands, gate types with large construction costs, or with reduced reliability such as rotating segment gates and inflatable gates become less desirable. The complexity and size of the sill structure, and the weight of the gate in rotating sector gates, are likely to vastly increase the cost of the barrier especially when considering a long total gated section. The inflatable gates, have never been used in flood protection barrier of this magnitude either, and questions about the various failure modes of the barrier and the dynamic behaviour of the gate type during wave loading make it hard to justify the choice of these barriers currently for the application in the New Haringvliet barrier. Additionally, the inspection of maintenance of these barriers in a span of this size might become an increasingly large problem.

Therefor, vertical lift gates and radial gates are considered the best options for use in the New Haringvliet barrier. As it pertains to the visual impact of the New Haringvliet barrier, it would be important to consider the desires of the various local stakeholders in the barrier design at later stages of the design process. Many storm surge barriers are often also considered as landmarks and thus proper design of the barrier's aesthetic and additional functions could bode well to the local stakeholders. In the case that a low-visual impact becomes a requirement, additional research into the operation, maintenance and reliability of the use of inflatable gates would be advised.

E.2.2. Assessment vertical lift-gate versus radial gate

Radial gates and vertical gates largely have similar benefits when it comes to their criteria and expected cost in the use of flood barriers. This is also reflected in the results of the gate type MCA. When comparing the two barrier types, there are some differences that can affect the choice between the two gate types:

- Radial gates rotate around a central trunnion that is located above the local water level, which is beneficial from a maintenance perspective. The trunnion, is however also a very complex part of the barrier as it is the focus of all hydraulic forces on the gate.
- Radial gates have lower piers, as they do not require lifting piers to suspend the gates above water. The piers are however, wider as they have to include both the trunnion and gate seal.
- Due to the fact that radial gates are supported by relatively slender arms, structures with larger radial gates such as the Eider barrier and Haringvlietsluices, often are constructed using a beam as a support allowing for multiple hinges along the length of a single gate.

In general, vertical lift gates are far more common in use in storm surge barriers, where radial gates are more commonly seen in weir and spillway applications. Vertical lift gates have the added benefit that they can also designed as navigation openings by increasing the height of the lifting towers, this can be seen in the Hartelkering and the Hollands IJsell barrier. This thesis will continue the design of the New Haringvliet barrier, using primarily vertical lifting gates.

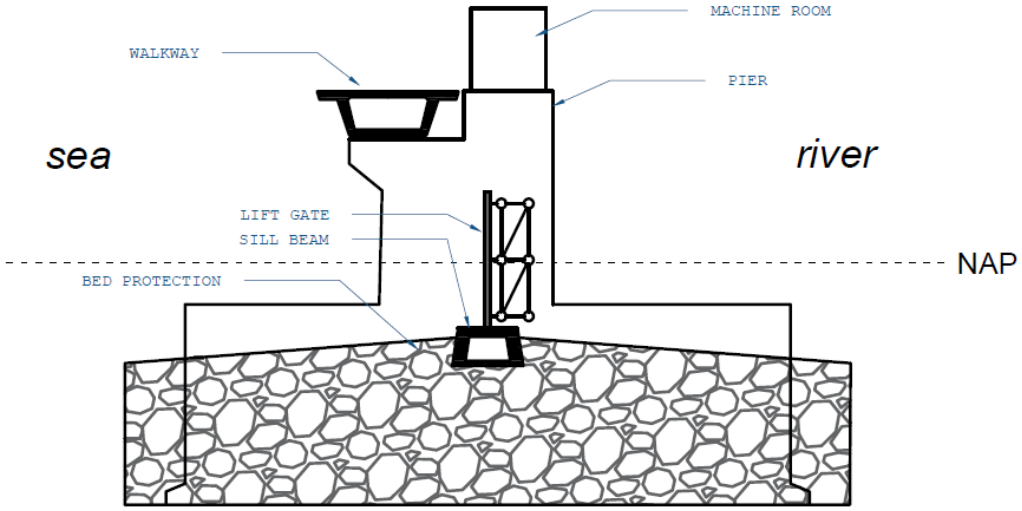

Figure E.7: Side view of an example layout for a lift-gate configuration of the gated barrier section

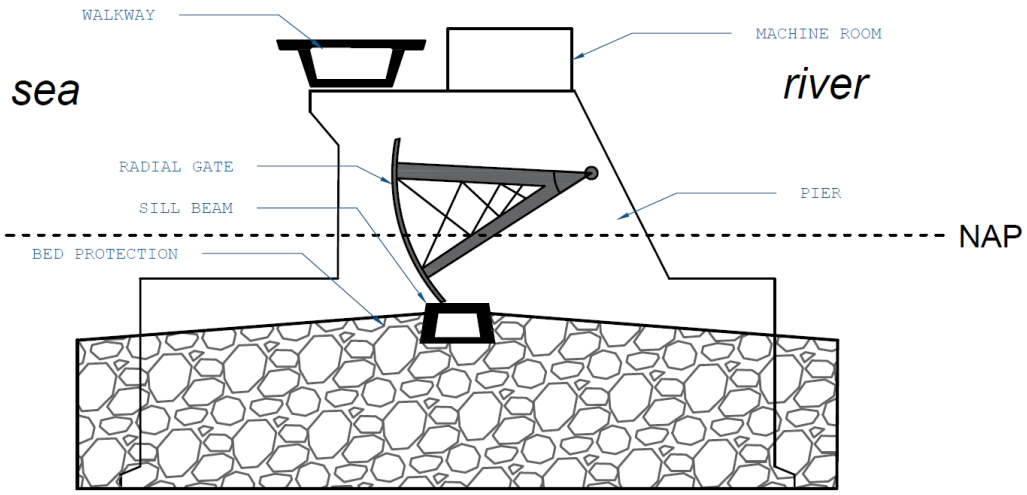

Figure E.8: Side view of an example layout for a proposed radial gate configuration of the gated barrier section

F

Gate Span Assesment

This is an appendix to section 7.1.5, and outlines the full gate span assessment that was done to motivate the choice in the barrier's gate span.

The choice of a gate span is a complex choice that affects the design of almost all individual barrier components, making the optimization of such a choice quite complex. To make a choice in the gate span of the flow gates in the New Haringvliet barrier, will be assessing the effects the span choice has on the dimensions and required position of the caisson foundation elements. This assessment, paired with a general discussion of the impact of the span choice on the other barrier elements, will then be used as a primary design consideration for the choice of the individual gate spans in the New Haringvliet barrier.

The choice of the span of an individual gate openings directly affects the design and the dimensions of the majority of the barrier's core elements. Vertical lift gates transfer their forces to the lifting towers and the foundation by bending. Increasing the span of an opening quadratically increases the maximum bending moment on the gate. The road girder and the sill beam, also experience quadratic bending moment increases for a linear increase in the gate span. The design of the bed protection is mostly unaffected by the differences in span lengths as the critical load scenario for the bed protection is the case where an individual gate fails to close during a storm. In this scenario, the head over the structure is determines the load on the bed protection at the downstream end of the structure. The machine room is only affected in the way that larger spans result in heavier gates, and so more heavy duty lifting equipment might be required.

The relation between the gate size and the piers however, is a more complex relation. The foundation caissons in the case of a prefab storm-surge barrier, are responsible for ensuring the stability of the overall structure. However, due to their large size the caissons are also subject to significant hydraulic loads. Meaning that changing the size of the caissons affects both the total loads on- as well as the resistances off the storm surge barrier.

Because of this relation, as well as the importance of the piers to the overall storm-surge barrier, the choice was made to select the span off an individual opening on it's effects on the design requirements of the caissons.

F.1. Hydraulic boundary conditions

The caissons elements will be evaluated and must suffice the requirements for rotational stability, horizontal stability and the vertical stability of the barrier. In order for the design of the barrier to suffice to the standard of the WBI2017, all the elements of the structure need to be designed so that the satisfy the reliability requirements shown in eq. (F.1). The corresponding design loads and conditions are shown in table F.1.

$$P_{f,STR} = \frac{P_{req} * \omega_{STR} * c}{N_{STR}} = \frac{5e-4 * 0.02 * 3}{3} = 1.0e-5 \tag{F.1}$$

where:

$P_{f,STR}$	= failure probability of the structure due structural failure	[−]
P_{req}	= required maximum failure probability of the flood defense section [-]	$[m/s^2]$
ω_{STR}	= failure probability factor for structural failure (= 0.02) [-]	$[m/s]$
N_{STR}	= length factor for structural failure failure mechanism (= 3)	$[m/s]$
c	= correction factor with regards to the correlation of failure due to structural failure and due to overtopping/overflow (= 3)	[−]

Parameter	Symbol	Value
Top of the sill	h_{sill}	-5.5m NAP
Top of the gate	h_{tog}	+6.0m Nap
Waterlevel North Sea	h_{NS}	+7.2m NAP
Waterlevel Haringvliet	h_{HV}	+2.0m NAP
Significant waveheight	$H_{s,d}$	3.96m

Table F.1: Design loads and conditions for the New Haringvliet barrier

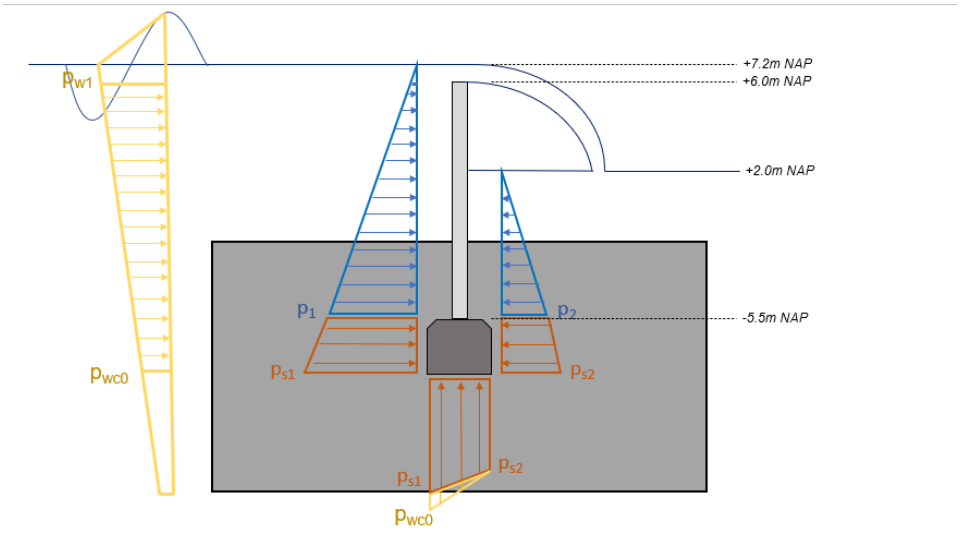

Figure F.1: The hydrostatic pressures on the gate and sill beam of the barrier that will be considered in the stability assessment (image NTS)

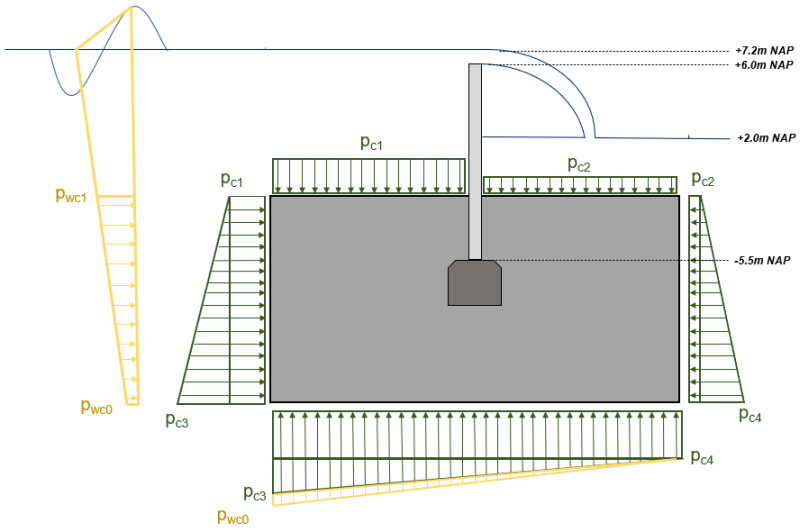

Figure F.2: The hydrostatic pressures on the caisson foundation of the barrier that will be considered in the stability assessment (image NTS)

F.2. Design Calculations

Figure F.1 and fig. F.2 show the the distribution of the hydrostatic pressure forces on the gate and sill beam, and the caisson foundation respectively. In this assessment, the dimensions and positions of the caisson will be varied. For the gates, the only variable that will be changed is the span of the gate. The gate will reach from the top of the sill beam (-5.5m NAP) to a level of +6m NAP when in it's closed position. The span evaluation will consider gate spans in the range of 40m - 100m. Currently, the largest single span vertical lift gates are in the order of 100m in length, so this was chosen as the upper limit in the evaluation.

For the self-weight of the caissons, an assumption was made for the ratio of the caisson to be 70% ballast (unit weight of $18 kN/m$) versus 30% concrete (unit weight of $25 kN/m$). The sill has beam modelled as a concrete hollow beam with a height and width of 5m and 8m respectively. The beam is assumed to be 40% concrete and the remainder of the cross-section is to be ballasted with water. Lastly, this assessment does not take into account the absence of the the self-weight of the gates, lifting towers and road girder. The soil pressures working on the foot were also not taken into account. This will yield a very conservative result for the stability of the elements.

The hydrostatic pressures at any point on the structure is a function of the pressure head and density of the water (eq. (F.2)). For the calculation of the pressures due to waves near the structure (indicated in yellow in fig. F.2 and fig. F.1), the Sainflou method was used.

$$p = \rho_w g h \tag{F.2}$$

where:

p	= water pressure	$[Pa]$
ρ_w	= density of water(= $1025 kg/m^3$)	$[kg/m^3]$
h	= pressure head	$[m]$

Sainflou method

The Sainflou method assumes complete reflection of the incoming wave, causing peaks in front of the structure with the magnitude of the incoming wave height. In addition to the incoming wave, height it also assumes an increase in the still water-level in-front of the structure due to the reflection of the incoming waves. In the critical load scenario considered for the current assessment, there will be significant overflow and overtopping of the gates. Thus the Sainflou method will overestimate the wave induced hydrostatic pressures on the structure. Therefor, the choice was made to assume no increase of the still waterlevel ($h_0 = 0$), but to still maintain full reflection of the wave. This is still likely to be an overestimation of the actual forces on the structure. But at this stage of the design process, this will be accepted as it will only result in a slightly more conservative design of the structure.

Equation (F.3) showns the equation and that leads to the maximum pressures at mean sea level according to the Sainflou method. The maximum pressure level near the bed is given by eq. (F.4). Between the two points a linear distribution of the pressures is assumed. Figure F.3 gives an visual overview of the pressure distribution according to the sainflou method.

$$p_1 = \rho_w g (H_{in} + h_0) \tag{F.3}$$

$$p_0 = \frac{\rho_w g H_{in}}{cosh(kd')} \tag{F.4}$$

where:

H_{in}	= incoming wave height	$[m]$
k	= wave number	$[rad/m]$
d'	= water depth above structure's foundation	$[m]$

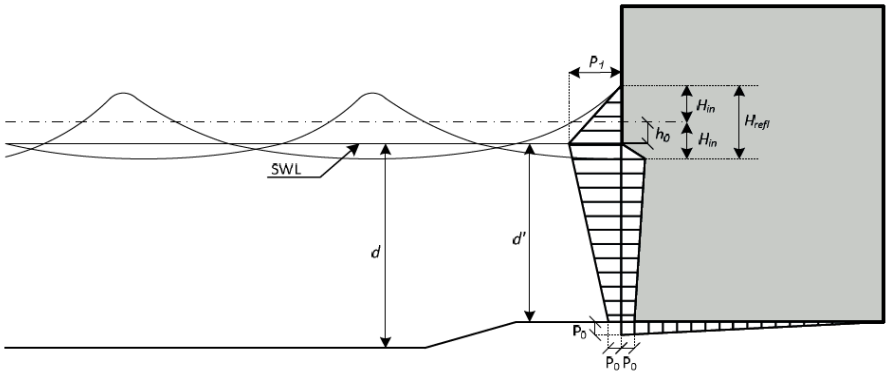

Figure F.3: Sainflou: wave pressure (image source: Molenaar and Voorendt (2019))

Stability calculations

In order to check if the caisson foundation suffices for a given gate span, the horizontal, rotational and vertical stability of the section will be evaluated. For each of the calculations, because it concerns the extreme load scenrio a safety factor of 1.2 is applied to the loads acting on the structure. This section of the report will give an overview of the respective stability calculations used in the evaluation.

Horizontal Stability
For structures founded on a shallow foundation, the friction forces between the subsoil and the structure should be large enough to resist the horizontal pressure forces on the barrier. For this scenario the normative load scenario occurs during the design conditions shown in table F.1. The large head difference across the barrier induces a large net horizontal force across the barrier, while simultaneously, the buoyant forces on the barrier are also relatively large. The friction coefficient is assumed to be $f = 0.6$, which coincides with the range of the values considered for cast concrete structures on clean-gravel/coarse sand. Similar values were also used in the Dutch Delta Works.

$$\sum H < f \sum V \tag{F.5}$$

where:

$\sum H$	= sum of all horizontal forces acting on the structure	$[kN]$
$\sum V$	= sum of all vertical forces acting on the structure	$[kN]$
f	= friction coefficient for the subsoil	$[-]$

Rotational Stability
In the case of a shallow foundation, the foundation and the subsoil are not capable of producing tensile forces to provide stability to the structure.. As long as the resultant force remains within the core, the subsoil will be able to provide the compressive forces needed for the structure to remain stable (Molenaar & Voorendt, 2019). The core of the structure is a region as wide as 1/6th of the width of the floor of the structure, at each side of

the middle of the structure fig. F.4. This yields the following relation with regards to the rotational stability of the structure.

$$e_r = \frac{\sum M_a}{\sum V} < \frac{1}{6} b \tag{F.6}$$

$\sum M_a$	= sum of all moments around the middle of the bottom of the structure	$[kNm]$
$\sum V$	= sum of all vertical forces acting on the structure	$[kN]$
b	= width of the structure	$[m]$

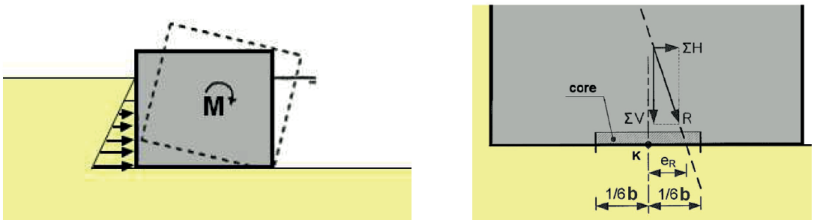

Figure F.4: Resultant forces at the barrier and their respective positions from the middle of the bottom of the concrete floor

Vertical Stability
The vertical stability assessment evaluates whether or not the vertical stresses induced by a critical load scenario of the barrier, exceed the maximum bearing capacity of the soil. As a first estimate, the bearing capacity of the subsoil is assumed to be in the order of $400 kN/m^2$ (value for densely packed sand).

$$\sigma_{k,max} < p'_{max} \tag{F.7}$$

$$\sigma_{k,max} = \frac{\sum V}{bl} + \frac{\sum M}{\frac{1}{6} l b^2} \tag{F.8}$$

$\sum M_a$	= sum of all moments around the middle of the bottom of the structure	$[kNm]$
$\sum V$	= sum of all vertical forces acting on the structure	$[kN]$
l	= length of the structure (= segment of 100m long)	$[m]$
b	= width of the structure	$[m]$

F.2.1. Preliminary Caisson Dimensions

In order to establish the caisson dimensions required for each gate span of the barrier, a layout where the top of the caisson aligns with the top of the sill-beams was chosen (fig. F.5). A layout with a higher caisson position, where the sill beam and the gate are further recessed into the caisson were also considered (fig. F.6). Such a layout was found to slightly improve the stability of the barrier, however, such a layout would also cause a significantly less efficient barrier design with regard to the effective cross-section of the barrier. Therefor such a barrier layout was not further considered for further evaluation.

While determining the dimensions of a caisson for a specific gate span, the increments of the width and length of the caisson were limited to steps of 5m, while the height was varied in steps of 2m at a time. An

overview of the design calculations can be found in appendix F. The results for the final caisson dimensions is given in table F.2. In order to limit the amount of dredging required at the final location, the height of the caissons was kept to a minimum.

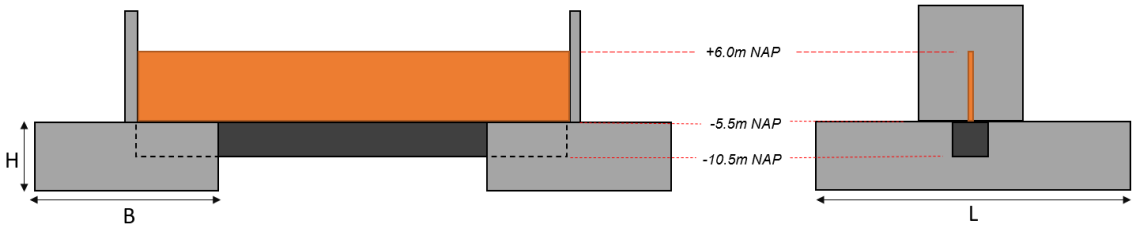

Figure F.5: Overview of the primary dimensions and relative positions of the primary barrier elements

Figure F.6: Alternate barrier layout, where the caissons are positioned higher relative to the other barrier elements

Gate span [m]		40	60	80	100
Caisson Dimensions [m]	B	20	25	30	30
	L	50	50	55	60
	H	12	14	14	16
Caisson Volume [m]	Total	12000	17500	23100	28800
Relative span increase [-]		1.0	1.5	2.0	2.5
Relative caisson volume increase [-]		1.00	1.46	1.93	2.41

Table F.2: Caisson dimensions for each respective gate span.

Gate span [m]		40	60	80	100
Stability unity check values [-]	Horizontal	1.02	1.00	1.02	1.04
	Rotational	1.53	1.22	1.37	1.29
	Vertical	1.66	1.30	1.36	1.17

Table F.3: The unity-check values of the various caissons with regard to the horizontal, rotational and vertical stability criteria (value must be large than 1.0 to suffice)

F.2.2. Recommendations

From the results for the caisson dimensions, it can be seen that the total volume of the caissons increases roughly proportional to the gate span of a section. This means that the choice in gate span will not significantly impact the total amount of material that is required for the construction of the caissons. One thing that should be noted however, is that a larger overall span for the individual gated sections would require a smaller total number of gated sections to come to reach the effective opening of the barrier. Figure F.7 gives an overview of the total number of caisson elements are required depending on the span size of each gate.

From a construction process point of view, a larger span would be greatly beneficial as it would require the construction of a smaller number of caissons. For the construction process this would have the following implications:

- There would be a reduction in the total amount of transport of caissons between the building dock and the final assembly location. Even though the elements might be larger, and thus would require more

effort to transport and place accurately. However, even the largest caissons in this case are of a feasibly manageable size.

- A smaller construction dock would be required. In the building dock, the individual caisson elements would have to be separated to allow for transport of materials and construction equipment throughout the building dock. Having fewer total elements to be constructed in the building dock would lead to a net reduction in the amount of space needed for these spaces, and thus also the total amount of space required in the building dock.

And thus based on the caisson elements and their relation to the gate span, it would be recommended to choose the section of a single gate opening as large ass possible. However, there are two additional important considerations to make with regards to the gate span selection of a storm-surge barrier:

1. Smaller spans cause generally less of a hydraulic load in the case of a partial failure to close of the barrier (failure of 1 - 2 gates)
2. Other elements such as the gates, walkway and sill beams will also become more complex and expensive as the span size increases.

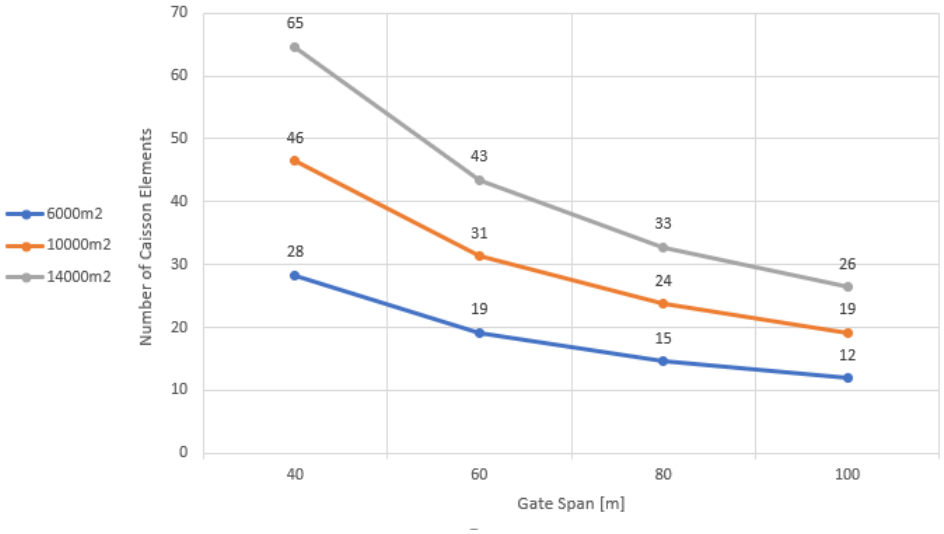

Figure F.7: The required number of caisson elements per gate span to complete an effective barrier cross-section of 6000m^2, 10000m^2 and 14000m^2

$$n = \frac{A_{barrier}}{L_{span} * d} \tag{F.9}$$

where:

$A_{barrier}$	= effective cross-section for the New Haringvliet barrier	[m^2]
n	= total number of gated sections	[−]
d	= depth of the sill relative to NAP (= 5.5m)	[m]
L_{span}	= gate span	[m]

It should be noted that the relation between the number of gate openings and the span of each gate is an inverse relation (see eq. (F.9)). Thus the larger the span becomes, the less effective the impact of increasing

the gate span is on the total number of required caisson elements. On the other hand however, the other structural elements, such as the gate, walkway, and sill beam are subject to distributed loads, and are subject to large bending moments, which scale quadratically with the span of the respective elements.

The final choice for the gate span is to select a single gate span of 80m. This was done as increasing the gate span to 100m would have a relatively small impact on the total number of caisson elements (between 3-7 elements depending on total barrier cross-section) that would have to be constructed and transported. While on the other hand there would still be a significant lower normative bending moment (36% reduction for a 80m span relative to 100m spans under a uniform distributed loads on a simple supported beam) that the sill-beam, walkway and gates would be subjected too, while also slightly reducing the hydraulic load in case of a failure to close of a barrier gate.

F.3. Schematic Overview of the Barrier and Forces

*1in

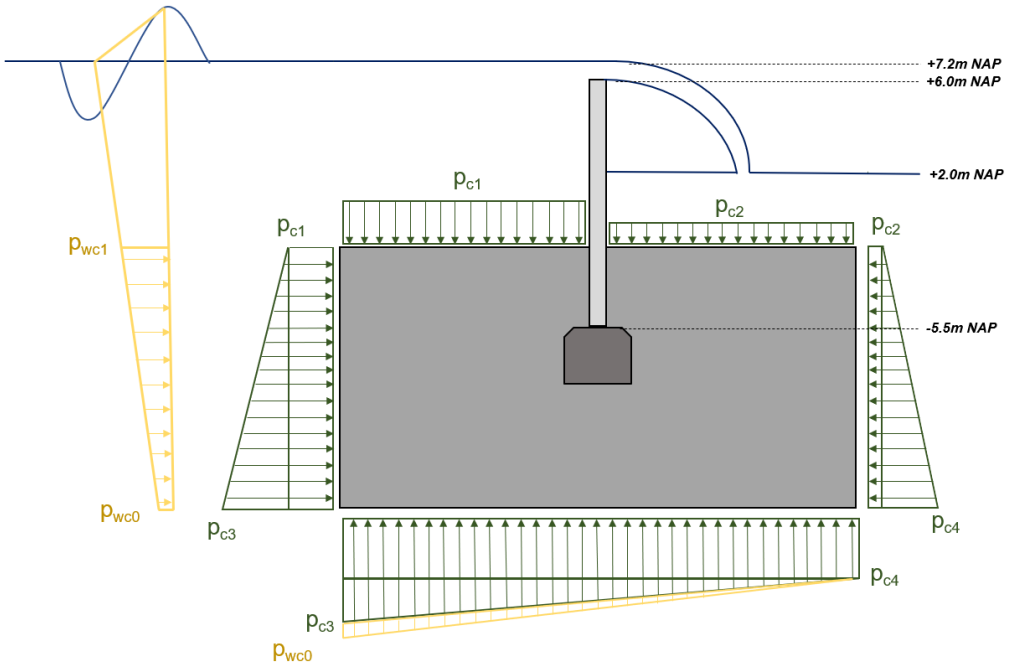

Figure F.8: Hydrostatic pressures on the caisson [Image NTS]

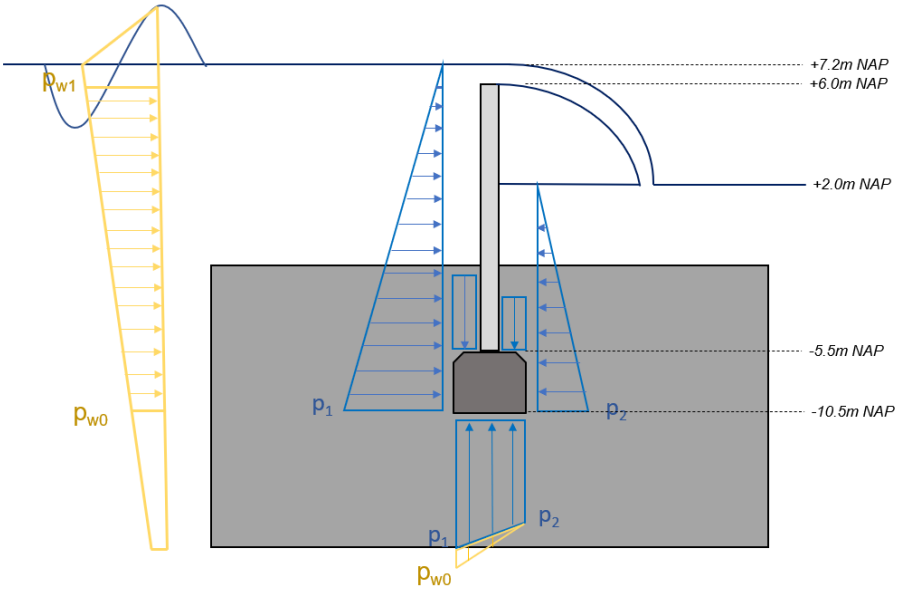

Figure F.9: Hydrostatic pressures on the sill and hydraulic gates [Image NTS]

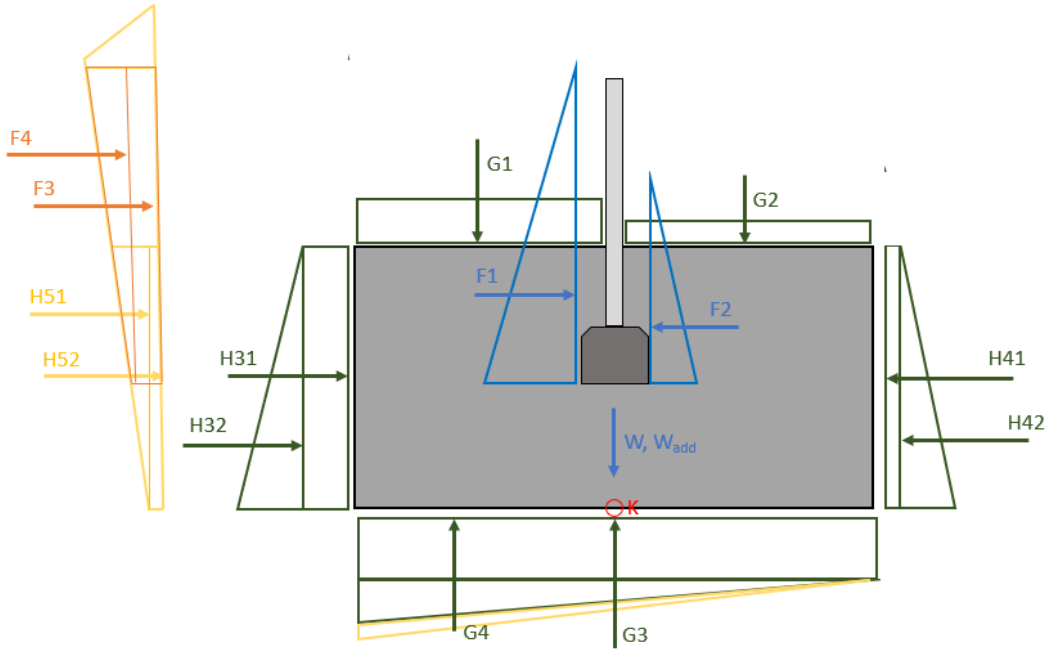

Figure F.10: Resultant hydrostatic forces on the caisson, gates, and sill [Image NTS]

F.4. Barrier Caisson Stability Calculation

This section will outline the calculations done in the stability assessment of the various gate span configurations for the barrier.

F.4.1. 40m Span Gate

Figure F.11: Overview of the spreadsheet calculations done for a 40m wide gate

F.4.2. 60m Span Gate

Figure F.12: Overview of the spreadsheet calculations done for a 60m wide gate

F.4.3. 80m Span Gate

Figure F.13: Overview of the spreadsheet calculations done for a 80m wide gate

F.4.4. 100m Span Gate

Figure F.14: Overview of the spreadsheet calculations done for a 100m wide gate

G

Scour protection

The bed protection near a hydraulic structure prevents structural damage to said structure by preventing erosion of the subsoil. Turbulence can still cause scour holes at the end of the applied bed protection, if there is insufficient sediment supply over the protection. When scour occurs, the majority of the erosion happens relatively quickly, after which it takes a longer period before an equilibrium scour depth is reached (Huis in 't Veld et al., 1982).

For the calculations with regards to the design of the scour protection, the following desing assumptions are used:

- The barrier will have an effective cross-section of 10000m2
- The critical water-level behind the barrier is +3m NAP (same as the Eastern- Scheldt Barrier)

The normative design conditions for the bottom protection of the New Haringvliet barrier, are generally based on one of three scenarios.

1. During a failure – to – close scenario of a storm surge
2. Overtopping / Overflow loading
3. Tidal in- or outflow conditions

Looking at the current Haringvliet sluices, the bottom protection on the North Sea side is designed to handle an extreme discharge of up to 25000m3/s. This is already significantly higher than the maximum expected possible river run-off that is expected to be about 16000-18000m3/s depending the future height of the inland river dikes. For the North Sea side of the New Haringvliet sluices, this will be the design parameter used for the bottom protection. As it pertains to the Haringvliet side of the barrier, an assessment of the three scenarios listed above will determine the design of the bottom protection.

G.1. Scour Protection Failure Modes

The normative situation with regards to the stability of the bottom protection of the New Haringvliet Barrier occurs when the barrier fails to close during a storm event. The worst situation would arise if a minimal section of the barrier fails, during a significant storm event. Such a scenario would cause a high head difference across the barrier, resulting in high flow velocities over the bottom protection. From a floodsafety perspective, the failure probability for the FTC failure mechanism is given in eq. (G.1).

$$P_{f,FTC} = \frac{P_{req} * \omega_{FTC}}{N_{FTC}} = \frac{5e-4 * 0.04}{1} = 2.0e-5 \tag{G.1}$$

where:

$P_{f,HT}$ = failure probability of the structure due to a failure to close [-]

P_{req} = required maximum failure probability of the flood defense section [-]

ω_{HT} = failure probability factor for failure to close = 0.04 [-]

N_{HT} = length factor for the FTC = 1 [-]

For a barrier with a large number of gates such as the New Haringvliet barrier, the failure probability can be calculated by assessing the combination of various partial failure scenarios and the probability that this coincides with a storm of a given strength (eq. (G.2)).

$$P_{f,FTC} = \sum (P_{f,i}(n_{gates}|h_{NS}) * P_i(h_{NS})) \tag{G.2}$$

where:

$P_f(n_{gates}|h_{NS})$ = the probability that a specific number of gates fail upon request, given the occurrence of h_{NS} large enough to cause significant in the hinterlands

h_{NS} = waterlevel on the North Sea

Evaluating the failure mode of the failure to close failure mechanism there are two failure types of failure to be considered:

1. failure due to an exceedance of the inland estuary's bearing capacity
2. failure due to erosion of the bottom-protection around the structure

Depending on the amount of gates that fail, and the degree of the waterlevel that is induced during a storm, different types of failure scenarios might occur. For design purposes, as a first approximation the values for closure reliability for the Eastern Scheldt barrier were used. To evaluate the range of various failure modes in a FTC scenario an assessment on the two end of the possible outcomes was done, an assessment into the failure of a single gate, and an assessment into the failure of all the gates to close.

G.1.1. Failure of a single gate

In the situation that one single gate was to fail, the main concern during a storm scenario would be the design of the bottom protection. If the majority of the barriers cross-section is closed off, the total discharge through the barrier would be limited, therefor limiting the increase of the waterlevel of the inland basin. Due to this being the case, the head across the barrier would be significantly large, inducing high flow velocities through the barrier.

At the Eastern Scheldt Barrier, the probability that a single gate fails during the manned operation of the structure, if 0.0116 per closure request. This is the fast majority of the total failure probability of the barrier, which has a cumulative probability of 0.13 for a certain number of gates to fail during a closure request. During a single gate failure, the amount of total discharge going through the gate is limited, making the possibility for the exceedance of the bearing capacity behind the New Haringvliet Barrier almost impossible. Therefor, in this situation, the bottom protection is normative from a design perspective.

When a large storm surge arises on the North Sea, and one single gate fails to open on request, the waterlevel in the basin will stay relatively low due to the overall limited amount of inflow into the basin, while the water-level on the North Sea increases at a fast pace, this will induce a high head difference over the barrier, causing large flow velocities across the bottom protection (fig. G.1).

From a probability point of view, the accepted likelihood of such a scenario occurring is linked to a storm with a minimum return period of 580 years eq. (G.3). However, this does not account for all the failure modes of the barrier and is therefor too optimistic of an estimate, but for now it gives a clear upper boundary for the allowable failure rate. For the design of the bed protection in this report a storm with a return period of 1/3000 years was selected.

$$P(h_{NS}) = \frac{P_{f,FTC}}{P_f(n_{gates})} = \frac{2E-5}{0.0116} = \frac{1}{580} per\,year \tag{G.3}$$

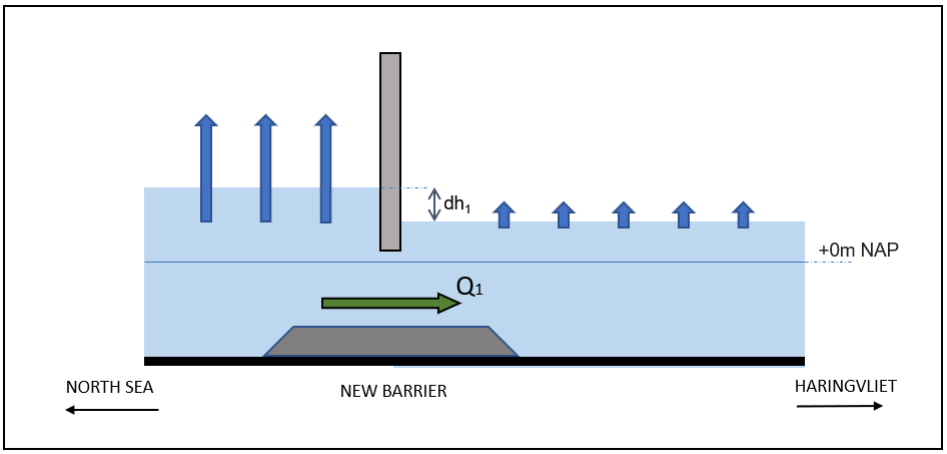

Figure G.1: Waterlevel progression during the failure of a single gate to close

G.1.2. Failure of Entire Barrier

In the case the entire barrier fails, the main concern is the exceedance of the basin storage capacity for the barrier. The failure of the entire barrier to close, would cause a rapid increase in the water-level in the basin, to the degree that it is assumed that any water-level on the North Sea above the threshold of +3m NAP would mandate flooding in the region. With the assumed sea-level rise of 1m, the return rate for storms with such a water level would be approximately 34 times per year (fig. G.2). The probability for the entire Eastern-Scheldt barrier to be subject to a FTC is 2.05E-5 per failure request. Calculating the failure rate of such a scenario occurring considering these values yields a failure rate that is higher than the acceptable rate (eq. (G.4)).

$$P(P_{f,FTC}) = 2.05E-5 * 33.9 = 6.95E-4 per\,year >> 2E-5 \tag{G.4}$$

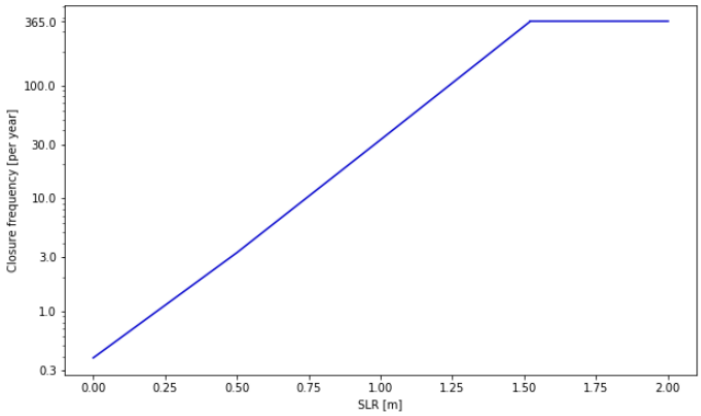

Figure G.2: Closure frequency for the New Haringvliet barrier, assuming various levels of SLR

G.1.3. Mitigation strategies

The initial estimates for the failure rates, based on the assessment in appendix G.1, are initial estimates that do not include additional mitigation measures for the possible failure scenario. Some mitigation measures are already included in the failure probabilities of the respective failure modes, however the assessment of various additional measures can lead to a better insight into the design measures possible to improve the redundancy of the flood defense system.

The failure of the entire barrier section, is difficult to solve due to the huge hydraulic load that is placed on the hinterland in such a scenario. The primary way to reduce the probability of this scenario occurring is by reducing the probability of the barrier to fail upon request. Failure scenarios where a large part of the barrier, or the entire barrier fails to close, are most likely due to large operational mistakes, mechanical issues in key part of the barrier, or due electrical issues. To counteract such errors from occurring, measures such as backup power supplies, mechanical back-up systems, and the storage of spare parts on location are key. Thus a reliability based design, that incorporated these measures in addition to rigid maintenance standards should be the first step in measures aimed to reduce the failure upon request rate to an acceptable rate.

Further measures that can be applied if the acceptable failure rate is still not met, can include some of the following options:

1. raising of the inland dikes to allow for less frequent barrier closure
2. operation of the Haringvlietsluices as backup
3. adjustment in barrier operation policy

1. Raising of the inland dikes could allow for an increase in the barrier's mandated closure level, impacting the closure rate of the barrier. Every 0.5m the barrier's closure level is raised, reduces the closure frequency by roughly a factor 10. However, given the fact that one of the primary aims of the Delta21 project is to minimize the raising of the dikes in the hinterlands this does not seem like the most desirable option. However, such an adjustment, that can still be made at later stages of the barrier's lifetime to potentially extend it's functionality might be helpful.

2. The second option to improve the system's reliability, is to operate the Haringvlietsluices as a back-up measure. If a storm occurs and the New Haringvliet barrier fails, the Haringvlietsluices could potentially be used as a back-up to avoid flooding. There are however some limitations to the effectiveness of this measure. Firstly, the operation of Delta21 as a primary flood defense might limit the funding, maintenance, and thus the reliability of the Haringvlietsluices. Secondly, the failure of both barriers during a given storm event might be strongly co-dependent, given that the operation of the Haringvlietsluices and the New Haringvliet barrier will both be done by the same organization (Rijkswaterstaat), might be subject to the same power

sources, and maintenance strategies. The last problem with this strategy is that in the case the operation of the Haringvlietsluices is required, Delta21's discharge functionalities will be rendered useless. The use of the Haringvlietsluices as a backup, is generally speaking a great option, however, care must be given to the practicality of the measure. Additionally the probability of a barrier failure occurring during a storm event, where also the Delta21 discharge capacity is required is most likely extremely small and probably within the bound of the acceptable failure rate. The exact benefit of this measure to the reliability of the system, and further assessments of the operation of the Haringvlietsluices, will not be assessed in this project.

3. The final measure is the adjustment of the barrier operational policy. If the closure reliability of the barrier becomes a problem in the future, sections of the barrier could potentially be permanently closed. Such a measure would have negative effects on the tide in the Haringvliet and Hollandsche Diep. However, it would reduce the barrier's effective cross-section in the case of barrier failure, which might reduce the flooding potential in the region.

H

Vertical lift gate design

This is an appendix to section 8.3, and feature skin plate design calculations as-well as additional MatrixFrame verification calculations.

H.1. Skin plate design

The first step in the design process, is the design of the skin plate and it's stiffeners. The skin plate thickness of the gates was chosen to be $t_{skin} = 20mm$. The skin plate will be supported by both longitudinal stiffeners and transverse girders that will transfer the forces to the main supporting structure of the gate. The first set of stiffeners that will be considered are the longitudinal stiffeners. A commonly used preliminary design rule to determine the maximum effective girder width of a stiffener or girder is given in eq. (H.1) (Daniel & Paulus, 2019). The equation shows that the maximum effective width over which the the stiffeners are effective is roughly 40 times the skin plate thickness, this yields a maximum stiffener spacing of $a = 800mm$. For the design of the stiffeners the design choice was made to space the longitudinal stiffeners 750mm apart, and the transverse girders 2500mm apart.

$$b_{eff,max} = 40 * t \tag{H.1}$$

where:

$b_{eff,max}$	= maximum effective skin plate width	$[mm]$
t	= skin plate thickness	$[mm]$

H.1.1. Longitudinal stiffeners

To dimension the longitudinal stiffeners the skin plate is divided in strips of 750mm, with each section being schematized as a beam on pinned supports. The pinned supports indicate the locations of the transverse stiffeners and are thus spaced 2500mm apart. To be conservative, the design pressure on the gate is taken to be uniform at a value of $q = 79.3kN/m^2 * 0.75m = 59.5kN/m$, the maximum pressure found along the gate for the design conditions. For a continuous beam on multiple pin supports, the largest bending moment occurs over the outer most pin-supports (fig. H.1). This was used as the normative design section for the stiffeners and thus the design bending moment for this section is $M_{d,1} = 40kNm$ for every 750mm wide section. The design of the longitudinal stiffeners shown in fig. H.2.

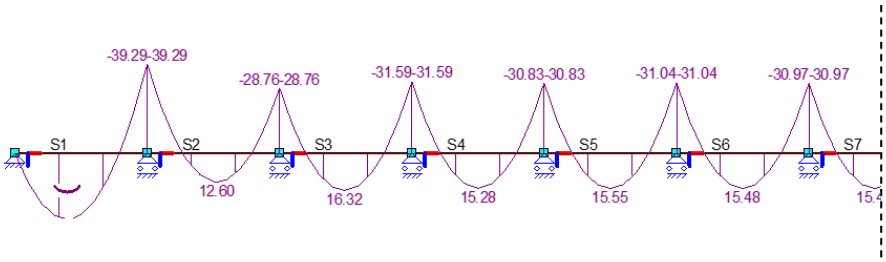

Figure H.1: Bending moment diagram for the normative section of a continuous pin-supported beam with a uniformly distributed load of $q = 59.5 kN/m$. The distance between supports is 2.5m each.

The maximum bending stresses occur in the upper (u) and lower (l) most fibres of the section (dashed section in fig. H.2). The maximum bending stresses are acceptable for a steel type of S355.

$$\sigma_{b,u} = \frac{-M_z\, z_u}{I_{zz}} = \frac{-40 * 10^6\, Nmm * -24\, mm}{26311122\, mm^4} = 43.4 N/mm^2 \tag{H.2}$$

$$\sigma_{b,l} = \frac{-M_z\, z_l}{I_{zz}} = \frac{-40 * 10^6\, Nmm * 166\, mm}{26311122\, mm^4} = -303.2 N/mm^2 \tag{H.3}$$

where:

σ_b	= bending stresses	$[N/mm^2]$
z	= distance from the centroid to the outer edge fibres of the cross-section	$[mm]$
M_z	= design bending moment	$[Nmm]$
I_{zz}	= mass moment of inertia in the z- plane	$[mm^4]$

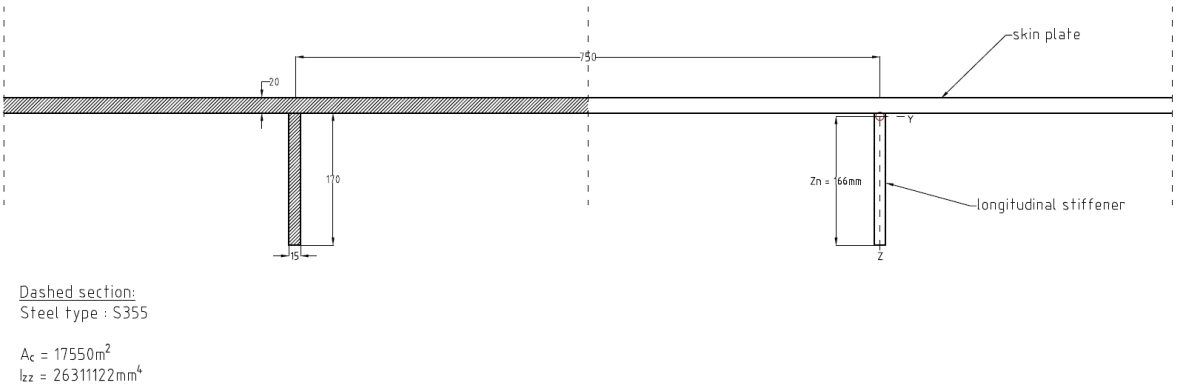

Figure H.2: Design dimensions of the longitudinal stiffeners, the right side indicates the location of the centre of mass of each section (skin plate and stiffener)

H.1.2. Transverse girders

As mentioned previously, the transverse girders are spaced 250mm apart. They are backed by two longitudinal beams that are the connection between the skin plate and the load bearing frame of the gates. To dimensions the transverse girders, the skin plate is once again divided into strips, this time with a width of

2500m. These strips are regarded as pin supported beams, with the supports being placed at the location of the longitudinal beams. An overview of the schematized system and the resulting bending moment diagram (per linear meter) is given in fig. H.3.

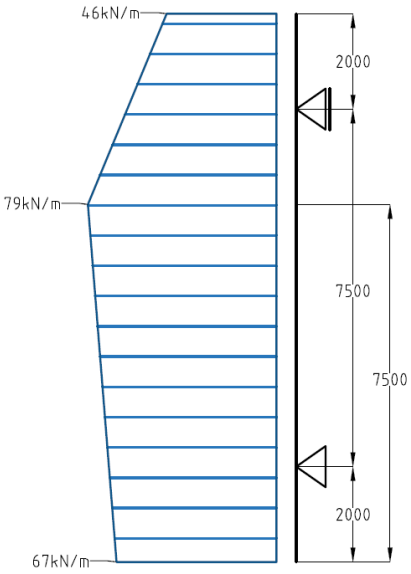

(a) Forces on the skin plate along the longitudinal direction

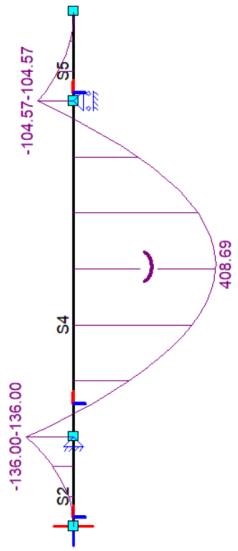

(b) Bending moments along the skin plate per meter (calculated using MatrixFrame

Figure H.3: Overview of the design load scenario along the longitudinal axis of the barrier per linear meter

The transverse girder that were designed are T-shaped sections (fig. H.4). The section was designed based on the maximum bending stresses that occur in the section. A design safety factor of 1.2 is applied. The design bending moment for the section is $M_z = 409 kNm/m * 2.5m * 1.2 = 1227 kNm$. The section suffices for a steel type of S355.

$$\sigma_{b,u} = \frac{M_z z_u}{I_{zz}} = \frac{1.22 * 10^9 \, Nmm * -88 \, mm}{1.946 * 10^9 \, mm^4} = -49.2 \, N/mm^2 \tag{H.4}$$

$$\sigma_{b,l} = \frac{M_z z_l}{I_{zz}} = \frac{1.22 * 10^9 \, Nmm * 497 \, mm}{1.946 * 10^9 \, mm^4} = 312.6 \, N/mm^2 \tag{H.5}$$

where:

σ_b	= bending stresses	$[N/mm^2]$
z	= distance from the centroid to the outer edge fibres of the cross-section	$[mm]$
M_z	= design bending moment	$[Nmm]$
I_{zz}	= mass moment of inertia in the z- plane	$[mm^4]$

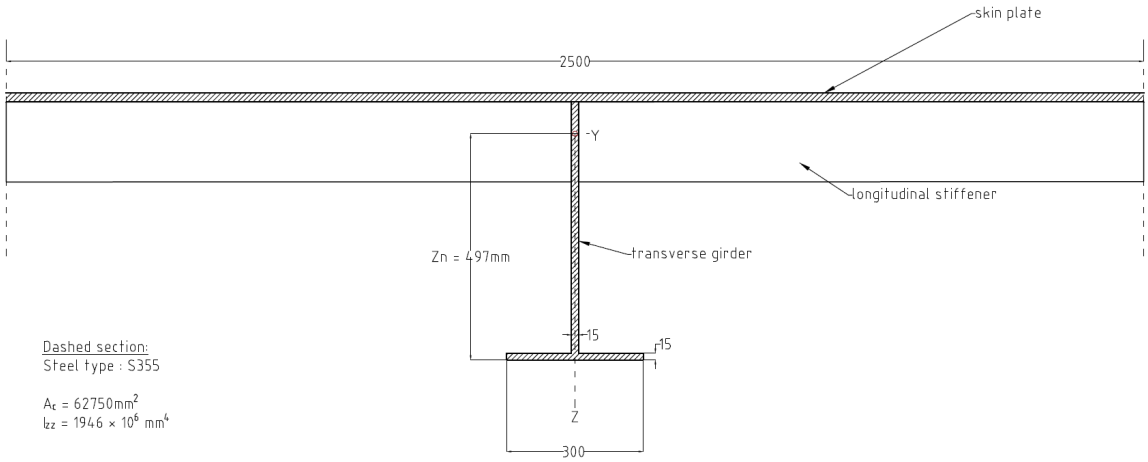

Figure H.4: Design dimensions of the transverse girders (skin plate and transverse girder)

H.2. Additional verification calculations

In this appendix, two additional verification calculations are shown.

Member check of S14: Axial loading and bending

$$\sigma_{max} = \frac{N}{A} + \frac{M\,z}{I} = +\frac{19714\,kN}{0.1225\,m^2} + \frac{7679\,kNm * 0.820\,m}{0.053\,m^4} = 279737 kN/m^2 < 355000 kN/m^2 \tag{H.6}$$

where:

σ_{max}	= maximum profile stresses	$[kN/m^2]$
z	= distance from the centroid to the outer edge fibres of the arched beam	$[m]$
A	= profile surface area	$[m^2]$
N	= normal forces in the member	$[m^4]$
M	= design bending moment	$[kNm]$
I	= mass moment of inertia in the relevant axis	$[m^4]$

Member check of S28 / S29: Axial buckling

$$N_{b,Rd} = \frac{\chi\,A\,f_y}{\gamma_s} = \frac{0.8 * 0.024 m^2 * 355000\ kN/m^2}{1.2} = 5680\ kN > 5160 kN \tag{H.7}$$

where:

χ	= axial buckling reduction factor for a HE500A profile with a length of 12000mm	$[-]$
A	= profile surface area	$[m^2]$
f_y	= yield strength of s335 steel	$[kN/m^2]$
γ_s	= safety factor	$[-]$

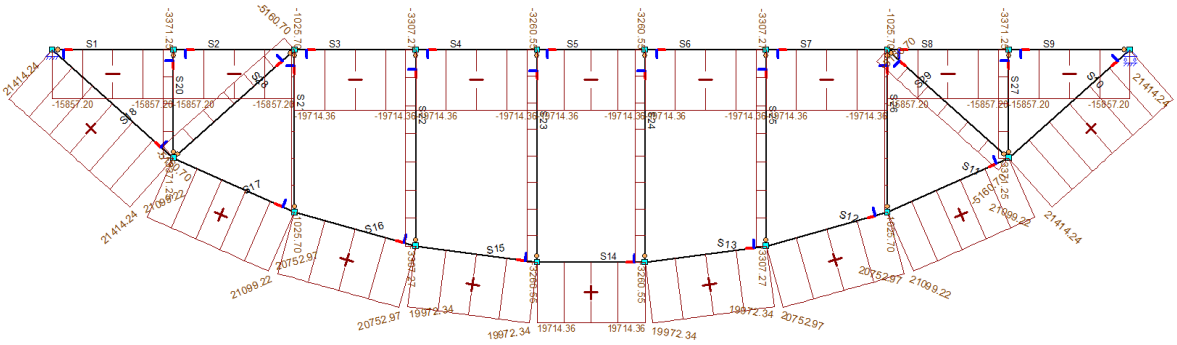

Figure H.5: Normal force diagram for the vertical lift gates

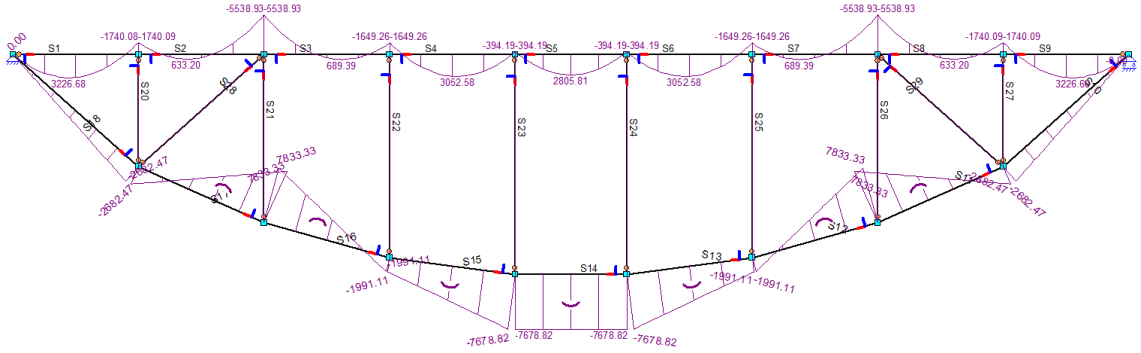

Figure H.6: Bending moment diagram for the vertical lift gates

H.3. Inverse loading of the hydraulic gates

Changing the side on which the gates are loaded, simply reverses the direction of the forces going through the respective member forces. Placing the gates in such an orientation would still suffice all the general strength calculations done for the design of the gates.

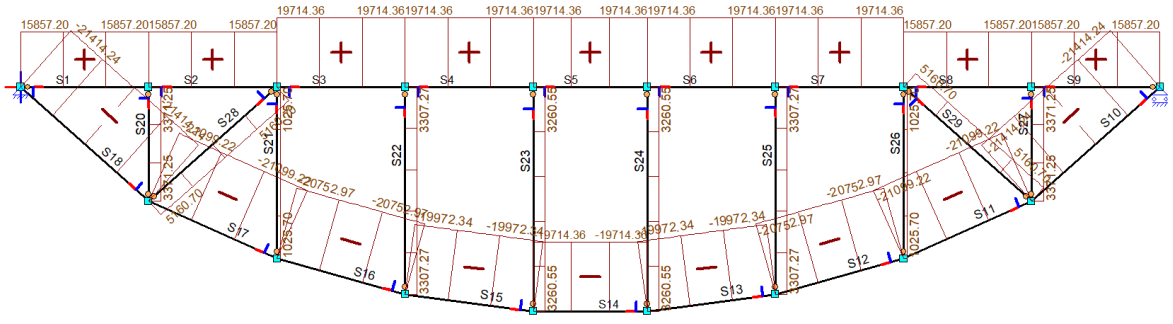

Figure H.7: Normal force diagram for the reverse loading of the vertical lift gates

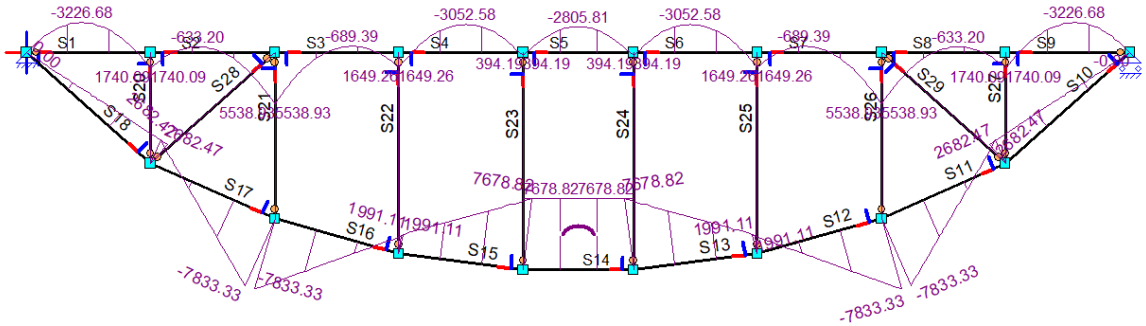

Figure H.8: Bending moment diagram for the reverse loading of the vertical lift gates